

INFORMATION TO USERS

This manuscript has been reproduced from the microfilm master. UMI films the text directly from the original or copy submitted. Thus, some thesis and dissertation copies are in typewriter face, while others may be from any type of computer printer.

The quality of this reproduction is dependent upon the quality of the copy submitted. Broken or indistinct print, colored or poor quality illustrations and photographs, print bleedthrough, substandard margins, and improper alignment can adversely affect reproduction.

In the unlikely event that the author did not send UMI a complete manuscript and there are missing pages, these will be noted. Also, if unauthorized copyright material had to be removed, a note will indicate the deletion.

Oversize materials (e.g., maps, drawings, charts) are reproduced by sectioning the original, beginning at the upper left-hand corner and continuing from left to right in equal sections with small overlaps.

Photographs included in the original manuscript have been reproduced xerographically in this copy. Higher quality 6" x 9" black and white photographic prints are available for any photographs or illustrations appearing in this copy for an additional charge. Contact UMI directly to order.

**ProQuest Information and Learning
300 North Zeeb Road, Ann Arbor, MI 48106-1346 USA
800-521-0600**

UMI[®]

**Polycaprolactone-*b*-Poly(ethylene oxide) Copolymer
Micelles: Physico-Chemical Characterization and
Application in Drug Delivery**

by

Christine Jane Allen

A thesis
submitted to the Faculty of Graduate Studies and Research
in partial fulfillment of the requirements for the degree of

Doctor of Philosophy

Department of Chemistry
McGill University
Montreal, Quebec
Canada, H3A 2K6

© Christine Jane Allen

September 1999



**National Library
of Canada**

**Acquisitions and
Bibliographic Services**

**395 Wellington Street
Ottawa ON K1A 0N4
Canada**

**Bibliothèque nationale
du Canada**

**Acquisitions et
services bibliographiques**

**395, rue Wellington
Ottawa ON K1A 0N4
Canada**

Your file Votre référence

Our file Notre référence

The author has granted a non-exclusive licence allowing the National Library of Canada to reproduce, loan, distribute or sell copies of this thesis in microform, paper or electronic formats.

The author retains ownership of the copyright in this thesis. Neither the thesis nor substantial extracts from it may be printed or otherwise reproduced without the author's permission.

L'auteur a accordé une licence non exclusive permettant à la Bibliothèque nationale du Canada de reproduire, prêter, distribuer ou vendre des copies de cette thèse sous la forme de microfiche/film, de reproduction sur papier ou sur format électronique.

L'auteur conserve la propriété du droit d'auteur qui protège cette thèse. Ni la thèse ni des extraits substantiels de celle-ci ne doivent être imprimés ou autrement reproduits sans son autorisation.

0-612-64495-2

Canada

ABSTRACT

This thesis describes the preparation, characterization and biological study of block copolymer aggregates as drug delivery vehicles. A novel method is described for the synthesis of biodegradable and biocompatible copolymers of polycaprolactone-*b*-poly(ethylene oxide). The copolymers and their aggregates are then characterized with special attention given to properties which are of most interest to applications in drug delivery such as copolymer composition, thermal behavior, critical water content, critical micelle concentration, partition coefficient of hydrophobic solubilizates, morphology of the aggregates and *in vitro* biocompatibility. The polycaprolactone-*b*-poly(ethylene oxide) copolymer micelles are first explored as a delivery vehicle for the neurotrophic agents FK506 and L-658,818. The *in vitro* delivery and biological activity of the micelle-incorporated drugs are confirmed in PC12 cell cultures. The *in vivo* biological distribution of the micelle-incorporated FK506 was assessed in Sprague Dawley rats both 6 and 24 hours following intravenous administration. Also, the biological activity of the micelle-incorporated FK506 was shown to be retained *in vivo* using the sciatic nerve crush model of peripheral neuropathy in Hanover Wistar rats. The question of whether or not the cellular internalization of the polycaprolactone-*b*-poly(ethylene oxide) micelles proceeds by an endocytotic mechanism is addressed in PC12 cell cultures. Finally, the polycaprolactone-*b*-poly(ethylene oxide) micelles are explored as a delivery vehicle for dihydrotestosterone. We report on several of the physico-chemical characteristics of the micelle-incorporated dihydrotestosterone as well as *in vitro* delivery in HeLa cells which have been cotransfected with the MMTV-LUC reporter gene and the androgen receptor.

RESUME

Cette thèse décrit la préparation, la caractérisation et l'étude biologique d'agrégats de copolymères bloc comme véhicules de relargage de médicaments. Une nouvelle méthode de synthèse de copolymères poly(caprolactone)-b-poly(oxyde d'éthylène), qui sont biodégradables et biocompatibles, est décrite. Les copolymères et leurs agrégats sont ensuite caractérisés, avec une attention particulière accordée aux propriétés qui sont les plus intéressantes dans le domaine de relargage des médicaments, par exemple la composition du copolymère, son comportement thermique, la concentration critique en eau, la concentration critique de micelles, le coefficient de partition des substances hydrophiques, les morphologies, et la biocompatibilité *in vitro*. Les micelles de polycaprolactone-*b*-poly(oxyde d'éthylène) sont tout d'abord étudiées comme véhicules de relargage d'agents neurotrophiques FK506 et L-658,818. Le relargage *in vitro* et l'activité biologique des médicaments incorporés dans les micelles sont confirmées sur des cultures de cellules PC12. La distribution biologique *in vivo* de FK506 incorporé dans les micelles a été vérifiée sur des rats Sprague Dawley à la fois 6 heures et 24 heures suivant une administration intraveineuse. Par ailleurs, on a montré que l'activité biologique de FK506 incorporé dans les micelles est conservée *in vivo* en utilisant le modèle d'écrasement du nerf sciatique dans la neuropathie périphérique chez des rats Hanover Wistar. On discute aussi le problème de savoir si l'internalisation cellulaire des micelles polycaprolactone-*b*-poly(oxyde d'éthylène) se passe par un mécanisme endocytotique dans des cultures de cellules PC12. Finalement, les micelles PCL-*b*-PEO sont explorées comme véhicule de relargage de dihydrotestosterone. Nous reportons plusieurs caractéristiques physico-chimiques des micelles contenant de la dihydrotestosterone, ainsi que le relargage *in vitro* dans des cellules HeLa qui ont été cotransfectées avec le gène rapporteur MMTV-LUC et le récepteur androgène.

Foreword

In accordance with Thesis Specifications of the "Guidelines for Thesis Preparation" (Faculty of Graduate Studies and Research, McGill University), the following text is cited:

"Candidates have the option of including, as part of the thesis, the text of one or more papers submitted or to be submitted for publication, or the clearly-duplicated text of one or more published papers. These texts must be bound as an integral part of the thesis.

If this option is chosen, connecting texts that provide logical bridges between the different papers are mandatory. The thesis must be written in such a way that it is more than a mere collection of manuscripts; in other words, results of a series of papers must be integrated.

The thesis must still conform to all other requirements of the "Guidelines for Thesis Preparation". The thesis must include: A Table of Contents, an abstract in English and French, an introduction which clearly states the rationale and objectives of the study, a review of the literature, a final conclusion and summary, and a thorough bibliography or reference list.

Additional material must be provided where appropriate (e.g. in appendices) and in sufficient detail to allow clear and precise judgment to be made of the importance and originality of the research reported in the thesis.

In the case of manuscripts co-authored by the candidate and others, the candidate is required to make an explicit statement in the thesis as to who contributed to such work and to what extent. Supervisors must attest to the accuracy of such statements at the doctoral oral defense. Since the task of the examiners is made more difficult in these cases, it is in the candidate's interest to make perfectly clear the responsibilities of all the authors of the co-authored papers."

This dissertation is written in the form of six original papers and two review articles, each of which comprises one chapter, with general conclusions contained in the final chapter. Following normal procedures, the papers and review articles have either been published, submitted or will be submitted shortly for publication in scientific journals. A list of the papers and review articles contained within each chapter is given below:

Chapter 1, section 1.2: *S.T.P. Pharma Sciences* **1999**, 9, 139-151.

Chapter 2: *Colloids and Surfaces B: Biointerfaces* **1999** accepted.

Chapter 3: *Macromolecules* **1997** 30, 7143-7150

Chapter 4: to be submitted to *Macromolecules*

Chapter 5: *Bioconjugate Chemistry* **1998**, 9, 564-573.

Chapter 6: a longer version will be submitted

Chapter 7: *Biochimica Biophysica Acta; Biomembranes* **1999** accepted.

Chapter 8: *Journal of Controlled Release* **1999** accepted.

Contributions of Authors

All of the papers were co-authored by the research director Dr. Adi Eisenberg. Also, several of the papers were co-authored by Dr. Dusica Maysinger as she supervised and directed all of the pharmacological studies. In Chapter 3, Dr. Jianxi Zhao is a co-author as he performed much of the early experimental work. In Chapters 4 - 8, Dr. Yisong Yu is a co-author as he synthesized all of the polycaprolactone-b-poly(ethylene oxide) copolymer samples. Also, in Chapter 4 Dr. Yisong Yu is a co-author as he performed the thermal analysis studies and determined the critical water content. Chapter 4 also includes Ms. Sachiko Chijiwa, an undergraduate student working under the direct supervision of the author. For Chapter 6, Dr. Jasenka Mrsic performed the biological functional assay (sciatic nerve crush paradigm). For Chapter 8, Dr. D. Maysinger performed the co-transfection of HeLa cells with the MMTV-LUC reporter gene and the androgen receptor. Also, Chapter 8 includes Ms. Jeannie Han, an undergraduate student working under the direct supervision of the author. Other than the aforementioned contributions to the chapters, all of the work presented in this dissertation was performed by the author.

I hereby give copyright clearance for the inclusion of the following paper, for which I am co-author, in the dissertation of Christine Allen.

"Partitioning of Pyrene between "Crew-Cut" Block Copolymer Micelles and H₂O/DMF Solvent Mixtures."

"Polycaprolactone-*b*-poly(ethylene oxide) Block Copolymer Micelles as a Novel Drug Delivery Vehicle for Neurotrophic Agents FK506 and L,685-818."

" Copolymer Drug Carriers: Conjugates, Micelles and Microspheres."

"Nano-Engineering Block Copolymer Aggregates for Drug Delivery."

"Cellular Internalization of PCL₂₀-*b*-PEO₄₄ Block Copolymer Micelles."

"Polycaprolactone-*b*-Poly(ethylene oxide) Copolymer Micelles as a Delivery Vehicle for Dihydrotestosterone."

"Synthesis and Characterization of a Biodegradable and Biocompatible Amphiphilic Diblock Copolymer of Polycaprolactone-*b*-Poly(ethylene oxide)."

"*In vivo* Study of Polycaprolactone-*b*-Poly(ethylene oxide) Micelles as a Delivery Vehicle for the Neurotrophic Agent FK506"



Dr. Adi Eisenberg
Department of Chemistry
McGill University
801 Sherbrooke St. West
Montreal, Quebec
Canada, H3A 2K6

Date: August 30 1999

I hereby give copyright clearance for the inclusion of the following papers for which I am co-author in the dissertation of Christine Allen.

"Polycaprolactone -*b*-Poly(ethylene oxide) Block Copolymer Micelles as a Novel Drug Delivery Vehicle for Neurotrophic Agents FK506 and L-685,818"

"Copolymer Drug Carriers: Conjugates, Micelles and Microspheres"

"Nano-Engineering Block Copolymer Aggregates for Drug Delivery"

"Cellular Internalization of PCL₂₀-*b*-PEO₄₄ Block Copolymer Micelles"

"Polycaprolactone -*b*-Poly(ethylene oxide) Copolymer Micelles as a Delivery Vehicle for Dihydrotestosterone"

"Synthesis and Characterization of a Biodegradable and Biocompatible Amphiphilic Diblock Copolymer of Polycaprolactone-*b*-Poly(ethylene oxide)"

Dr. D. Maysinger

Date: 9/7/1999

Dr. D. Maysinger
Department of Pharmacology and Therapeutics
McGill University
3655 Drummond St.
Montreal, Quebec
Canada
H3G 1Y6

I hereby give copyright clearance for the inclusion of the following paper, for which I am co-author, in the dissertation of Christine Allen.

"Synthesis and Characterization of a Biodegradable and Biocompatible Amphiphilic Diblock Copolymer of Polycaprolactone-*b*-Poly(ethylene oxide)."



Sachiko Chijiwa
Department of Chemistry
McGill University
801 Sherbrooke St. West
Montreal, Quebec
Canada, H3A 2K6

Date: August 30th, 1999

I hereby give copyright clearance for the inclusion of the following paper, for which I am co-author, in the dissertation of Christine Allen.

"Polycaprolactone-*b*-poly(ethylene oxide) Block Copolymer Micelles as a Novel Drug Delivery Vehicle for Neurotrophic Agents FK506 and L,685-818."

"Cellular Internalization of PCL₂₀-*b*-PEO₄₄ Block Copolymer Micelles."

"Polycaprolactone-*b*-Poly(ethylene oxide) Copolymer Micelles as a Delivery Vehicle for Dihydrotestosterone."

"Synthesis and Characterization of a Biodegradable and Biocompatible Amphiphilic Diblock Copolymer of Polycaprolactone-*b*-Poly(ethylene oxide)."

"*In vivo* Study of Polycaprolactone-*b*-Poly(ethylene oxide) Micelles as a Delivery Vehicle for the Neurotrophic Agent FK506"


Dr. Yisong Yu

Date: Aug. 20, 1999

Acknowledgements

I would especially like to thank Professor Eisenberg, Professor Lennox and Professor Hogan for having made a deep and lasting impression in my life over these past few years. Professor Eisenberg has supervised and directed my research throughout the years during which time he shared with me his overwhelming enthusiasm for science. His faith in my abilities has strengthened my own sense of self-confidence and enabled me to strive to greater heights in my professional life. I have thoroughly enjoyed so many of the discussions that we have had over the years. I am also grateful to Professor Lennox for having provided me with support and positive words of encouragement especially in the early stages of this degree. His positive influence was crucial in enabling me to settle in during my first year at McGill University. I am thankful to Professor Hogan for having given me the opportunity to uncover my true love for teaching. I thank him also for his advice and guidance over these past years.

I am also grateful to the Chemistry Department and especially Professor Eisenberg and Professor Maysinger for enabling my research project to be interdisciplinary as it includes experimental work in areas of both Chemistry and Pharmacology. In this connection I would like to thank Dr. Maysinger for having directed and supervised all pharmacological aspects of the research. I also thank Dr. Maysinger for having given me the opportunity to learn various aspects of both pharmacology and biology.

In addition, I feel truly blessed for having been surrounded by such an incredibly supportive laboratory group. I would first like to thank Matthew Moffitt, Lifeng Zhang, and Neil Cameron for sharing their wisdom with me and always being willing to provide me with both sound and solid advice. I have always felt I could especially count on the friendship of Carl Bartels, Neil Cameron, and Anne Noronha. I also thank Muriel Corbiere, Patrick Lim Soo, Luc Desbaumes, Yisong Yu, Hongwei Shen, Kui Yu, Jeannie Han, Owen Terreau, Sachiko Chijiwa, Diane Goodman, Chris Wilds, Andrea Bardel, Colleen Williams, Anne Morinville and Natalia Kucic for their friendship.

I am grateful to the following individuals for sharing their technical expertise:

- Dr. H. Vali for teaching me various electron microscopic techniques and also for insightful scientific discussions

- Ms. Jeannie Mui and Ms. Matilda Cheung for help with sample preparation and operation of the electron microscopes
- Dr. Peter McGarry (Paprican) for graciously allowing me to use the fluorometer and always being willing to provide advice in terms of the operation of the instrument
- Anne Morinville and Natalia Kucic for helpful advice and technical assistance in the cell culture room (also thank-you to Anne for editing my written work over the years)
- Professor Grosser for helpful discussions on release kinetics and pharmacokinetics
- Dr. Yisong Yu for his scientific advice and helpful input
- Dr. Jianxi Zhao for teaching me how to operate the fluorometer
- Muriel Corbiere for translation of the abstract from english into french

I am sincerely grateful to NSERC, FCAR and the Chemistry Department of McGill University for financial assistance. I would also like to thank the Chemistry Department for providing me with the opportunity to be both a teaching assistant and laboratory demonstrator over the years.

Finally, I would like to thank my parents for their unbelievable support and encouragement throughout my life. They have taught me that with faith and hard work anything is possible. Thank-you Mom and Dad for always believing in me and my dreams. I would also like to thank my brother, Greg, for providing a strong shoulder to lean on when I needed it most. I am also grateful to my extended family for their show of support, especially my aunts, Brenda Rothwell and Jill Young, my uncle, Roxy Young, and my grandmother, Veleda Amm. I am very thankful for the wonderful friends that have stood by me throughout these years. My incredible friends, Jennifer Timmons and Alynn Shafer thank-you mostly for listening but also for your positive words of encouragement. Thank-you to my dearest friend, Paul McManus, for his daily support during the final stages of thesis preparation. I also thank all of the friends that have kept me laughing: Christine Bennett, Michelle Bennett, Elaine Silver, Tara Leyden, Claire Busu, Helen Vakos, and my little cousin Emily Rothwell.

Table of Contents

Abstract.....	ii
Resume.....	iii
Foreword.....	iv
Acknowledgements.....	x
Table of Contents.....	xii
List of Tables.....	xix
List of Figures.....	xx
List of Abbreviations.....	xxvii
CHAPTER 1. General Introduction.....	1
1.1. The Role and Relevance of Drug Delivery Vehicles Today.....	1
1.2. Delivery Vehicles Based on Copolymer Materials.....	2
1.2.1. Copolymer Properties Influencing Rational Design.....	5
1.2.1.1. Polymer-Drug Conjugates and Macromolecular Conjugates.....	5
1.2.1.2. Block Copolymer Micelles.....	6
1.2.1.3. Micro(nano)particles.....	14
1.2.2. Copolymer Colloidal Carriers: Strengths/Weaknesses.....	23
1.3. Scope of the Thesis.....	25
1.4. References.....	27
CHAPTER 2. Nano-engineering Block Copolymer Aggregates for Drug	
Delivery.....	32
2.1. Introduction.....	32
2.2. The Micelle as a Whole.....	35
2.2.1. Methods of Micelle Preparation.....	35
2.2.2. Methods of Drug Incorporation.....	37
2.2.3. Micelle Stability.....	38
2.2.3.1. Thermodynamic Stability.....	38
2.2.3.2. Kinetic Stability.....	39
2.2.4. Micelle Size.....	40

2.2.5. Size Population Distribution	41
2.3. The Micelle Corona: Steric Barrier	41
2.3.1. PEO as the Corona-Forming Block.....	42
2.3.1.1. Steric Stabilization.....	43
2.3.2. Corona-Forming Blocks Other than PEO.....	44
2.4. The Micelle Core: Cargo Space.....	46
2.4.1. Loading Capacity.....	46
2.4.1.1. Compatibility between the Solubilizate and the Core- Forming Block.....	46
2.4.1.2. Other Factors which Influence Drug Loading.....	49
2.4.2. Release Kinetics.....	51
2.4.2.1. Polymer Drug Interactions.....	51
2.4.2.2. Localization of the Drug within the Micelle.....	52
2.4.2.3. Physical State of the Micelle Core.....	52
2.4.2.4. Other Factors which Influence Release Kinetics.....	53
2.5. Morphology.....	54
2.5.1. The Potential Relevance of Morphologies of Block Copolymer Aggregates in Drug Delivery.....	54
2.5.2. Morphologies of Crew-Cut Aggregates.....	55
2.5.3. Morphogenic Factors.....	58
2.5.3.1. Copolymer Composition	58
2.5.3.2. Copolymer Concentration.....	59
2.5.3.3. Presence of Added Acid, Base or Salt.....	59
2.5.3.4. Common Organic Solvent used in Micelle Preparation.....	60
2.6. Conclusion.....	62
2.7. References.....	64
 CHAPTER 3. Partitioning of the Hydrophobic Solubilizate, Pyrene, between a Model Micelle System and the External Medium.....	 70
3.1. Partitioning of Pyrene between “Crew-Cut” Block Copolymer Micelles and H ₂ O/DMF Solvent Mixtures.....	72

3.1.1. Introduction.....	72
3.1.2. Theoretical Aspects.....	74
3.1.2.1. Fluorescence.....	74
3.1.2.2. Pyrene Monomer Fluorescence.....	75
3.1.2.3. Calculation of the Amount of Pyrene Absorbed.....	75
3.1.2.4. Calculation of I_3^U from the Partition Coefficient.....	78
3.1.2.5. Relationship between K_V and K	78
3.1.2.6. Calculation of Free Energy of Transfer.....	79
3.1.3. Experimental Section.....	79
3.1.3.1. Materials.....	79
3.1.3.2. Methods	80
3.1.4. Results and Discussion.....	81
3.1.4.1. Pyrene in the Solvent Mixture.....	81
3.1.4.2. Pyrene Partitioning in Micellar Solutions.....	82
3.1.4.3. Calculation of the Amount of Pyrene Absorbed.....	84
3.1.4.4. Partition Coefficient.....	88
3.1.4.5. Calculation of I_3^U , $[Py]_M / [Py]$, and Pyrene Molecules / Micelle....	88
3.1.4.6. Mass Equilibrium Constant and Free Energy of Transfer.....	94
3.1.5. Conclusions.....	96
3.1.6. References.....	97

CHAPTER 4. Synthesis and Characterization of a Biodegradable and Biocompatible Amphiphilic Copolymer of Polycaprolactone- <i>b</i>-Poly-(ethylene oxide)	100
4.1. Synthesis and Characterization of a Biodegradable and Biocompatible Amphiphilic Copolymer of Polycaprolactone-<i>b</i>-Poly(ethylene oxide)	101
4.1.1. Introduction.....	101
4.1.2.Experimental Section.....	103
4.1.2.1. Materials.....	103
4.1.2.2. Methods.....	104

4.1.3. Results and Discussion.....	109
4.1.3.1. Synthesis of Polycaprolactone- <i>b</i> -Poly(ethylene oxide) Copolymers.....	109
4.1.3.2. Thermal Behavior of PCL- <i>b</i> -PEO Copolymers.....	113
4.1.3.3. Aggregation Studies of the PCL- <i>b</i> -PEO Copolymers by Static Light Scattering Measurements.....	118
4.1.3.4. Crystallization of PCL block during micellization.....	123
4.1.3.5. CMC Determination.....	123
4.1.3.6. Determination of Micelle Morphology.....	126
4.1.3.7. Incorporation of Hydrophobic Solubilizes.....	128
4.1.3.8. Loading Efficiency of the PCL- <i>b</i> -PEO Micelles for CM-DiI as a Function of Polycaprolactone Block Length.....	129
4.1.3.9. <i>In vitro</i> Biocompatibility of the PCL- <i>b</i> -PEO Micelles.....	131
4.1.4. Conclusion.....	134
4.1.5. References.....	135

**CHAPTER 5. Polycaprolactone -*b*-Poly(ethylene oxide) Copolymer Micelles
as a Novel Drug Delivery Vehicle for Neurotrophic Agents
FK506 and L-685,818.....**

5.1. FK506: Therapeutic Effects and Mechanisms of Action.....	139
5.1.1. Therapeutic Effects of FK506.....	141
5.1.1.1. FK506 as an Immunosuppressive Agent.....	141
5.1.1.2. FK506 as a Neuroprotective and Neuroregenerative Agent	144
5.1.1.3. FK506 as a Dermatological Agent.....	147
5.1.2. Drug Delivery Vehicles for FK506.....	147
5.2. <i>In vitro</i> Model to Assess Delivery and Biological Activity of Micelle- Incorporated FK506.....	150
5.2.1. PC12 Cell Cultures.....	150
5.2.2. FK506 Potentiates NGF in PC12 Cell Cultures.....	151
5.3. PCL- <i>b</i> -PEO Micelles as a Delivery Vehicle for the Neurotrophic Agents FK506 and L-685,818.....	152

5.3.1. Introduction	152
5.3.2 Experimental Section.....	155
5.3.2.1. Materials.....	155
5.3.2.2. Methods.....	156
5.3.3. Results.....	160
5.3.3.1 Micelle Size Distributions.....	160
5.3.3.2. <i>In vitro</i> Stability Studies	161
5.3.3.3. Determination of the Partition Coefficient for Pyrene.....	161
5.3.3.4. Cell Survival in the presence of the PCL- <i>b</i> -PEO Micelles.....	161
5.3.3.5. Cell Uptake of Pyrene Incorporated Micelles.....	162
5.3.3.6. <i>In vitro</i> Studies of free form FK506 and L-685,818 and micelle- incorporated FK506 and L-685,818.....	162
5.3.3.7. Dose-response curves for NGF, FK506 and L-685,818 without Micelles.....	162
5.3.3.8. Dose-response curves for the Combined Effect of NGF and FK506 or L-685,818 without Micelles.....	163
5.3.3.9. <i>In vitro</i> effect of micelle-incorporated FK506 and L-685,818 along with NGF.....	163
5.3.4. Discussion	164
5.3.4.1 Characterization of the PCL- <i>b</i> -PEO Micelles.....	164
5.3.4.2 Determination of the Partition Coefficient for Pyrene between the PCL- <i>b</i> -PEO Micelles and Water.....	167
5.3.4.3. <i>In vitro</i> Biocompatibility of the PCL- <i>b</i> -PEO Micelles.....	171
5.3.4.4. Cell Uptake of Pyrene-Incorporated Micelles	171
5.3.4.5. PCL- <i>b</i> -PEO Micelles as a Delivery System for FK506 and L- 685,818.....	174
5.3.5. References	179

CHAPTER 6. <i>In vivo</i> Study of Polycaprolactone-<i>b</i>-Poly(ethylene oxide)	
Micelles as a Delivery Vehicle for the Neurotrophic agent	
FK506.....	184

6.1. <i>In vivo</i> Study of PCL-<i>b</i>-PEO Micelles as a Delivery Vehicle for the Neurotrophic Agent FK506.....	186
6.1.1. Introduction	186
6.1.2. Materials and Methods.....	187
6.1.2.1. Materials.....	187
6.1.2.2. Methods.....	188
6.1.3. Results.....	190
6.1.3.1. <i>In vitro</i> Release Kinetics.....	190
6.1.3.2. Biodistribution of Micelle-Incorporated FK506 in Non-Neural Tissue.....	192
6.1.3.3. Biodistribution of Micelle-Incorporated FK506 in Neural Tissue.....	192
6.1.3.4. Behavioral Assessment of Functional Recovery.....	192
6.1.4. Discussion.....	197
6.1.5. Conclusions.....	201
6.1.6. References.....	202

CHAPTER 7. Cellular Internalization of PCL₂₀-*b*-PEO₄₄ Block Copolymer

Micelles.....	204
7.1. Endocytosis.....	205
7.2. The Cellular Internalization of the PCL ₂₀ - <i>b</i> -PEO ₄₄ Micelles.....	207
7.2.1. Introduction.....	207
7.2.2 Materials and Methods.....	208
7.2.2.1. Materials	208
7.2.2.2. Experimental Methods.....	209
7.2.3. Results and Discussion.....	212
7.2.3.1 Characteristics of the PCL- <i>b</i> -PEO Micelles Employed in the Cellular Internalization Studies.....	212
7.2.3.2. Cellular Uptake Studies	212
7.2.4. References.....	220

CHAPTER 8. PCL-<i>b</i>-PEO Micelles as a Delivery Vehicle for other	
Hydrophobic Drugs such as Dihydrotestosterone.....	222
8.1. <i>In vitro</i> Model to Assess the Delivery and Biological Activity of Micelle	
Incorporated Dihydrotestosterone	223
8.2. Polycaprolactone- <i>b</i> -Poly(ethylene oxide) Copolymer Micelles as a	
Delivery Vehicle for Dihydrotestosterone.....	224
8.2.1. Introduction	224
8.2.2. Materials and Methods.....	226
8.2.2.1. Materials.....	226
8.2.2.2. Methods.....	226
8.2.3. Results	229
8.2.3.1. Loading Capacity of PCL ₂₀ - <i>b</i> -PEO ₄₄ Micelles for	
Dihydrotestosterone.....	229
8.2.3.2. Apparent Partition Coefficient for DHT between the Micelles	
and the External Medium.....	231
8.2.3.3. Number of Molecules Loaded per Micelle.....	232
8.2.3.4. <i>In vitro</i> Release Kinetic Profile of Micelle-Incorporated DHT	234
8.2.3.5. <i>In vitro</i> Studies.....	234
8.2.4. Discussion.....	238
8.2.5. Conclusion.....	241
8.2.6. References.....	242

CHAPTER 9. Conclusions, Contributions to Original Knowledge and	
Suggestions for Future Work.....	245
9.1. Conclusions and Contributions to Original Knowledge.....	245
9.2. Suggestions for Future Work.....	250

List of Tables

Table 1.1. List of several of the block copolymer materials which have been used to form micellar delivery systems and the drugs which have been incorporated.	9
Table 1.2. Several of the performance dependent parameters of block copolymer micelle delivery systems and a few examples of each.	11
Table 1.3. List of several of the copolymer materials which have been used to form micro or nanoparticles and drugs which have been incorporated	18
Table 1.4. The two primary methods employed for the steric stabilization of microparticles. The first method requires the use of block copolymers containing a PEO block, the second method involves surface modification of the microparticle with PEO containing conjugates.	19
Table 2.1. A list of several of the biocompatible polymers that have been employed as core-forming blocks.	33

List of Figures

- Figure 1.1.** The basic architecture and size of copolymer drug carriers (*after* DONBROW, M., ed. *Microcapsules and Nanoparticles in Medicine and Pharmacy*, CRC Press, 1992.) 3
- Figure 1.2.** A schematic of the different polymers which can be created depending on the number of types of repeat units; homopolymer (one type), copolymer (two or more types). Copolymers may be random, block or graft according to the arrangement of repeat units. 4
- Figure 1.3.** An illustration of the three categories of block copolymer micelles distinguished on the basis of the method of drug incorporation. "Micellar microcontainers" include physically entrapped drug, "polymeric drugs" are formed from copolymer-drug conjugates and "block ionomer complexes" contain charge bearing drugs or molecules which interact with the core-forming block via electrostatic interactions. 7
- Figure 1.4.** An illustration of the two main categories of microparticles, namely, microspheres and microcapsules. Also, an example, of surface modification of the microparticle, with a block copolymer containing a poly(ethylene oxide) block, to produce sterically stabilized particles. 15
- Figure 2.1.** A schematic of the two principle methods employed for the preparation of block copolymer micelles. 35
- Figure 2.2.** The key physical properties of the micelle corona that influence factors important in terms of the capabilities of micelles as drug carriers. 42
- Figure 2.3.** The properties of the core and drug which have the most profound influence on both the loading capacity of the micelle and release kinetics of the drug. 47
- Figure 2.4.** A schematic of the "ideal micelle system" including the most favorable properties for the micelle as a whole, the core and the corona. 63
- Figure 3.1.** Fluorescence emission spectrum of pyrene (1.5×10^{-9} mol/g) in 85%/15% H₂O/DMF at a copolymer concentration of 5.6×10^{-4} g/g. 77

Figure 3.2. Intensity (I_3^V) as a function of water content in the solvent mixture in the absence of copolymer. Pyrene concentration = 1.5×10^{-9} mol/g. 82

Figure 3.3. Semilogarithmic plots of the fluorescence intensity (I_3^U) as a function of polymer concentration in different solvent mixtures. Symbols represent the experimental values for the various solvent mixtures expressed as %H₂O/ %DMF; (◆) 90/10, (●) 85/15, (●) 80/20, (Δ) 70/30, (■) 60/40, (□) 40/60, (Δ) 20/80. The curves were calculated using eq. 7. 83

Figure 3.4. Semilogarithmic plots of $[Py]_M/[Py]$ vs copolymer concentration in different solvent mixtures. Symbols represent the experimental values for the various solvent mixtures expressed as %H₂O/ %DMF; (◆) 90/10, (●) 85/15, (●) 80/20, (Δ) 70/30, (■) 60/40, (□) 40/60, (Δ) 20/80. The curves were calculated using eq. 6. 86

Figure 3.5. Logarithmic plot of the number of pyrene molecules per micelle as a function of polymer concentration for the various DMF/H₂O solvent mixtures. 87

Figure 3.6. Plot of $[Py]_M/[Py]_v$, obtained from fluorescence data, vs copolymer concentration in g/mL for the 85% /15% H₂O/DMF mixture. From this plot the partition coefficient of pyrene calculated by eq. 5. 89

Figure 3.7. A semilogarithmic plot of partition coefficient (K_v) vs water content in the solvent mixture. 90

Figure 3.8. Semilogarithmic plots of the fluorescence intensity (I_3^U) as a function of polymer concentration for the 80%/20% H₂O/DMF solvent mixture. Symbols represent the experimental values. The curves were calculated using eq. 7, for a range of values of I_{3max} . 93

Figure 3.9. Semilogarithmic plots of the mass equilibrium constant (K) and the free energy (ΔG^0) of pyrene transfer from solvent phase to the micellar cores as functions of water content in the solvent mixture. 95

Figure 4.1. SEC traces of PEO homopolymer and PCL-*b*-PEO copolymers 111

Figure 4.2. ^1H -NMR spectrum of PCL- <i>b</i> -PEO copolymer	112
Figure 4.3a.: The conversion of ϵ -CL monomer versus polymerization time initiated by PEO diethyl aluminum macroinitiator in THF.	114
Figure 4.3b. The relationship between the molecular weight (M_n) and the conversion of ϵ -CL monomer in THF.	115
Figure 4.4. Thermographs of various PCL- <i>b</i> -PEO copolymers:	
A) PCL ₁₄ - <i>b</i> -PEO ₄₄ B) PCL ₂₀ - <i>b</i> -PEO ₄₄	
C) PCL ₄₀ - <i>b</i> -PEO ₄₄ D) PCL ₁₅₀ - <i>b</i> -PEO ₄₄	116
Figure 4.5. Thermographs of repeated runs of on one PCL ₄₀ - <i>b</i> -PEO ₄₄ copolymer :	
A) first run, B) second run, C) third run.	117
Figure 4.6. Plot of the scattered light intensity as a function of added water content for different concentrations (shown in brackets next to each curve) of PCL ₉₆ - <i>b</i> -PEO ₄₄ in THF.	119
Figure 4.7. The semilogarithmic plot of the critical water content versus the copolymer concentration for various PCL- <i>b</i> -PEO copolymers in THF.	120
Figure 4.8. Plot of the micelle fraction as a function of the water increment beyond the critical water content for various PCL- <i>b</i> -PEO copolymers. The insert shows the plot against the absolute water content (1 wt%).	122
Figure 4.9. Thermographs of various PCL- <i>b</i> -PEO aggregates:	
A. PCL ₉₀ - <i>b</i> -PEO ₄₄ ; B. PCL ₄₅ - <i>b</i> -PEO ₄₄ ; C. PCL ₃₅ - <i>b</i> -PEO ₄₄	124
Figure 4.10. A semilogarithmic plot of the ratio of I_{338}/I_{333} of pyrene versus the copolymer concentration.	125
Figure 4.11a and b) The freeze-fracture/freeze etch electron micrograph of a 1% (w/w) solution of PCL ₂₀ - <i>b</i> -PEO ₄₄ copolymer.	127
Figure 4.12 a) Plot of the % loading efficiency of CM-DiI versus the block length of polycaprolactone in the copolymer used to form the PCL- <i>b</i> -PEO aggregates.	130
Figure 4.12b) Plot of the % loading efficiency of CM-DiI versus the PCL ₂₀ - <i>b</i> -PEO ₄₄ copolymer concentration.	132
Figure 4.13. The plot of the % cell survival versus the incubation time in PC12 cell cultures.	133

Figure 5.1.1: Structure of FK506 ($R_1 = H$, $R_2 = \text{allyl}$)	139
Figure 5.1.2: Schematic of FK506/FKBP12 inhibition of transcription of the IL-2 gene, as shown in ref. 34	141
Figure 5.1.3: A schematic of the inhibition of the production of NO by FK506/FKBP12, as found in cortical cultures.	143
Figure 5.1.4: The Structure and Activity of the FKBP12 ligands; FK506 and L-685,818,.	145
Figure 5.3.1.a) Particle size distribution of a 0.02% (w/w) solution of the PCL ₂₀ -b-PEO ₄₄ copolymer micelles.	165
Figure 5.3.1.b) Particle size distribution of a 0.1% (w/w) solution of the PCL ₂₀ -b-PEO ₄₄ copolymer micelles.	166
Figure 5.3.2.a) The I_3/I_1 ratio for pyrene in a solution of PCL ₁₄ -b-PEO ₄₄ copolymer micelles and a DMF/H ₂ O solvent mixture.	168
Figure 5.3.2. b) The semilogarithmic plot of the partition coefficient for pyrene in a solution of the PCL- <i>b</i> -PEO micelles and a range of H ₂ O/DMF solvent mixtures.	170
Figure 5.3.3. The <i>in vitro</i> biocompatibility of the PCL- <i>b</i> -PEO (14- <i>b</i> -44 and 20- <i>b</i> -44) micelles (0.02 to 1% w/v) as determined by the Alamar Blue survival assay. The results were confirmed by the Trypan Blue assay. Each data point represents the average of 3 independent experiments, from 6-8 wells.	172
Figure 5.3.4. The change in the relative emission intensity of: pyrene in the supernatant (■), and cells (○), at 390 nm, over a 24 hour period. PC 12 cells were exposed to PCL ₁₄ - <i>b</i> -PEO ₄₄ micelles containing pyrene and the change in the fluorescence intensity was measured at 4, 8 and 24 hour time points.	173
Figure 5.3.5. The degree of neurite-like outgrowth in PC 12 cells incubated with either NGF, FK506 r L-685,818, over a 48 hour period (n=3-4). The concentration of NGF incubated with the cells was C1 = 0.1, C2 = 0.5, C3 = 1, C3 = 5, C4 = 10, C5 = 50 ng/mL, the concentrations of FK506 or L-685,818 was C1 = 1, C2 = 5, C3 = 10, C4 = 100, C5 = 500 nM.	

The degree of differentiation in the control (absence of any treatment) is taken to be 100 % differentiation.

175

Figure 5.3.6. The effect of micelle-incorporated FK 506 and NGF (5 ng/mL) on the neurite-like outgrowth in PC 12 cells over a 48 hour period (n= 3-4). Control = PC 12 cells in the absence of any treatment. Bars 1-9 are PC 12 cells treated with the following: Bar 1 = 5 ng/mL NGF, Bar 2 = PCL₂₀-b-PEO₄₄ micelles, Bar 3= micelle-incorporated FK506 (1 nM), Bars 4-6 = FK506 (Bars 4,5,6 = 1, 10, 100 nM respectively) along with 5 ng/mL NGF; Bars 7-9 = micelle-incorporated FK506 (Bars 7,8,9 = 1, 10, 100 nM respectively) along with 5 ng/mL NGF.

177

Figure 5.3.7. The effect of micelle-incorporated L-685,818 and NGF (5 ng/mL) on the neurite-like outgrowth in PC 12 cells over a 48 hour period (n = 3-4). Control = PC 12 cells in the absence of any treatment. Bars 1-9 are PC 12 cells treated with the following: Bar 1 = 5 ng/mL NGF, Bar 2 = PCL₂₀-b-PEO₄₄ micelles, Bar 3 = micelle-incorporated L-685,818 (10 nM), Bars 4-6= L-685,818 (Bars 4, 5, 6 = 10, 100, 1000 nM respectively) along with 5 ng/mL NGF; Bars 7-9= micelle-incorporated L-685,818 (bars 7,8,9 = 10, 100, 1000 nM respectively) along with 5 ng/mL NGF.

178

Figure 6.1. The *in vitro* release profiles of ³H-FK506 alone and PCL₂₀-b-PEO₄₄ micelle incorporated-³H-FK506 as measured by the dialysis method.

191

Figure 6.2.a) The biodistribution in non-neural tissue (expressed in terms of % of total dose) of radiolabeled FK506, 6 and 24 hours following intravenous injection of PCL-b-PEO micelle incorporated FK506 into male Sprague Dawley rats (n=3-4).

193

Figure 6.2.b) The biodistribution in non-neural tissue (expressed in terms of % of total dose/g tissue) of radiolabeled FK506, 6 and 24 hours following intravenous injection of PCL-b-PEO micelle incorporated FK506 into male Sprague Dawley rats (n=3-4).

194

Figure 6.3.a) The distribution in neural tissue (expressed in terms of % of total dose) of radiolabeled FK506, 6 and 24 hours following intravenous injection of PCL-*b*-PEO micelle incorporated FK506 into male Sprague Dawley rats (n=3-4). (The abbreviations are as follows hypot.= hypothalamus; stria. = striatum; thal. = thalamus; hipp. = hippocampus; cort. = cortex; pit. = pituitary; r. of b. = rest of brain; cereb. = cerebellum).

195

Figure 6.3.b) The biodistribution in neural tissue (expressed in terms of % of total dose/g tissue) of radiolabeled FK506, 6 and 24 hours following intravenous injection of PCL-*b*-PEO micelle incorporated FK506 into male Sprague Dawley rats (n=3-4). (The abbreviations are as follows hypot.= hypothalamus; stria. = striatum; thal. = thalamus; hipp. = hippocampus; cort. = cortex; pit. = pituitary; r. of b. = rest of brain; cereb. = cerebellum).

196

Figure 6.4. The endurance time attained for each of the animal groups (Hanover Wistar rats, n=6 per experimental group) studied on the rotarod apparatus over a 20 day period. Treated animals received 5 mg/kg of the micelle-incorporated FK506 solution on days 0, 6 and 12 following the sciatic nerve crush.

198

Figure 7.1.1. The intracellular trafficking pathway of pino-and phagocytosis.

205

Figure 7.1.2. The Five Methods of Endocytosis: A schematic of the five methods of endocytosis (A = Phagocytosis, B = Macropinosome, C = Clathrin – Coated Vesicle, D = Non-Clathrin Coated Vesicle, E = Calveolae. The size of the vesicles formed by each mode are not drawn to scale (Adapted from Lamaze and Schmid, *Current Opinion in Cell Biology* 1995, 573-580.)

205

Figure 7.2.1.a) The temperature and pH dependence of the cellular internalization of PCL₂₀-*b*-PEO₄₄ micelle-incorporated ³H-FK506 in PC12 cell cultures. Each bar represents the mean of 4 samples ± S.D.

213

Figure 7.2.1.b) The temperature and pH dependence of the cellular internalization

of PCL₂₀-*b*-PEO₄₄ micelle-incorporated DiI in PC12 cell cultures. Each bar represents the mean of 4 samples \pm S.D. 214

Figure 7.2.2. The time dependence of the uptake of ³H-FK506 alone (■) and PCL₂₀-*b*-PEO₄₄ micelle-incorporated ³H-FK506 (●) in PC12 cell cultures over a four hour period. Each point represents the mean of 4 samples \pm S.D. 216

Figure 7.2.3. The effect of various pharmacological manipulations on the cellular internalization of PCL₂₀-*b*-PEO₄₄ micelle-incorporated ³H-FK506 in PC12 cell cultures. Each bar represents the mean of 4 samples \pm S.D. 217

Figure 8.1: The plot of the apparent partition coefficient for DHT (left axis) between the PCL₂₀-*b*-PEO₄₄ micelles and the external medium versus the amount of DHT added during micelle preparation. The amount of DHT loaded into the PCL₂₀-*b*-PEO₄₄ micelles (right axis) versus the amount of DHT added during micelle preparation. 230

Figure 8.2: The percentage of the weight of drug loaded to the total weight of micelle cores (left axis) versus the amount of drug added during micelle preparation. The plot of the number of molecules of DHT loaded per micelle (right axis) versus the amount of DHT added during micelle preparation. 233

Figure 8.3: The release of DHT alone, 8mM micelle-incorporated DHT, 40mM micelle-incorporated DHT over time. 235

Figure 8.4: The *in vitro* biocompatibility of PCL₂₀-*b*-PEO₄₄ micelles in HeLa cells for 24-72 hours as measured relative to the untreated control which is taken to be 100% survival. 236

Figure 8.5: The luciferase activity in HeLa cells cotransfected with MMTV-LUC and the androgen receptor and treated with either nothing (control), 100nM DHT alone, empty PCL₂₀-*b*-PEO₄₄ micelles or PCL₂₀-*b*-PEO₄₄ micelle-incorporated DHT 100nM. 237

List of Abbreviations

ADR	Adriamycin
BfA	Brefeldin A
BSA	Bovine serum albumin
CHT	Chymotrypsin
CMC	Critical micelle concentration
CNS	Central nervous system
CPP	1,3-bis(carboxyphenoxy)propane
CsA	Cyclosporin A
DHT	Dihydrotestosterone
DLS	Dynamic light scattering
DMEM	Dulbecco's modified eagle medium
DMF	Dimethylformamide
DMSO	Dimethyl sulfoxide
DNA	Deoxyribonucleic acid
DOG	2-Deoxyglucose
Dox	Doxorubicin
DRG	Dorsal root ganglia
EPR	Enhanced permeability and retention
EVA	Ethylene vinyl acetate
FKBP	FK506 binding protein
GA	Glycolic acid
GM-CSF	Granulocyte macrophage colony stimulating factor
GPC	Gel permeation chromatography
GR	Glucocorticoid receptor
GRE	Glucocorticoid response elements
HPMA	(2-hydroxypropyl)methacrylamide
HSP	Heat shock protein
IL	Interleukin
IMC	Indomethacin
LA	Lactic acid
LUC	Luciferase
MMTV	Mouse mammary tumor virus
MTT	3-(4,5-Dimethylthiazol-2-yl)-2,5-Diphenyltetrazolium Bromide
Nagg	Aggregation number
Naz	Sodium azide
NGF	Nerve growth factor
NF-AT	Nuclear factor of activate T cells
NMDA	N-methyl-D-aspartate
NMR	Nuclear magnetic resonance
NO	Nitric oxide
NOS	Nitric oxide synthase
oMMA	Oligo(methyl methacrylate)
PAAc	Poly(acrylic acid)
PBLA	Poly-benzyl-L-aspartate

PBS	Phosphate buffer saline
PBLA-<i>b</i>-PEO	Poly(β-benzyl L aspartate)-<i>b</i>-poly(ethylene oxide)
PCL-<i>b</i>-PEO	Polycaprolactone -<i>b</i>- poly(ethylene oxide)
PEG	Poly ethylene glycol
PEO	Poly (ethylene oxide)
PLA	Poly(lactic acid)
PLGA	Poly(lactic –co-glycolic acid)
PLL-<i>b</i>-PEG	Poly(L-lysine)-<i>b</i>-poly(ethylene glycol)
Poly (MePEGCA- co-HDCA)	Poly(methoxypolyethyleneglycol cyanoacrylate-co-hexadecyl cyanoacrylate)
PPO	Poly (propylene oxide)
PS	Polystyrene
Py	Pyrene
RES	Reticuloendothelial system
SA	Sebacic acid
SEC	Size exclusion chromatography
T_g	Glass transition temperature
THF	Tetrahydrofuran
T_m	Melting temperature
TMA	Trimellitylimido anhydride
Tyr	Tyrosine

Dedicated to
my incredible parents
Curt and Suzanne Allen
for their
continual support and encouragement

CHAPTER 1

GENERAL INTRODUCTION

The overall goal of this thesis is the development and characterization of a novel drug delivery vehicle for lipophilic agents. The delivery vehicle is formed from amphiphilic polycaprolactone-b-poly(ethylene oxide) copolymers which self-assemble to form aggregates containing a hydrophobic core that serves as cargo space for lipophilic drugs.

At the time that these studies began, research spanning decades had been carried out on the development of carriers to enhance the therapeutic efficacy of various drugs. However, the ultimate goal of drug delivery research has been to achieve site-specific delivery and since this dream has not yet been fully realized there is still much research to be done in this area. The introduction is divided into three sections, the first is a discussion of the role and relevance of drug delivery vehicles today, the second describes the delivery vehicles that have been based on copolymer materials while the third summarizes the overall scope of the thesis as well as a breakdown of the contents within each chapter.

1.1. The Role and Relevance of Drug Delivery Vehicles Today

The purpose of a drug delivery vehicle is to enable the full therapeutic potential of a drug to be maximally exploited while ensuring the safety of the patient [1-4]. Specifically, a drug delivery vehicle should fulfill some of the following roles: (1) provide controlled release so the drug is maintained at therapeutically relevant levels for a

prolonged period of time, (2) reduce drug induced systemic toxicity by targeting the drug to a specific site, (3) decrease the amount of drug needed to reach therapeutically effective levels by stabilizing the drug, optimizing its metabolism and/or preventing its rapid elimination, (4) overcoming the drugs transport limitations and the defense mechanisms of the multi-drug resistance phenotype.

Role 1 and 2 are of great significance since they can potentially lead to a reduction in health care costs while also providing a less invasive means of treating the patient. Most importantly the advantages which accompany the use of drug delivery vehicles must outweigh any potential risks. The drug delivery vehicle must be biologically inert meaning: stable, non-toxic, biocompatible and non-immunogenic. The vehicle and its components produced following biodegradation must not accumulate in the body, they require a specific means of elimination. The creation of the ideal drug delivery vehicle requires a firm understanding of both materials science and human physiology and pharmacology. In this way, the most successful design may require an interdisciplinary approach, bringing together members from the biomedical field and the field of materials science.

1.2. Delivery Vehicles Based on Copolymer Materials

Synthetic copolymer materials have been used as the essential building blocks of drug carriers in the form of polymer-drug conjugates [5-14], block copolymer micelles [15-37] and micro(nano)particles [38-66] (Figure 1.1). Copolymer materials are also commonly used in the surface modification of micro(nano)particles in order to produce sterically stabilized particles [62-64, 67]. The copolymer materials employed in these preparations afford a degree of versatility which is difficult to attain with other synthetic or natural homopolymers.

Copolymers are formed from two or more monomeric units which, following polymerization, are arranged in a specific manner depending on the type of copolymer desired. Random, block, graft or various other configurations are possible (Figure 1.2) [68]. The copolymer materials employed in the preparation of drug carriers are often block copolymers, which consist of a block or sequence of one repeat unit coupled to a


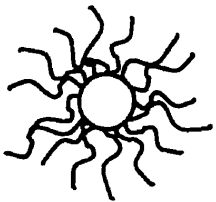

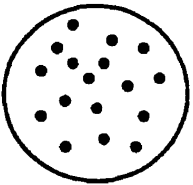
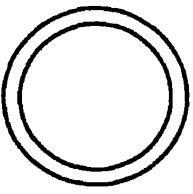
<u>Drug Carrier</u>		<u>Diameter</u>
Copolymer-Drug Conjugate		5 - 10 nm
Block Copolymer Micelle		10 - 100 nm
Microsponge		5 - 80 μm
Microsphere		0.1 - 2000 μm
Microcapsule		1 - 2000 μm

Figure 1.1: The basic architecture and size of copolymer drug carriers (*after* DONBROW, M., ed. Microcapsules and Nanoparticles in Medicine and Pharmacy, CRC Press, 1992.)

block of another repeat unit [68]. Microspheres are also commonly formed from random copolymers. The advantage to using block copolymers over random copolymer materials is the much narrower total molecular weight and sequence distributions for block copolymers [68, 69]. For some block copolymers, much better control may be exercised

Homopolymer	AAAAAAAAAAAAA
Random Copolymer	ABAAABABBABBBA
Block Copolymer	
Diblock	AAAAAABBBBBBBB
Triblock	AAAABBBBBBBAAAA
Graft Copolymer	AAAAAAAAAAAAA
B	B
B	B
B	B
B	B

Figure 1.2: A schematic of the different polymers which can be created depending on the number of types of repeat units; homopolymer (one type), copolymer (two or more types). Copolymers may be random, block or graft according to the arrangement of repeat units (for more details see [ref. 68]).

over the copolymer properties due to the ionic polymerization techniques used to synthesize the copolymer. For random copolymers, the condensation or free radical polymerization techniques employed can often only afford broad molecular weight distributions.

It is the presence of the second or third block, especially if one block is hydrophilic while the other is hydrophobic, that broadens the range of properties of the polymer which may be manipulated. The key properties of the copolymer are its block

composition, molecular weight, molecular weight distribution, and copolymer ratio. The versatility afforded by the use of block copolymers is largely due to the ease with which the key properties of the material can be controlled. The design of a vehicle for a particular drug requires a firm understanding of the properties of the copolymer which will enable a drug carrier with the desired characteristics to be created. Polymer-drug conjugates, block copolymer micelles and micro(nano)particles can be tailor-made to suit a particular application through careful manipulation of the properties of the copolymer materials from which they are formed.

1.2.1. Copolymer Properties Influencing Rational Design

1.2.1.1. *Polymer-drug Conjugates and Macromolecular Conjugates*

Polymer-drug conjugates and macromolecular conjugates are produced by the covalent binding of a water-soluble polymer to a drug or protein molecule, respectively [5-13]. The water-soluble polymers often used are copolymers such as N-(2-hydroxypropyl)methacrylamide (HPMA) containing oligopeptide side-chains [5-8], poly(styrene-co-maleic acid) [10], and poly(ethylene oxide-propylene oxide) [12,13].

Design of the copolymer drug conjugate requires that consideration be given to several parameters such as the molecular weight of the polymer [12], the nature of the covalent linkage between the drug and the copolymer [8-12], the number of drug molecules and targeting moieties linked to each polymer molecule and the placement of the individual polymer blocks within the polymer-drug conjugate [12].

The nature of the covalent linkage between the drug and the copolymer is of prime importance. The linkage should be stable within the bloodstream, but easily cleaved or hydrolyzed once the conjugate has reached the target site. The attachment of a copolymer molecule to the drug has been found to ensure that endocytosis is the mechanism of cellular uptake and, following cell entry, the polymer-drug conjugate ends up within the lysosomal compartment [11]. Thus, site-specific delivery is enhanced by the use of a covalent bond between the drug and the polymer which is hydrolyzable within the lysosomal compartment [11].

The use of the copolymer composed of N-(2-hydroxypropyl)methacrylamide and oligopeptide side-chains is especially attractive as the drug and targeting moieties can be

covalently linked to amino acids within the side-chains [5,8]. The amino acid sequence within the oligopeptide side-chain can vary, but is most often chosen to be a lysosomally degradable sequence [8]. The importance of a degradable linkage is clearly seen in work involving HPMA conjugates of the anti-cancer drug, adriamycin, where the use of a non-degradable linkage does not result in the visible presence (monitored by fluorescence) of any adriamycin within the nucleus following a 24 hour incubation period with HepG2 cells [5].

Jelinkova et al. found that the amino acid sequence of the oligopeptide side-chain can influence the degree of intracellular accumulation of anti-Thy 1.2-HPMA-DOX [8]. It was suggested that an increase in the hydrophobicity of the oligopeptide side-chain enhances cellular uptake. This has been seen by other groups also studying HPMA-drug conjugates [9].

The properties of macromolecular conjugates composed of protein molecules coupled to amphiphilic diblock copolymers such as poly(propylene oxide)-*b*-poly(ethylene oxide) can vary depending on which block the protein molecule is bound to [12]. Topchieva reported that protein conjugates with the hydrophilic block placed next to the protein (protein-PEO-PPO) were able to translocate through the cell while constructs with the hydrophobic block placed next to the protein (protein-PPO-PEO) were unable to accomplish membrane translocation [12]. In this same study, only the protein-PEO-PPO conjugates were able to translocate through the cell. The unmodified proteins (BSA, CHT, and cytochrome c) and their PEO conjugates were unable to translocate through the cell. This demonstrates the degree to which block copolymers with properly placed blocks are able to alter the properties of the protein. The thermal stability of the protein has also been found to be affected by the placement of the blocks within the block copolymer of the conjugate [13].

1.2.1.2. Block Copolymer Micelles

Block copolymer micelles are formed from synthetic amphiphilic di- or tri- block copolymers (Figure 1.3). In aqueous solution, the micellar aggregates consist of a hydrophobic core surrounded by a hydrophilic shell or corona [25, 35]. The core of the micelle acts as a microreservoir for the incorporation of hydrophobic drugs while the

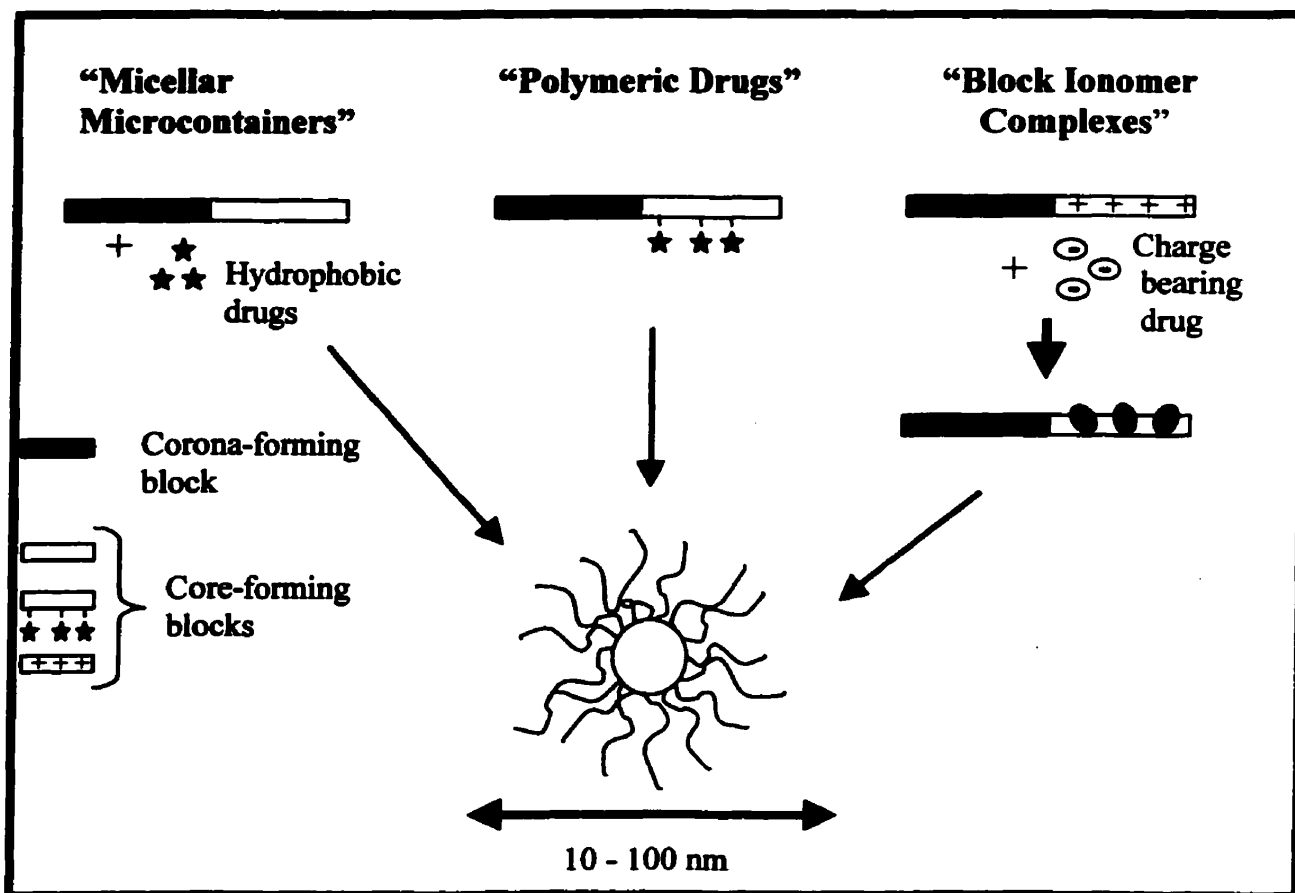


Figure 1.3: An illustration of the three categories of block copolymer micelles distinguished on the basis of the method of drug incorporation. "Micellar microcontainers" include physically entrapped drug, "polymeric drugs" are formed from copolymer-drug conjugates and "block ionomer complexes" contain charge bearing drugs or molecules which interact with the core-forming block via electrostatic interactions [35].

hydrophilic shell serves as an interface between the hydrophobic core of the micelle and the external environment. Block copolymer micelles may also be formed from diblocks which include a hydrophilic block and a charged block. In this case, the charged block interacts with a charge-bearing drug to form the neutral core-forming portion of the micelle [31, 34]. In almost all cases the hydrophilic shell – forming block has been poly(ethylene oxide) with a molecular weight which is usually between 1000 and 12 000 g/mole but has been up to 20 000 [27]. Also the length of the hydrophobic block is usually less than or equal to the length of the hydrophilic block [26]. Many polymers have been tried as the hydrophobic or charged core-forming block of the micelles (Table 1.1).

The nature and properties of the copolymer material which form the micelles largely determine its success as a drug carrier for various drugs. The material properties influence characteristics such as size, stability, loading capacity, release kinetics and more.

Size Block copolymer micelles are typically between 10-100 nm in diameter [35] (Table 1.2). The size of individual micelles is largely determined by the aggregation number (N_{agg}) which is the number of single chains that aggregate to form a micelle.

The hydrophilicity and hydrophobicity of the copolymer and its molecular weight are two factors which influence the aggregation number. Generally, it has been found that copolymers with longer hydrophobic blocks have higher aggregation numbers and those with longer hydrophilic blocks have lower aggregation numbers. It is also known that the aggregation number for diblock copolymers is larger than that of triblock copolymers of identical molecular weight and composition [70]. The 10-100 nm size range mentioned above is typical of single primary micelles; however, often secondary aggregates are present in solution [23,71]. The actual nature of these larger aggregates remains to be determined. Winnik's group suggested that secondary aggregates of PS-*b*-PEO may be either onion-like aggregates or clusters of individual single micelles [71]. Kataoka's group was in agreement with the latter suggestion to describe the secondary aggregates they encountered with PBLA-*b*-PEO micelles [23, 30].

Morphology In most cases the shape of the micelles has been spherical or near spherical. However, Eisenbergs group has recently developed methods for the

Block Copolymers	Drugs Incorporated
polycaprolactone - <i>b</i> - poly(ethylene oxide) [15,16]	Indomethacin [15] FK506 [16] L-685-818 [16]
poly(N-isopropylacrylamide) - <i>b</i> - poly(ethylene glycol) [17]	
poly(γ -benzyl-L-glutamate)- <i>b</i> -poly(ethylene oxide) [18]	clonazepam [18]
oligo(methyl methacrylate)- <i>b</i> -poly(acrylic acid) [19]	doxorubicin hydrochloride [19]
poly(aspartic acid)- <i>b</i> -poly(ethylene oxide) [20]	lysozyme [20] adriamycin [37] cisplatin [24]
poly(ethylene oxide)- <i>b</i> -poly(propylene oxide)- <i>b</i> -poly(ethylene oxide) (Pluronic TM) [36]	doxorubicin [36] cisplatin [36]
poly(D,L-lactide)- <i>b</i> -methoxy poly(ethylene glycol) [22]	paclitaxel [22] testosterone [29]
poly(β -benzyl L aspartate)- <i>b</i> -poly(α -hydroxy ethylene oxide) [26]	doxorubicin [26]
poly(β -benzyl L aspartate)- <i>b</i> -poly(ethylene oxide) [30]	doxorubicin [30] indomethacin [23]
poly(L-lysine)- <i>b</i> -poly(ethylene glycol) [31,34]	DNA [31,34]
polyspermine- <i>b</i> -poly(ethylene oxide) [35]	oligonucleotide [35]

Table 1.1: List of several of the block copolymer materials which have been used to form micellar delivery systems and the drugs which have been incorporated.

preparation of block copolymer aggregates of various morphologies [72-74]. The wide range of morphologies includes spheres, rods, vesicles, tubules, large compound micelles and many more [72-74].

Stability The stability of micelles is highly dependent on their critical micelle concentration, which is the minimum polymer concentration required for micelle formation (Table 1.2). The lower the value of the cmc the greater the thermodynamic stability of micelles in dilute solution. Once the micelles have been diluted to a point which is below the cmc, they will disassemble into single chains, if thermodynamics is operative. The elimination of copolymer materials will be facilitated by the eventual disassembly of the micelle into single chains and excretion by the kidney [35]. Elimination of single chains by this method requires that the molecular weight of the block copolymer be below the renal filtration limit [26]. Thus, the cmc of the micellar drug delivery vehicle should be adjusted so that it be high enough to allow the carrier to remain in the circulation for a certain period of time, but low enough to enable the eventual disassembly of the micellar vehicle.

The nature of the copolymer, the block ratio and molecular weight are all key determinants of the critical micelle concentration. It has been found that both the hydrophobic and hydrophilic blocks influence the cmc, with the influence of the hydrophobic block being much stronger [75]. For both diblock and triblock copolymer micelles it has been shown that an increase in the length of the hydrophobic segment will result in a decrease in the cmc [75,76]. Block copolymers of poly(ethylene oxide)-*b*-poly(propylene oxide)-*b*-poly(ethylene oxide) (PEO-PPO-PEO) with a constant PEO block length showed a decrease in their cmc value as the PPO block length was increased. In a similar study, the cmc was found to show a slight increase when the PEO block length of the PEO-*b*-PPO-*b*-PEO copolymers was increased while maintaining a constant PPO block length [76,77]. Also, when the PPO/PEO ratio is held constant, an increase in the molecular weight of the whole copolymer causes a decrease in the cmc [77].

It has been found that the cmc of triblock copolymers is typically higher than that of diblock copolymers with the same block copolymer molecular weight and composition [70]. The higher cmc found for triblock copolymers is said to be due to the energy

Properties of Micellar Delivery System	Block Copolymer	Values
Size (diameter)	PBLA- <i>b</i> -PEO [23, 30] PLA- <i>b</i> -PEO [29] PLA:PEO 1.5:2 PLA:PEO 2:5 PLL- <i>b</i> -PEO [31] PEO- <i>b</i> -PPO- <i>b</i> -PEO	1° micelles 19 nm [23, 30] 2° aggregates 115 nm [23] 19.8 nm [29] 25.3 nm [29] 1° complex (with DNA) 48.5 nm [31] 2° complex (with DNA) 140 nm [31] 14.6 nm [33, 36]
CMC	PBLA- <i>b</i> -PEO [23] PLA- <i>b</i> -PEO [29] PBLG- <i>b</i> -PEO [27] PBLG:PEO 1:1 PBLG:PEO 1:3 PEO- <i>b</i> -PPO- <i>b</i> -PEO [33]	18 µg/mL [23] 35 µg/mL [29] 1.5 µg/mL [27] 2.0 µg/mL [27] 0.03 % w/v [33]
Hydrophilic shell PEO molecular weight	PLA- <i>b</i> -PEO [29] PDLLA- <i>b</i> -PEO [28] PLA- <i>b</i> -PEO [29] PBLA- <i>b</i> -PEO [23]	2 000 [29] 2 000 [28] 5 000 [29] 12 000 [23]
Hydrophobic core drug loading capacity	PBLA- <i>b</i> -PEO [23] PBLA- <i>b</i> -PEO [30] Dox-PBLA- <i>b</i> -PEO [32] PLA- <i>b</i> -PEO [29] PLA:PEO 1.5:2 PLA:PEO 2:5 PLA:PEO 1.5:2 PLA:PEO 2:5 PBLG- <i>b</i> -PEO [27] PBLG:PEO 1:1 PBLG:PEO 1:3 PDLLA- <i>b</i> -PEO [28]	Indomethacin 20.4-22.1 % w/w [23] doxorubicin 12 % w/w [30] doxorubicin 16% w/w [32] testosterone .74 %w/w [29] testosterone .34 %w/w [29] sudan black B 63.9 %w/w [29] sudan black B 59 %w/w [29] clonazepam 48.2 (mol %) [27] clonazepam 24.7 (mol %) [27] paclitaxel 50 mg/mL [28]

Table 1.2: Several of the performance dependent parameters of block copolymer micelle delivery systems and a few examples of each.

contribution required to fold the middle hydrophobic block in order to keep the two hydrophilic end blocks out of the micelle core [70].

The rate of single chain exchange between micelles depends on the glass transition temperature of the core-forming block [23]. For a block such as polystyrene the rate of exchange would be very slow at room temperature since the core would be in a frozen glassy state [25,78,79].

Drug Loading Capacity

Drug incorporation into block copolymer micelles can proceed via physical entrapment, covalent conjugation or ionic interaction and, depending on the type of incorporation, the micelles may be referred to as micellar microcontainers, polymeric drugs or block ionomer complexes, respectively [35].

The degree of non-covalent incorporation or physical entrapment of a hydrophobic drug into a micelle is determined by the partition coefficient of the drug between the micellar core and the surrounding aqueous medium. Several studies have been performed involving the measurement of the partition coefficient of various compounds between micellar cores and an aqueous medium [80-82]. Overall, it has been found that the greatest degree of solubilization will be achieved when the environment within the micelle core is highly compatible with the solubilizate [83,84]. This highlights the importance of the compatibility between the hydrophobic core-forming block and the drug to be incorporated. It is the hydrophobic interaction between the hydrophobic block and the drug which enhances incorporation [28]. For this reason, an increase in the hydrophobic block content within the copolymer has been commonly found to increase incorporation [29]. Hurter and Hatton found that the partitioning of hydrophobic solubilizates into poly(ethylene oxide-*b*-propylene oxide) micelles increased with both an increase in the poly(propylene oxide) content of the copolymer and its molecular weight [85].

For micelles with hydrophobic cores, the incorporation efficiency is also increased as the hydrophobicity of the drug is increased. Hagan et al. compared the loading capacity of PLA-PEG (1.5:2) micelles for testosterone ($\log P = 3.35$) and Sudan Black ($\log P = 7.6$) which differ in their degree of hydrophobicity (measured by the $\log P$ value which is the octanol : water partition coefficient). They found that the amount of drug

incorporated (w/w) was greatest for the most hydrophobic compound, Sudan Black, 63.9%, while the amount for Testosterone was only 0.74% [29].

Covalent incorporation of hydrophobic drugs requires a covalent bond between the hydrophobic block of the copolymer and the drug to be incorporated. In this way, the core of the micelle is formed by the hydrophobic block-drug conjugate. In some cases incorporation of the hydrophobic drug has been both covalent and non-covalent. Yokoyama et al. found that the physical entrapment of adriamycin into poly(ethylene glycol)-*b*-poly(aspartic acid) with chemically conjugated adriamycin was most efficient for the micelles with the greatest amount of chemically conjugated adriamycin. Thus, in this case, physical entrapment is enhanced when the drug is also chemically conjugated to the core-forming block [21]. In these studies, poly(ethylene glycol)-*b*-poly(aspartic acid) micelles containing only the chemically conjugated drug were found to have no anti-tumor activity. This low activity of the chemically conjugated drug is most often found to be attributed to the slow release of the free drug from the block copolymer [21].

When a charged drug or molecule is to be incorporated into the micelle it is necessary to use a block copolymer with a hydrophilic block and a charged block of opposite charge with respect to the drug to be incorporated. Diblock copolymers with a poly(ethylene oxide) block and a polycationic block such as polyspermine, or poly(L-lysine) have been complexed with DNA to form polyion micellar aggregates [31,34,35]. For instance, diblock copolymer micelles formed from poly(ethylene oxide)-*b*-polyspermine have been shown to form complexes with DNA [35]. The polyspermine block is cationic and interacts with the negatively charged phosphate groups of the DNA, to form a hydrophobic complex. The core of the micelles include polyspermine, the core forming block, complexed to DNA and the poly(ethylene oxide) blocks form the hydrophilic shell at the surface of the micelles [35]. Kabanov et al. [35] studied the enzyme degradation of a 19-mer oligonucleotide when both free and when incorporated into micelles of poly(ethylene oxide)-*b*-polyspermine in serum at 37°C. The incorporation of the 19-mer into the block copolymer micelle was found to greatly increase its stability against enzymatic digestion. An increased stability of DNA to nuclease attack when incorporated in micellar aggregates was reported by Katayose et al. [31, 34] for salmon testes DNA or Col E1 plasmid DNA complexed within poly(ethylene

glycol)-*b*-poly(L-lysine) micelles. In this study it was found that the degree to which the DNA complexed within the block copolymer aggregates was protected from DNase I digestion depended on the length of the poly(L-lysine) core-forming block [34]. An increase in the length of the poly(L-lysine) block increased the extent to which the DNA was protected [34].

Release Kinetics The release profile of a physically entrapped drug from block copolymer micelles has been largely found to be a function of the strength of the interactions between the drug and the micelle core. Conditions which may somehow weaken the hydrophobic-hydrophobic interaction between the drug and the micelle core will accelerate the release rate. La et al. found the release of indomethacin (IMC) from poly(ethylene oxide)-poly(β -benzyl L-aspartate) micelles was greatly enhanced when the pH of the external medium was altered from 1.2 to 7.4 at 37°C [23]. At pH 1.2 the carboxylic acid groups (pKa of IMC is 4.5) are not ionized, but when the pH is increased to 7.4, these groups are ionized; this weakens the interaction between IMC and the poly(β -benzyl L-aspartate) core [23].

The rate of release is also controlled by the state of the micelle core, depending on whether it is solid or liquid like in nature [30]. The state of the core, as mentioned previously, is largely determined by the glass transition temperature of the core forming block.

1.2.1.3. Micro(nano)particles

Micro(nano)particles may be divided into two groups: microspheres and microcapsules [57,58,66]. Microspheres contain drug in solution or solid form dispersed within a polymer matrix while microcapsules contain concentrated drug within the core which is surrounded by a polymeric shell (Figure 1.4) [57,58].

Several different copolymers have been tried as materials to produce micro or nanoparticles (Table 1.3); of these, the most common has been poly(lactide-co-glycolide) [57,58]. Many groups have explored the way in which the key properties of the copolymer affect several of the carrier's performance dependant parameters, such as size, shape, polydispersity, surface properties, drug loading capacity, drug release profile and rate of biodegradation of the vehicle [44-50, 53-55, 61, 65].

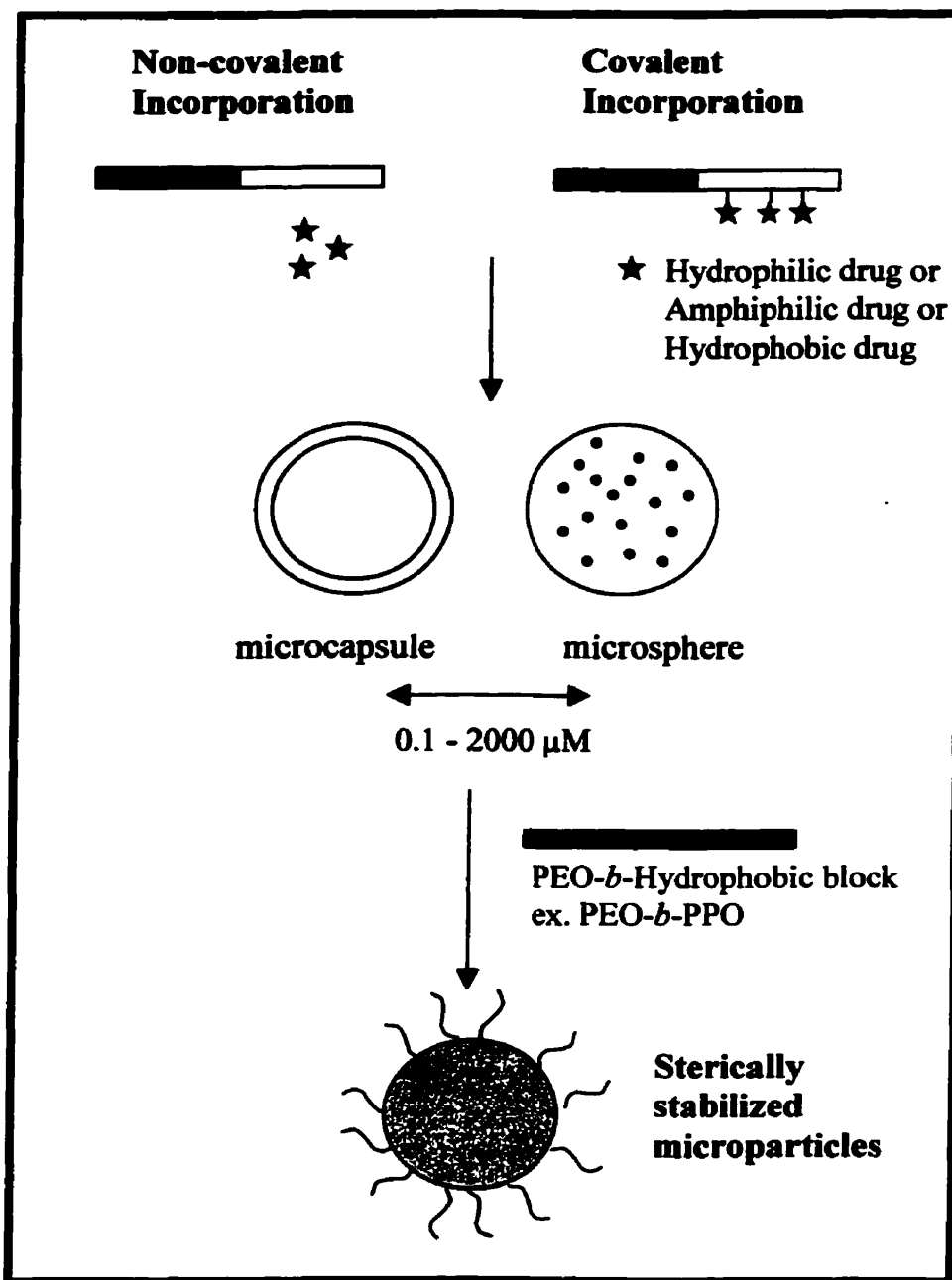


Figure 1.4: An illustration of the two main categories of microparticles, namely, microspheres and microcapsules. Also, an example, of surface modification of the microparticle, with a block copolymer containing a poly(ethylene oxide) block, to produce sterically stabilized particles.

Size, Morphology and Polydispersity

The size range of microparticles which have been produced is quite broad, ranging from approximately 0.1 μm to up to 2 mm [57]. The copolymer composition, copolymer ratio and molecular weight are primary determinants of the size of microparticles produced. Generally, an increase in the molecular weight of block copolymers with the same copolymer composition will result in an increase in the size of microparticles [53,65]. Wang et al. found the size of poly(lactic-co-glycolic acid) (PLGA) microspheres (LA/GA 75/25) increased from 27.6 μm to 38.7 μm when the molecular weight of the copolymer was increased from 5 000 to 20 000 [53]. A change in copolymer ratio while maintaining a constant molecular weight also affects the particle size, for instance PLGA microspheres with a 75/25 LA/GA ratio had a diameter of 30.1 μm , while microspheres with a 50/50 LA/GA ratio had a diameter of 43.2 μm [53].

To date, the microparticles produced have all been spherical or near-spherical in shape.

Surface Properties Several of the key surface properties for microspheres are charge, porosity and degree of hydrophilicity / hydrophobicity. Two of the determinants of surface porosity have been found to be the molecular weight of the copolymer and the copolymer ratio [53]. In a study involving PLGA microspheres the number of micropores was found to increase with both an increase in molecular weight and LA content [53]. The increase in the number of micropores with increased LA content was attributed to a difference in the rate of precipitation of LA compared to GA during the preparation of the microparticles: LA precipitates faster than GA.

The presence of poly(ethylene oxide) at the surface of microparticles provides a means of increasing surface hydrophilicity and produces a steric barrier which will inhibit interaction with various biological components. The PEO at the surface of the microparticles acts as a steric stabilizer providing a barrier which acts to discourage surface adhesion or interaction with various biological components. Proteins will often adsorb to the surface of a material within only the first few minutes of its exposure, especially if the material is charged or hydrophobic [86,88]. The binding of a protein to a surface is an energetically favorable process owing to the increase in entropy which accompanies adsorption. Protein adsorption can cause damage or lysis of the vehicle, inducing leakage of the drug entrapped within the carrier; this makes it near impossible to

predict the release profile of the drug from the carrier. Surface adsorption of opsonins will enhance RES clearance of the vehicle from the system preventing the carrier from fulfilling its role. The presence of long flexible polyethylene oxide chains at the surface of the vehicle will sterically stabilize the vehicle by creating entropic and osmotic forces which outweigh the protein - surface attractive forces such as van der Waals or hydrophobic interactions [87,88].

Microparticles which PEO present at their surface have been found to have an extended circulatory half-life and a reduced liver uptake when administered intravenously [65,67]. The increase in circulation time owing to the inhibition of RES uptake has been found to be largely dependant on the surface density of PEO chains [54, 62, 65].

There are two primary methods by which PEO may be introduced at the surface of microparticles; one involves using PEO containing materials to produce the microparticles and the other requires the surface modification of the microparticles with PEO containing conjugates (Table 1.4).

Surface modification of microparticles employs, poly(ethylene oxide) (PEO) conjugates, which are most commonly either triblock copolymers of polypropylene-*b*-poly(ethylene oxide)-*b*-polypropylene oxide (PPO-PEO-PPO) or diblock copolymers such as PPO-PEO. These conjugates are grafted to the surface of microspheres or adsorbed via hydrophobic interaction between the microsphere surface and the hydrophobic block(s) of the conjugate.

Many studies have revealed that the surface density of PEO is the factor which determines the degree to which the microparticles are sterically stabilized by surface modification. Flocculation tests are often used to study the stability of particles which have been surface modified by PEO-conjugates [38]. This type of study includes the measurement of the salt concentration or temperature required to induce flocculation of the particles. The greater the degree of steric stabilization of the particles the more they are resistant to the addition of a salt solution or to a temperature change. Flocculation tests were carried out by Coombes et al. [38] on PLG (poly-DL-lactide-co-glycolide) microparticles sterically stabilized by PEG-dextran conjugates containing various degrees of substitution of PEG within the conjugate. In this study the concentration of sodium chloride required to induce flocculation was found to be 0.01M, 1M, and 4M for PLG

Copolymer Materials	Drug Incorporated
poly(sebacic acid-co-1,3-bis(p-carboxyphenoxy)propane) [60]	-
poly(b-hydroxybutyrate-hydroxyvalerate) [45]	bovine serum albumin [45]
poly(lactide-co-glycolide) [46, 49]	phosphorylcholine [46] cisplatin [49]
poly(D,L-lactic-co-glycolic acid)- <i>b</i> -polyethylene glycol [61]	lidocaine [61] prednisolone [61]
poly(methyl methacrylate-acrylic acid) [47]	α -amylase [47]
poly(acrylamide-co-acrylic acid) [48]	-
poly(fumaric-co-sebacic anhydride) [50]	dicumarol [50]
poly(lactic acid)- <i>b</i> -polyethylene glycol- <i>b</i> -poly(lactic acid) [59]	bovine serum albumin [59]
poly(lactic acid)-co-poly(ethylene glycol) [62, 64]	tetanus toxoid [64]
poly(D,L-lactide-co-glycolide)- <i>b</i> -poly(ethylene glycol)- <i>b</i> -poly(D,L-lactide-co-glycolide) [51, 59]	BSA [59]
poly(sebacic acid)- <i>b</i> -polyethylene glycol [61]	lidocaine [61]
poly(vinyl alcohol)- <i>b</i> -polyethylene glycol [61]	lidocaine [61]
poly(ϵ -caprolactone)- <i>b</i> -polyethylene glycol [61]	lidocaine [61] prednisolone [61]
poly(D,L-lactide)-co-poly- ϵ -caprolactone [52]	17 beta estradiol [52] progesterone [52]

Table 1.3: List of several of the copolymer materials which have been used to form micro or nanoparticles and drugs which have been incorporated.

Method of Steric Stabilization of Microparticles		Comments
1. PEO containing copolymer used to form particles	<p>PLA-<i>b</i>-PEO [62, 65]</p> <p>Poly(MePEGC A-co-HDCA) [41]</p>	<p>-PLA-PEO particles circulate for several hours while PLA particles modified by surface adhesion of surfactants cleared by RES in minutes [62]</p> <p>-PLA-PEO particles were phagocytized 9 times less than particles made from PLA alone [65].</p> <p>-the cytotoxicity of the peglyated nanoparticles towards mouse peritoneal macrophages was reduced and the presence of PEO improved the degradability of poly(hexadecyl cyanoacrylate) [41]</p>
2. Surface adhesion of PEO-conjugate		
PEO mol.wt	2000 [62] 5000 [38] 12 000 [61]	
% substitution (e.g. PEO-Dextran)	1.2% -9% [38]	-conjugate with highest degree of PEO substitution was able to stabilize microparticles the most [38].
copolymer ratio	PEO _n - <i>b</i> -PPO _m - <i>b</i> -PEO _n - n = 98, m = 39 or m = 67 [40]	-the longer PPO block (m=67) prevented <i>in vitro</i> attachment to Kuppfer cells to a greater extent than copolymer with shorter PPO (m=39) [40]
diblock vs. triblock	PEO- <i>b</i> -PPO PEO- <i>b</i> -PPO- <i>b</i> -PEO [39]	-triblock able to stabilize particles more than diblock [39]

Table 1.4: The two primary methods employed for the steric stabilization of microparticles. The first method requires the use of block copolymers containing a PEO block, the second method involves surface modification of the microparticle with PEO containing conjugates.

microparticles which were not modified or surface modified with PEG-dextran conjugates containing 1.2 % or 9 % PEG, respectively. The surface adhesion of the PEG-dextran conjugate containing the highest substitution of PEG most likely produces particles with a higher surface density of PEG on the surface of the microparticles. Also, Coombes et al. [39] found that a 2M and 4M concentration of NaCl were needed to flocculate PLG microspheres which were surface modified with PEO-*b*-PPO (5:1) or PEO-*b*-PPO-*b*-PEO (70% PEO content) respectively. The greater degree of steric stabilization achieved by surface modification with the triblock is said to be due to the higher surface density of PEO which results through use of the triblock copolymer.

However, microparticles formed from biodegradable polymers (e.g. PLA, PLGA) which are surface modified by PEO containing surfactants have been found to be less resistant to RES uptake than microparticles formed from diblock copolymers containing PEO [62]. Microparticles formed from PLA-*b*-PEO were found to circulate for several hours in the bloodstream while PLA microparticles surface modified with a PEO containing copolymer were taken up by the RES within minutes [62]. The reduced stability of the microparticles modified by surface adhesion may be due to the desorption of the surface adsorbed copolymers *in vivo* [65]. For this reason it may be more favorable to limit surface modification of microparticles to chemical conjugation of PEO containing copolymers rather than surface adhesion [65]. However, this introduces another step into microparticle production which is otherwise unnecessary if block copolymers containing PEO are used as the materials to form the particles.

Drug Loading Capacity Microparticles are quite versatile in that they are able to act as carriers for drugs with a wide range of physico-chemical properties [57,58]. Microparticle carriers have been designed for hydrophobic, hydrophilic and charge-bearing drugs. There are two primary types of incorporation; non-covalent or physical entrapment and covalent incorporation. Non-covalent incorporation involves no covalent interaction between the drug and the copolymer material, while for covalent incorporation the drug is covalently linked to the copolymer [58].

The molecular weight of the copolymer as well as the copolymer ratio influence the loading capacity of the microparticle. However, there appears to be no trend that is

evident in terms of changes in the molecular weight of the copolymer or the copolymer composition and the effect on the loading capacity. Wang et al. found that for microparticles formed from poly(lactic-co-glycolic acid) with a copolymer ratio of 75/25 (LA/GA) and increasing the molecular weight from 5000 to 10000 or 20 000 the drug trapping efficiency of taxol was 84.4%, 95.5% and 82.7% respectively [53]. In the same study when the molecular weight of the copolymer was held at 10 000 and the copolymer ratio was 100/0, 75/25, 50/50 (LA/GA) the drug trapping efficiency was 28.6, 95.5, and 86.6% respectively [53]. In addition, Lecorre et al. found that PLGA microspheres with a constant copolymer ratio of 50:50 LA/GA and a molecular weight of 9000 or 12000 had approximately the same encapsulation efficiency for etidocaine; 96.4% and 95.4% respectively [55]. In the same study a large difference was seen for the trapping efficiency of local anaesthetics which have a more hydrophilic (mepivacaine, lidocaine) character versus those that are more hydrophobic (bupivacaine, etidocaine). The 9000 mol. wt. PLGA polymer with a 50:50 LA/GA had drug trapping efficiencies of 96.4 and 96% for etidocaine and bupivacaine while for mepivacaine and lidocaine the trapping efficiencies were only 19.6% and 54.8% respectively [55].

Drug Release Profile In many cases, the release of hydrophobic drugs from microparticles has been found to be strongly correlated with the rate of erosion of the matrix material [53,89]. For hydrophilic drugs the release has been found to be largely by simple diffusion and erosion of the matrix [53]. The rate of erosion is largely related to both the copolymer composition and molecular weight. An increase in the overall hydrophilicity of the copolymer will increase the rate of erosion and, in turn, increase the release rate. Thus, an increase in the copolymer ratio in favor of the most hydrophilic block, such as GA in the case of PLGA will increase the release rate of hydrophobic drugs [53]. This is clearly seen in a study by Chiba et al. on poly(TMA-Tyr:SA:CPP) microspheres where an increase in the length of either the TMA-Tyr or SA hydrophilic polymer blocks caused an increase in the release rate of BSA, while an increase in the length of the hydrophobic block CPP decreased the rate of release [44]. In this case they found that the protein release could be extended from a few days to a month by simply changing the block ratio of the copolymer [44].

Perrachia et al. recently produced nanoparticles from multiblock copolymers in which the block copolymers were composed of a hydrophobic block such as poly(ϵ -caprolactone), poly(L-lactic acid) or poly(sebacic acid) coupled to one block or multiblocks of polyethylene glycol (e.g. R-b-PEG, R-(PEG)₃; R= hydrophobic block) [61]. They found that while the drug is contained within the hydrophobic core of the nanoparticle, an increase in the PEG block length from 5000 to 20 000 decreased the release rate of the drug.

The molecular weight of the whole copolymer will also affect the release rate of the drug from the microparticle. During microparticle preparation, the copolymers with a higher molecular weight will precipitate at a faster rate, often resulting in an increased degree of surface porosity [53, 55]. The increased porosity at the surface of the microsphere will enhance the release of hydrophobic drug molecules which are present in the microsphere matrix as a "particulate dispersion" [53, 55]. However, the increased degree of porosity will not enhance the release of hydrophilic drugs, as they are present within the microsphere in a "molecular dispersion" [55].

Rate of Biodegradation The physical properties of polymers can largely determine their rate of biodegradation. The glass transition temperature (T_g) and the melting temperature (T_m), if it is crystalline, are two important parameters affecting a polymer's biodegradability [68]. Below its glass transition temperature, a polymer is glassy, above this temperature it is rubberlike and above its melting temperature (if it is crystalline) it becomes a viscous liquid [68]. The T_g and T_m values determine the permeability and chain mobility of the polymer at a specific temperature. The chain mobility and permeability will then, in turn, affect the rate of biodegradation by controlling water access to hydrolytically unstable bonds [90]. The T_g and T_m of a polymer are highly dependent on their molecular weight. Thus, the nature of the individual blocks in a copolymer, as well as their length will have a major effect on the biodegradation rate of the copolymer.

Biodegradation of PLGA requires hydrolysis of the ester linkages within the polymer backbone [56]. In a study performed on microspheres formed from several different PLGA copolymers of varying block ratios (LA/GA; 90:10, 80:20, 70:30, 50:50) the rate of biodegradation, monitored by measurement of the presence of degradation

products, was found to increase with increasing GA content. GA is the more hydrophilic block within the copolymer and thus it was expected to be the primary site for hydrolysis [56].

In summary, the properties of the copolymer clearly play a large role in determining the characteristics of the drug delivery vehicle created. However, the degree to which the material properties influence each of the three categories of drug carriers is quite different. In each case the size and stability of the carrier is highly dependent on material properties. Yet, with microspheres, their size and stability are often equally dependent on the techniques employed during preparation.

In terms of loading capacity, the maximum for polymer drug conjugates is mostly limited to the amount which may be loaded without precipitation [37]. For microspheres, the loading capacity varies with the copolymer properties, but in many cases the variation occurs in an unpredictable manner [53,55]. The loading capacity of micellar microcontainers or block copolymer micelles with physically entrapped drugs is determined by the compatibility between the drug and the core-forming block (table 1.2).

The degree to which the copolymer materials can be manipulated to design the most suitable drug carrier for a particular application is limited to our knowledge of material properties and their effect on several of the carrier's parameters. The development of drug carrier technology still requires more systematic studies on material properties and their impact on the drug carrier created.

1.2.2. Copolymer Colloidal Carriers: *Strengths/Weaknesses*

Polymer-drug conjugates, micelles and micro or nanoparticles formed from copolymers are each very distinct types of drug delivery systems. The design of each type of system has been spurred by the same overall goal of increasing the therapeutic potential of various drugs. However, each of these individual categories of drug carriers has its own strengths and weaknesses.

For instance, polymer-drug conjugates, micelles and micro or nanoparticles all increase the hydrodynamic volume of the incorporated drug relative to that of the free drug. This increased size enables passive targeting to tumor tissue. The passively targeted delivery of anti-cancer drugs to tumors is facilitated by the "enhanced

permeability and retention (EPR) effect" seen in tumor tissue [14]. The net result of the EPR effect is an increased accumulation of drug carrier within the tumor tissue. However, the size limitation or cut-off for tumor vascular permeability has been reported to be approximately 400 nm [91]. The polymer-drug conjugates and block copolymer micelles which have been designed are well below this limit [14,35].

The size range of polymer-drug conjugates (5-7 nm non-targeted, 10-15 nm targeted) [14] is not only ideal for accumulation within solid tumors but also facilitates the avoidance of RES uptake. The colloidal copolymer carriers such as micelles and microparticles must be strategically designed so to inhibit or delay RES uptake as a means of increasing their circulation time. The micelle systems which have been produced are quite favorable in terms of their avoidance of RES uptake owing to both their small size (10-100 nm) and their PEO coat [25, 30, 35]. Yet owing to the large size of some microparticles their circulation time can be quite short. However, surface modification with PEO-conjugates, has, in some cases, greatly enhanced the circulation time of microparticles [61, 67].

The covalent bond within a polymer-drug conjugate can prove to be both advantageous and disadvantageous. In the past, a common problem which plagued this type of system was the release of the drug within the bloodstream owing to premature hydrolysis of the covalent bond [11]. Most of the newly designed systems contain covalent linkages which are only hydrolysed within the lysosomal compartment of the cell [11]. This enables selective release of the drug within the cell rather than within the bloodstream. Unfortunately, the covalent linkage can also prevent or inhibit the drug's activity [92]. Overall, the properties of the covalent linkage must be optimized so to prevent both premature hydrolysis in the bloodstream and loss of activity at the target site. This problem is not only known to polymer-drug conjugates but also to colloidal carriers wherein the drug is coupled to the copolymer. In some cases, chemical conjugation of the drug has had no or little *in vivo* activity relative to the drug which is physically entrapped within the delivery system [21, 35].

The type of drugs each delivery system can carry as well as their loading capacities are also different. The loading capacity of polymer-drug conjugates for hydrophobic drugs is limited by the eventual precipitation of the system [37]. However,

colloidal carriers can often be loaded with notable quantities of hydrophobic solubilize. The ability of the colloidal carriers to create a microenvironment which masks or protects the drug is also noteworthy.

1.3. Scope of the Thesis

This dissertation is devoted to the preparation, physico-chemical characterization and biological study of block copolymer micelles as drug delivery vehicles. The different types of block copolymer micellar delivery vehicles as well as a brief review of the literature in this area has been provided in section 1.2.1.2 of this Chapter.

In Chapter 2, we outline many of the properties of micelles which determine their ability to deliver various drugs, and also address the factors which influence or control each of these individual properties. The discussion draws from both the literature on block copolymer micelles which is related to drug delivery and that which is more general and unrelated to that topic. In this way, we hope to bring together information which will allow for block copolymer micelles to be tailor-made as carriers for the effective delivery of specific drugs.

In Chapter 3, we describe our first study of the partitioning of the model hydrophobic solubilize, pyrene, between block copolymer micelles and the external medium. The micelle system studied is formed from polystyrene-*b*-polyacrylic acid (PS-*b*-PAA) crew-cut copolymers. The PS-*b*-PAA copolymer system is not completely representative of the biocompatible, biodegradable copolymer systems commonly used for drug delivery. However, this study sets the stage for further investigations into the partitioning of pyrene and other hydrophobic solubilizes between micelles and the external medium.

In Chapter 4, we report on a novel method of synthesis of a biocompatible and biodegradable copolymer system formed from poly(caprolactone)-*b*-poly(ethylene oxide) (PCL-*b*-PEO). The characterization of the copolymers as well as the physico-chemical characterization of the copolymer aggregates are also described. Special attention is given to properties of the micelles which are of most interest in terms of their applications in drug delivery.

In Chapter 5, we report on our initial *in vitro* studies which explore the potential of the PCL-*b*-PEO copolymer micelles as drug delivery vehicles. FK506 and its structural analogue L-685,818 were the first biologically active model compounds that we chose for our study of the PCL-*b*-PEO micelles as drug carriers. The neurotrophic drugs FK506 and L-685,818 were incorporated into the PCL-*b*-PEO micelles and the *in vitro* delivery was assayed by monitoring the degree of differentiation achieved in cultures of PC 12 rat pheochromocytoma cells.

In Chapter 6, we report on the *in vitro* release kinetics of FK506 from the PCL-*b*-PEO copolymer micelles as well as the *in vivo* biodistribution of the micelle-incorporated drug, 6 and 24 hours following intravenous injection into male Sprague Dawley rats. Also, the extent to which the micelle-incorporated FK506 is able to enhance functional recovery in rats whose sciatic nerves have been lesioned is assessed using a behavioral study.

In Chapter 7, we address the question of whether or not the PCL-*b*-PEO micelles are internalized into PC12 cells by an endocytotic mechanism. Various pharmacological manipulations are employed in order to study the cellular internalization of the copolymer micelles.

In Chapter 8, we report on the physico-chemical characterization and *in vitro* study of PCL₂₀-*b*-PEO₄₄ micelles as a delivery vehicle for dihydrotestosterone. The biological activity and *in vitro* delivery of the micelle-incorporated DHT is evaluated in HeLa cells which have been cotransfected the MMTV-LUC reporter gene and the androgen receptor.

Finally, Chapter 9 includes a discussion of conclusions, contributions to original knowledge and suggestions for future work.

1.4. References

1. Gregoriadis G. *TIBS*. **1995**, 13, 527,.
2. (a) Langer R. *Annals of Biomedical Engineering* **1995**, 23, 101; (b) Langer R. *Science* **1990**, 249, 1527; (c) Langer R. *Nature* **1998**, 392 suppl. 30, 5.
3. Jain K. *TiPS* **1998**, 19, 155.
4. Duncan R. *Journal of Drug Targeting* **1997**, 5, 1.
5. Omelyanenko V., Kopeckova P., Gentry C., Kopecek J. *J. Control. Release* **1998**, 53, 25.
6. Duncan R., Vasey P.A., Kaye S.B., Cassidy J.- The CRC Experience. EORTC Early Drug Development Meeting 1995, June 21-24, **1995**, Corfu, Greece, p.60.
7. Stastny M., Ulbrich K., Strohalm J., Rossmann P., Rihova B. *Transplantation* **1997**, 63, 1818.
8. Jelinkova M., Strohalm J., Plocova D., Subr V., St'astny M., Ulbrich K., Rihova B. *J. Control. Release* **1998**, 52, 253.
9. Duncan R., Seymour L.W. O'Harre K.B., Flanagan P.A., Wedge S., Hume I.C., Ulbrich K., Strohalm J., Subr. B., Spreafico F., Grandi M., Ripamonti M., Farao M., Suaroto. *J. Control. Release* **1992** 19, 331,.
10. Maeda H., Matsumoto T., Konno T., Iwai K., Ueda M. *J. Protein Chem.* **1984**, 3, 181.
11. Putnam D., Kopecek J. *Bioconjugate Chem.* **1995** 6, 483.
12. Topchieva I.N., *ACS Symposium Series* **1997**, 680, 193.
13. Topchieva I.N., Efremova N.V., Khvorov N.V., Magretova N.N. *Bioconjugate Chem*, **1995**, 6, 380.
14. Omelyanenko V., Gentry C., Kopeckova P., Kopecek J. *Int. J. Cancer*. **1998**, 75, 600.
15. Yeon Kim S., Gyun Shin, I.L., Moo Lee, Y. *J. Control. Release* **1998**, 51, 13.
16. Allen C., Yu Y., Maysinger D., Eisenberg A. *Bioconjugate Chem.* **1998**, 9, 564.
17. Chung J.E., Yokoyama M., Aoyagi T., Sakurai Y., Okano T. *J. Control. Release* **1998**, 53, 119.
18. Jeong, Y.I., Cheon J.B., Kim S.H., Nah J.W., Lee Y.M., Sung Y.K., Akaike T., Cho C.S. *J. Control. Release* **1998**, 51, 169.
19. Inoue T., Chen G.H., Nakamae K., Hoffman A.S. *J. Control. Release* **1998**, 51, 221.
20. Harada A., Kataoka K. *Macromolecules* **1998**, 31, 288.

21. Yokoyama M., Fukushima S., Uehara R., Okamoto K., Kataoka K., Sakurai Y., Okano T. *J. Control. Release* **1998**, 50, 79.
22. Ramaswamy, M., Zhang X., Burt H.M., Wasan K.M. *J. Pharm. Sci.* **1997**, 86, 460.
23. La S.B., Okano T., Kataoka K. *J. Pharm. Sci.* **1996**, 85, 85.
24. Yokoyama M., Okano T., Sakurai Y., Suwa S., Kataoka K. *J. Control. Release* **1996** 39, 351.
25. Kwon G.S., Okano T. *Adv. Drug Deliv. Rev.*, **1996**, 21, 107.
26. Cammas S., Matsumoto T., Okano T., Sakurai Y., Kataoka K. *Mat. Sci. and Eng.* **1997**, C4, 241.
27. Nah, J.W., Jeong Y.I., Cho C.S. *J. Polym. Sci.: Part B: Polym. Phys.*, **1998**, 36, 415.
28. Zhang X., Burt H.M., Von Hoff D., Dexter D., Mangold G., Degen D., Oktaba A.M., Hunter W.L. *Cancer Chemother. Pharmacol.*, **1997**, 40, 81.
29. Hagan S.A., Coombes A.G.A., Garnett M.C., Dunn S.E., Davies M.C., Illum L., Davis S.S. *Langmuir* **1996**, 12, 2153.
30. Kwon G., Naito M., Yokoyama M., Okano T., Sakurai Y., Kataoka K. *J. Control. Release* **1997**, 48, 195.
31. Katayose S., Kataoka K. *Bioconjugate Chem.* **1997**, 8, 702.
32. Yokoyama M., Okano T., Kataoka K. *J. Controlled Rel.* **1994**, 32, 269.
33. Miller D.W., Batrakova E.V., Waltner T.O., Alakhov V.Y., Kabanov A.V. *Bioconjugate Chem.* **1997**, 8, 649.
34. Katayose S., Kataoka K. *J. Pharm. Sci.* **1998**, 87, 160.
35. Kabanov A.V., Alakhov V.Y. " Micelles of Amphiphilic Block Copolymers as Vehicles for Drug Delivery " In *Amphiphilic Block Copolymers: Self-Assembly and Applications* edited by Alexamdris P., Lindman B., Elsevier, Netherlands, 1998.
36. Alakhov V.Y., Moskaleva E.Y., Batrakova E.V., Kabanov A.V. *Bioconjugate Chem.* **1996**, 7, 209.
37. Yokoyama, M., Miyauchi M., Yamada N., Okano T., Sakurai Y., Kataoka K. *Cancer Res.*, **1990**, 50, 1693.
38. Coombes A.G.A., Tasker S., Lindblad M., Holmgren J., Hoste K., Toncheva V., Schacht E., Davies M.C., Illum L., Davis S.S. *Biomaterials.* **1997**, 18, 1153.

39. Coombes A.G.A., Scholes P.D., Davies M.C., Illum L., Davis S.S. *Biomaterials* **1994**, 15, 673.
40. Harper, G.R., Davis S.S., Davies M.C., Norman M.E., Tadros T.F., Taylor D.C., Irving M.P., Waters J.A., Watts J.F. *Biomaterials*, **1995**, 16, 427.
41. Peracchia M.T., Vauthier C., Desmaele D., Gulik A., Dedieu J.C., Demoy M., Dangelo J., Couvreur P. *Pharm Res.* **1998**, 15, 550.
42. Burt H.M., Jackson J.K., Bains S.K., Liggins R.T., Oktaba A.M., Arsenault A.L., Hunter W.L. *Cancer Letters* **1995**, 88, 73.
43. Yoshikawa H., Seebach S. *Biological and Pharmaceutical Bulletin.* 1996, 19, 1527.
44. Chiba, M., Hanes, J., Langer R. *Biomaterials*, **1997**, 18, 893.
45. Atkins, T.W., Peacock, S.J. *J. Biomat. Sci. -Polym. Ed.* **1995**, 7, 1065..
46. Allaoui-Attarki, K., Fattla E., Pecquet S., Trolle S., Chachaty, E., Couvreur P., Andremont, A. *Vaccine* **1998**, 16, 685.
47. Aksoy, S., Tümtürk H., Hasirci, N. *J. Biotech.* **1998**, 60, 37.
48. Nagashima, S., Ando, S., Makino, K., Tsukamoto T., Ohshima, H. *J. Colloid and Interface Sci.* **1998**, 197, 377.
49. Takahata H., Lavelle E.C., Coombes A.G.A., Davis S.S. *J. Control. Release* **1998**, 50, 237.
50. Chickering III, D.E., Jacob J.S., Desai T.A., Harrison M., Harris W.P., Morrell, C.N., Chaturvedi, P., Mathiowitz, E. *J. Control. Release* **1997**, 48, 35.
51. Itoi K., Tabata C.Y., Ike O., Shimizu Y., Kuwabara M., Kyo M., Hyon S.H., Ikada Y. *J. Control. Release* **1996**, 42, 175.
52. Nowak M., Buntner B., Bero M., Gorski J., Kajdaniuk D., Glogowska-Szelag J., Plewka A. *Acta Pharmaceutica Hungarica* **1996**, 66, 153.
53. Wang Y.M., Sato H., Horikoshi I. *J. Control. Release* **1997**, 49, 157.
54. Harper G.R., Davis S.S., Davies M.C., Norman M.E., Tadros T.F., Taylor D.C., Irving M.P., Waters J.A., Watts J.F., *Biomaterials* **1995**, 16, 427.
55. Le Corre P., Rytting J.H., Gajan V., Chevanne F., Le Verge R. *J. Microencapsulation*, **1997**, 14, 243.
56. Park. T. G. *Biomaterials* **1995**, 16, 1123.

57. Donbrow, M., ed. *Microcapsules and Nanoparticles in Medicine and Pharmacy*, CRC Press, 1992.
- 58.(a) Chen Y., Burton M.A., Gray B.N., *Pharmaceutical and Methodological Aspects of Microparticles*. (b) Willmott N., *Agents for Microsphere Incorporation: Physicochemical Considerations and Physiological Consequences of Particle Embolization*. In *Microspheres and regional cancer therapy*. Edited by Willmott N., Daly J.M., Boca Raton: CRC Press, 1994.
59. Li, X.Y., Volland C., Kissel L. *J. Control. Release* **1995**, 32, 121.
60. Gao J., Niklason L., Zhao X.M., Langer R. *J. Pharm. Sc.* **1998**, 87, 246.
61. Peracchia M.T., Gref R., Minamitake Y., Domb A., Lotan N., Langer R. *J. Control. Release* **1997**, 46, 223.
62. Vittaz, M., Bazile, D., Splenhauer, G., Verrechia, T., Veillard, M., Puisieux, F., Labarre, D. *Biomaterials* **1996**, 17, 1575.
63. Tan J.S., Butterfield, D.E., Voycheck, C.L., Caldwell, K.D., Li, J.T. *Biomaterials* **1993**, 14, 823.
64. Tobio, M., Gref, R., Sanchez, A., Langer, R., Alonso, M.J. *Pharm. Res.* **1998**, 15, 270.
65. Gref R., Domb A., Quellec P., Blunk T., Muller R.H., Verbavatz J.M., Langer R. *Adv. Drug Deliv. Rev.* **1995**, 16, 215.
66. Maysinger D., Morinville A. *TIBTECH.* **1997**, 15, 410.
67. Torchilin V.P. *J. Microencapsulation* **1998**, 15, 1.
68. Cowie J.M.G., *Polymers: Chemistry and Physics of Modern Materials* 2nd Ed., Blackie Academic and Professional, New York, 1994.
69. Wilczek-Vera G., Danis Paul O., Eisenberg A. *Macromolecules* **1996**, 29, 4036.
70. Nagarajan R., Ganesh K. *J. Colloid and Interface Sci.* **1996** 184, 489.
71. Xu R., Winnik M.A., Hallett F.R., Riess G., Croucher M.D. *Macromolecules* **1991**, 24, 87.
72. (a)Zhang L. Eisenberg A. *Science* **1995**, 268, 1728: (b) Zhang L, Yu K., Eisenberg A. *Science* **1996**, 272, 1777.
73. Yu K., Zhang L., Eisenberg A. *Langmuir* **1996**, 12, 5980.
74. Zhang L., Bartels C., Yu Y., Shen H., Eisenberg A. *Phys. Rev. Lett.* **1997**, 79, 5034.

75. Kwon G., Naito M., Yokoyama M., Okano T., Sakurai Y., Kataoka K. *Langmuir* **1993**, 9, 945.
76. Alexandridis P., Athanassiou V., Fukuda S., Hatton T.A. *Langmuir* **1994**, 10, 2604.
77. Alexandridis P., Holzwarth J.F., Hatton T.A. *Macromolecules* **1994**, 27, 2414.
78. Prochaska K., Kiserow D., Ramireddy C., Tuzar Z., Munk. P., Webber S.E.-
Macromolecules **1992**, 25, 454.
79. Kiserow D., Prochaska K., Ramireddy C., Tuzar Z., Munk. P., Webber S.E.
Macromolecules **1992**, 25, 461.
80. Wilhelm, M.; Zhao, C.-L.; Wang, Y.; Xu, R.; Winnik, M.A.; Mura, J.-L.; Riess, G.;
Croucher, M.D. *Macromolecules* **1991**, 24, 1033.
81. Kabanov, A.V, Nazarova, I.R., Astafieva I.R., Batrakova E.V., Alakhov V.Y.,
Yarostavov A.A., Kabanov V.A. *Macromolecules* **1995**, 28, 2303.
82. Zhao, J., Allen, C., Eisenberg, A. *Macromolecules* **1997**, 30, 7143.
83. Nagarajan, R.; Barry, M.; Ruckenstein, E. *Langmuir*, **1986**, 2, 210.
84. Tian, M.; Arca, E.; Tuzar, Z.; Stephen, E.; Webber, S.E.; Munk, P. *J. Polym. Sci.:
Part B: Polym. Phys.* **1995**, 33, 1713.
85. Hurter, P.A.; Hatton, T.A. *Langmuir* **1992**, 8, 1291.
86. Muller R.H., Colloidal Carriers for Controlled Drug Delivery and Targeting:
Modification, Characterization and *In vivo* Distribution, CRC Press Inc., Florida,
1991.
87. Lee J.H., Lee H.B., Andrade J.D. *Prog. Polym. Sci.* **1995**, 20, 1043.
88. Elbert D. L. Hubbell J.A. *Annu. Rev. of Mater. Sci.* **1996**, 26, 365.
89. Heller. J. *Biomaterials* **1980**, 1, 51.
90. Ottenbrite R.M., Fadeeva N., "Polymer Systems for Biomedical Applications an
Overview" In Polymeric Drugs and Drug Administration edited by Ottenbrite R.M.,
American Chemical Society, Washington D.C., 1994, pp. 1-14.
91. Yuan F., Dellian M., Fukurama D., Leunig M., Berk D.A., Torchilin V.P., Jain R.K.,
Cancer Res. **1995**, 55, 3752.
92. Kaneda Y., Yamamoto Y., Kamada H., Tsunoda S., Tsutsumi Y., Hirano T., Mayumi
T., *Cancer Res.* **1998**, 58, 290.

CHAPTER 2

NANO-ENGINEERING BLOCK COPOLYMER MICELLES FOR DRUG DELIVERY

2.1. Introduction

Micelles formed from amphiphilic di or tri block copolymers have been explored in recent years as carriers for hydrophobic drugs [1-32]. In an aqueous environment, the hydrophobic blocks of the copolymer form the core of the micelle while the hydrophilic blocks form the corona or outer shell. The hydrophobic micelle core serves as a microenvironment for the incorporation of lipophilic drugs, while the corona shell serves as a stabilizing interface between the hydrophobic core and the external medium.

To date, the greatest contributions in this area have been made by the groups of Kabanov [1-8] and Kataoka [9-21]. Kabanov's work initially focused mostly on micelles formed from Pluronic™ triblock copolymers as delivery vehicles for drug targeting across the blood brain barrier [1, 2]. The Kabanov group was the first to demonstrate that Pluronic™ unimers inhibit the P-gp-mediated drug efflux system in both bovine brain microvessel endothelial cells and Caco-2 monolayers [3, 4, 5]. In recent years, his research has also expanded to include block ionomer complexes as carriers for DNA [6, 7]. The work of Kataoka's group has largely focused on micelles formed from copolymers containing a poly(amino acid) core-forming block, as delivery vehicles for anti-cancer drugs [9-13]. However, his research has also centered on the use of "polyion complex micelles" as carriers for charged molecules such as DNA or enzymes [14, 15]. Recently, the groups of Kataoka and Okano have developed thermo-responsive micelles from poly(N-isopropylacrylamide)-*b*-poly(styrene) copolymers [16].

Several other groups have also done research in this area [23-32]. Such a high level of activity has brought a great deal of diversity to this field, since most groups have introduced their own micelle system formed from copolymers which contain a unique hydrophilic-hydrophobic block combination. In almost all cases, the hydrophilic block has been poly(ethylene oxide) for reasons which will be discussed in section 2.2. By contrast to the universal use of poly(ethylene oxide) as the hydrophilic block, a much wider range of hydrophobic blocks have been explored (Table 2.1). Thus the uniqueness associated with the different copolymer systems largely

Biocompatible Core-Forming Polymers	Refs.
poly(aspartic acid)	9, 15
poly(β -benzyl L aspartate)	13, 17
polycaprolactone	25, 32
poly(γ -benzyl-L-glutamate)	27
poly(D,L-lactide)	24, 30
poly(L-lysine)	14
poly(propylene oxide)	1, 4
polyspermine	7
oligo(methyl methacrylate)	26

Table 2.1. A list of several of the biocompatible polymers that have been employed as core-forming blocks.

originates from the choice of the hydrophobic block. The various PEO-hydrophobic block combinations have given rise to a number of micelle systems which have distinct physico-chemical properties and different characteristics important to their suitability as drug carriers. Also, micelles containing a specific hydrophobic block have been found to be more effective as carriers of some specific drug rather than other drugs. Unfortunately, the synthesis and manipulation of many of the biocompatible block copolymers is difficult. For this reason, few systematic studies have been performed whereby one parameter (e.g. core block length) is varied and the effect of this variation on the micelle's characteristics such as size, stability, loading capacity and release kinetics, is measured. Also, due to the fact that there are such a large number of variables which influence micelle properties, it may be unrealistic for groups in the area of drug delivery to explore all of the relevant parameters in a systematic way. However, the PPO-PEO based block copolymers are available commercially, and for this reason many studies have been done on this system.

In studies completely unrelated to drug delivery, a number of groups have investigated many of the physico-chemical parameters of block copolymers micelles in a very systematic way [33-56]. Several reviews have resulted from this work [57-61]. These studies involve micelles which are most often formed from non-biocompatible copolymers, yet the information obtained may be used to gain insight into the biocompatible systems.

The aim of this review is twofold; first we aim to outline many of the properties of micelles which determine their ability to deliver various drugs, and second, we address the factors which influence or control each of these individual properties. Several of the key performance related properties are loading capacity, release kinetics, circulation time, biodistribution, size, size population distribution and stability, all of which are discussed in this review. In addition, the last section is dedicated to the discussion of the morphology of block copolymer aggregates as another potential performance related parameter. The morphology of the block copolymer aggregates, in so far as it affects drug delivery, has not been addressed to date, primarily because it was not possible to prepare reproducibly a wide range of morphologies. This has now become possible, and section 2.5. discusses the preparation and potential relevance of block copolymer aggregates of different morphologies in drug delivery [61].

The method and extent to which each of the micelle parameters can be manipulated has been described most systematically and thoroughly in literature which is unrelated to drug delivery. For this reason, this review draws from both the literature on block copolymer micelles which is related to drug delivery and that which is more general and unrelated to that topic. In this way, we hope to bring together information which will allow for block copolymer micelles to be tailor-made as carriers for the effective delivery of specific drugs.

The review is divided into five major sections, the first of which is the introduction (2.1.). The second section (2.2.) covers performance related properties of the micelle as a whole, including methods of preparation, stability, as well as size and size population distributions of the micelles. The third (2.3.) and fourth (2.4.) sections deal with the two principal working parts of the micelle, the corona which acts as the

stabilizing interface between the core and the external medium and the micelle core which act as the cargo space for lipophilic drugs. More specifically, in section three, aspects related to the micelle corona are discussed; these include the use of poly(ethylene oxide) as the corona forming block, the use of hydrophilic polymer blocks other than PEO and the concept of steric stabilization. In section 2.4, the two core-related parameters, loading capacity and release kinetics, are discussed in detail with special emphasis placed on factors which may be used to alter both of these parameters. In section 2.5, we discuss the relevance of block copolymer aggregates of different morphologies in drug delivery and the various methods by which aggregates with these morphologies can be prepared.

2.2 The Micelle as a Whole

2.2.1. Methods of Micelle Preparation There are two principal methods for the

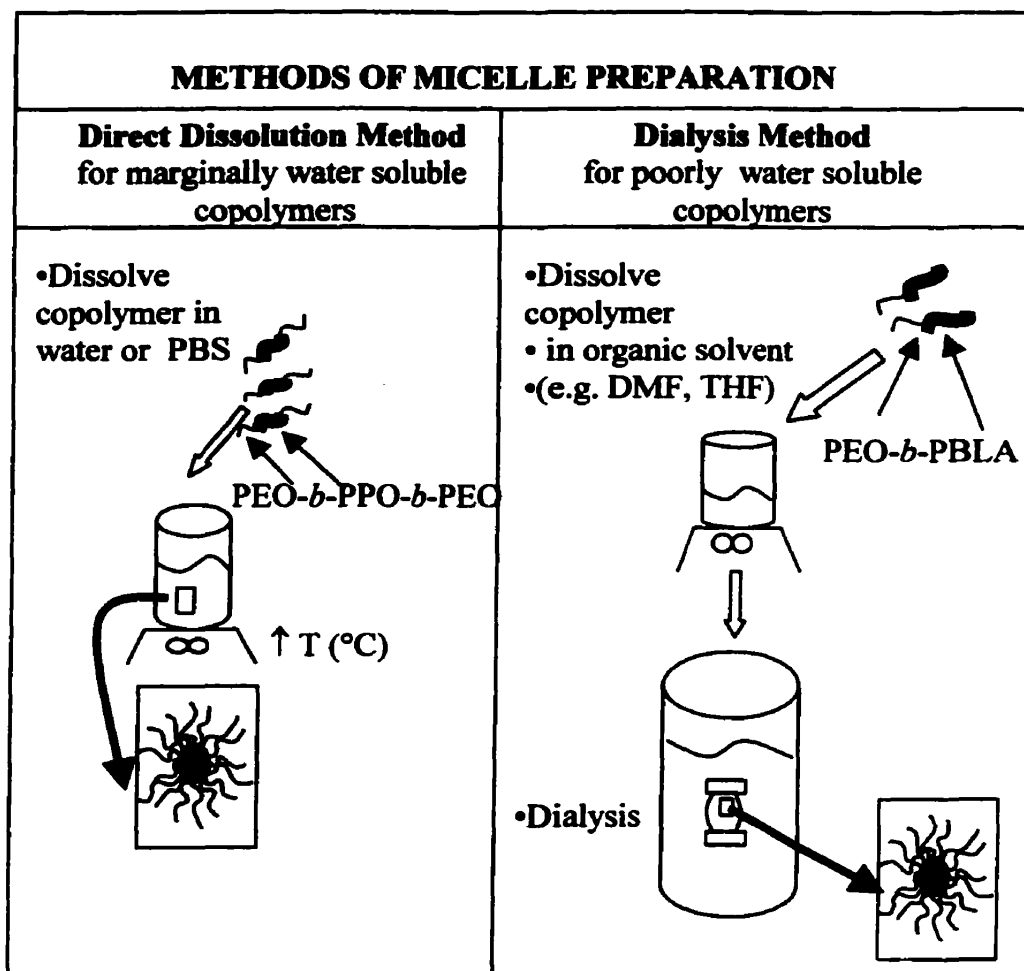


Figure 2.1. A schematic of the two principle methods employed for the preparation of block copolymer micelles.

preparation of block copolymer micelles, the direct dissolution method and the dialysis method, as outlined in Figure 2.1. The choice of which method to use depends mostly on the solubility of the block copolymer in water. To this point, mostly star-type micelles have been investigated as drug carriers. Star-type micelles are formed from block copolymers which have corona-forming blocks that are longer than the core-forming blocks. If the copolymer is marginally soluble in water, the direct dissolution method is employed, whereas if the copolymer is poorly soluble in water, the dialysis method is usually employed.

The direct dissolution simply involves adding the copolymer to water or another aqueous medium such as phosphate buffer saline. The micelles formed from the PEO-b-PPO-b-PEO copolymers are routinely formed by direct dissolution, but in some cases the copolymer and water are mixed at elevated temperatures to ensure micellization [8].

The dialysis method is often used when micelles are to be formed from a copolymer that is not easily soluble in water [17, 25]. In this case, the copolymer is first dissolved in a common organic solvent that is miscible with water such as dimethylformamide, tetrahydrofuran, or dimethylacetamide. The copolymer solvent mixture is stirred and then dialyzed against bidistilled water. During the process of dialysis micelle formation is induced and the organic solvent is removed.

The size and size population distribution of micelles produced using the dialysis method may vary depending on the organic solvent employed [17, 25]. In addition, the weight fraction or yield of micelles obtained was also found to vary with the choice of organic solvent. For example, in a study by La et al. [17], the use of DMSO as the organic solvent gave rise to PEO-b-PBLA micelles which were only 17 nm in size; however, only 6% of the copolymer formed micelles. Yet, when DMAc was used, the micelles were obtained in high yield, with an average particle size of 19 nm and a narrow size distribution ($d_w/d_n = 1.27$) [17]. In this way, the dialysis method provides a means of tailoring the size and size population distribution of the micelles.

Recently, our group has been working on crew-cut micelle systems formed from a variety of copolymers such as PS-b-PAA, PS-b-PEO and PCL-b-PEO [32, 62, 63]. Crew-cut aggregates are formed from copolymers which have core-forming blocks that are

longer than the corona-forming blocks. These copolymers are thus insoluble in water and therefore must first be dissolved in a common organic solvent. For this reason, the method of preparation employed involves the initial dissolution of the copolymer in a common organic solvent followed by the slow addition of water at a very slow rate. Self-assembly occurs at some critical water content which depends on the physical properties of the block copolymer, primarily the length of the hydrophobic block and the copolymer concentration. The copolymer in the organic/water solvent mixture is then dialyzed against bidistilled water. Our studies have found that the size, size distribution and morphology of the micelles can depend on both the common organic solvent employed and the rate of water addition to the copolymer solvent mixture [64]. Once again this demonstrates the many parameters of the micelles (size, size population distribution and morphology) that can be manipulated by simple variations within the method of preparation.

2.2.2 Methods of Drug Incorporation The method of drug incorporation employed will depend mostly on the method of micelle preparation used for the particular block copolymer in question. If the micelles are formed by direct dissolution in water, than an aliquot of a copolymer water stock solution is often added to a vial which contains the drug to be incorporated. For example, a drug stock solution in acetone is made and then an aliquot is added to an empty vial, the acetone is allowed to evaporate, and then the copolymer/water mixture is added. However, the drug may also be incorporated by the oil in water emulsion method, in which case the drug is added dropwise in a solvent such as chloroform to the micelle solution in water. The drug is incorporated as the solvent evaporates.

Finally, if the micelles are prepared by the dialysis method, then the drug is added with the copolymer to the common organic solvent and then the preparation proceeds as described above for the micelles alone. In some cases, the oil in water emulsion method is also used for the incorporation of drugs into micelles prepared by the dialysis method [18].

In a study by La et al., the amount of indomethacin (IMC) entrapped into PEO-*b*-PBLA micelles was measured when both the dialysis method and the oil in water emulsion method were employed as methods of drug incorporation [18]. The amount of IMC entrapped into the PEO-*b*-PBLA micelles was found to be 20.4% (w/w) and 22.1% (w/w) when the dialysis method and oil in water emulsion method were employed, respectively [18].

For the incorporation of drugs into crew-cut micelle systems, the slow addition of water method may be employed, as described previously. For example, the copolymer and drug are dissolved in the organic solvent and stirred for several hours. Water is then added at a slow rate and then the solutions are dialyzed against bidistilled water.

2.2.3. Micelle Stability The stability of block copolymer micelles includes two different concepts thermodynamic stability and kinetic stability. A micelle is thermodynamically stable relative to disassembly to single chains in pure water if the total copolymer concentration is above the critical micelle concentration (CMC). The critical micelle concentration (CMC) is the copolymer concentration below which only single chains exist but above which both micelles and single chains are present. However, even if a micelle system is below its CMC, it may still be kinetically stable and survive at least for some period or time, if the core is large and the core material is below the T_g or if it is crystalline and thus physically crosslinked.

2.2.3.1. Thermodynamic Stability A delivery system is subject to “sink conditions” or severe dilution upon intravenous injection into an animal or human subject. In an average individual, the total blood volume is approximately 5L. For example, following the intravenous injection of 1 mL of a 1% (w/w) PCL₂₁-*b*-PEO₄₄ micelle solution, the concentration of copolymer in the blood would be 2 mg/L [32]. Therefore it is very important to know the critical micelle concentration of a particular copolymer. The CMC for PCL₂₁-*b*-PEO₄₄ is 2.8×10^{-7} mole/L or 1.2 mg/L [31]. However, the copolymer concentration of 2mg/L is below the value of the CMC of many of the other block copolymers that have been explored as micellar delivery vehicles. The CMC values for PBLA-*b*-PEO have been reported to range between 5-18 mg/L [17,21] while the CMC for

a PLA-*b*-PEO system was found to be 35 mg/L [24]. The CMC values for several PEO-*b*-PPO-*b*-PEO systems were reported to range between 300-500 mg/L [4]. In some cases, injecting a larger volume or a more concentrated micellar solution would prevent the copolymer concentration from falling below the CMC immediately upon injection.

However, it may prove to be more advantageous to begin with a copolymer system with a lower CMC value. The CMC of a copolymer is determined by many factors, some of which are the nature and length of the core-forming block, length of the hydrophilic block and the presence of hydrophobic solubilizers. The nature and length of the core-forming block have the most profound effect on the CMC. Amphiphilic copolymers which contain a highly hydrophobic block have lower CMC values in water than those which include the less hydrophobic blocks. The CMC values for PS-*b*-PEO copolymers, which contain the highly hydrophobic polystyrene block, range between 1-5 mg/L [46].

For a series of copolymers, if the core-forming block is kept constant, an increase in the molecular weight of the core-forming block will decrease the CMC [52]. To a lesser extent, if the length of the core-forming block is maintained at a constant length, than a increase in the length of the hydrophilic block will cause an increase in the value of the CMC [52, 53].

The use of a copolymer system with a low CMC value may increase the *in vivo* stability of the micelles. However, in many papers, the disassembly of micelles into single chains is mentioned to be advantageous since this will facilitate elimination of the copolymer material from the body via the kidneys. Therefore, the ideal micelle system will be stable to sink conditions encountered upon injection and will facilitate elimination by eventual disassembly into single chains.

2.2.3.2. Kinetic Stability The disassembly of micelles at copolymer concentrations below the CMC has been reported to be quite slow for some copolymer systems [18-20]. The rate of disassembly depends, among others, upon the physical state of the micelle core [18]. Micelles formed from copolymers containing a hydrophobic block which has a high glass transition temperature will tend to disassemble more slowly than those with a low glass transition temperature.

The rate of disassembly is likely affected by many of the same factors which affect the rate of unimer exchange between micelles. The unimer exchange rate has been found to be dependent on many factors such as content of solvent within the core, the hydrophobic content of the copolymer and the lengths of both the hydrophilic and hydrophobic blocks [37, 38, 41, 43, 44, 48, 49]. For example, Creuz et al. studied micelles formed from poly((dimethylamino)alkyl methacrylate)-b-sodium methacrylate and found that the rate of unimer exchange decreased with an increase in the hydrophobic/hydrophilic balance of the copolymer [48].

In addition, there is also evidence that the incorporation of hydrophobic compounds into block copolymer micelles may enhance micelle stability. For example, in a study by Kataoka's group, they found that both the physical entrapment and/or chemical conjugation of adriamycin (ADR) into the micelle core increased the structural stability of the poly(ethylene glycol)-poly(aspartic acid) (PEG-P(Asp)) micelles [12]. In their study, they assessed the stability of the micelle by gel exclusion chromatography. They found that the stability of the micelle increased as the amount of chemically conjugated adriamycin was increased, and also that the physical entrapment of adriamycin into the PEG-P(Asp)ADR micelles further enhanced micellar stability. They suggested that the presence of both the physically entrapped and chemically conjugated drug increased the hydrophobic interactions within the core, producing micelles which were more tightly packed [12].

2.2.4. Micelle Size

The size of colloidal particles is one of the properties which largely influences the circulation time and organ distribution of the vehicle. Particles which are less than 200 nm are said to be less susceptible to RES clearance, and those less than 5 μm have access to small capillaries [36]. Also, the size of the carrier may influence its mechanism of entry into cells, which may, in turn, influence the kinetics and extent of cell uptake.

The size of micelles is controlled by several factors, among which are the length of the core-forming block and the length of the corona forming block [36]. Several

different groups have contributed to this area of research, and as a result scaling relations have been developed [36, 50, 51, 65].

2.2.5. Size Population Distribution

A common problem with most block copolymer micelle systems has been the presence of a bimodal population distribution [16, 32]. The larger aggregates are believed to be clusters of individual primary micelles which have aggregated due to hydrophobic-hydrophobic interactions between the cores of the micelles [16]. This aspect will be discussed further in section 2.2.

A bimodal population distribution may be unfavorable for a drug delivery system; however, this depends upon the stability of the aggregates. Clearly, micelles of approximately 10 nm in size and those of 200 nm in size are likely to have different circulation times and biodistributions. However, if the large aggregates are not stable and break into individual primary micelles upon dilution, then they may not present a problem. For example, in our study with PCL-*b*-PEO micelles, we found that as the micelle solution was diluted from 0.2% (w/w) to 0.01% (w/w) the population of larger aggregates decreased in favor of the smaller population [32].

2.3. The Micelle Corona: Steric Barrier

The micelle shell acts as a stabilizing interface between the hydrophobic micelle core and the external medium (Figure 2.2). The properties of the outer shell will predominantly affect the biodistribution of the micelle and thereby that of the incorporated drug as well as its pharmacokinetic parameters. In most cases the hydrophilic shell-forming block is poly(ethylene oxide) with a molecular weight which is usually between 1000 to 12 000 g/mole and a length which is greater than or equal to the length of the core-forming block. Poly(ethylene oxide) has also been used to increase the biocompatibility and enhance the colloidal stability of other types of delivery vehicles such as nanoparticles [67], microspheres [68], and liposomes [69]. The stability imparted by poly(ethylene oxide) is due to an effect termed steric stabilization; this effect is most likely enhanced by PEO's unique solution properties [70-72].

2.3.1. PEO as the Corona-Forming Block

In the bulk, PEO is a non-ionic crystalline, thermoplastic water-soluble polymer [70, 71]. Its water solubility is reported to be unlimited at room temperature for all degrees of polymerization [70]. Many close structurally related polyethers cannot achieve nearly the same degree of water solubility as PEO. The high degree of hydration and large excluded volume induce repulsive forces which contribute to the stabilization of a PEO coated surface.

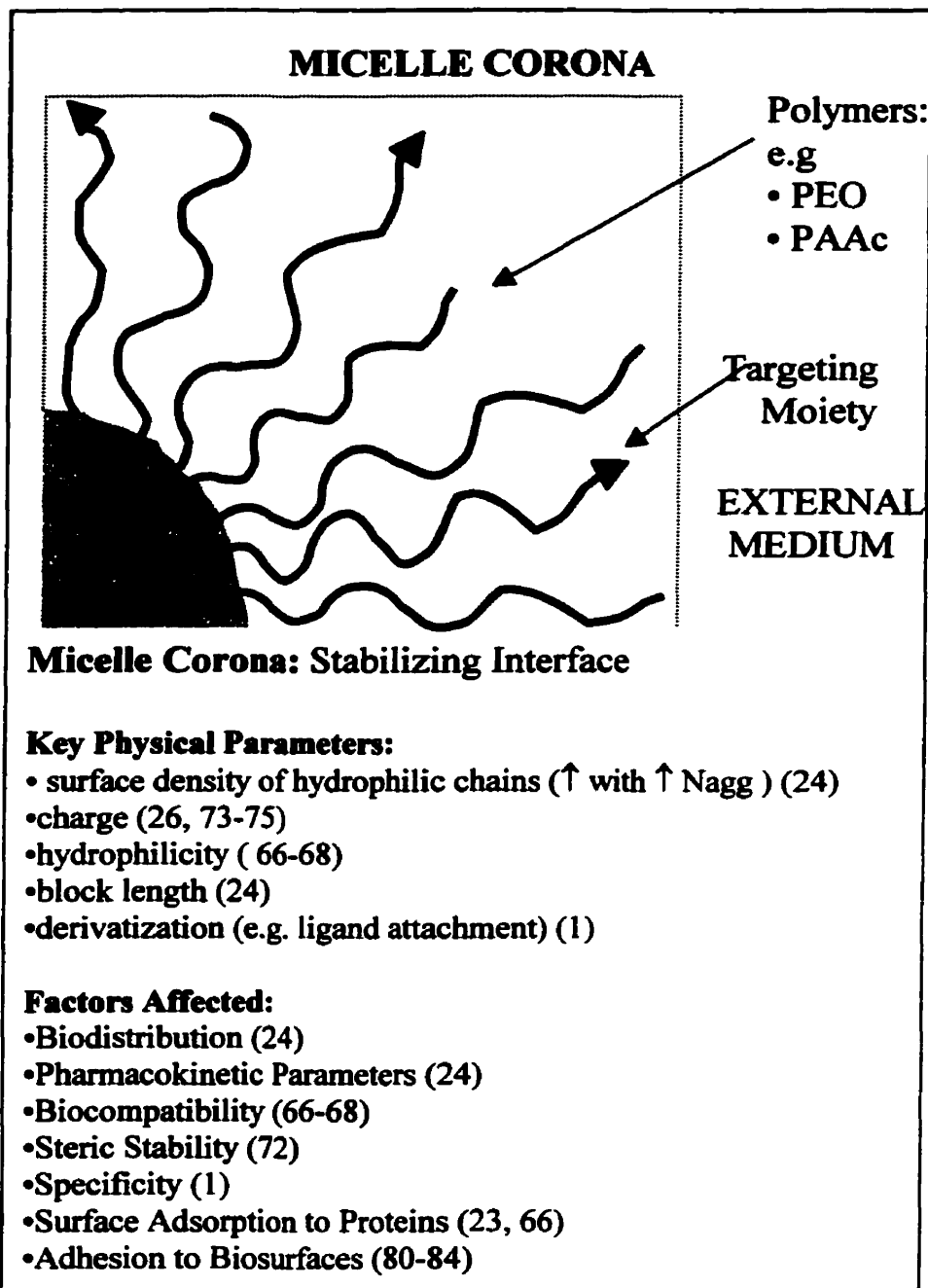


Figure 2.2. The key physical properties of the micelle corona that influence factors important in terms of the capabilities of micelles as drug carriers.

2.3.1.1. Steric Stabilization The steric stabilization of colloidal particles in an aqueous medium may be achieved by surface fixation of neutral water-soluble stabilizing moieties such as long chains of poly(ethylene oxide) [72]. The stabilizing moieties will create steric repulsive forces which will compete with the interparticle van der Waals attractive forces. Coagulation is prevented if the repulsive forces overwhelm the attractive forces operative between the particles.

The outer PEO shell of micelles may inhibit the surface adsorption of biological components. Proteins adsorb to the surface of a foreign material within the first few minutes of exposure to the blood, especially if the surface is charged or hydrophobic [23]. The adsorption of proteins to the surface of a drug delivery vehicle can cause damage and lysis of the vehicle, inducing leakage of the drug entrapped within the carrier. This makes it nearly impossible to predict the pharmacokinetics of a drug incorporated in such a system. Also, protein surface adsorption can lead to the interference of many biochemical pathways such as the complement cascade, the coagulation cascade and the fibrinolysis cascade [70]. The interference of these pathways can have serious implications since they play a central role in maintaining homeostasis. Surface opsonization of proteins which are part of the reticuloendothelial system will attract phagocytic macrophages which take up the vehicle and the net result is accumulation in the liver, spleen and lungs [66]. RES clearance decreases the circulation time of the vehicle in the bloodstream, reducing the vehicle's chance of successfully reaching its target site.

The PEO shell is also important in micelles as it may influence the extent to which primary micelles aggregate to form large secondary clusters. The aggregation of micelles leads to a larger average particle size for a specific micelle population; this, in turn, may have a profound effect on the overall biodistribution of the vehicles. Larger particles are said to be more susceptible to clearance by the RES and may also be unable to enter small capillaries and other sites which are accessible to smaller particles.

The extent to which the PEO corona is able to sterically stabilize the micelle depends on both the surface density of PEO and the thickness of the PEO shell [18]. The surface density of the PEO shell will influence the amount of core material which remains exposed to the aqueous medium. It is believed that van der Waals interactions between

the exposed cores are responsible for secondary aggregation of micelles resulting in the formation of large clusters [17]. The density of PEO at the surface of the micelle will be determined by the aggregation number or the number of copolymer chains per micelle. The larger the aggregation number of the micelle the more PEO blocks at the micelle surface [24].

The biodistribution of the micelle-incorporated drug will largely be determined by the surface properties of the vehicles such as charge, degree of hydrophilicity and steric stability. This effect is clearly seen in a study by Hagan et al. on the biodistribution of two block copolymer micelle systems formed from PLA-b-PEO copolymers where one system had a PLA:PEO ratio of 1.5:2 and the other had a PLA: PEO ratio of 2:5 [24]. The PLA-b-PEO system with a ratio of PLA:PEO of 1.5:2 has a higher density of PEO at the surface of the micelle due to the large aggregation number of this system in comparison to the 2:5 PLA-b-PEO system. The high PEO surface density of the 1.5:2 PLA-b-PEO system led to an improved biodistribution with reduced liver uptake [24].

2.3.2. Corona-Forming Blocks Other Than PEO There has been little investigation into the use of hydrophilic corona-forming blocks other than PEO in drug delivery. For many of the reasons described previously, PEO has been the most popular choice of hydrophilic polymer in block copolymers used to form micellar drug carriers. However, Inoue et. al., for example, reported on the development of micelles formed from the amphiphilic copolymer oligo(methyl methacrylate) (oMMA) and poly(acrylic acid) (PAAc) [26]. In an aqueous environment, this block copolymer produces micelles with a negative charge at the surface of the micelle.

The use of a charged corona-forming block leads to the question of whether or not it is biologically and/or physically more favorable for the drug carrier to have a neutral or charged surface. Previous studies performed on liposomes with a charged surface have revealed that following intravenous injection, their fate *in vivo* is largely dependent on their surface charge. Work by Gregoriadis et al. and Senior et al. found that the presence of negatively charged groups at the surface of liposomes decreased their circulation time and enhanced their accumulation in both the liver and the spleen [73, 74]. Liposomes

with a positive charge at the surface were found to have enhanced uptake in both the lungs and the liver [75]. However, in later studies, it was found that if the negative charge at the surface of the liposomes was shielded by "bulky hydrophilic groups" their circulation time was actually enhanced [76]. Papahadjopoulos suggested that the negative charge at the surface of the liposomes requires direct contact with certain biological components (plasma proteins or cell-surface receptors) in order to result in a decrease in the circulation time of the vehicle [76, 77].

In many studies, it has been found that the presence of negative charge at the surface of the vehicle will enhance the extent of *in vitro* uptake into various cell lines. For example, Bajoria et al., found that both anionic and neutral unilamellar liposomes were taken up into trophoblast cells more readily than cationic liposomes of the same size [78]. Also, Yu et al. found that the *in vitro* cell uptake of negatively charged liposomes into hepatocytes was greater than the uptake of neutral or cationic liposomes [79]. In addition, they found that the cationic liposomes gave rise to the highest plasma concentrations. For this reason they suggested that cationic liposomes may be most appropriate for use when liver uptake is to be avoided while negatively charged liposomes are more useful for delivery to the liver [79].

Several delivery systems with charged surfaces have been designed [80-84] for delivery to mucosal surfaces which include the lower and upper respiratory tracts, the gastrointestinal tract and the urogenitary tract [85]. Many groups have found that for delivery to mucosal surfaces, it is advantageous to use a delivery system with a bioadhesive surface. In a study by Akiyama et al. the use of mucoadhesive microspheres with poly(acrylic acid) at the surface resulted in the accumulation of a greater amount of drug in the stomach and higher drug plasma concentration levels in comparison to those obtained with non-mucoadhesive microspheres [82]. The mucoadhesive properties allow for increased gastrointestinal residence times which may aid gastrointestinal absorption. Also, discussions by Bailey et al. demonstrate that the particle size and charge of therapeutic aerosols may provide a means of targeting specific regions of the lung [86].

Therefore, if we consider the information available on other delivery systems (liposomes, microparticles, hydrogels etc.) with charged surfaces, it is clear that there is a

need for the exploration of micelle systems with a negatively charged corona-forming blocks such as the system described by Inoue et al. [26]. The charged systems may be most useful for delivery to mucosal surfaces and may afford the development of effective oral and aerosol block copolymer micellar formulations.

2.4. The Micelle Core: Cargo Space

2.4.1 Loading Capacity The micelle core serves as the cargo space for various lipophilic drugs (Figure 2.3). However, this cargo space is limited; for instance, a typical 1% (w/w) PCL-*b*-PEO (20-b-44) micelle solution ($N_{agg} = 125$) contains only approximately 0.5 % core volume [32]. This means that in a 1 mL aliquot of this 1% (w/w) micelle solution only 5 μ L is core volume. In order to exploit maximally the minimal loading space available, we must manipulate the many factors which control the loading capacity and loading efficiency.

Several of the major factors which influence both the loading capacity and loading efficiency of block copolymer micelles are nature of the solute, nature of the core-forming block, core block length, total copolymer molecular weight, solute concentration and, to a lesser extent, the nature and block length of the corona. Many studies have indicated that the overriding factor is the compatibility between the solubilize and the core-forming block.

2.4.1.1. *Compatibility between the Solubilize and the Core-Forming Block*

Many studies have explored the influence of properties of the solubilize on their extent of incorporation into block copolymer micelles. Several of the important properties of the solubilize that have been identified are molecular volume, interfacial tension against water, polarity, hydrophobicity, charge and degree of ionization

Studies by Nagarajan et al. demonstrated that the amount of solubilize incorporated decreases with an increase in the molecular volume of the solubilize [34]. They also found a correlation between the interfacial tension of the solubilize against water and the extent of incorporation into block copolymer micelles. Aromatic hydrocarbons are incorporated to a greater extent in comparison to aliphatic hydrocarbons owing to their lower interfacial tension against water [34].

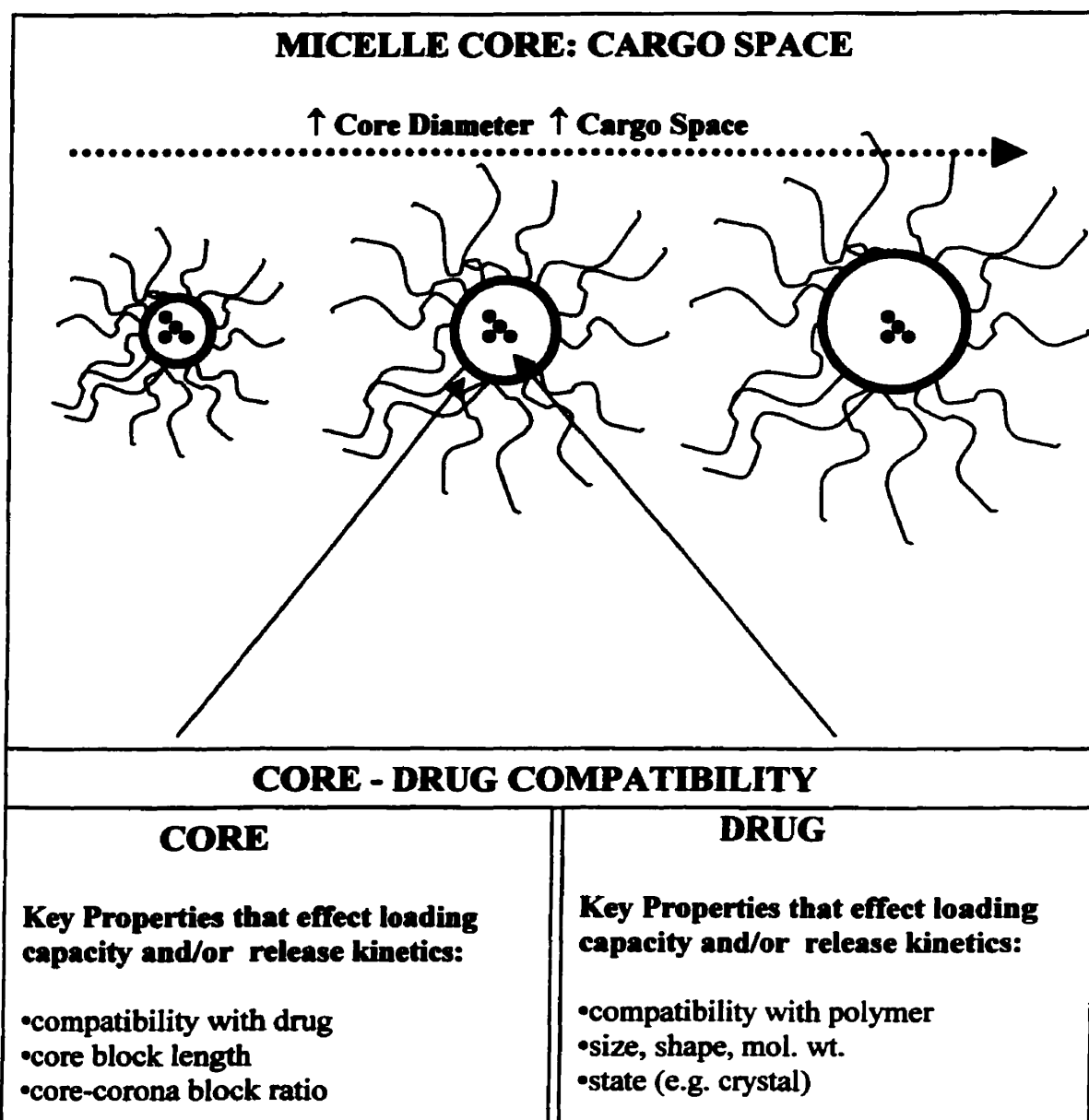


Figure 2.3. The properties of the core and drug which have the most profound influence on both the loading capacity of the micelle and release kinetics of the drug.

The nature of the solute, including polarity, hydrophobicity, charge and degree of ionization, have also been found to influence greatly the incorporation; however, this is entirely dependent on the nature of the core-forming block. It is the compatibility between the solute and the core-forming block that can be used to enhance incorporation most effectively. One parameter which has been used to assess compatibility between the polymer and the solubilizte is the Flory-Huggins interaction parameter. This interaction parameter (χ_{sp}) between the solubilizate and the core-forming block is described by the following equation:

$$\chi_{sp} = (\delta_s - \delta_p)^2 V_s / RT$$

where χ_{sp} = interaction parameter between the solubilize (s) and the core-forming polymer block (p), δ_s = the Scatchard-Hildebrand solubility parameter of the solubilize, δ_p = the Scatchard-Hildebrand solubility parameter of the core-forming polymer block and V_s = the molar volume of the solubilize [34, 54].

The lower the positive value of the interaction parameter (χ_{sp}) the greater the compatibility between the solubilize and the core-forming block. The highest degree of compatibility will be reached when $\delta_s = \delta_p$. Note, that if specific interactions are present, e.g. ionic interactions, the value of χ may even be negative. The possible complexity of polymer drug interactions suggests that the largest amount of drug loaded per micelle will be reached when the core-forming block is most suitably matched with the drug to be loaded. Due to the fact that each drug is unique, this suggests that no one core-forming block will enable maximum loading levels to be achieved for all drugs. For this reason, it is unlikely that any one micelle system will serve as a universal delivery vehicle for all drugs. In the same way, it is equally unlikely that any one drug will be as efficiently delivered by all block copolymer micelle systems. For instance, the partition coefficient for the model hydrophobic compound, pyrene, between micelles and water has been measured in several different block copolymer systems. The results obtained revealed the partition coefficients to be of the order of 10^2 for PEO-*b*-PPO-*b*-PEO [8], 10^3 for PCL-*b*-PEO [31], 10^4 for PBLA-*b*-PEO [19], 10^5 for PS-*b*-PEO (and PS-*b*-PAA) [46, 56]. From the results we see that the partition coefficient for pyrene is higher in systems with cores which are less polar [19]. Therefore, it appears reasonable to expect that more polar compounds will be most easily loaded into micelles in which the cores are more polar. For example, Kim et al. [25] obtained an indomethacin content of 42.2% in micelles formed from PEO-*b*-PCL while La et al. obtained an indomethacin content of only 22.1 (wt) % for micelles formed from PEO-*b*-PBLA [17]. These studies demonstrate the need to match a drug with certain properties with a copolymer containing a core-forming block which has similar properties.

The environment within the core may be made to be more compatible for a specific drug by attaching drug molecules to the core-forming block. This was shown in

studies by Yokoyama et al. who found that the physical entrapment of adriamycin was higher in micelles formed from adriamycin conjugated copolymer (PEO-*b*-P(Asp(ADR))) than in micelles formed from the PEO-*b*-P(Asp) copolymer alone [12].

Aside from polymer-drug compatibility and interactions, there are other factors which influence the extent of incorporation of a solubilize into block copolymer micelles. These will be discussed below.

2.4.1.2. Other Factors which Influence Drug Loading

Length of the Core-Forming Block For a copolymer with a constant hydrophilic block length, an increase in the length of the core-forming block has been found to increase the partition coefficient of the solubilize between the micelles and the external medium [39, 42]. Yu et al. measured the partition coefficient for pyrene between water and PCL-*b*-PEO micelles formed from copolymers with constant PEO block length and different PCL block lengths [31]. The partition coefficient was found to increase from 240, 760, 1450, for micelles formed from PCL-*b*-PEO with the same PEO block length and 14, 21 and 40 units of caprolactone, respectively [31].

An increase in the length of the core-forming block has been found to decrease the critical micelle concentration (cmc) and also cause an increase in the core size per micelle which, in turn, results in an increased loading capacity per micelle [54]. For example, for any one block copolymer system, as one increases the length of the core-forming block the aggregation number increases, resulting in a larger core size and thus a larger cargo space per micelle. However, due to the increase in the aggregation number per micelle, the total number of micelles in solution will decrease per unit mass of polymer. In addition, Kabanov's group has found a clear reciprocal relationship between the cmc and the length of the core-forming block [6].

Length of the Corona-Forming Block A significant increase in the length of the hydrophilic block can both increase the critical micelle concentration and decrease the aggregation number. The increase in the cmc will cause fewer chains to be present as micelles and thus available for drug loading. The smaller fraction of copolymer chains in

micelle form decreases the degree of solubilization since there is a smaller hydrophobic volume [42].

Nature of the Corona-Forming Block The effect of the nature of the corona-forming block on incorporation is once again a question of compatibility. The Flory-Huggins interaction parameter between the drug and the corona-forming block may be considered in this context. If the interaction between the corona-forming block and the drug is favorable, even if only slightly, some of the drug may be present in the outer shell. In studies by Gadelle et al. PEO-b-PPO-b-PEO micelles were found to have a higher affinity for chlorobenzene than for benzene; this was unexpected, since the χ_{sp} for benzene ($\chi = .0014$) is lower than that for chlorobenzene ($\chi_{sp} = .0068$) [54]. However, some of the chlorobenzene may have been solubilized in the outer shell since the χ_{sp} (PEO) for chlorobenzene ($\chi_{sp}(\text{PEO}) = .1711$) is lower than that for benzene ($\chi_{sp}(\text{PEO}) = .2483$) [54].

Likely, amphiphilic drugs with a low $\chi_{sp}(\text{core block})$ for the hydrophobic portion of the molecule and a low $\chi_{sp}(\text{corona block})$ for the hydrophilic portion of the molecule will be well solubilized at the interface of the micelle and in the near-corona region.

Copolymer Concentration In theoretical studies by Xing et al. the solubilization capacity was found to increase to the saturation level (maximum loading level) with an increase in the copolymer concentration [42]. The copolymer concentration at which the saturation level is reached is largely influenced by the interaction between the solubilize and the core-forming block, where stronger interactions enable saturation to be reached at lower polymer concentrations [42]. Several studies indicate that there are two patterns of solubilization, one in which the extent of solubilization increases with copolymer concentration, and another in which the degree of solubilization is independent of the copolymer concentration [42, 54]. Hurter and Hatton found that the solubilization of naphthalene into micelles formed from a range of PEO-b-PPO-b-PEO copolymers was independent of copolymer concentration for micelles formed from copolymers with a high hydrophobic content. In the same studies, it was found that the extent of solubilization did increase with copolymer concentration for the micelles formed from copolymers with high hydrophilic block contents [87-89].

Solute Concentration The presence of a hydrophobic solubilize has been found to enhance the aggregation of amphiphilic copolymer molecules. Studies by Mattice et al. employing Monte Carlo simulations to study the solubilization of small molecules into triblock copolymer micelles revealed that the solubilize can enhance the aggregation of copolymer molecules [42]. The enhancement of the aggregation lowers the CMC value, leading to an increased number of micelles present in solution [42, 54]. Increasing the solute concentration has also been found to increase the aggregation number of the copolymer which causes larger micelles to be produced. This is reported to increase the solubilization capacity per micelle [42].

Clearly, there are a large number of factors which influence both the loading efficiency and loading capacity of block copolymer micelles. However, the most important factor identified to date is the compatibility between the drug and the core-forming block. For this reason, the choice of which polymer to employ as the core-forming block is most crucial. The copolymer-drug match should be made on the basis of many of the parameters described above. Once the copolymer system has been chosen the other properties (block copolymer length, copolymer mol. wt., copolymer concentration) may be modified as needed.

2.4.2. Release Kinetics

The release of drugs from block copolymer micelles will depend upon the rate of diffusion of the drug from the micelles, micelle stability and the rate of biodegradation of the copolymer. If the micelle is stable and the rate of biodegradation of the copolymer is slow, the release rate will be mostly influenced by several of the following factors: the strength of the interactions between the drug and the core-forming block [17], the physical state of the micelle core [13], the amount of drug loaded [25], the molecular volume of the drug, the length of the core-forming block [25] and the localization of the drug within the micelle.

2.4.2.1. Polymer-Drug Interactions The stronger the interaction between the drug and the core-forming block the slower the release of the drug from the micelle. For

example, studies by La et al. found that the *in vitro* release rate of indomethacin from PBLA-*b*-PEO micelles increased with increasing pH of the external medium. As the pH of the medium is increased, more of the carboxylic acid groups become ionized, weakening the hydrophobic-hydrophobic interaction which holds the drug within the micelle core [17].

Strong polymer-drug interactions will enhance loading and decrease the release rate of the drug from the micelles. For this reason, a compromise must be achieved such that both the loading level and the release kinetics of the drug are optimized.

2.4.2.2. Localization of the Drug within the Micelle The incorporated drug may lie within the micelle core, at the interface between the micelle core and the corona or even within the corona itself. The localization of the drug will largely depend upon its physical properties and the interaction parameters between the drug and the micelle core and corona – forming blocks [40,45]. It has been found that the more soluble compounds are localized in the inner corona or the core-corona interface while the more hydrophobic compounds are situated mostly in the micelle core [40].

The release rate of the drug will largely be a function of its localization within the micelle. The outer corona region of the micelle is quite mobile; as a result, release from this area will be rapid. The release of drug localized in the corona or at the interface is said to account for “burst release” from the micelle [40].

2.4.2.3. Physical State of the Micelle Core The state of the micelle core, whether it be liquid-like or solid-like, will have a large influence on the rate of release of drugs from the micelle core. The physical state of the core under normal physiological conditions (37°C) will depend largely upon the glass transition temperature of the core-forming block and the degree of crystallinity, if any. Below the glass transition temperature the polymer is in a solid-like state, while above it the polymer is in a liquid-like state, although the changes in properties such as viscosity are usually gradual [90]. Micelles containing polystyrene cores are glassy at room temperature since the glass transition temperature of polystyrene is ca.100°C; however, if a solvent can diffuse into the core, plasticization can lower the T_g appreciably. Many of the biocompatible polymers have glass transition temperatures which are well below that of polystyrene. For

instance, the glass transition temperatures for several of the biocompatible polymers are 35°C for Poly(glycolic acid) (mol. wt. 50 000), 54°C for Poly(L-lactic acid) (mol. wt. 50 000), -62°C for Polycaprolactone (mol. wt. 44 000) and -75°C for Poly(propylene oxide) [91]. The movement of a drug from a glassy core will be slower in comparison to the movement of drugs out of cores which are more mobile. This effect was seen, for example, in studies by Teng et al. who found that the diffusion constant for pyrene in poly(styrene) is less than it is in poly(tert-butyl acrylate). This result was expected since the T_g of polystyrene is 100°C while that of poly(tert-butyl acrylate) is 42°C [40].

In addition, micelle cores formed from the more hydrophilic polymers may contain appreciable amounts of water. The release of drugs from cores of this nature has been found to proceed rapidly [40].

2.4.2.4. Other Factors Influencing Release Kinetics

The Length of the Core-Forming Block The properties of the micelle core, including core radius, influence the release rate if the drug is primarily situated in the micelle core. The longer the core-forming block, the larger the core, and the slower the release of the drug from the micelle.

However, the release kinetics of drugs which reside at the core-corona interface or in the outer shell do not have to diffuse through the core, and are thus not influenced by the core radius or length of the core-forming block [45]. For example, Hruska et al. found that the exit rate coefficient for the fluorescent probe BAN was independent of the size of the micelle since it resides close to the core surface [45].

Molecular Volume of the Drug The size or molecular volume of the drug will affect its rate of diffusion from the micelle [40]. Drugs with larger molecular volumes will have a smaller diffusion constant resulting in a decreased release rate. Once again, the burst release or release of drugs localized at the micelle surface should be independent of the molecular volume.

The Physical State of the Drug in the Micelle The physical state of the drug within the delivery vehicle can have a significant effect on the release kinetics. The drug which has been incorporated into the micelles may not be well dissolved or solubilized in the

copolymer. Several groups have identified cases where drugs which are incorporated into delivery vehicles are not dissolved in the polymer; instead, they exist in another form [92-94] e.g. as crystals dispersed within the micelle core. If the drug is dissolved molecularly, it may act as a plasticizer and lower the glass transition temperature of the core-forming block; this, in turn, may accelerate the release. However, if the drug is present as a crystal, it may instead act as a reinforcing filler, especially if strong interactions between the polymer and the surface of the crystallite are present, which may cause an increase in the glass transition temperature.

2.5. Morphologies of Block Copolymer Aggregates

To this point, the effect of the morphology of the aggregates on their efficiency as drug carriers has remained virtually unexplored. In most papers, if the morphology was reported, it was spherical. This morphology is most likely to be encountered, since most of the micelle systems which have been tried as drug carriers are star-type systems which are known to produce spheres.

In contrast, amphiphilic block copolymer systems which form crew cut aggregates have been shown to produce a wide range of morphologies [61-65, 95-108]. The crew-cuts are formed from highly asymmetric block copolymers in which the length of the core-forming block is much greater than that of the corona-forming block. The morphologies include spheres, rods, vesicles, lamellae, large compound micelles, tubules, hexagonally packed hollow hoops and many more [61-65, 95-105]. The number of morphologies that can be reproducibly formed in a highly controlled manner is of some interest, because the usefulness of aggregates other than spheres in drug delivery, while not established, is certainly an intriguing possibility.

2.5.1. The Potential Relevance of Morphologies of Block Copolymer Aggregates in Drug Delivery

There are good reasons for suspecting that morphologies other than spheres may be of interest in drug delivery. The physical parameters of drug delivery systems, such as size and surface charge, have been shown to have a substantial influence on the effectiveness of the drug delivery system in terms of its capability to deliver certain

drugs. As previously mentioned, the biodistribution, circulation time and mechanism and extent of cell uptake are altered by changing the surface properties and/or size of the drug carrier. The striking influence of these two physical parameters suggests that it may be worthwhile to explore the morphology of the carrier as another performance related physical parameter.

The various morphologies could be used for different applications in drug delivery. For instance, rod shaped aggregates will likely have different loading capacities and release kinetics than their spherical counterparts. The rod-like aggregates may be most useful in the preparation of aerosol formulations whereby their thin tubular structure may facilitate access to the different parts of the lung, because the aerodynamic properties of rods have been shown to be more suitable than those of spheres [109].

Block copolymer vesicles can be made to contain hydrophilic compounds, as has been shown for liposomes [69, 73, 74-76] and a copolymer system [110]. In this way a cocktail of vesicles and micelles could be used to deliver a combination of hydrophilic and hydrophobic drugs. There are many hydrophobic/hydrophilic drug combinations which are synergistic, one example is NGF and FK506. The use of sphere/vesicle combinations will first require the complete *in vivo* characterization of both systems. These studies are necessary to ensure that the release kinetics, biodistribution and pharmacokinetic parameters of drugs incorporated into both systems are suitable for this purpose.

If crew-cut copolymer systems are to be used for drug delivery, one should be at least aware of what conditions produce which morphologies. This will be discussed in Sect. 2.5., which will also mention the conditions under which some pitfalls may be encountered.

2.5.2. Morphologies of Crew-Cut Aggregates An aqueous solution of stable crew-cut aggregates cannot be formed by direct dissolution into water due to the large hydrophobic content of the core-forming block. The preparation requires initial dissolution of the block copolymer in a common organic solvent (DMF, dioxane or THF), and then slow addition of a material which is a good solvent for the hydrophilic blocks

but a precipitant for the hydrophobic blocks (e.g. water or methanol) [61-65, 95-105]. An aqueous solution can then be obtained by dialyzing against water in order to remove the common organic solvent. The addition of the precipitant increases the Flory Huggins parameter between the solvent mixture and the core-forming block. This increasingly uncomfortable environment for the hydrophobic blocks provides the driving force for micelle formation. If, during the process of water addition, one crosses stability regions for different morphologies, as is frequently the case with crew-cut copolymer systems, then mixtures of morphologies can result. However, this can sometimes be avoided by the dissolution of the copolymer in a specific solvent/ precipitant mixture at a particular copolymer concentration that is known to yield a single morphology. Frequently, however, regions are encountered where morphologies can coexist under thermodynamic equilibrium. Thus, a knowledge of both the thermodynamics and kinetics of the micellization process are needed, and these are under active study.

A large number of morphological studies have been carried out by our group, primarily using polystyrene-*b*-poly(acrylic acid) and polystyrene-*b*-poly(ethylene oxide) copolymers with a wide range of copolymer compositions [61-65, 95-105]. These studies have revealed that the formation of various morphologies of crew-cut aggregates may be explained by a force balance effect involving the following three components: the degree of stretching of the core-forming blocks, the interfacial energy between the micelle core and the solvent, and the inter-corona chain interactions [62, 96]. The force balance also determines the structural parameters of an the existing morphology such as size, core dimensions, Nagg etc. A very brief description of the three force components may be useful at this point.

The degree of stretching (S_c) may be defined as the ratio of the core radius to the copolymer chain end to end distance in the unperturbed state. An increase in the degree of stretching of the core-forming blocks results in a loss in entropy for the system. For spherical micelles the degree of stretching will increase with an increase in the core radius.

The inter-corona interactions provide another mechanism for morphological change. In an ionizable block such as PAA, the inter-corona interactions may be both

steric and electrostatic in nature. The strength of the interactions is inversely proportional to the area per corona chain at the core/corona interface. For spherical micelles the surface area per chain increases with decreasing aggregation number of the micelles. For each individual morphology, spheres, rods, vesicles, the area per corona chain decreases with an increase in the dimension of the PS region. However, in comparing different morphologies with the same dimension of the PS region (e.g. sphere or rod diameter, vesicle wall thickness), the area per corona chain decreases from spheres to rods to vesicles [61]. The interfacial energy between the core and corona regions generally increases with an increase in the water content in the solvent mixture. This progressive increase is a driving force for the minimization of the total interfacial area, and leads to an increase in the aggregation number per micelle but a decrease in the total number of micelles [61].

The structural parameters of the resulting morphology will be a result of the balance achieved between these three forces. For instance, for spherical crew-cut micelles, the addition of water (one of the morphogenic factors) increases the interfacial energy between the core and the corona; in response to such a perturbation, the system will tend to decrease the total interfacial area. This is accomplished by increasing the diameter of the micelles through increasing the aggregation number, and thus results in a consequent decrease in the total number of micelles. However, in the process, the degree of stretching increases and the inter-corona repulsions increase, and at some point one of two things can happen. The process comes to an end and the aggregation number can not increase further due to the presence of strong inter-corona repulsions; this occurs if the corona chains are long as is the case in the star-type micelles. However, if the corona chains are short and the repulsions are weak, the core-size expansion continues until some critical point is reached at which the degree of stretching is too large to support the spherical morphology, at which point the morphology changes. The occurrence of either of these two events depends not only on the relative lengths of the two blocks, but also on the other morphogenic factors to be discussed later.

The balance of forces which results in morphological control can be exercised by controlling a number of different parameters. The resulting morphology depends on coil

dimensions and interfacial energy; there are several different variables which may be used to control this. These variables include, among others, block copolymer composition, copolymer concentration, type and concentration of added ions and the nature of the common solvent used in micelle preparation. The studies on the PS-*b*-PAA system have enabled several of the morphogenic factors and their effects to be identified, these will now be discussed.

2.5.3. Morphogenic Factors

2.5.3.1. Copolymer Composition

Effect on the Degree of Stretching The value for the degree of stretching of the PS core forming block has been found to depend on the copolymer composition by the following equation: $S_c \sim N_{PS}^{-0.1} N_{PAA}^{-0.15}$. This equation applies to spherical micelles in aqueous solution which do not contain any remaining organic solvent in their cores [96]. It should be recalled that, prior to dialysis, the micelle cores are swollen with common organic solvent; as a result, the value of S_c is greater than it is following dialysis. The equation demonstrates that an increase in the length of the core and/or corona forming blocks, while keeping the other block constant, will lead to a decrease in the degree of stretching of the core-forming blocks. For example, consider a spherical micelle containing a long poly(acrylic acid) block and a polystyrene block of some particular length. If the length of the poly(acrylic acid) is decreased, the degree of stretching of the core will increase, and at some point the morphology can change to produce rod shaped aggregates. The decrease in the length of the poly(acrylic acid) block decreases inter-corona repulsions and thus allows more copolymer chains to pack into one micelle. By contrast, if one were to begin with a spherical micelle and decrease the polystyrene block length, the morphology will not change. Yet, if one takes a rod shaped micelle and then decrease the polystyrene block length, eventually the decrease in the degree of stretching will result in a change to a spherical morphology.

Effect on Inter-Corona Interactions The area per corona chain for spherical micelles is related to the copolymer composition by the following relation: $A_c \sim N_{PS}^{0.6} N_{PAA}^{0.5}$. The area per corona chain increases with an increase in the length of the core

and/or corona forming blocks [96]. Since the inter-corona interactions are inversely proportional to the area per corona chain, this means that an increase in the length of either blocks will lead to an increase in the inter-corona chain repulsions.

Consider a PS-*b*-PAA copolymer with a constant PS block length and a decreasing PAA block length. Let us begin with spherical micelles formed from copolymers with long PAA block lengths, in which the aggregation number is mostly restricted by the intercorona repulsions. As the PAA block length is decreased, the intercorona repulsions become less important, and instead, the aggregation number is restricted by the degree of stretching of the core-forming blocks. Eventually, a further decrease in the length of the PAA blocks will lead to a change in morphology from spheres to rods and even to vesicles. For example [61, 96], for a series of PS-*b*-PAA copolymers with a constant PS block length but different PAA block lengths, 200-*b*-21, 200-*b*-15, 200-*b*-8 the morphologies obtained were spheres, cylinders and vesicles respectively, for which the degrees of stretching of the PS blocks were calculated to be 1.41, 1.26, and 0.99. If the three copolymer systems had each formed spherical morphologies, the degree of stretching in each case would have been 1.41, 1.47, 1.62. The change in morphology from spheres, to rods to vesicles led to a decrease in the degree of stretching of the core-forming blocks, and, in turn, to a decrease in the free energy of the system.

2.5.3.2. Copolymer Concentration An increase in the copolymer concentration in solution will increase the aggregation number of the micelles [61, 101]. The increased aggregation number means the chains in the core will be stretched, which results in the production of rods under conditions that would previously have produced spheres or vesicles under conditions that would previously have produced rods. Therefore, using the same PS-*b*-PAA copolymer in the same solvent, one can obtain different morphologies by simply changing the copolymer concentration. For example, it was reported that the aggregates formed from PS(410)-*b*-PAA(25) at an initial copolymer concentration of 2wt % were spherical, if the concentration was 2.6wt% rod-like micelles were formed, and for a 4wt % solution vesicles were formed (with a few rods also present in solution).

2.5.3.3. Presence of Added Acid, Base or Salt The presence of ions influences the morphology of the micelles by effecting the strength of the inter-corona

chain interactions [63, 97]. Several studies were performed on solutions of PS-*b*-PAA copolymers in the presence of various ions including HCl, CaCl₂, NaCl, NaOH. The addition of electrolytes to the PS-*b*-PAA solutions was either found to strengthen or weaken the inter-corona repulsive interactions, depending on the nature of the ions added. PAA in a DMF/water mixture is slightly ionized, so the addition of HCl protonates the ionic sites resulting in a decrease in the inter-corona repulsions; this decrease in turn, will cause the morphology to change from spheres to rods to vesicles. On addition of CaCl₂, the Ca²⁺ ions will bind to the carboxylate groups and in this way decrease inter-corona repulsions, which will have the same effect as the addition of HCl. The addition of NaCl will also decrease inter-corona repulsions, but in this case by providing electrostatic shielding of the few ionic sites on the chain. By contrast, the addition of NaOH in small quantities ionizes the poly(acrylic acid), which increases inter-corona repulsions for electrostatic reasons. As a result, the increase in the concentration of NaOH changes in the morphology from vesicles to spheres.

2.5.3.4. Common Organic Solvent used in Micelle Preparation For the preparation of the crew-cut aggregates, the block copolymer is initially dissolved in a common organic solvent prior to the slow addition of water. The choice of common organic solvent employed has been found to have a profound effect on the morphology obtained. The detailed explanation of this effect is quite complicated, because a change in the solvent employed will have an effect on three of the six interaction parameters involved. The six interaction parameters are: polymer A – polymer B, solvent – polymer A, solvent – polymer B, solvent – precipitant, precipitant – polymer A and precipitant – polymer B. The change in the interaction parameters will change the coil dimensions but usually to a different extent for the corona and core blocks. The precipitant may also be changed from water to, for example, methanol; this will also change three interaction parameters. For this reason, it is difficult to predict which morphology will be produced by changing either the common organic solvent or the precipitant employed. However, if we know that by using one common organic solvent we get, for example, spheres, and with another we get vesicles; then by using a mixture of the two organic solvents we can obtain the intermediate morphology.

It is important to keep in mind that an interplay between thermodynamics and kinetics is operative in all of the examples described above. The rate of morphological change is a function of the solvent content in the core, which, in turn, is determined by water content in the solvent mixture outside the core. The higher the water content the slower the kinetics. This can be illustrated by a recent study [106], which involved the mixing of two different copolymer (PS(1140)-b-PAA(165) and PS(170)-b-PAA(33)) micelle solutions in DMF/water solvent mixtures with different DMF/water ratios. For the (PS(1140)-b-PAA(165) copolymer system alone the micelles produced are 38nm in diameter, while for the PS(170)-b-PAA(33)) copolymer system the micelles are 25 nm in diameter. When the two copolymer micelle solutions are mixed at a 5 wt.% water content, a single micelle population is obtained following a 24 hour period. By contrast when the added water content is 11 wt.% the individual micelle populations remained intact following the 24 hour period. Thus, for a particular rate of water addition, a water content will be reached above which the morphology no longer changes over the experimental time scale, and the system can be considered to be frozen. At that point the morphology reflects the equilibrium that was prevalent under conditions (water content) when equilibrium was still operative. It should also be recognized that because of the generally slower kinetics in block copolymer systems when compared to small molecule amphiphiles, it is very easy to trap morphologies which are intermediates in the transition from one morphology to another. For example, a morphology consisting of vesicles with hollow rods in the walls running parallel to the wall was recently documented, this morphology is an intermediate in the transition from vesicles to hexagonally packed hollow rods or hoops [105].

To this point we have discussed only three morphologies in detail, spheres, rods and vesicles. However, a wide range of other morphologies have been prepared in our studies, several of which may be of interest in drug delivery. These aggregates of various morphologies are stable, low free energy structures; and it is thus not surprising that several of them show a great similarity to biological structures commonly found in nature. The biological structures include for example; the smooth endoplasmic reticulum

(bicontinuous rods), microtubules (tubules) and vesicles (endosomes, cells and several others).

2.6. Conclusion

Figure 2.4 summarizes many of the most favorable characteristics of the “ideal micelle system”. *The Micelle as a Whole* should be less than 100 nm in diameter in order to avoid RES uptake and to facilitate access to cells and tissues. A narrow size distribution is favored over a broad distribution due to the unpredictable change in both the drug’s pharmacokinetic parameters and organ biodistribution which may result from a broad micelle size distribution. The micelle should be stable to “sink conditions” encountered upon injection. The lifetime of the micelle should be longer than the time required for it to reach its target site. *The Micelle Corona* must act as an effective steric barrier while also providing sufficient coverage of the core. Also, modification of the corona may also enable the micelle to be targeted to a specific site. *The Micelle Core* should have a high loading capacity and allow for a controlled drug release profile. Core-drug compatibility has been found to be one of the key determinants for the loading capacity of the micelle.

It is difficult to produce micelles which possess all of the ideal performance related properties. Largely, this is due to the fact that many of the performance related properties are influenced by the same factors. As demonstrated in Table 5, a change in one factor can influence many different properties of the micelle. For example, the loading capacity per micelle may be enhanced by increasing the length of the core-forming block, yet this may also increase the size of the micelle. For this reason, it may be necessary to assign priority to the different properties of the micelle and in this way compromise in order to create the best possible micellar delivery vehicle.

To this point, the morphology of the micellar delivery vehicles has not yet been explored as a performance related property. However, due to the overwhelming influence of other physical properties such as size and surface charge, it seems necessary to investigate morphology as another potentially important property. The extent to which

the micelles with various morphologies may be reproducibly prepared also encourages exploration in this area.


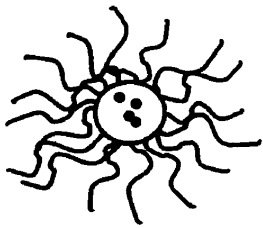
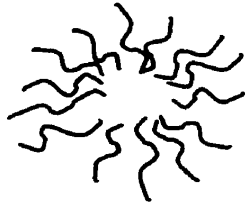
<p><i>The Micelle Core</i></p>  <p>Cargo Space</p>	<p><i>The Micelle as a Whole</i></p> 	<p><i>The Micelle Corona</i></p>  <p>Stabilizing Interface</p>
<ul style="list-style-type: none"> • high loading capacity • controlled release profile <p>high degree of compatibility between the drug and core - forming block</p>	<ul style="list-style-type: none"> • suitable size between 10 - 100nm • high degree of stability low CMC • slow rate of disassembly 	<ul style="list-style-type: none"> • efficient steric barrier <p>high surface density of poly(ethylene oxide)</p> <p>corona shell of sufficient thickness</p> <ul style="list-style-type: none"> • effective coverage of core

Figure 2.4. A schematic of the “ideal micelle system” including the most favorable properties for the micelle as a whole, the core and the corona.

2.7. References

1. Kabanov A.V., Chekhonin V.P., Alakhov V.Y., Batrakova E.V., Lebedev A.S., Melik-Nubarov N.S., Arzhakov S.A., Levashov A.V., Morozov, G.V., Severin E.S., Kabanov V.A., *FEBS Lett.* **1989**, 258, 343.
2. Kabanov A.V., Batrakova E.V., Melik-Nubarov N.S., Fedoseev N.A., Dorodnich T.Y., Alakhov V.Y., Chekhonin V.P., Nazarova I.R., Kabanov A. V., *J. Controll. Rel.* **1992**, 22, 141.
3. Alakhov V.Y., Moskaleva E.Y., Batrakova E.V., Kabanov A.V., *Bioconjugate Chem.* **1996**, 7, 209.
4. Miller D.W., Batrakova E.V., Waltner T.O., Alakhov V.Y., Kabanov A.V., *Bioconjugate Chem.* **1997**, 8, 649.
5. Batrakova E.V., Han H.Y., Alakhov V.Y., Miller D.W., Kabanov A.V., *Pharmaceutical Research* **1998**, 15, 850.
6. Alakhov V.Y., Kabanov A.V., *Exp. Opin. Invest. Drugs* **1998**, 7, 1453.
7. Kabanov A. V., Kabanov V.A., *Advanced Drug Delivery Reviews* **1998**, 30, 49.
8. Kabanov A.V., Nazarov I.R., Astafieva I.V., Batrakova E.V., Alakhov V.Y., Yaroslavov A.A., Kabanov V.A., *Macromolecules* **1995**, 28, 2303.
9. Yokoyama M., Miyauchi M., Yamada N., Okano T., Sakurai Y., Kataoka K., Inoue S., *Cancer Res.* **1990**, 50, 1693.
10. Yokoyama M., Kwon G.S., Okano T., Sakurai Y., Naito M., Kataoka K., *Journal of Controlled Release* **1994**, 28, 59.
11. Kwon G., Suwa S., Yokoyama M., Okano T., Sakurai Y., Kataoka K., *Journal of Controlled Release* **1994**, 29, 17.
12. Yokoyama M., Fukushima S., Uehara R., Okamoto K., Kataoka K., Sakurai Y., Okano T., *Journal of Controlled Release* **1998**, 50, 79.
13. Kwon G., Naito M., Yokoyama M., Okano T., Sakurai Y., Kataoka K., *Journal of Controlled Release* **1997**, 48, 195.
14. Katayose S., Kataoka K., *Journal of Pharmaceutical Sciences* **1998**, 87, 160.
15. Harada A., Kataoka K., *Macromolecules* **1998**, 31, 288.

16. Cammas S., Suzuki K., Sone C., Sakurai Y., Kataoka K., Okano T., *Journal of Controlled Release* **1997**, 48, 157.
17. La S.B., Okano T., Kataoka K., *Journal of Pharmaceutical Sciences* **1996**, 85, 85.
18. Kwon G.S., Okano T., *Advanced Drug Delivery Reviews* **1996**, 21, 107.
19. Kwon G.S., Naito M., Kataoka K., Yokoyama M., Sakurai Y., Okano T., *Colloids and Surfaces B: Biointerfaces* **1994**, 2, 429.
20. Kwon G.S., Kataoka K., *Advanced Drug Delivery Reviews* **1995**, 16, 295.
21. Kwon G., Naito M., Yokoyama M., Okano T., Sakurai Y., Kataoka K., *Langmuir* **1993**, 9, 945.
22. Maysinger D., Morinville A., *Trends Biochem. Sci.* **1997**, 15, 410.
23. Muller R.H., *Colloidal Carriers for Controlled Drug Delivery and Targeting*. CRC Press, Boca Raton, Florida, 1991.
24. Hagan S.A., Coombes A.G.A., Garnett M.C., Dunn S.E., Davies M.C., Illum L., Davis S.S. *Langmuir* **1996**, 12, 2153.
25. Kim S.Y., Shin I.G., Lee Y.M., Cho C.S., Sung Y.K., *Journal of Controlled Release* **1998**, 51, 13.
26. Inoue, T., Chen G., Nakamae K., Hoffman A.S., *Journal of Controlled Release* **1998**, 51, 221.
27. Jeong, Y.I., Cheon J.B., Kim S.H., Nah J.W., Lee Y.M., Sung Y.K., Akaike T., Cho C.S. *J. Control. Release* **1998**, 51, 169.
28. Nah, J.W., Jeong Y.I., Cho C.S. *J. Polym. Sci.: Part B: Polym. Phys.* **1998**, 36, 415.
29. Zhang X., Burt H.M., Von Hoff D., Dexter D., Mangold G., Degen D., Oktaba A.M., Hunter W.L. *Cancer Chemother. Pharmacol.* **1997**, 40, 81.
30. Ramaswamy, M., Zhang X., Burt H.M., Wasan K.M.- *J. Pharm. Sci.* **1997**, 86, 460.
31. Yu, Y., Allen C., Chijiwa S., Maysinger D., Eisenberg A., *Macromolecules*, submitted.
32. Allen C., Yu Y., Maysinger D., Eisenberg A., *Bioconjugate Chemistry* **1998**, 9, 564.
33. Nagarajan R., Ganesh K., *Journal of Colloid and Interface Science* **1996**, 184, 489.
34. Nagarajan R., Barry M., Ruckenstein E., *Langmuir* **1986**, 2, 210.
35. Nagarajan R., *Current Opinion in Colloid and Interface Science* **1997**, 2, 282.

36. Nagarajan R., Ganesh K., *J. Chem Phys.* **1989**, 90, 5843.
37. Tian M., Qin A., Ramireddy C., Webber S.E., Munk P., Tuzar Z., Prochazka K., *Langmuir* **1993**, 9, 1741.
38. Prochaska K., Kiserow D., Ramireddy C., Tuzar Z., Munk. P., Webber S.E *Macromolecules* **1992**, 25, 454.
39. Tian M., Arca E., Tuzar Z., Webber S. E., Munk P., *Journal of Polymer Science: Part B: Polymer Physics*, **1995**, 33, 1713.
40. Teng Y., Morrison M.E., Munk P., Webber S.E., *Macromolecules* **1998**, 31, 3578.
41. Pacovska M., Prochazka K., Tuzar Z., Munk P., *Polymer* **1993**, 34, 4585.
42. Xing L., Mattice W.L., *Macromolecules* **1997**, 30, 1711.
43. Wang Y., Kausch C.M., Chun M., Quirk R.P., Mattice W.L., *Macromolecules* **1995**, 28, 904.
44. Haligolu T., Bahar I., Erman B., Mattice W.L., *Macromolecules* **1996**, 29, 4764.
45. Hruska Z., Piton M., Yekta A., Duhamel J., Winnik M.A., Riess G., Croucher M.D., *Macromolecules* **1993**, 26, 1825.
46. Wilhelm M., Zhao C.L., Wang Y., Xu R., Winnik M.A., *Macromolecules* **1991**, 24, 1033.
47. Xu R., Winnik M.A., *Macromolecules*, **1991**, 24, 87.
48. Creutz S., van Stam J., De Schryver F.C., Jerome R., *Macromolecules* **1998**, 31, 681.
49. Creutz S., van Stam J., Antoun S., De Schryver F.C., Jerome R., *Macromolecules* **1997**, 30, 4078.
50. deGennes P.G., In Solid State Physics, Liebert, L. Ed., Academic Press, New York, 1978, supplement 14, p.1.
51. Halperin A., *Macromolecules* **1987**, 20, 2943.
- 52.a) Astafieva I., Zhong X.F., Eisenberg A., *Macromolecules* **1993**, 26, 7339;
(b) Astafieva I., Khougaz K., Eisenberg A., *Macromolecules* **1995**, 28, 7127-7134.
- 53.a) Alexandridis P., Holzwarth J.F., Hatton T.A.- *Macromolecules* **1994**, 27, 2414; (b)
Alexandridis P., Athanassiou V., Fukuda S., Hatton T.A., *Langmuir* **1994**, 10, 2604.
54. Gadelle F., Koros W.J., Schechter R. S., *Macromolecules* **1995**, 28, 4883.
55. Halperin A., Alexander S., *Macromolecules* **1989**, 22, 2403.

56. Zhao J., Allen C., Eisenberg A., *Macromolecules* **1997**, 30, 7143.
57. Price, C. In *Developments in block copolymers*; Goodman, I., Ed.; Applied Science Publishers: London, 1982; Vol. 1, p 39.
58. Selb, J.; Gallot, Y. In *Developments in block copolymers*; Goodman, I., Ed.; Applied Science Publishers: London, 1985; Vol. 2, p 27.
59. Riess, G; Hurtrez, G; Bahadur, P. *Encyclopedia of Polymer Science and Engineering*, 2nd ed.; Wiley: New York, 1985; Vol. 2, p 324.
60. Chu, B.; Zhou, Z. in *Non-ionic Surfactants: Polyoxyalkylene Block Copolymers*, V. M. Ed.; Marcel Dekker, Inc.: New York; 1996, pp67.
61. Zhang L., Eisenberg A., *P.A.T.* **1998**, 9, 677.
62. Zhang L., Eisenberg A., *Science* **1995**, 268, 1728.
63. Zhang L., Yu K., Eisenberg A., *Science* **1996**, 272, 1777.
64. Chen, L., Eisenberg A., manuscript in preparation.
65. Zhang L., Barlow J., Eisenberg A., *Macromolecules* **1995**, 28, 6055.
66. Gref R., Domb A., Quellec P., Blunk T., Muller R.H., Verbavatz J.M., Langer R., *Advanced Drug Delivery Reviews* **1995**, 16, 215.
67. Gref R., Minamitake Y., Peracchia M.T., Trubeskoy V., Torchilin V., Langer R., *Science* **1994**, 263, 1600.
68. Tobio, M., Gref, R., Sanchez, A., Langer, R., Alonso, M. J., *Pharm. Res.* **1998**, 15, 270.
69. Allen T.M., *Adv. Drug Deliv. Rev.* **1994**, 13, 285.
70. Elbert D. L., Hubbell J.A., *Annual Review of Material Science* **1996**, 26, 365.
71. Lee J.H., Lee H.B., Andrade J.D., *Progress in Polymer Science* **1995**, 20, 1043.
72. Hunter R.J., *Foundations of Colloid Science* Vol. 1., Oxford University Press, New York, 1991.
73. Gregoriadis G., Senior J., *FEBS Lett.* **1980**, 119, 43.
74. Senior J., Crawley J.C.W., Gregoriadis G., *Biochim Biophys. Acta* **1985**, 839,1.
75. Mauk M.R., Gamble R.C., Baldeschwieler J.D., *Proc. Natl. Acad. Sci. USA.* **1980**, 77, 4430.
76. Papahadjopoulos D., *Journal of Liposome Research* **1996**, 6, 3.

77. Lee K.D., Hong K., Papahadjopoulos D., *Biochim Biophys. Acta* **1992**, 1103, 185.
78. Bajoria R., Sooranna S.R., Contractor S.F., *Human Reproduction* **1997**, 12, 1343.
79. Yu H.Y., Lin C.Y., *Journal of the Formosan Medical Association* **1997**, 96, 409.
80. Kuntz R.M., Saltzman W.M., *Trends in Biotechnology* **1997**, 15, 364.
81. Inoue, T., Chen G.H., Hoffman A.S., Nakamae K., *Journal of Bioactive and Compatible Polymers* **1998**, 13, 50.
82. Akiyama Y., Nagahara N., Nara E., Kitano M., Iwasa S., Yamamoto I., Azuma J., Ogawa Y., *Journal of Pharmacy and Pharmacology* **1998**, 50, 159.
83. Gershanik T., Benzeno S., Benita S., *Pharmaceutical Research* **1998**, 15, 863.
84. Calvo R., Remunanlopez C., Vilajato J.L., Alonso M.J., *Colloid and Polymer Science* **1997**, 275, 46.
85. Lowrey J.A., Savage N.D.L., Palliser D., Corsinjimenez M., Forsyth L.M.G., Hall G., Lindley S., Stewart G.A., Tan K.A.L., Hoyne G.F., Lamb J.R., *International Archives of Allergy and Immunology* **1998**, 116, 93.
86. Bailey A.G., Hashish A. H., Williams T.J., *Journal of Electrostatics* **1998**, 44, 3.
87. Hurter P. N., Hatton T.A., *Langmuir* **1992**, 8, 1291.
88. Hurter P. N., Scheutjens J.M.H.M., Hatton T.A., *Macromolecules* **1993**, 26, 5592.
89. Hurter P. N., Scheutjens J.M.H.M., Hatton T.A., *Macromolecules* **1993**, 26, 5030.
90. Cowie J.M.G., *Polymers: Chemistry and Physics of Modern Materials* 2nd Ed., Blackie Academic and Professional, New York, 1994.
91. Ratner, B.D., Hoffman, A.S., Schoen, F.J., Lemons J.E., *Biomaterials Science: An Introduction to Materials in Medicine*, Academic Press, New York (1996).
92. Benoit J.P., Courteille F., Thies C., *Int. J. Pharm.* **1986**, 29, 95.
93. Cavalier M., Benoit J.P., Thies C., *J. Pharm. Pharmacol.* **1986**, 38, 249.
94. Donbrow M., *In vitro Release from Microcapsules and Microspheres In Microcapsules and Nanoparticles in Medicine and Pharmacy*. CRC Press Boca Raton, 1992.
95. Desjardins A., Eisenberg A., *Macromolecules* **1991**, 24, 5779.
96. Zhang L., Eisenberg A., *J. Am. Chem. Soc.*, **1996**, 118, 3168.
97. Zhang L., Eisenberg A., *Macromolecules* **1996**, 29, 8805.

98. Yu K., Eisenberg A., *Macromolecules* **1996**, 29, 6359.
99. Yu K., Zhang L., Eisenberg A., *Langmuir* **1996**, 12, 5984.
100. Yu Y., Zhang L., Eisenberg A., *Langmuir* **1997**, 13, 2578.
101. Zhang L., Eisenberg A., *Macromol. Symp.* **1997**, 113, 221.
102. Yu Y., Eisenberg A., *J. Am. Chem. Soc.* **1997**, 119, 8383.
103. Yu K., Eisenberg A., *Macromolecules* **1998**, 31, 3509.
104. Yu K., Bartels C., Eisenberg A., *Macromolecules* in press.
105. Zhang L., Bartels C., Yu Y., Shen H., Eisenberg A., *Phys. Rev. Letters.* **1997**, 79, 5034.
106. Zhang L., Shen H., Eisenberg A., *Macromolecules* **1997**, 30, 1001.
107. Massey J., Power K.N., Manners I., Winnik M.A., *Journal of the American Chemical Society* **1998**, 120, 9533.
108. Tao J., Stewart S., Liu G., Yang M., *Macromolecules* **1997**, 30, 2738.
109. Johnson D.L., Polikandritou-Lambros M., Martonen T.B., *The Journal of Drug Delivery and Targeting of Therapeutic Agents* **1996**, 3, 9.
110. Ding J.F., Liu G.J., *Journal of Physical Chemistry B* **1998**, 102, 6107.

CHAPTER 3

PARTITIONING OF THE HYDROPHOBIC SOLUBILIZATE, PYRENE, BETWEEN A MODEL MICELLE SYSTEM AND THE EXTERNAL MEDIUM

In section 3.1., we describe our first study of the partitioning of the model hydrophobic solubilize, pyrene, between block copolymer micelles and the external medium. The micelle system studied is formed from polystyrene-*b*-polyacrylic acid (PS-*b*-PAA) crew-cut copolymers. The PS-*b*-PAA copolymer system is not completely representative of the biocompatible, biodegradable copolymer systems commonly used for drug delivery. The polystyrene core-forming block is more hydrophobic and has a higher glass transition temperature than most of the biocompatible and/or biodegradable polymers which are usually used as core-forming blocks. Also, as mentioned in Chapter 2 polyacrylic acid has only recently been tried as the corona-forming block in a micellar system designed for drug delivery. However, this study sets the stage for further investigations into the partitioning of pyrene and other hydrophobic solubilizes between micelles and the external medium

If a hydrophobic solubilize is placed in an aqueous solution containing block copolymer micelles, it will partition between the micelles and the external medium. The partition coefficient of the drug is of key importance as it will largely influence the pharmacokinetic parameters of the micelle-incorporated drug *in vivo*. However, the measurement of the partition coefficient of a specific compound in a micelle solution requires that it be detectable by a sensitive analytical method. Unfortunately, many drugs

do not have absorption or fluorescence properties that allow for routine detection. Also, radiolabeled analogues of a specific drug are not always readily available and are otherwise very expensive. For this reason, model compounds are often employed in the early stages of the development and characterization of a drug delivery vehicle. Pyrene is one of the most common hydrophobic model compounds employed for the initial characterization of micellar delivery vehicles formed from block copolymers.

In section 3.1. and 4.1 we describe the results of several experiments whereby we exploited the unique fluorescence properties of pyrene. This includes the measurement of the partition coefficient of pyrene between PS-b-PAA (section 3.1.) and PCL-b-PEO (section 4.1.) micelles and the external medium. Also, pyrene was used to measure the critical micelle concentration of the PCL-b-PEO copolymers as well as the micropolarity of the polycaprolactone micelle core (section 4.1.).

In each of the experiments performed using pyrene, care was taken to ensure that excimer formation did not occur. For some compounds, such as pyrene, at high concentrations a dimer may be formed between a molecule in the excited singlet state and a molecule in the ground state. The dimer, known as an excimer, results in a red – shift in the fluorescence emission spectrum owing to the energy expended on the interaction between the ground and excited state molecules. Excimer formation is a concern when aromatic molecules such as pyrene are studied. Pyrene was only used at relatively low concentrations in all of the experiments. However, because of the excimer formation pyrene cannot be used to measure such parameters as the maximum loading capacity of the micelles. Pyrene is also not an ideal model compound due to its overwhelmingly high degree of hydrophobicity; most drugs are not as hydrophobic as pyrene. With these concerns in mind pyrene does serve as a useful probe for the initial study of a new micellar vehicle.

3.1. Partitioning of Pyrene between "Crew-Cut" Block Copolymer Micelles and H₂O/DMF Solvent Mixtures

3.1.1. Introduction

Self-assembling colloidal carriers have been receiving much attention as potential drug delivery systems [1-5]. Such systems include micelles formed either from small-molecule surfactants or from amphiphilic block copolymers. Low molecular weight surfactants are frequently considered for pharmaceutical use due to their low toxicity [6-7]. However, their application in drug delivery is restricted due to their relatively low capacity for drug loading [11-12]. Similar to surfactants, amphiphilic block copolymers with hydrophobic and hydrophilic segments are generally self-assembled in the form of micelles in aqueous media. In these micelles, the hydrophobic blocks constitute the core and the hydrophilic blocks, along with the solvent (which can have a variable water content), form the corona. Some block copolymer micelles have been studied for drug delivery; these include poly(aspartic acid)-b-poly(ethylene glycol) [13], poly(B-benzyl L-aspartate)-b-poly(ethylene oxide) [14], poly(oxyethylene)-b-poly(isoprene)-b-poly(oxyethylene) [15], poly(oxyethylene)-b-poly(oxypropylene)-b-poly(oxyethylene) [16], and many others.

Several laboratories have recently studied the incorporation of model hydrophobic materials by the block copolymer micelles [17-19]. Nagarajan et al.[17a] compared the solubilization of aromatic and aliphatic hydrocarbons in poly(ethylene-propylene oxide) and poly(N-vinylpyrrolidone-styrene) block copolymer micelles. They found that the solubilize which is more compatible with the core-forming block is solubilized to a greater extent. A thermodynamic treatment of hydrocarbon solubilization was presented by the same group for both diblock and triblock copolymer molecules [17b]. Their results demonstrated that the core radius, the corona thickness and the aggregation number for the diblock copolymer micelles are much larger than those for the triblock copolymer micelles of identical molecular weights and block compositions. Tian et al.[18] determined the solubilization of organic substances by styrene-methacrylic acid block copolymer micelles using light scattering measurements, and suggested that the

compounds which interact favorably with polystyrene are solubilized to a much larger extent than the compounds which interact less favorably.

Solubilization within the core is controlled by the partition coefficient of the material between the hydrophobic micellar core and the hydrophilic aqueous phase. The pharmacokinetic behavior of the system in terms of controlled release will also depend upon this partitioning. Therefore, the partition coefficients of hydrophobic materials within micellar systems of both surfactant molecules and block copolymers have been studied by various groups. A fluorescence quenching technique developed by Auger et al. [8] enabled measurement of the naphthalene partition coefficient in aqueous solutions of non-ionic surfactant micelles. One significant benefit of using this technique is that the partitioning of naphthalene can be determined for both saturated and unsaturated solutions. Itoh et al. [9] used fluorescence measurements to determine the partition coefficient of pyrene in aqueous solutions of n- β -octyl glucoside micelles. They also calculated the free energy of transfer of pyrene from the solvent water phase to the micellar cores. Moroi et al. [10] compared the solubilization of several cyclic aromatic hydrocarbons in 1-dodecane sulfonic acid micelles. They found that the first stepwise association constant increased in order from benzene to naphthalene to anthracene to pyrene. These studies clearly indicate that control over solubilization is largely exerted by hydrophobic interactions between the solubilizate and the micelle core.

Pyrene partitioning between the poly(styrene-ethylene oxide) block copolymer micellar phase and the water phase was studied by Wilhelm et al. using fluorescence measurements [19]. The partition coefficient of pyrene was found to have a value of the order of 10^5 . In a previous paper from this laboratory, the partition coefficient of pyrene between the polystyrene-*b*-poly(acrylic acid) block copolymer micelles and water phase was also reported to be of the order of 10^5 [20]. Hurter and Hatton [21] examined the partitioning of three polycyclic aromatic hydrocarbons, naphthalene, phenanthrene and pyrene, between water and micelles formed by poly(ethylene oxide-propylene oxide) block copolymers. The micelle-water partition coefficient was found to increase with both an increase in the polypropylene oxide content of the copolymer and with and increase in molecular weight. Kabanov et al. suggested an approach for the calculation of

the partition coefficient from the emission spectrum of pyrene between Pluronic micelles of poly(oxyethylene-b-oxypropylene-b-oxyethylene) triblock copolymers and bidistilled water [16].

Crew-cut micelles have recently been the subject of extensive research in this laboratory [22-26]. The crew-cuts are formed from amphiphilic block copolymer chains with long hydrophobic core forming blocks and short hydrophilic blocks [22]. The long hydrophobic blocks prevent simple micelle preparation in pure water, rather a dual solvent system such as DMF and H₂O must be employed. The crew-cut micelle earned its name due to its thin hydrophilic brush like shell which surrounds a large hydrophobic core. The crew-cut micelles as a drug delivery system may have an enhanced capacity for the solubilization of non-polar drugs due to their large hydrophobic cores. In this study, the polystyrene-b-polyacrylic acid micelles serve as a model crew-cut system and pyrene as the model for a hydrophobic drug.

In this communication we report on the calculation of the partition coefficient (K_v) of pyrene between crew-cut micelles of polystyrene-b-polyacrylic acid and an H₂O/DMF solvent mixture. We examine the effect of water content in the solvent mixture on both the total amount of pyrene incorporated into micelles and the number of molecules incorporated per micelle. The relationship between the partition coefficient (K_v) and the mass equilibrium constant (K) is obtained and the free energy of transfer of pyrene from the solvent mixture to the micelles is given in terms of K .

3.1.2. Theoretical Aspects

3.1.2.1. Fluorescence

Wilhelm et al. [19] and Kabanov et al. [16] suggested different fluorescence methods to calculate the partition coefficient for pyrene in micellar solutions. The approach described by Wilhelm et al. [19] is based on monitoring changes in the intensity ratio $I_{338}/I_{332.5}$ in the excitation spectrum of pyrene. The method proposed by Kabanov et al. [16] involved examination of the fluorescence emission intensity of pyrene at $\lambda = 395\text{nm}$. Our fluorometric approach is a hybrid version of these methods with a few minor modifications. We monitor changes in the intensity of the third vibrational band and the

first vibrational band (I_3/I_1) in the emission spectrum of pyrene in various DMF/H₂O solvent mixtures. The I_3/I_1 ratio is used to calculate both the amount of pyrene absorbed into the micelle cores, the number of pyrene molecules per micelle and the partition coefficient of pyrene. The partition coefficients determined this way are then used to recalculate the I_3/I_1 ratios, the amount of pyrene absorbed and the number of pyrene molecules per micelle. A comparison of the experimental and recalculated I_3/I_1 ratios will enable a check of the self-consistency of the approach. This will also enable any shortcomings or breakdowns which may arise through the use of this fluorescence method to be revealed.

3.1.2.2. Pyrene Monomer Fluorescence

Pyrene has commonly been used as a hydrophobic fluorescence probe, to evaluate the polarity of various environments [9,27,28]. The fluorescence emission spectrum of pyrene shows some vibrational bands which are affected by the polarity of the surrounding environment of the probe molecules. Specifically, changes in the relative intensity of the 1st and 3rd vibrational bands in the pyrene emission spectrum have proven to be reliable tools in examining the polarity of the microenvironment [9,27,28].

Figure 3.1 presents the monomer fluorescence spectrum for pyrene in aqueous solution (pyrene conc. = 1.5×10^{-9} mol/g). The concentration is low to avoid excimer formation. As is customary, the five predominant peaks or vibrational bands in the spectrum are numbered from left to right as one to five. The first vibrational band (0-0 band) shows significant intensity variation in response to changes in polarity; for instance, considerable intensity enhancement is observed in a polar solvent. The third vibrational band demonstrates only minimal intensity variation in response to changes in microenvironment polarity. Thus, the intensity ratio of vibrational band three to vibrational band one, i.e. the intensity of peak three normalized with reference to peak one, is strongly related to the polarity of the surrounding medium of the pyrene.

3.1.2.3. Calculation of the Amount of Pyrene Absorbed.

The intensity of fluorescence emission (I) at wavelength λ may be written as:

$$I = k\phi(1 - 10^{-\epsilon_l I[Py]}) = K_a \phi \epsilon_\lambda [Py] \quad (1)$$

where $K_a = kl \times \ln 10$; k is an instrumental constant, l the cell path length, ϵ_λ the molecular decadic extinction coefficient at wavelength λ , ϕ the quantum yield, and $[Py]$ = the total concentration of pyrene = $[Py]_M + [Py]_V$, M the concentration of pyrene in micelles, V the concentration of pyrene in the solvent.

For pyrene in a copolymer micellar solution, the fluorescence intensity of the third vibrational band is [16,19]:

$$\begin{aligned} I_3^U &= K_a(\phi_V \epsilon_{3,V} [Py]_V + \phi_M \epsilon_{3,M} [Py]_M) \\ &= K_a(\phi_V \epsilon_{3,V} [Py] + (\phi_M \epsilon_{3,M} - \phi_V \epsilon_{3,V}) [Py]_M) \end{aligned} \quad (2)$$

where the superscript U refers to the micellar solution.

For the same concentration of pyrene in the same solvent mixture in the absence of copolymer, the emission intensity (I_3^V) may be described as:

$$I_3^V = K_a \phi_V \epsilon_{3,V} [Py] \quad (3)$$

Thus

$$\begin{aligned} \frac{I_3^U - I_3^V}{I_3^V} &= \frac{\phi_M \epsilon_{3,M} - \phi_V \epsilon_{3,V}}{\phi_V \epsilon_{3,V}} \times \frac{[Py]_M}{[Py]} \\ &= \left(\frac{\phi_M \epsilon_{3,M}}{\phi_V \epsilon_{3,V}} - 1 \right) \times \frac{[Py]_M}{[Py]} \\ &= \left(\frac{I_{3,\max.}}{I_{3,\min.}} - 1 \right) \times \frac{[Py]_M}{[Py]} \end{aligned} \quad (4)$$

where $I_{3,\max.}$ is the fluorescence intensity when all the pyrene is in the micelle cores and $I_{3,\min.}$ is the fluorescence intensity when all the pyrene is in the solvent. If both $I_{3,\max.}$ and $I_{3,\min.}$ are known, the absorbed amount of pyrene in the micelles may be calculated.

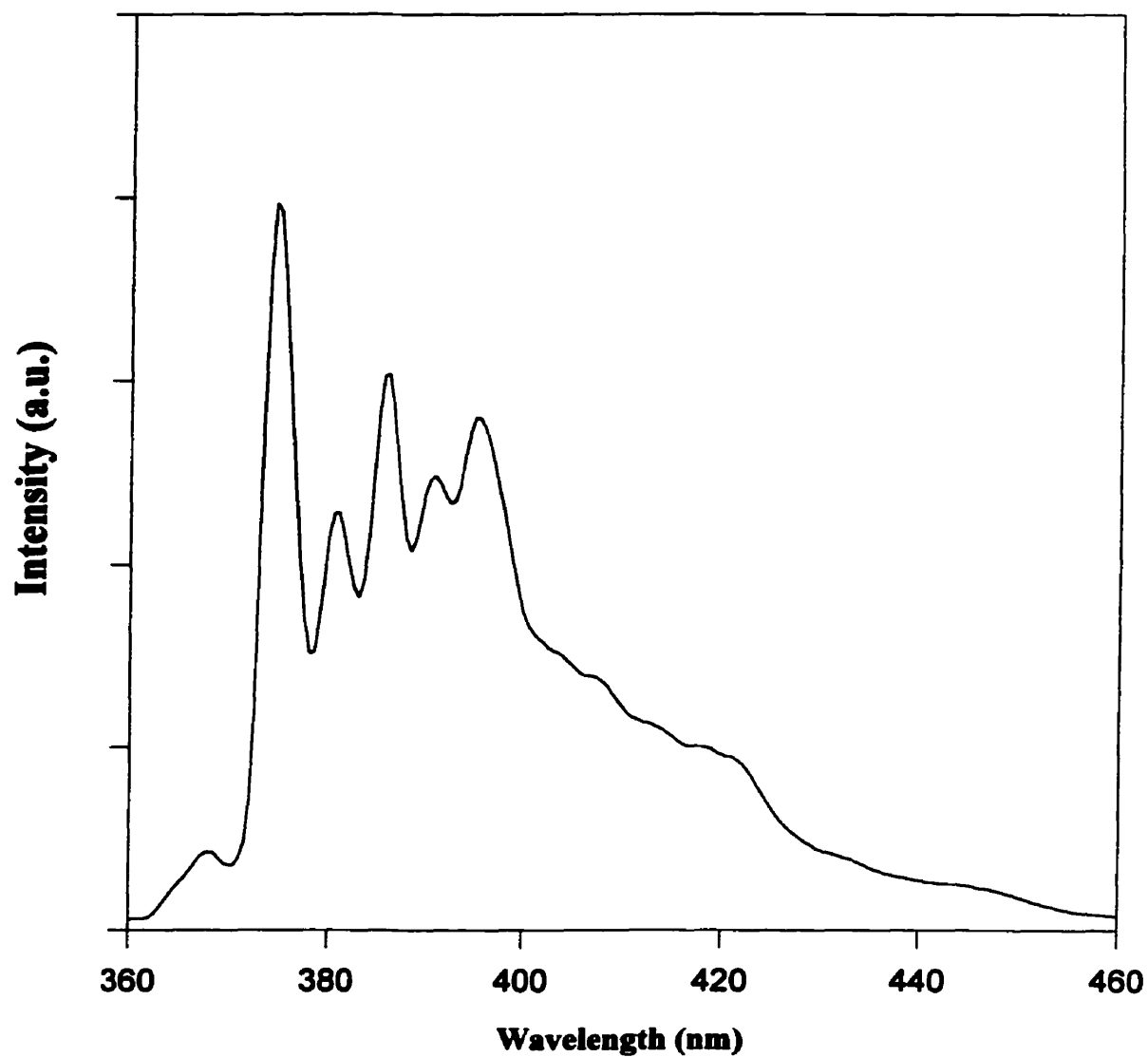


Figure 3.1. Fluorescence emission spectrum of pyrene (1.5×10^{-9} mol/g) in 85%/15% $\text{H}_2\text{O}/\text{DMF}$ at a copolymer concentration of 5.6×10^{-4} g/g.

3.1.2.4. Calculation of I_3^U from the Partition Coefficient.

Wilhelm et al [19] suggested that pyrene binding to the micelles may be described as a simple partition equilibrium between a micellar phase and a solvent phase. They provided an equation to describe the relationship between the partition coefficient (K_v) and the ratio of pyrene in the micellar phase to pyrene in the solvent phase.

$$\frac{[Py]_M}{[Py]_V} = \frac{K_V \chi_{PS} C}{\rho_{PS}} \quad (5)$$

Where χ_{PS} is the weight fraction of polystyrene in the polymer, ρ_{PS} is the density of the polystyrene core of the micelle and C is the concentration of polymer in g/mL. In this expression, the measurements are assumed to be insensitive to micellar association of polymer molecules.

From eq (5), we get

$$\frac{[Py]_M}{[Py]} = \frac{K_V \chi_{PS} C}{\rho_{PS} + K_V \chi_{PS} C} \quad (6)$$

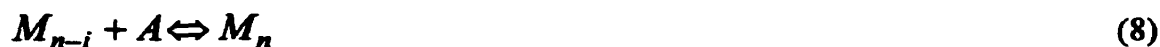
Substituting into eq (4) and rearranging

$$I_3^U = \left(\frac{I_{3,\max.}}{I_{3,\min.}} - 1 \right) \times \frac{K_V \chi_{PS} C}{\rho_{PS} + K_V \chi_{PS} C} \times I_3^V + I_3^V \quad (7)$$

In this way, we can theoretically calculate I_3^U from the measured partition coefficient K_v . The absorbed amount of pyrene can also be calculated in terms of the measured partition coefficient K_v using eq (6).

3.1.2.5. Relationship between K_v and K .

Hunter [29] suggested a kinetic approach with



to describe the distribution of probe molecule A between the micelles and the solvent phase, where M_n is a micelle containing n probe molecules and A is a probe molecule in the surrounding solvent. In the present case, A= Py(pyrene).

If there is no limit to the number of solubilized molecules per micelle, then the mass equilibrium constant, K , of the distribution of pyrene molecules is:

$$K = \frac{[Py]_M}{C_M^o [Py]_V} \quad (9)$$

where $[Py]_M$ and $[Py]_V$ are the pyrene concentrations in the micelle and in the solvent phase, respectively. C_M^o is the micellar concentration, i.e.

$$C_M^o = \frac{(C - cmc)}{N} \quad (10)$$

where C is the concentration of polymer, cmc is the critical micelle concentration, N is the aggregation number. In the present case, the cmc is very small [30]. Equation (10) thus becomes

$$C_M^o = \frac{C}{N} \quad (11)$$

Substituting both the eq (11) and the eq (5) into eq (9), we get

$$K = \frac{NK_V \chi_{PS}}{\rho_{PS}} \quad (12)$$

From this equation, the mass equilibrium constant K can be calculated through the partition coefficient K_V if the aggregation number N is known.

3.1.2.6. Calculation of Free Energy of Transfer.

From the mass equilibrium constant K , we have

$$\Delta G^o = -RT \ln K \quad (13)$$

where ΔG^o is the free energy of transfer of pyrene molecules from the solvent phase to the micelles.

3.1.3. Experimental Section

3.1.3.1. Materials.

The block copolymer used was polystyrene-*b*-poly(acrylic acid) (PS(500)-*b*-PAA(60)) containing 500 styrene repeat units and 60 acrylic acid repeat units. This block copolymer

was synthesized by sequential anionic polymerization of styrene monomer followed by *tert*-butyl-acrylate monomer. The polymerization process was carried out in tetrahydrofuran (THF) at -78 °C under nitrogen gas. Before the addition of *tert*-butyl-acrylate monomer, an aliquot of the reaction medium was withdrawn to obtain the styrene chain, which had an identical polystyrene chain length to that in the diblock copolymer which was to be synthesized subsequently. A more detailed description of the procedures was given in a previous communication [31]. The block copolymer had a narrow distribution of molecular weights, and the polydispersity index, (M_w/M_n) estimated by gel permeation chromatography (GPC), was 1.04. The synthesized block copolymers were hydrolyzed to the acid form (PS-*b*-PAA) in toluene at 110 °C reflux overnight by using *p*-toluene sulfonic acid as the catalyst (5 mol% relative to the polyacrylate content). Pyrene was purchased from Aldrich Chemical (USA) and was recrystallized two times in ethanol.

3.1.3.2. Methods

Preparation of Solutions.

Sample solutions were prepared by adding known amounts of pyrene in acetone to each of a series of empty flasks, following which the acetone was evaporated. The amount of pyrene was chosen so as to give a pyrene concentration in the final solution of 1.5×10^{-9} mol/g. Different amounts of polymer in *N,N*-dimethylformamide (DMF) were then added. The initial volumes of the solutions were *ca.* 2mL. Micellization of the polymer was achieved by adding water at a rate of 1 drop every 10 s. The addition of water was continued until the desired water content was reached. The polystyrene-*b*-poly(acrylic acid) block copolymer used here was found to have a very low cmc and to form spherical micelles with an aggregation number of 160 when water content added exceeds 5% [24,30]. All the sample solutions were stirred overnight before fluorescence measurement.

Fluorescence Measurements.

Steady-state fluorescent spectra were measured using a SPEX Fluorolog 2 spectrometer in the right-angle geometry (90° collecting optics). For the fluorescence

measurements, 3 mL of solution was placed in a 1.0-cm square quartz cell. All spectra were run on air-equilibrated solutions. For fluorescence emission spectra, λ_{ex} was 339 nm, and for excitation spectra, λ_{em} was 390 nm. Spectra were accumulated with an integration time of 1 s/0.5 nm.

3.1.4. Results and Discussion

3.1.4.1. *Pyrene in the Solvent Mixture.*

The effect of water content in the solvent mixture on the intensity ratio of peak3/peak1 (i.e. I_3 normalized to I_1 , here we simply represent it as I_3^V , V means solvent) in the absence of polymer, is shown in Fig. 3.2. With increasing water content, I_3^V is enhanced. Generally, the peak ratio is affected by two factors: the dipole moment of the solvent and its dielectric constant [28]. When the dipole moment of the solvent decreases, the peak ratio increases, and for any two given solvents with the same dipole moment, the one with the smaller dielectric constant has the higher peak ratio. Based on these premises, Kalyanasundaram and Thomas [28] gave a larger value for the I_3/I_1 peak ratio in water than in DMF, which is in agreement with our result. In the present case, a linear relationship between I_3^V vs. water content was found over the range of 20-85% water content (see Fig. 3.2). At 90% water, a sharp increase in I_3^V was observed. The value of I_3^V in pure water is .53, while that in pure DMF is .55 [27].

3.1.4.2. *Pyrene Partitioning in Micellar Solutions.*

It should first be noted, that the experimental points in Figures 3.3, 3.4, and 3.5 will be discussed now in sections 3.1.4.2 and 3.1.4.3 while the lines found in these figures will be discussed later in section 3.1.4.5. The experimental points in Figure 3.3 show the normalized I_3^U as a function of polymer concentration. The measured values of I_3^U (symbols) reveal changes with both the polymer concentration and the solvent composition. In all cases the polymer concentration is far above that of the cmc for this diblock copolymer [30]. It is seen that with an increase in polymer concentration, the I_3^U

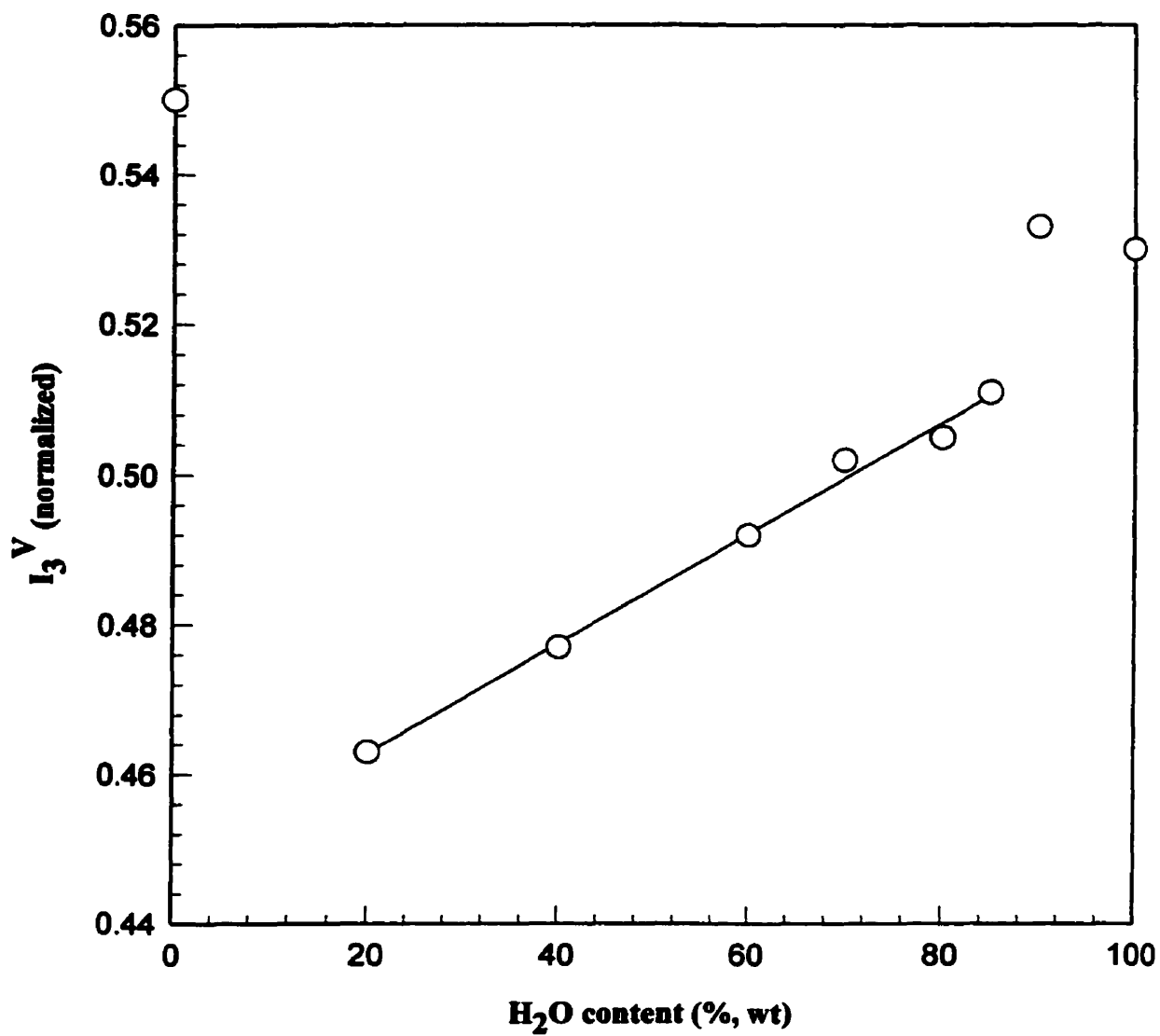


Figure 3.2. Intensity (I_3^V) as a function of water content in the solvent mixture in the absence of copolymer. Pyrene concentration = 1.5×10^{-9} mol/g.

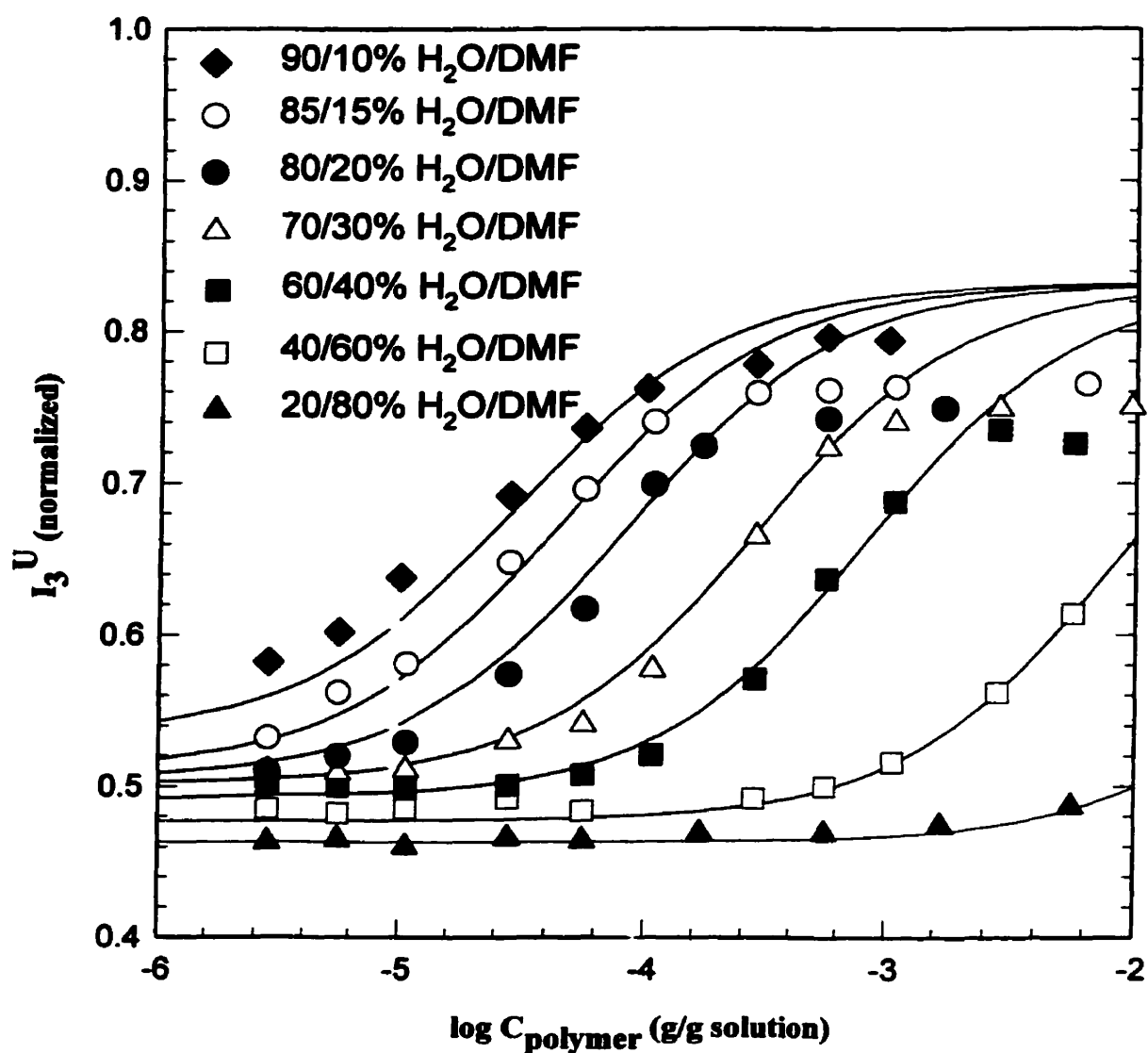


Figure 3.3. Semilogarithmic plots of the fluorescence intensity (I_3^U) as a function of polymer concentration in different solvent mixtures. Symbols represent the experimental values for the various solvent mixtures expressed as %H₂O/ %DMF; (◆) 90/10, (○) 85/15, (●) 80/20, (Δ) 70/30, (■) 60/40, (□) 40/60, (▲) 20/80. The curves were calculated using eq. 7.

increases until it reaches a plateau. In a micellar solution, the I_3^U reflects the combined contributions of both the pyrene molecules in the micellar cores and those in the solvent phase. It is well known that the peak3/peak1 intensity ratio has a larger value for pyrene in a hydrophobic environment in comparison to that in a hydrophilic one [9,27,28]. Thus, the increase in I_3^U means that more pyrene molecules are incorporated into the micelles with increasing polymer concentration. However, I_3^U remains small but almost constant over the range of low polymer concentration, particularly in the solvent mixture with low water contents.

At a constant concentration of polymer, I_3^U increases with increasing water content in the solvent mixture. Solvent mixtures with higher water contents have a significantly lower capacity to accommodate pyrene molecules, and more solute is thus incorporated into the micelle cores, leading to an increase in I_3^U . This result suggests that an increase in solvent polarity may be a simple preparative method to achieve high loading of hydrophobic solubilize.

3.1.4.3. Calculation of the Amount of Pyrene Absorbed

In order to calculate the amount of absorbed pyrene using equation (4), the two parameters, $I_{3,\min}$ and $I_{3,\max}$, must first be obtained. Here we chose the I_3^V value (Fig. 3.2) measured in the solvent mixture with 1.5×10^{-9} mol/g pyrene in the absence of copolymer to be equivalent to $I_{3,\min}$ for the corresponding micelle solution.

In the polymer micellar solutions, as previously described, the total fluorescence intensity I_3^U is a result of combined contributions of pyrene molecules in the micelles and in the solvent mixture. Since the saturation solubility of pyrene in water is very low (1.2×10^{-7} M at 22 °C [19]), the contribution to the pyrene fluorescence in the aqueous micellar solution, at the highest polymer concentrations, is predominantly due to pyrene in the micelle cores. Therefore in order to obtain an upper limit $I_{3,\max}$ value the series of plateau values of I_3^U at the highest polymer concentrations were plotted as a function of

water content in the solvent mixture, and were then extrapolated to 100% water content. The value of 0.83 was obtained as the present upper limit for $I_{3,\text{max}}$.

Figure 3.4 shows a semilogarithmic plot of the fraction of pyrene incorporated in the micelles, expressed as $[\text{Py}]_{\text{M}}/[\text{Py}]$, as a function of the logarithm of the polymer concentration, for each solvent mixture. The experimental data shows that the absorbed amount of pyrene increases for increasing polymer concentrations. Since the solutions used are all above the cmc, increasing the polymer concentration results in an increase in the number of micelles in solution. Clearly, the total number of pyrene molecules incorporated increases as more micelles are present. However, as the number of micelles is increased, the ratio of the total number of pyrene molecules per micelle is decreased. This is clearly seen in Figure 3.5, the logarithmic plot of the number of molecules per micelle as a function of polymer concentration for the various solvent mixtures. The diagonal line (in Figure 3.5) represents the ratio of the total number of pyrene molecules per micelle if one assumes that all molecules are incorporated into the micelles. The diagonal line shows that the maximum possible number of pyrene molecules per micelle decreases linearly on a log-log plot as the polymer concentration is increased. The experimental points in Figure 3.5 show that each micelle solution reaches a maximum number of molecules per micelle at a different polymer concentration, depending on the water content in the solvent mixture. The greater the water content in the solvent mixture, the lower the polymer concentration required to reach the maximum number of molecules per micelle. Another phenomenon that is worth noting is that the 60, 70 and 80% water content solutions have a fairly wide plateau region over which the number of molecules incorporated is independent of the polymer concentration. This plateau extends over one magnitude of polymer concentration (1×10^{-5} - 1×10^{-4} g/g) and the plateau value increases with increasing water content such that for the 60% solution the plateau is seen at 10 molecules / micelle while for the 70% solution it is at 32 and for the 80% it's at 100 molecules/micelle. This is quite interesting when it is considered that over this concentration range the number of micelles present in solution has increased by an order of magnitude, yet the number of pyrene molecules per micelle remains practically constant.

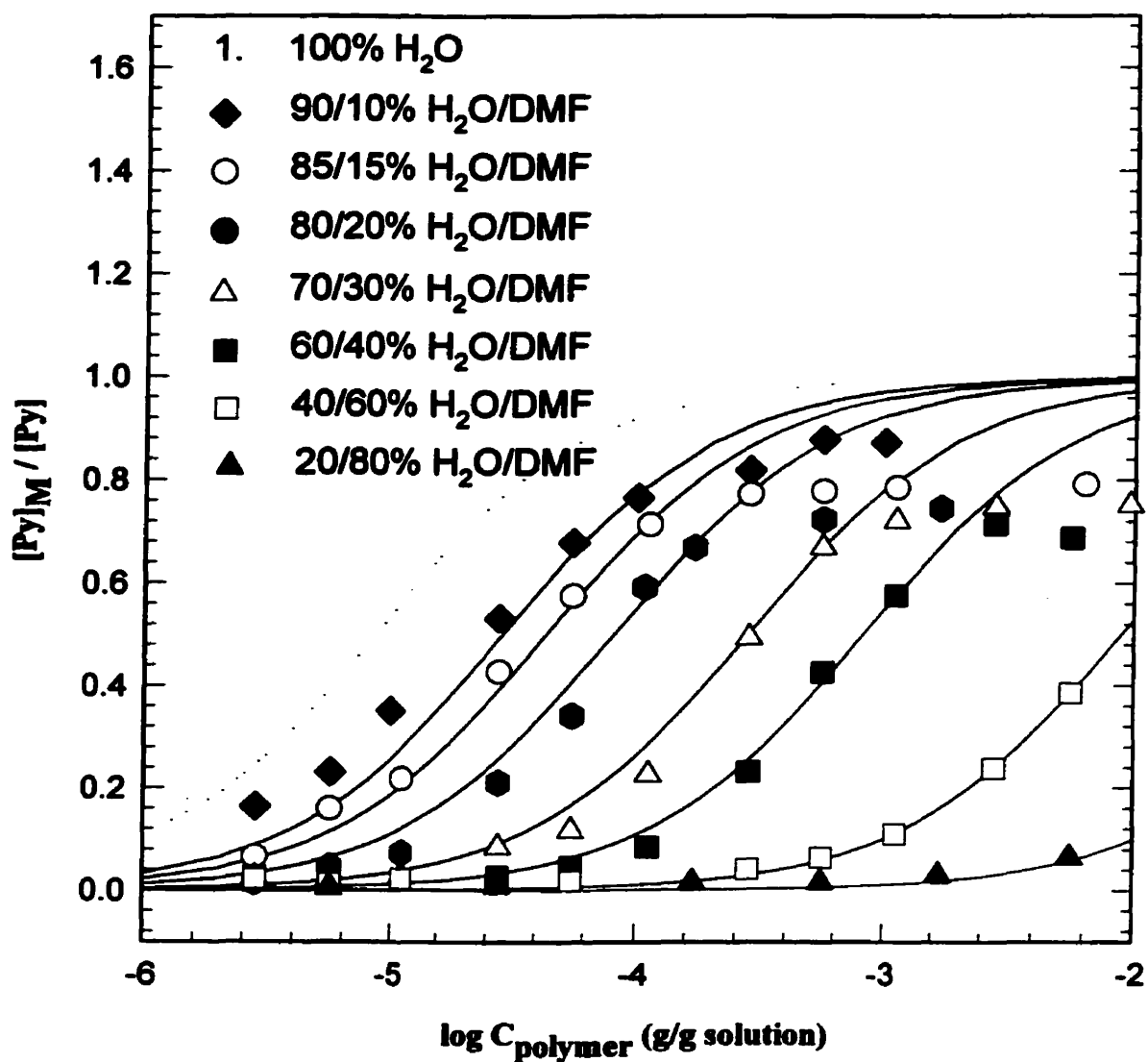


Figure 3.4. Semilogarithmic plots of $[Py]_M/[Py]$ vs copolymer concentration in different solvent mixtures. Symbols represent the experimental values for the various solvent mixtures expressed as %H₂O/ %DMF; (◆) 90/10, (○) 85/15, (●) 80/20, (△) 70/30, (■) 60/40, (□) 40/60, (▲) 20/80. The curves were calculated using eq. 6.

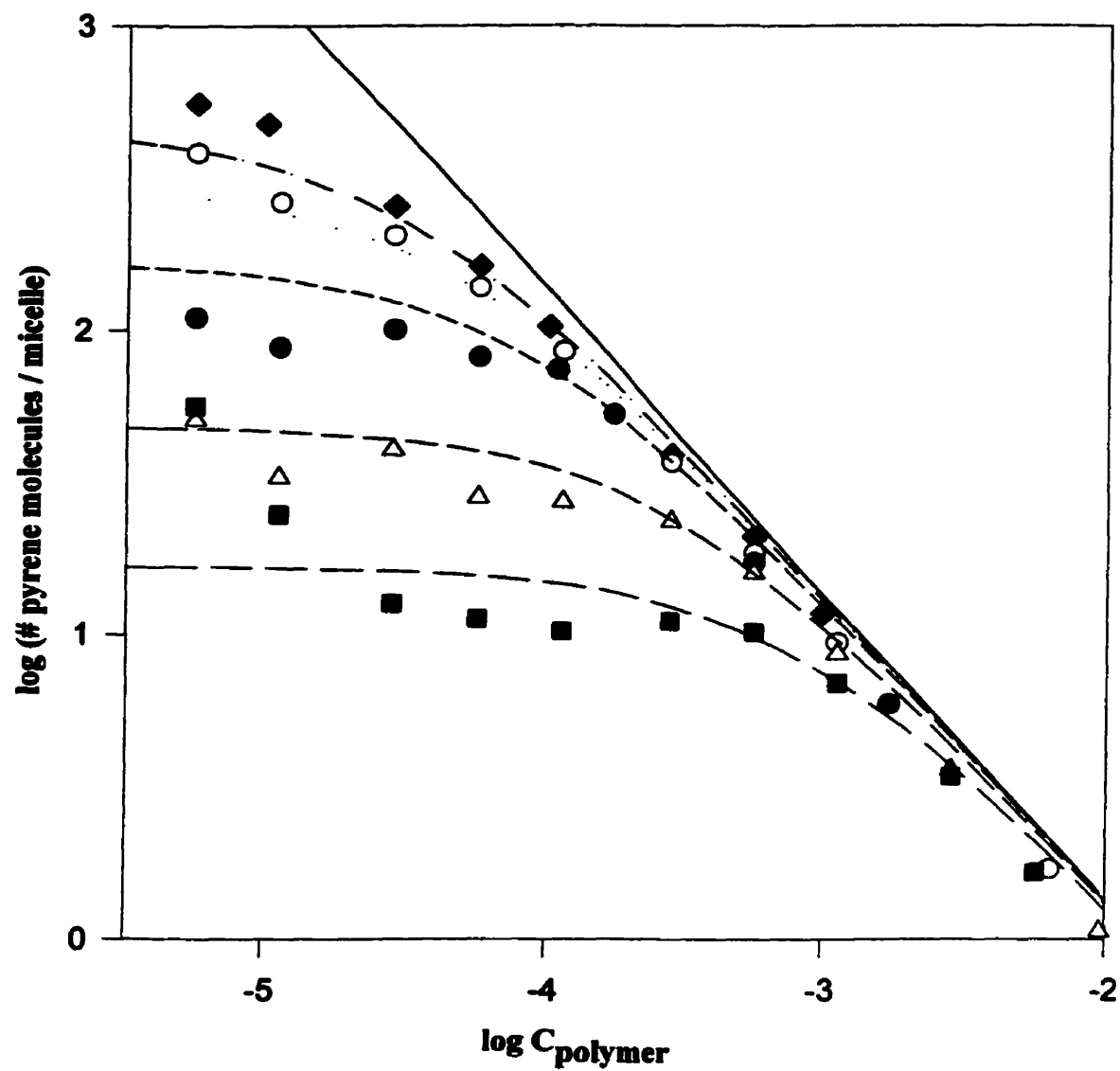


Figure 3.5. Logarithmic plot of the number of pyrene molecules per micelle as a function of polymer concentration for the various DMF/H₂O solvent mixtures.

3.1.4.4. Partition Coefficient

The $[Py]_M/[Py]_V$ values for each solvent mixture were obtained from the fluorescence data are plotted against copolymer concentration. Figure 3.6 shows the $[Py]_M/[Py]_V$ vs. copolymer concentration plot for the 85/15% H_2O/DMF solvent mixture; such plots were made for each solvent mixture. The slope of Figure 3.6 is used in the calculation of the partition coefficient K_V in terms of equation 5, as suggested by Wilhelm et al.[19]. Figure 3.7 shows a semilogarithmic plot of the partition coefficient as a function of water content in the solvent mixture. K_V increases with increasing water content in the solvent mixture. The dependence of $\log K_V$ on solvent composition is seen to be linear. For pure water, K_V is 1.3×10^5 calculated from this linear relationship. This value is close to that reported by Wilhelm et al [19] who suggested that the K_V values range from 2×10^5 to 4×10^5 for pyrene partitioning between the micelles of polystyrene-poly(ethylene oxide) diblock and poly(ethylene oxide)-polystyrene-poly(ethylene oxide) triblock copolymers and the water phase. We previously obtained similar values for K_V , ranging from 1.9×10^5 to 2.5×10^5 , for pyrene partitioning between the micelles of polystyrene-*b*-poly(acrylic acid) diblock copolymers and water [20].

In the solvent mixture of 50% water content. K_V equals to 4.2×10^2 which is 1000 times smaller than that in aqueous solution. This again demonstrates the strong influence of solvent environment on the partitioning of pyrene between the micellar and solvent phases.

3.1.4.5. Calculation of I_3^U , $[Py]_M/[Py]$, and Pyrene Molecules / Micelle.

Knowing the value of K_V as a function of water content, we are now able to calculate *a priori* the plots for I_3^U , $[Py]_M/[Py]$, and the number of molecules/micelle for a range of polymer concentrations (1×10^{-6} - 1×10^{-2}) in solvents of variable water content. The calculations are described below and plots are shown as the lines in Figs. 3.3, 3.4 and 3.5.

The Calculated Values of I_3^U

Using the upper limit value for $I_{3,max.}$, and the respective values for $I_{3,min}$ the curves, were calculated by eq. 7 and are shown in Fig. 3.3. They are in good agreement

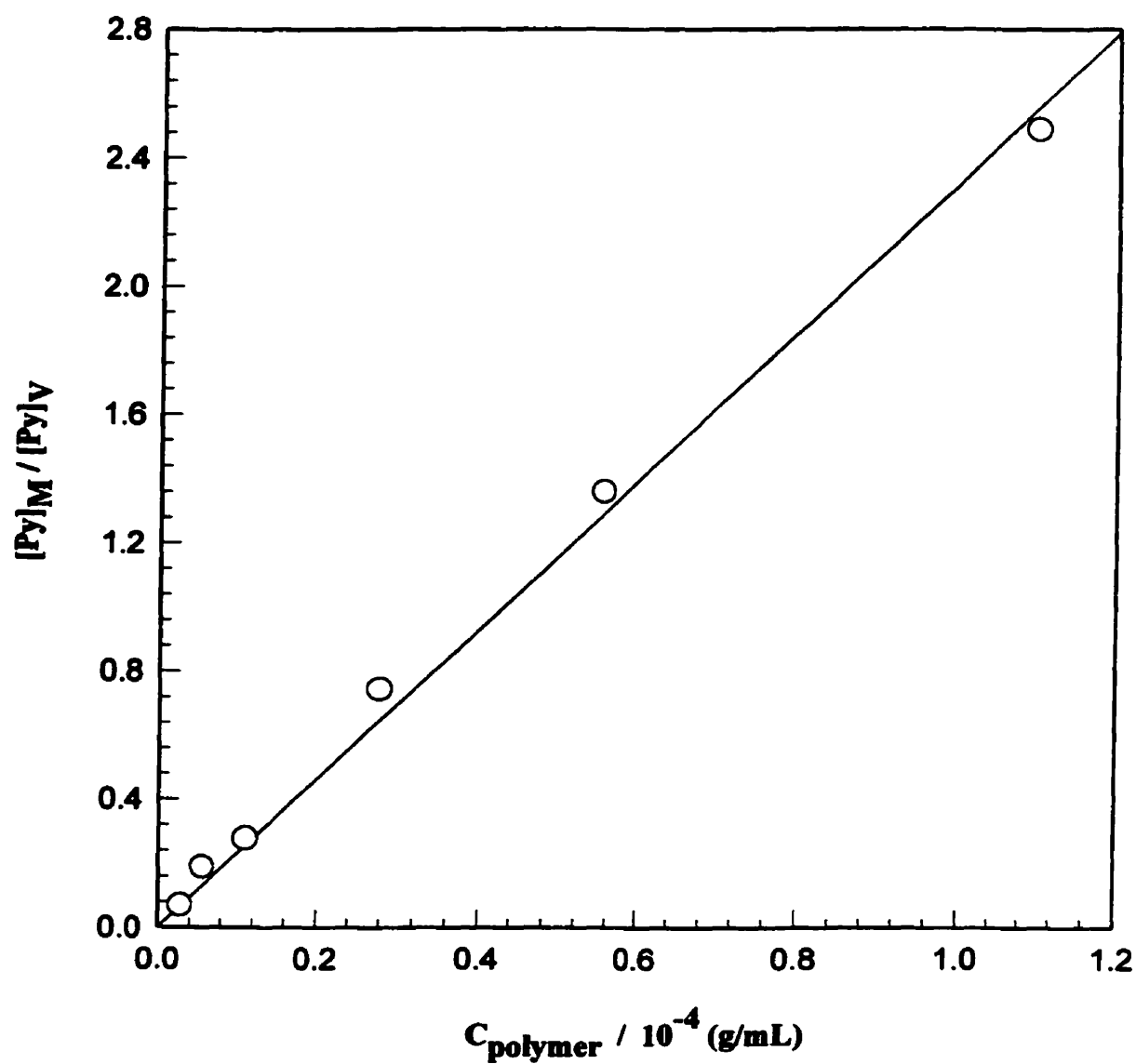


Figure 3.6. Plot of $[\text{Py}]_{\text{M}}/[\text{Py}]_{\text{v}}$, obtained from fluorescence data, vs copolymer concentration in g/mL for the 85% /15% $\text{H}_2\text{O}/\text{DMF}$ mixture. From this plot the partition coefficient of pyrene calculated by eq. 5.

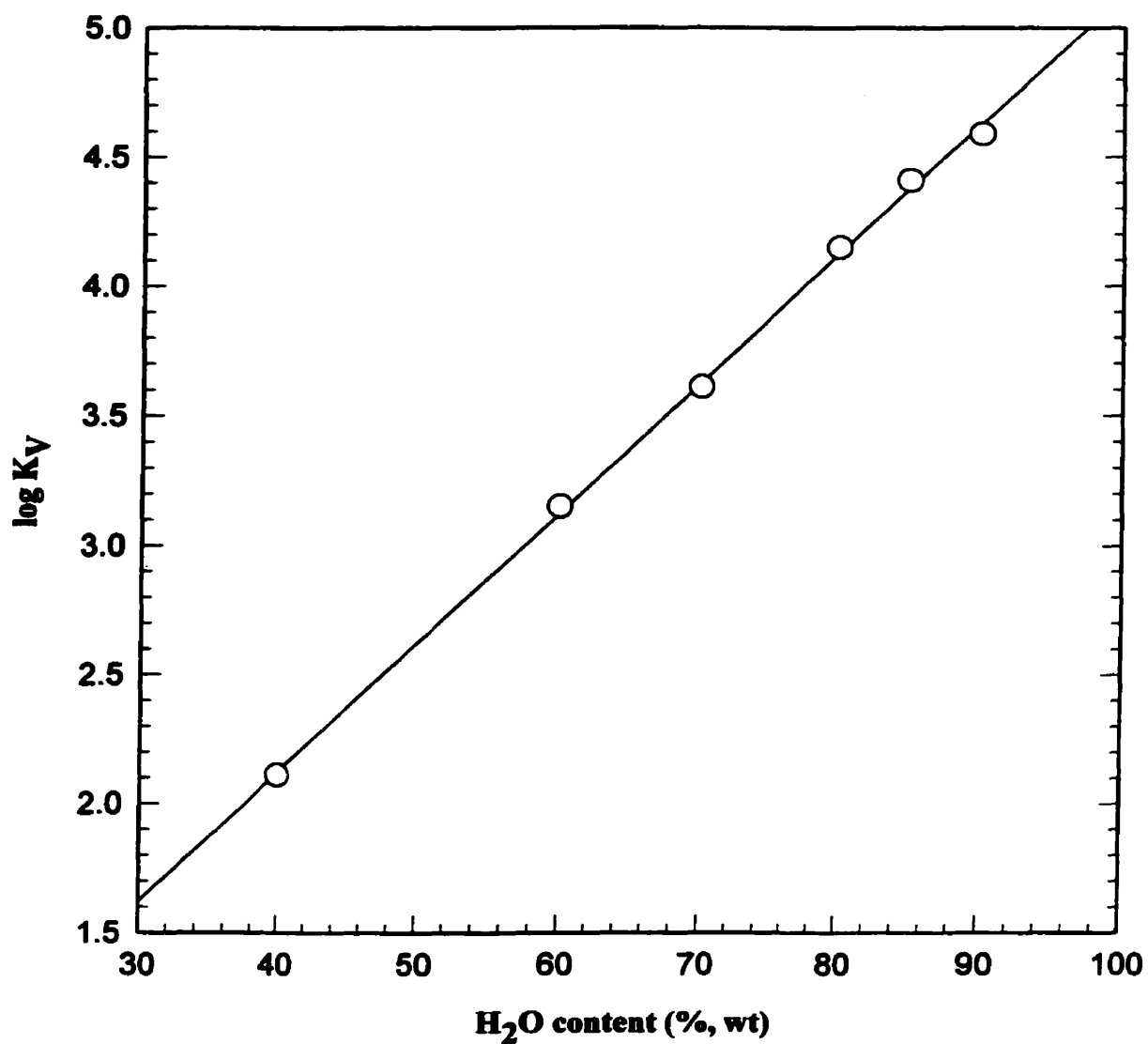


Figure 3.7. A semilogarithmic plot of partition coefficient (K_V) vs water content in the solvent mixture.

with the experimental data over the range of low and medium polymer concentrations (1×10^{-6} - 1×10^{-4}). However, there is a deviation in the plateau region found at high polymer concentrations. One possible interpretation of the deviation is given below.

Low Polymer Concentration Region.

At low polymer concentrations, the calculated curves obtained using equation 7 and the upper limit $I_{3,\max}$ value fit the experimental points quite well. The I_3^U calculated values match the I_3^U experimental values which approach the $I_{3,\min}$ values for each solvent mixture. The agreement between the I_3^U calculated and experimental values at low polymer concentrations may be explained as follows: In the present case, the density of polystyrene is close to 1 ($\rho_{PS}=1.04\text{g/mL}$). When the polymer concentration is very low, the fraction term in the right hand side of eq.7 may be simplified to

$$\frac{K_V \chi_{PS} C}{\rho_{PS} + K_V \chi_{PS} C} \approx \frac{K_V \chi_{PS} C}{\rho_{PS}} \approx K_V \chi_{PS} C \quad (14)$$

Thus, since $K_V \chi_{PS} C \ll 1$ and $I_{3,\max} / I_{3,\min} \gg 1$, I_3^U becomes

$$I_3^U \approx I_{3,\max} K_V \chi_{PS} C + I_{3,\min} \approx I_{3,\min}. \quad (15)$$

As described above, the I_3^V was adopted as the corresponding $I_{3,\min}$. For solvents of low water content, when the polymer concentration is very low, the majority of the pyrene molecules remain in the solvent phase. Thus, the contribution of pyrene to the fluorescence intensity arises mainly from pyrene in the solvent phase.

High Polymer Concentration Region.

When the polymer concentration is very high, the fraction term

$$\frac{K_V \chi_{PS} C}{\rho_{PS} + K_V \chi_{PS} C} \approx 1 \quad (16)$$

We therefore have

$$I_3^U \approx I_{3,\max}. \quad (17)$$

Therefore, the calculated curves reach a plateau at the value of $I_{3,\max}$ as shown in Fig. 3.3. The $I_{3,\max}$ plateau value describes the intensity of emission when all the pyrene is in the micelle core.

In Figure 3.3, the theoretical I_3^U curves were calculated using .83 as the value for $I_{3,\max}$, which assumes no DMF in the core. The calculated theoretical curves deviate from the experimental points in the plateau region. This deviation seems to increase with decreasing water content. One possible explanation for this deviation is based on the premise that the $I_{3,\max}$ value should not be the same for all solvent mixtures, since in each case there will be a different amount of DMF in the polystyrene core. With this in mind, the calculated curves were then recalculated using $I_{3,\max}$ values which ranged from the individual plateau values for each solvent mixtures curve to the maximum extrapolated value of .83. It was found (Figure 3.8) that the lower limit $I_{3,\max}$ value yields a calculated curve that is in agreement with the experimental points at higher polymer concentrations. However, the calculated $I_{3,\max}$ curve recalculated using the upper limit $I_{3,\max}$ value is in good agreement with experimental points obtained at lower polymer concentrations. Thus for each solvent mixture, the experimental points are best fit by one calculated curve at low polymer concentrations and another at high polymer concentrations. However, the polymer concentration at which point the crossover occurs between the experimental data being best fit by one calculated curve to another varies for each solvent mixture. As the water content in the solvent mixture is increased, the polymer concentration at which point this change occurs is decreases. Interestingly, the polymer concentration at this point of variation appears to coincide with the polymer concentration at which the experimental points approach the diagonal line in Figure 3.5.

The calculated curves for the fraction of pyrene incorporated into the micelles (Fig. 3.4) were also calculated by eqn.6, from the obtained partition coefficients (Fig. 3.7). Naturally, these curves follow the same pattern as the calculated I_3^U curves.

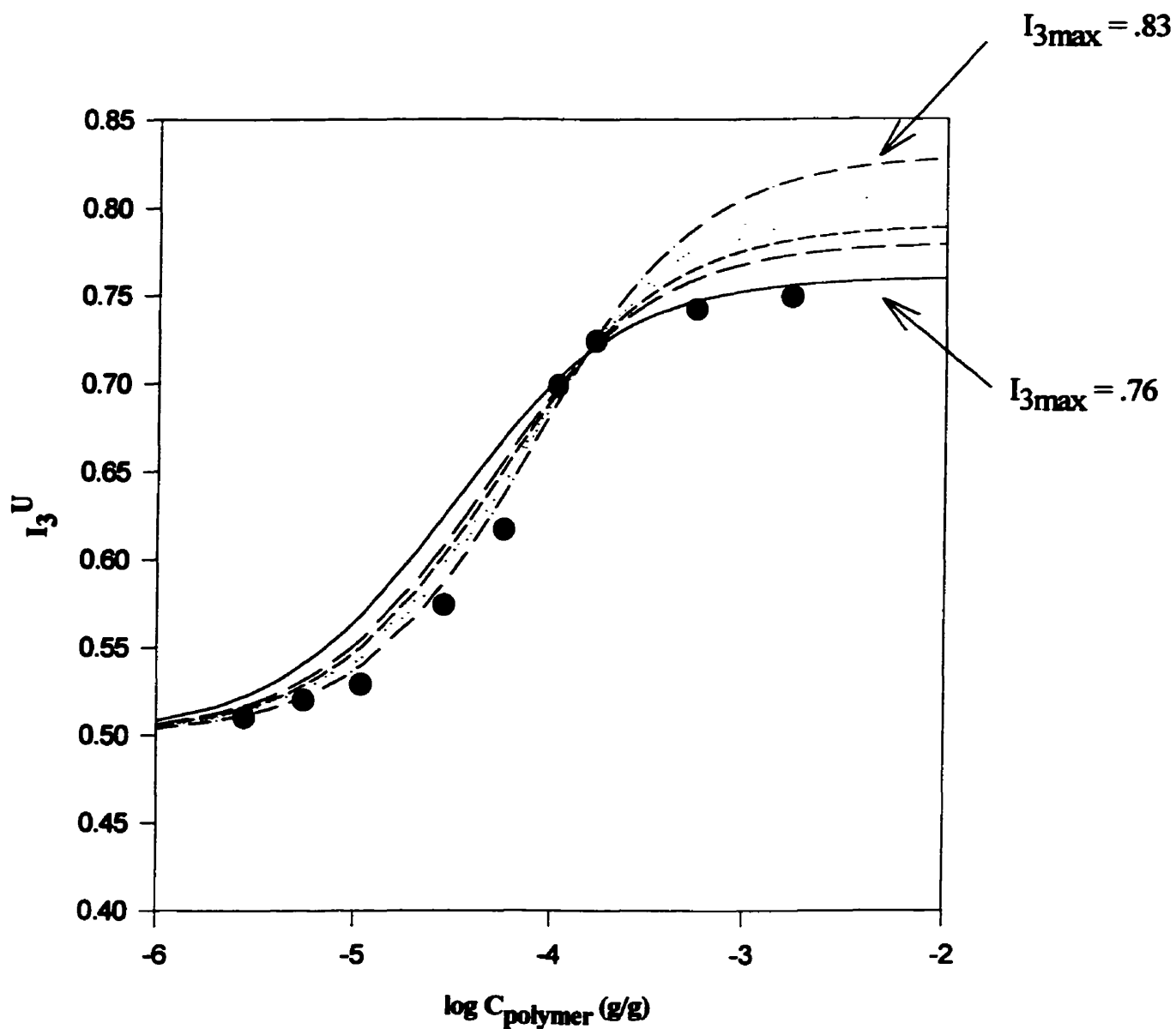


Figure 3.8. Semilogarithmic plots of the fluorescence intensity (I_3^U) as a function of polymer concentration for the 80%/20% H₂O/DMF solvent mixture. Symbols represent the experimental values. The curves were calculated using eq. 7, for a range of values of $I_{3\text{max}}$.

Calculated Number of Pyrene Molecules / Micelle

From the partition coefficients, the number of pyrene molecules incorporated per micelle in each polymer solution has been recalculated using equation 6. The recalculated values (shown as the lines in Figure 3.5) are in good agreement with the experimental points

at high polymer concentrations (1×10^{-4} - 1×10^{-2} g/g). However the recalculated values deviate from the experimental points at low polymer concentrations (1×10^{-6} - 1.5×10^{-4} g/g). This deviation is most pronounced for the solutions having the 60% and 70% water contents.

3.1.4.6. Mass Equilibrium Constant and Free Energy of Transfer.

In the present system, the aggregation number of the micelles is known to be 160 (24). The mass equilibrium constant (K) can thus be calculated in terms of eq.12, and is shown in Fig. 3.9 as a function of water content in the solvent mixture. From the equilibrium constant, the corresponding free energies (ΔG°) of transfer of pyrene from the solvent phase to the micelle cores were calculated by eq. 13, and are shown in Fig. 3.9. ΔG° decreases linearly with increasing water content and thus is driving the increased incorporation of pyrene into the micelle cores. Moroi et al. [10] indicated that the solubilization was controlled mainly by hydrophobic interaction between the solubilizates and the micellar cores. An increase in the hydrophobicity of the blocks which constitute the cores of micelles will generally improve solubilization [32-34]. The present results suggest further that a change in solvent composition such that it is made increasingly incompatible with the solubilizate will also enhance solubilization. This may be a convenient method to maximize the loading of hydrophobic materials into micelle cores.

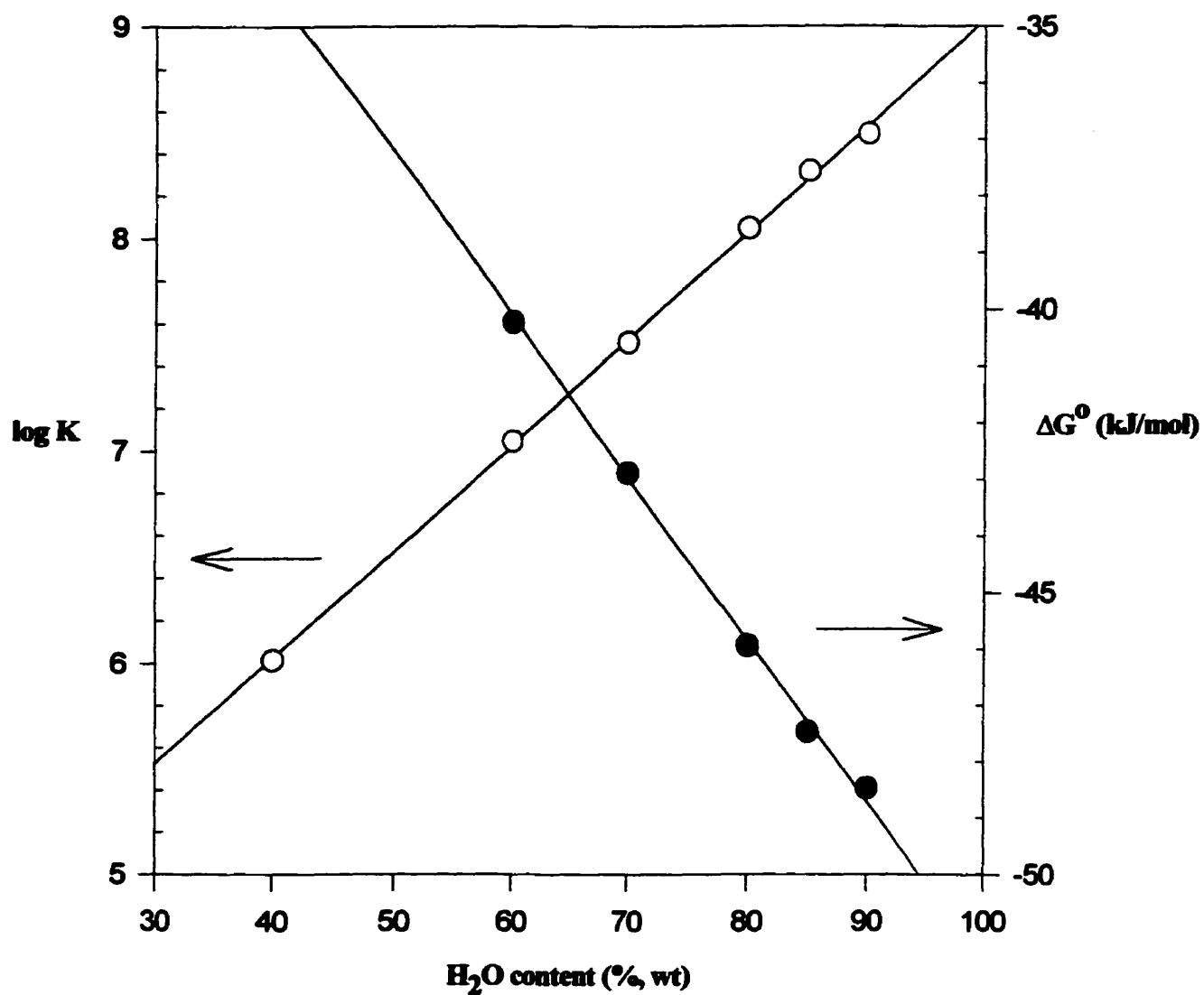


Figure 3.9. Semilogarithmic plots of the mass equilibrium constant (K) and the free energy (ΔG°) of pyrene transfer from solvent phase to the micellar cores as functions of water content in the solvent mixture.

3.1.5. Conclusions

The partitioning of pyrene between the crew-cut micelles of polystyrene-*b*-poly(acrylic acid) and the H₂O/DMF solvent mixture was studied as a function of both polymer concentration and water content in the solvent mixture. The fluorescence measurement of I_3^U enabled determination of the amount of pyrene absorbed, the number of pyrene molecules incorporated per micelle and also K_v . Since K_v increased linearly with increasing water content, the total amount of pyrene incorporated into the micelles also increases. The number of pyrene molecules per micelle was found to vary with both solvent composition and polymer concentration.

In the second part of the paper, using only the value of K_v and its variation with water content, we calculated *a priori* I_3^U , the amount of pyrene absorbed and the number of pyrene molecules incorporated per micelle. The experimental values obtained were then compared with the theoretically calculated values in order to assess the overall consistency of the fluorescence method. As described, deviations were found at the highest polymer concentrations between the two sets of values of I_3^U , and at the lowest polymer concentrations for the values of pyrene molecules incorporated per micelle.

In addition, K_v was used to calculate the equilibrium constant, which in turn enabled the calculation of the free energy of transfer of pyrene from the solvent phase to the micelle phase. The free energy of transfer was shown to decrease with increasing water content in the solvent mixture, as expected. It thus appears that the loading of hydrophobic materials into micelles may be enhanced by gradually changing the solvent composition such that it becomes increasingly hostile to the solubilizate.

3.1.6. References

1. Lawrence, M.J. *Chem. Soc. Rev.* **1994**, 417
2. Yokoyama, M. *Critical Rev. in Therapeutic Drug Carrier Systems* **1992**, 9, 213
3. Ottenbrite, R.M.; Fadeeva, N. "Polymer Systems for Biomedical Applications an Overview" In Polymeric Drugs and Drug Administration (Ottenbrite, R.M., ed.) Americal Chemical Society, Washington D.C., **1994**
4. Kwon, G.S.; Kataoka, K. *Advanced Drug Delivery Reviews* **1995**, 16, 295
5. Kabanov, A.V., Alakhov V.Y., Micelles of Amphiphilic Block Copolymers as Vehicles for Drug Delivery In Amphiphilic Block Copolymers: Self-Assembly and Applications (P.Alexandris and B. Lindman, eds.) Elsevier, Netherlands, **1997**.
6. Attwood, D.; Florence, A.T. *Surfactant Systems. Their Chemistry, Pharmacy and Biology* Chapman and Hall, London, **1983**
7. Florence, A.T. *Techniques of Solubilization of Drugs* Ed. Yalkowsky, S.H.; Marcel Dekker, Inc., New York, **1981**
8. Auger, R.L.; Jacobson, A.M.; Domach, M.M. *Environ. Sci. Technol.* **1995**, 29, 1273
9. Itoh, H.; Ishido, S.; Nomura, M.; Hayakawa, T.; Mitaku, S. *J. Phys. Chem.* **1996**, 100, 9047
10. Moroi, Y.; Mitsunobu, K.; Morisue, T.; Kadobayashi, Y.; Sakai, M. *J. Phys. Chem.* **1995**, 99, 2372.
11. Engstrom, S.; Lindahl, L.; Wallin, R.; Engblom, J. *Int. J. Pharm.* **1992**, 86, 137.
12. Wahlgren, S.; Linstrom, A.L.; Friberg, S.E. *J. Pharm. Sci.* **1984**, 73, 1484.
13. (a) Yokoyama, M.; Okano, T.; Sakurai, Y.; Ekimoto, H.; Shibazaki, C.; Kataoka, K. *Cancer Res.* **1991**, 51, 3229. (b) Yokoyama, M.; Miyauchi, M; Yamada, N.; Okano, T.; Sakurai, Y.; Kataoka, K.; Inoue, S. *Cancer Res.* **1990**, 50, 1693. (c) Yokoyama, M.; Inoue, S.; Kataoka, K.; Yui, N.; Okano, T.; Sakurai, Y. *Makromol. Chem.* **1989**, 190, 2041. (d) Yokoyama, M.; Miyauchi, M; Yamada, N.; Okano, T.; Sakurai, Y.; Kataoka, K.; Inoue, S. *J. Controlled Release* **1990**, 11, 269 (e) Kwon, G.S.; Suwa, S.; Yokoyama, M.; Okano, T.; Sakurai, Y.; Kataoka, K. *J. Controlled Release* **1994**, 29, 17

14. (a) Kwon, G.; Maito, M.; Yokoyama, M.; Okano, T.; Sakurai, Y.; Kataoka, K. *Langmuir* **1993**, 9, 945 (b) Kwon, G.; Maito, M.; Kataoka, K.; Yokoyama, M.; Sakurai, Y.; Okano, T. *Colloids Surfaces B: Biointerfaces* **1994**, 2, 429
15. Rolland, A.; O'Mullane, J.; Goddard, P.; Brookman, L.; Petrak, K. *J. Appl. Polym. Sci.* **1992**, 44, 1195
16. Kabanov, A.V, Nazarova, I.R., Astafieva I.R., Batrakova E.V., Alakhov V.Y., Yarostavov A.A., Kabanov V.A. *Macromolecules* **1995**, 28, 2303-2314
17. (a) Nagarajan, R.; Barry, M.; Ruckenstein, E. *Langmuir* **1986**, 2, 210
18. Tian, M.; Arca, E.; Tuzar, Z.; Stephen, E.; Webber, S.E.; Munk, P. *J. Polym. Sci.: Part B: Polym. Phys.* **1995**, 33, 1713
19. Wilhelm, M.; Zhao, C.-L.; Wang, Y.; Xu, R.; Winnik, M.A.; Mura, J.-L.; Riess, G.; Croucher, M.D. *Macromolecules* **1991**, 24, 1033
20. Astafieva, I.; Zhong, X.F.; Eisenberg, A. *Macromolecules* **1993**, 26, 7339
21. Hurter, P.N.; Hatton, T.A. *Langmuir* **1992**, 8, 1291
22. Gao, Z., Varshney, S.K., Wong S., Eisenberg, A. *Macromolecules* **1994**, 27, 7923
- 23.(a) Zhang, L.; Eisenberg, A. *Science* **1995**, 268, 1728 (b)Zhang, L.; Eisenberg, A. *Journal of the American Chemical Society* **1996**, 118, 3168 (c) Zhang, L.; Eisenberg, A. *Macromolecules* **1996**, 29, 8805.
24. Zhang, L., Barlow R.J., Eisenberg, A. *Macromolecules* **1995**, 28, 6055
25. (a)Zhang, L.; Yu K., Eisenberg, A. *Science* **1996**, 272, 1777 (b) Zhang, L.; Yu K., Eisenberg, A. *Langmuir* **1996**, 12, 5980.
26. Yu K., Eisenberg, A. *Macromolecules* **1996**, 29, 6359.
27. Dong, D.C.; Winnik, M.A. *Can. J. Chem.* **1984**, 62, 2560.
28. Kalyanasundaram, K.; Thomas, J.K. *J. Am. Chem. Soc.* **1977**, 99, 2039.
29. Hunter, T.F. *Chem. Phys. Lett.* **1980**, 75, 152.
30. Zhang, L.; Shen, H.; Eisneberg, A. manuscript in preparation.
31. Zhong, X-F.; Varshney, S.K.; Eisenberg, A. *Macromolecules*, **1992**, 25, 7160.
32. Al-Saden, A.A.; Whately, T.L.; Florence, A.T.; *J. Colloid Interface Sci.* **1982**, 90, 303.
33. Anton, P.; Koberle, P.; Laschewsky, A.; *Makromol. Chem.* **1993**, 194, 1

34. Jacobs, P.T.; Geer, R.D.; Anacker, E.W. *J. Colloid Interface Sci.* **1972**, *39*, 611.

CHAPTER 4

SYNTHESIS AND CHARACTERIZATION OF A BIODEGRADABLE AND BIOCOMPATIBLE AMPHIPHILIC DIBLOCK COPOLYMER OF POLY(ϵ -CAPROLACTONE)-*B*-POLY(ETHYLENE OXIDE)

To date many different micelles from block copolymers have been introduced for applications in drug delivery. However, as described in Chapter 2 it is unlikely that there will be one universal micelle system that will be best suited as a delivery vehicle for all lipophilic drugs. The physico-chemical properties of the micelles formed from the various biocompatible copolymers are different). The synthesis of new biocompatible and biodegradable copolymers will enable the development of micelles with unique properties as drug delivery vehicles. In this way eventually, a pool of different copolymers will be available from which the most suitable copolymer could be used for the delivery of a specific compound. For this reason, we chose to develop a new micelle system formed from poly(caprolactone)-*b*-poly(ethylene oxide) (PCL-*b*-PEO) copolymers. The properties of the polycaprolactone core-forming block such as hydrophobicity, polarity and glass transition temperature will enable the PCL-*b*-PEO micelles to be unique from other previously developed systems. In section 4.1 the synthesis and characterization of the PCL-*b*-PEO copolymers are described as well as the physico-chemical characterization of the PCL-*b*-PEO micelles.

4.1. Synthesis and Characterization of a Biodegradable and Biocompatible Amphiphilic Copolymer of Poly(ϵ -Caprolactone)-*b*-Poly(ethylene oxide)

4.1.1. Introduction

Micelles formed from amphiphilic block copolymers have recently received much attention as potential delivery vehicles for hydrophobic drugs [1-8]. In an aqueous environment, the amphiphilic nature of the copolymer allows it to self-assemble to form micelles such that the hydrophobic blocks form the core of the micelle while the hydrophilic blocks form the outer shell or corona. To this point, the copolymer micelle systems studied as drug carriers have mostly been star-type micelles. Such micelles are formed from block copolymers which have corona-forming blocks that are usually longer than the core-forming blocks, and in this way they are most often spherical in shape and have an extended corona.

By contrast, crew-cut copolymer aggregates are formed from copolymers which contain corona-forming blocks that are much shorter than the core-forming blocks. Crew-cut aggregates have been found to exhibit a wide range of interesting morphologies including spheres, cylinders, vesicles, large compound micelles and many more [9]. To this point, the crew-cut aggregates that have been explored were formed from non-biocompatible and non-biodegradable copolymers such as polystyrene-*b*-poly(acrylic acid) and polystyrene-*b*-poly(ethylene oxide). The use of crew-cut aggregates of different morphologies in drug delivery has not yet been investigated.

In this paper we report on the synthesis and characterization of a series of PCL-*b*-PEO copolymers which have a constant PEO block length and different PCL block lengths, such that the copolymer aggregates produced range from star-type (e.g. PCL₃-*b*-PEO₄₄) to near crew-cut systems (e.g. PCL₁₅₁-*b*-PEO₄₄). We also describe characterization studies of the PCL-*b*-PEO aggregates, focusing on those properties which are of most interest to applications in drug delivery. The two components of the copolymer, poly(caprolactone) and poly(ethylene oxide), are known to be both biodegradable and biocompatible [8].

Several groups have studied the use of triblock and diblock copolymers formed from poly(ϵ -caprolactone) and poly(ethylene oxide) copolymers in drug delivery [10-12] and several methods have been reported for the synthesis of PCL-*b*-PEO block copolymers [13-15]. Perret et al. [13] described the anionically initiated copolymerization of ϵ -CL by PEO-sodium to provide ether-ester block copolymers; however, the resulting copolymers were found to be contaminated with a significant amount of homopolycaprolactone. The presence of homopolymer was attributed to an equilibrium cyclic oligomerization in the anionic polymerization when metal alkyl oxides are the living species. Cerrai et al.[14] exploited non-catalyzed polymerization of ϵ -CL initiated by poly(ethylene oxide) to obtain almost pure block copolymers; however, the polymerization rate was very slow and the length of the PCL blocks were short even when the polymerization was performed at very high temperature (185 °C) for long periods of time (several weeks). Recently, Bogdanov et al.[15] reported another approach to the synthesis of PCL-*b*-PEO copolymer which involves carrying out the copolymerization in the bulk at 130 °C for 24 hours in the presence of stannous octoate as the catalyst. The copolymers obtained contain high molecular weight polycaprolactone, and the polydispersities of the copolymers were not reported.

The present paper is divided into two parts; the first includes a description of the copolymer synthesis and characterization, while the second discusses the characterization of the copolymer aggregates. The synthesis involves a new method for the preparation of PCL-*b*-PEO copolymers which produces copolymers with a relatively narrow molecular weight distribution and long poly(ϵ -caprolactone) blocks. The copolymerization may be carried out at ambient temperature within a short period of time and with a high degree of control. The characterization of the copolymer includes the determination of the copolymer composition, thermal behavior, critical water content and critical micelle concentration. The copolymer composition was determined by GPC and ¹H-NMR, while differential scanning calorimetry was used to study thermal behavior. Static light scattering measurements were employed to determine the critical water content values and a fluorimetric method was used to find the critical micelle concentrations. In the second part of the paper, we focus on several of the characteristics of the PCL-*b*-PEO aggregates,

such as electron microscopic analysis and incorporation studies of two different lipophilic compounds, pyrene and CM-DiI. The partition coefficient of pyrene between the micelles and water is determined for aggregates formed from copolymers with the same PEO block length but different polycaprolactone block lengths. Pyrene is also employed to measure the micropolarity of the polycaprolactone core. The incorporation of CM-DiI into the aggregates formed from different PCL-*b*-PEO copolymers is also studied. Finally, we report on the *in vitro* biocompatibility of several of the PCL-*b*-PEO copolymers, as we are interested in studying the aggregates formed from the series of PCL-*b*-PEO copolymers as carriers for various hydrophobic drugs.

In recent papers we have demonstrated the usefulness of one of the PCL-*b*-PEO copolymers, PCL₂₁-*b*-PEO₄₄, as a material used to form carriers for various lipophilic drugs such as the neurotrophic agents [8] FK506 and L-685,818, as well as for dihydrotestosterone [16]. The success of these studies has encouraged an interest in exploring a broader range of PCL-*b*-PEO aggregates, formed from copolymers of the same PEO block length but different PCL block lengths.

4.1.2. Experimental Section

4.1.2.1. Materials Tetrahydrofuran (Aldrich) was purified by refluxing it over a sodium bezophenone complex under nitrogen, a blue-violet color indicating a solvent free of oxygen and moisture. It was further distilled over poly(styryllithium) under reduced pressure in the final purification step. ϵ -Caprolactone (Aldrich) was twice dried over CaH₂ at room temperature and distilled under reduced pressure. Ethylene oxide (Matheson) was first purified with CaH₂ and then distilled over *n*-butyllithium just before use. Diphenylmethylpotassium (Ph₂CHK) was prepared at room temperature by reacting diphenylmethane with potassium naphthalene in THF for 24 h. Naphthalene potassium resulted from the reaction of potassium with naphthalene in THF at room temperature. Diethylaluminum chloride (Aldrich) in hexane was filtered prior to use. Pyrene was purchased from Aldrich Chemical Co.. The fluorescent dye, CM-DiI, was purchased from Molecular Probes Co.. The tissue culture reagents were all purchased from Gibco BRL. The

Alamar Blue was purchased from Biosource Camarillo and the Trypan Blue from Gibco BRL.

4.1.2.2. Experimental Methods

Copolymer Synthesis Sequential anionic polymerization of ethylene oxide and ϵ -caprolactone was carried out under an inert atmosphere in a previously flamed glass reactor equipped with a rubber septum. Syringes and stainless steel capillaries were used in order to transfer solvent, monomer, and initiator. THF and diphenyl methyl potassium, which were used as the solvent and the initiator, were first charged into the reactor. Pre-purified ethylene oxide monomer was slowly added to the initiator solution of known concentration at $-78\text{ }^{\circ}\text{C}$. The temperature was slowly increased from -78 to $+30\text{ }^{\circ}\text{C}$ over a period of 30 minutes. Thereafter, the reaction mixture was kept at $30\text{ }^{\circ}\text{C}$ for 24 hours. Then an aliquot of the reaction medium was withdrawn for analysis by GPC in order to determine the molecular weight of the first block. The equivalent amount of diethylaluminum chloride in hexane was added dropwise into the polymerization solution, followed by the addition of ϵ -CL monomer. Polymerization of ϵ -CL was performed at $25\text{ }^{\circ}\text{C}$ for *ca.* 20 hours. The polymerization was stopped by adding a 10-fold excess of HCl solution relative to aluminum. The polymers were recovered by precipitation into cold hexane and were dried under vacuum at room temperature for one week. The pure PEO-*b*-Poly(ϵ -CL) block copolymers were white powders.

Copolymer Characterization

Determination of the Copolymer Composition Size exclusion chromatography (SEC) was used to measure the degree of polymerization and polydispersity of the polymers. SEC was carried out in THF at room temperature using a Waters 510 liquid chromatography unit equipped with two Gel Columns (Styragel HR1 and HR4) and a refractive index detector (Varian RI-4). Millennium software was utilized. Polyethylene oxide standards were used for calibration to calculate the molecular weight of the PEO blocks. The degree of polymerization of the Poly(ϵ -CL) blocks were measured by Nuclear magnetic resonance (^1H -NMR) relative to the degree of polymerization of PEO block. ^1H -

NMR spectra were recorded on a Varian XL-300 spectrometer at room temperature. CDCl_3 was used as solvent with tetramethylsilane as an internal standard.

Study of Thermal Behavior The thermal properties of the PCL-*b*-PEO samples were analyzed using a Perkin Elmer DSC, model DSC-7. The samples were heated at a rate of 10°C per minute over a single heating cycle.

Determination of the Critical Water Content The copolymer solutions were prepared by dissolution of the copolymers in a common solvent, i.e. N,N-dimethylformamide (DMF), tetrahydrofuran (THF) or 1,4-dioxane. The solvents DMF, THF, and dioxane (Aldrich, HPLC grade) were used as received without further purification. All solutions were filtered through a membrane filter with a nominal pore size of 0.45 μm . Deionized water (Milli Q) was added with a micro-syringe.

The light scattering measurements were carried out on a DAWN-F multiangle laser photometer (Wyatt Technology, Santa Barbara, CA) equipped with a He-Ne Laser (632.8 nm). All measurements were carried out at room temperature. The scattered light intensity was recorded 15 minutes after each water addition and during this time interval the solutions were stirred.

Determination of the Critical Micelle Concentration The CMC of three different PCL-*b*-PEO copolymers of variable PCL block length was determined by fluorescence based on previously developed methods [17-19]. A specific aliquot of a PCL-*b*-PEO copolymer stock solution in chloroform was added to empty vials such that the final concentration of polymer in solution ranged from 1×10^{-9} to 2×10^{-4} g/mL. The chloroform was then allowed to evaporate and 4 mL of water was added to each vial. The vials were capped and stirred for 4 hours at 50°C. Each vial and contents were weighed prior to and following the heating period in order to ensure that water loss had not occurred. An aliquot of a pyrene stock solution in acetone was added to another set of empty vials such that the final concentration of pyrene in the solution would be 6×10^{-7} M. The acetone was allowed to evaporate and a 3 mL aliquot of the corresponding previously prepared polymer solutions in water was added

to each vial. The solutions were then left to stir for 2 hours at 50°C and then overnight at room temperature.

Steady-state fluorescence emission spectra were obtained using a SPEX Fluorolog-2 spectrometer in the right angle geometry. The fluorescence excitation spectra were obtained with $\lambda_{em} = 390\text{nm}$. For each solution the ratio of I_{338}/I_{333} was measured.

Micelle Characterization

Micelle Preparation Ten milligrams of PCL-*b*-PEO block copolymer was dissolved in up to 0.2 g of dimethylformamide and stirred for four hours. Micellization was induced by dropwise addition of 0.8 g of water at a rate of approximately one drop every ten seconds. The micelles were placed in a dialysis bag and dialyzed against MilliQ distilled water. The water was changed every hour for the first four hours and then every three hours for the next twelve hours.

Electron Microscopic Analysis Several different preparative techniques were tried in order to determine the optimal method for the electron microscopic analysis of this system. For the basic method of preparation a drop of the micelle solution was placed on a copper grid which was precoated with formvar and then coated with carbon. The excess solution was removed and the sample grid was allowed to dry. The sample grids were then shadowed with a platinum (Pt/C:95/5) filament. For the freeze-fracture/freeze-etch technique a small drop of a 1% (wt) PCL-*b*-PEO micelle solution was placed in the center of a sample holder and dipped into liquid nitrogen-cooled liquid propane (-140°C). After approximately 5 seconds, the sample holder was removed and placed into a liquid nitrogen bath. The sample holder was then placed in the freeze-fracture apparatus (Balzers 300) wherein the temperature ranged between -100 to -120°C. Sample fracture was performed using a liquid nitrogen cooled knife. Following freeze-fracture and freeze etch, the fracture plane was shadowed with platinum/carbon (95:5) at a 30° angle and then coated with carbon at a 90° angle. The Pt/C replica was floated off the holder using distilled water and placed onto uncoated copper grids. The sample grids were analyzed by transmission electron microscopy using a JEOL microscope.

Incorporation of Hydrophobic Solubilizates

Determination of the Partition Coefficient for Pyrene between the PCL-*b*-PEO Micelles and Water The fluorescence method employed to determine the partition coefficient has been described in detail elsewhere [17,19,20]. The method involves the determination of the partition coefficient of pyrene between mixed water/DMF solvent mixtures (60-90% water content) and block copolymer micelles (concentration PCL-*b*-PEO ranging from 1×10^6 to 1×10^{-2} g/g), at 25°C. The method is based on the sensitivity of pyrene to the hydrophobicity and polarity of its microenvironment. The intensity ratio of the vibrational band three to the vibrational band one (I_3/I_1) in the fluorescence emission spectrum of pyrene reflects the polarity of the surrounding environment of the pyrene molecules. The I_3/I_1 ratio can then be used to calculate the total amount of pyrene incorporated into the micelles, and from this the partition coefficient for pyrene between the micelles and a water/DMF mixture may be calculated. A semilogarithmic plot of the values of the partition coefficient for pyrene between the various DMF/water mixtures versus water content can then be extrapolated to 100% water in order to obtain the partition coefficient for pyrene between the PCL-*b*-PEO micelles and water.

An aliquot of pyrene in acetone was added to each of a series of sample vials such that the final concentration of pyrene in solution would be 1.5×10^{-9} mol/g. The acetone was allowed to evaporate, at which point different amounts of PCL₂₁-*b*-PEO₄₄ or PCL₄₀-*b*-PEO₄₄ copolymer were added to each vial followed by the addition of a specific amount of DMF. The solutions were left to stir for four hours, at which point micellization was achieved by the dropwise addition of water. The solutions were then allowed to stir overnight.

Steady-state fluorescence emission spectra were obtained using a SPEX Fluorolog-2 spectrometer in the right angle geometry. For each fluorescence measurement ca. 3 mL of solution was placed in a quartz cell. The fluorescence emission spectra were obtained with $\lambda_{\text{ex}} = 339 \text{ nm}$.

Measurement of the Micropolarity of the Micelle Core A series of samples were prepared in the same manner as described above for the determination of the partition coefficient for pyrene between the micelles and a DMF/water solvent mixture. However,

following preparation the samples were taken and dialyzed against Milli Q water in order to remove the organic solvent. The fluorescence emission spectra of each sample were acquired and the value of the I_3/I_1 ratio was recorded.

Measurement of the Loading Efficiency of the PCL-*b*-PEO Micelles for the Fluorescence Probe CM-DiI as a Function of Polycaprolactone Block Length or Copolymer Concentration The preparation of micelle-incorporated solubilizes requires the initial dissolution of a quantity of both the solubilize and the polymer in an organic solvent. During micellization, only a certain proportion of the dye will be incorporated into the micelles, and during dialysis both incorporated and non-incorporated drug will be lost. The loading efficiency is the ratio (expressed as a percentage) of the amount of hydrophobe in the micelles following dialysis to the total amount of hydrophobe initially dissolved in solution.

In order to measure the amount of CM-DiI in the micelle solutions a standard curve was produced for 0.01 – 1 uM CM-DiI in a DMF/water mixture (2.5 % water content). The fluorescence emission intensity at 570 nm ($\lambda_{\text{ex}} = 553\text{nm}$) was measured for each solution. A log-log plot was then made of the emission intensity versus CM-DiI concentration. The slope of this line along with the fluorescence emission intensity at 570 nm for each micelle solution was used to calculate the amount of CM-DiI present in the aliquots of each micelle solution.

For the sample preparation an aliquot of CM-DiI in DMF was initially added to several empty vials such that the final concentration of CM-DiI was 1×10^{-8} moles/g. An aliquot of a stock solution of PCL₂₁-*b*-PEO₄₄ in DMF was then added to each vial such that the final concentration of copolymer in solution was 1×10^{-2} g/g for the measurement of the loading efficiency as a function of block length and 1×10^{-5} to 1×10^{-1} g/g for measurement of the loading efficiency as a function of copolymer concentration. DMF was then added up to .2 g and the solution was allowed to stir for several hours. Micellization was induced by the dropwise addition of MilliQ water (.8g). The solution was allowed to stir overnight and was then dialyzed against MilliQ water. Following dialysis, a 100 uL aliquot of the micelle

solution was added to 3.9 mL of DMF in order to disrupt the micelles. The solutions were allowed to stir for several hours prior to measuring the fluorescence emission spectra (Perkin Elmer LS 50) of each solution.

***In vitro* Biocompatibility of the PCL-*b*-PEO Micelles of Variable PCL Block Length in PC12 Cell Cultures.**

PC12 cells were employed for all *in vitro* studies. The cells were maintained in DMEM supplemented with 10% horse serum, 5% fetal calf serum, 500ug/mL penicillin and 500ug/mL streptomycin at 37°C in 5% CO₂. The cells were plated in 24 well plates and cultured in RPMI medium supplemented with 5% fetal bovine serum. Aliquots of the 1% (wt) PCL-*b*-PEO micelle solution were added to the individual wells to make the final concentration of micelles in the wells to range from 0.004 – 0.2% (w/v). Control wells consisting of cells alone were used in each experiment. The micelles were incubated with the cells for both four and five day periods, at which point cell viability was analyzed using both the Alamar Blue survival assay and Trypan Blue exclusion dye assay, which have been described in detail elsewhere [8].

4.1.3. Results and Discussion

4.1.3.1. Synthesis of poly(*caprolactone*)-*b*-poly(*ethylene oxide*) Copolymers

The synthesis of the PCL-*b*-PEO copolymers was carried out by ring-opening polymerization of ethylene oxide, initiated by diphenyl methyl potassium, in THF at 30 °C for 24 hours. Following the addition of the desired amount of initiator into THF, the solution was cooled to –78 °C and the ethylene oxide monomer, in liquid form at –78 °C, was added dropwise to the initiator solution. As the temperature was raised from –78 to 30 °C (over a period of *ca.* 0.5 hour) the deep red color of the diphenyl methyl potassium solution faded as a result of the initiation reaction. The polymerization lasted 24 hours at 30°C. An aliquot of the reaction medium was withdrawn for analysis by GPC in order to determine the molecular weight of the PEO block. In keeping with previous results, the PEO has a relatively narrow and symmetric molecular weight distribution as shown by the SEC trace in Figure 4.1.

Poly(ethylene oxide) end-capped with diethylaluminum was obtained as a result of the addition of the equivalent amount of diethylaluminum chloride into the PEO-potassium

solution. Polymerization of ϵ -CL, initiated by PEO-diethylaluminum, was performed at 25 °C for *ca.* 20 hours. The polymerization was stopped by the addition of acid (0.1M HCL).

Aluminium alkoxides have proved to be very successful in the synthesis of polyesters such as poly(ϵ -caprolactone) and poly(D,L or L,L) lactides [21]. This coordination-insertion type of polymerization can be considered living polymerization and yields linear chains of a predictable molecular weight and narrow molecular weight distribution. Poly(ethylene oxide)-diethyl aluminum was obtained by the reaction of diethylaluminum chloride and poly(ethylene oxide) potassium, and was used as the macroinitiator for ϵ -caprolactone polymerization. SEC traces from the copolymerization reaction are also shown in Figure 4.1. The peaks in the SEC traces are narrow and symmetrical; however, the polydispersity of the block copolymer broadens somewhat with an increase in the PCL block length. For example, as shown in Figure 4.1, the polydispersity increases from 1.07 to 1.12 when the PCL block length is increased from a molecular weight of 5000 to 17 000.

It is worth mentioning that the copolymerization of ϵ -caprolactone initiated directly by poly(ethylene oxide) potassium did not give a pure block copolymer. The molecular weight distribution of the resulting copolymer was relatively broad and tailing on the low molecular weight side, and indicated the presence of homopolycaprolactone in the final product. A cyclic equilibrium oligomerization might be responsible for the formation of homopolymer.

Since it is not possible to measure the molecular weight of the second block in the diblock copolymer by GPC, another technique was required. Proton nuclear magnetic resonance ($^1\text{H-NMR}$) has been widely used for the determination of copolymer composition, provided that each component contains protons whose resonance is unique and distinguishable. Figure 4.2 shows a typical $^1\text{H-NMR}$ spectrum of a PCL-*b*-PEO copolymer. The sharp single resonance centered at 3.6 ppm is due to the methylene protons of the oxyethylene units of PEO; two equally intense triplets at 4.1 ppm and 2.3 ppm and a multiplet at about 1.5 ppm is due to the methylene protons of the oxycarbonyl-1,5-

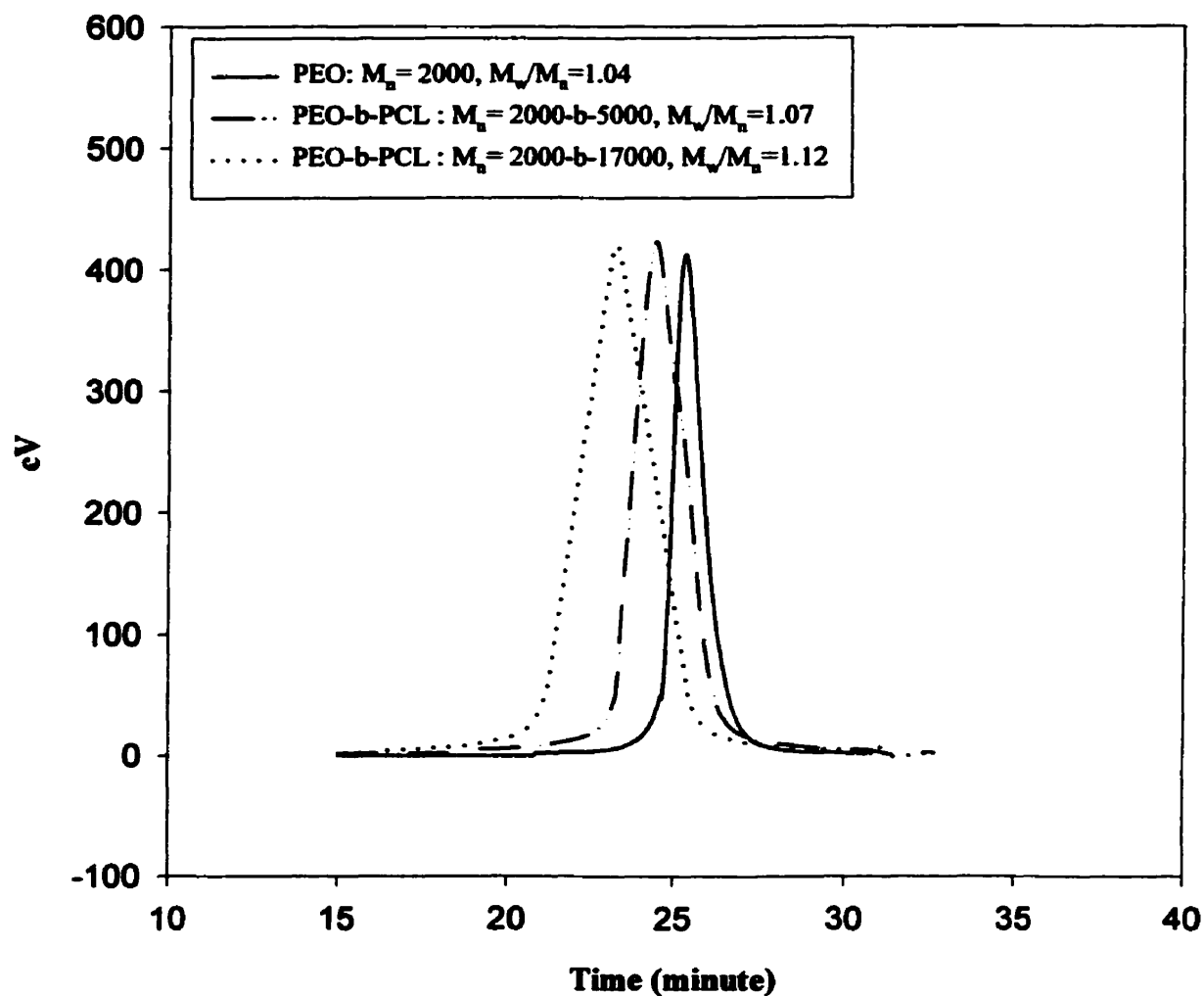


Figure 4.1. SEC traces of PEO homopolymer and PCL-b-PEO copolymers

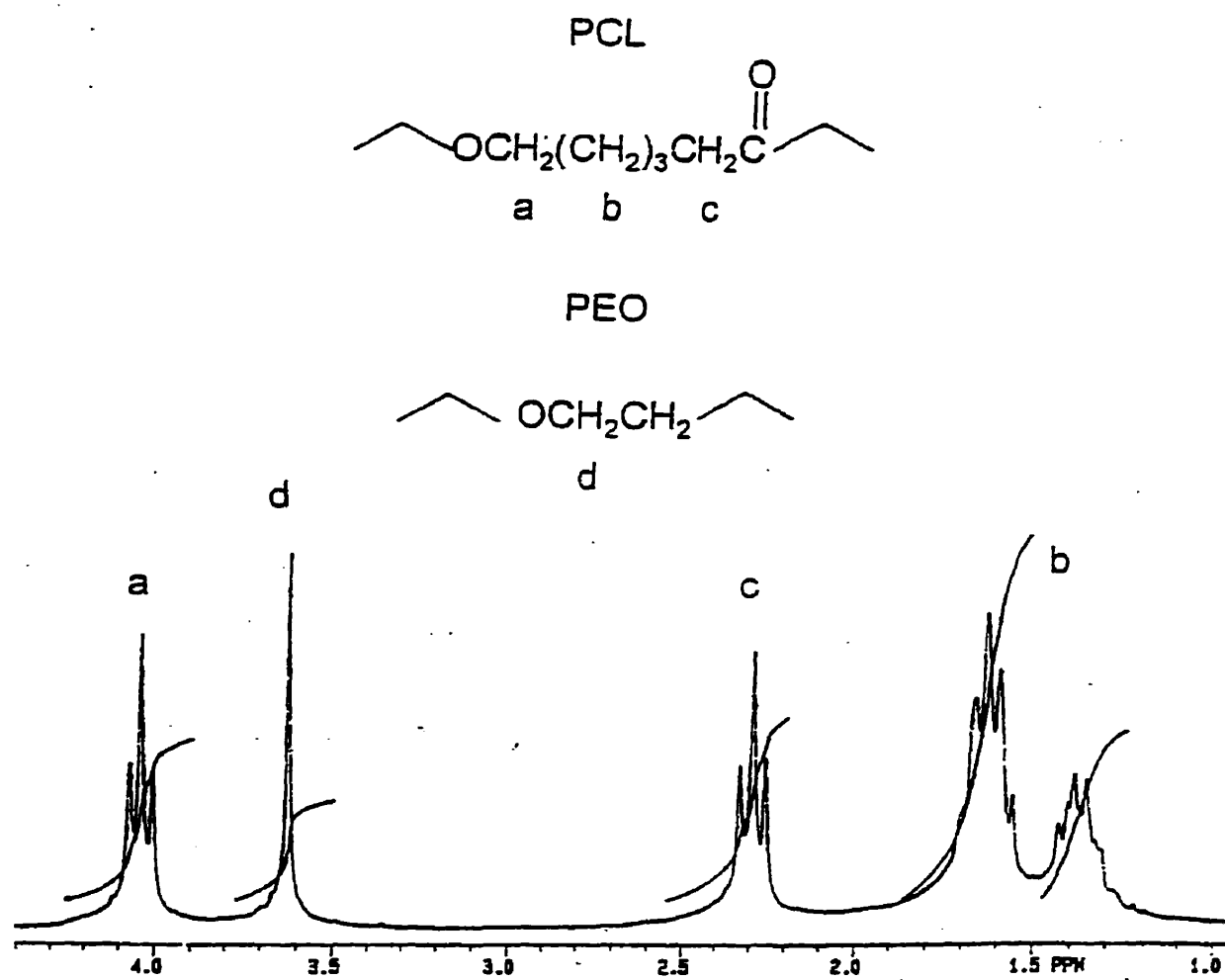


Figure 4.2. ^1H -NMR spectrum of PCL-*b*-PEO copolymer.

pentamethylene unit of a homosequence derived from CL ring opening. The mole fraction of each component in the block copolymer can be determined from the integral peak area ratio, and the degree of polymerization of the PCL block can be calculated relative to the degree of polymerization of the PEO block.

The time-conversion relationship for the ϵ -CL polymerization illustrated in Figure 4.3a shows that the polymerization of ϵ -CL is completed within 20 h. Figure 4.3b shows a linear increase of the degree of polymerization of the polycaprolactone with the degree of monomer conversion. This result confirms that the ring-opening polymerization of ϵ -CL is a living process without significant side reactions, such as chain transfer or termination.

4.1.3.2. Thermal Behavior of PCL-*b*-PEO Copolymers

Differential scanning calorimetry (DSC) measurements were carried out in order to broaden the polymer characterization to include information on the thermal behavior of the PCL-*b*-PEO copolymers. Figure 4.4, shows the thermographs of the copolymers with varying PCL block lengths. Trace A corresponds to the copolymer containing the highest PEO content, and displays a single endotherm starting at near 40 °C, which is very close to the melting temperature of crystalline PEO homopolymer of a similar molecular weight; for example, the melting temperature of PEO with a molecular weight of 1500 was reported to be 45°C [22]. This suggests that the melting of PEO in the block copolymer is responsible for this endotherm. Even after the addition of a few units of PCL, the PEO block retains a very high degree of crystallinity. When the PCL content increases, a second endotherm appears at 54 °C appears (traces B and C). With a further increase in the PCL block length, and a consequent decrease in the PEO content, the first endotherm disappears (trace D). The second endotherm peaking at 56°C is due to the melting of polycaprolactone. It is interesting to note that for a polycaprolactone block length of 14 (trace A) there appears to be no crystallinity in the polycaprolactone chains while in a copolymer with 150 caprolactone units the crystallinity of the PEO appears to be negligible (trace D). Thermographs from repeated runs on one PCL₄₀-*b*-PEO₄₄ diblock copolymer are shown in Figure 4.5. Trace A, the first run, displays two endotherms which start at 41 and 54°C, while traces B and C, the

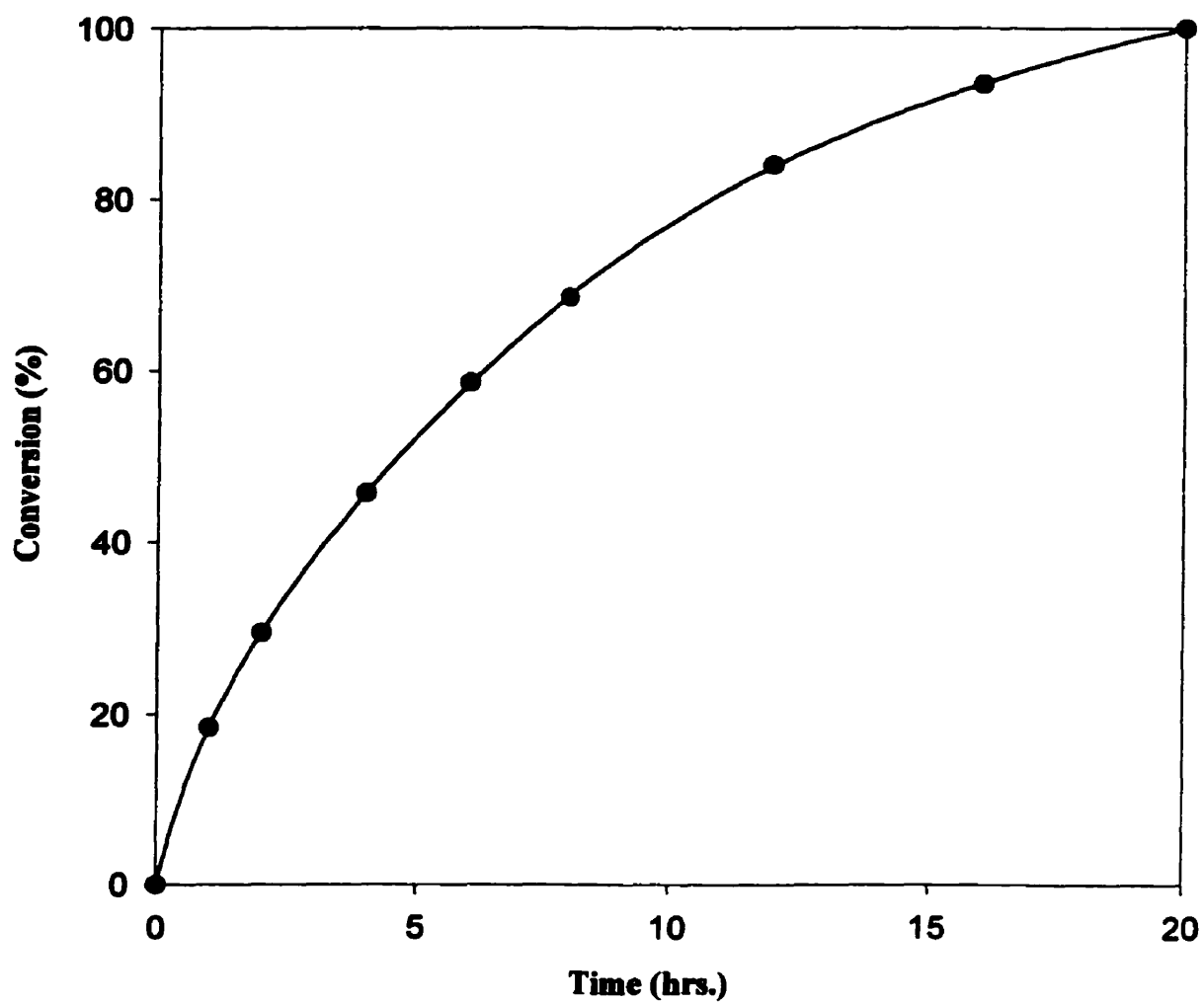


Figure 4.3a.: The conversion of ϵ -CL monomer versus polymerization time initiated by PEO diethyl aluminum macroinitiator in THF.

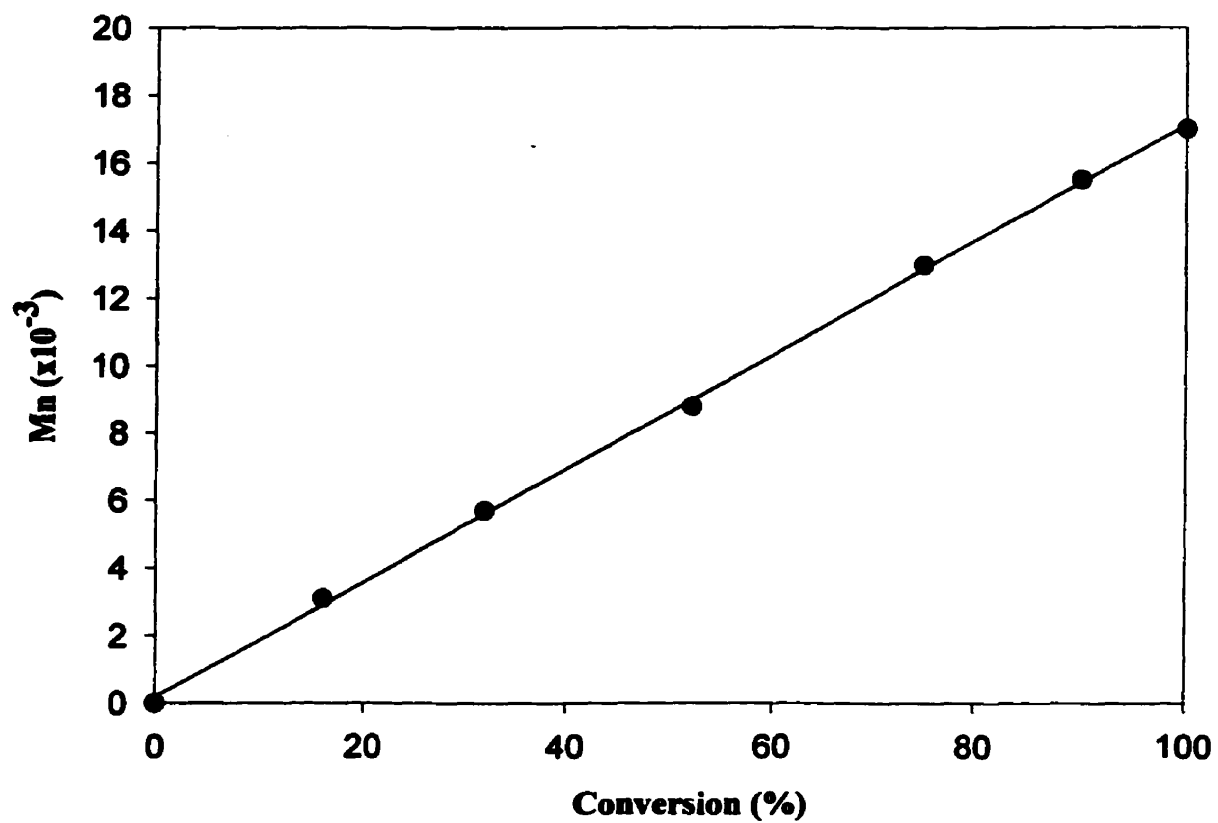


Figure 4.3b. The relationship between the molecular weight (M_n) and the conversion of ϵ -CL monomer in THF.

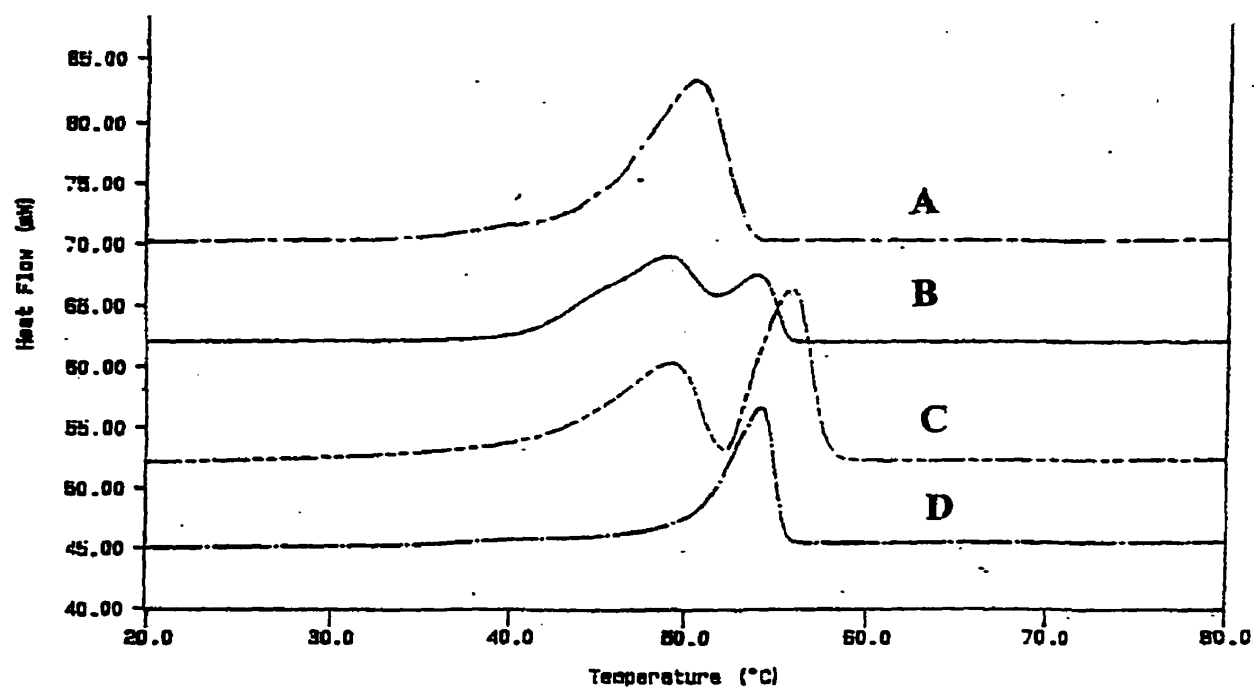


Figure 4.4. Thermographs of various PCL-b-PEO copolymers:

- A) PCL₁₄-b-PEO₄₄ B) PCL₂₀-b-PEO₄₄
 C) PCL₄₀-b-PEO₄₄ D) PCL₁₅₀-b-PEO₄₄

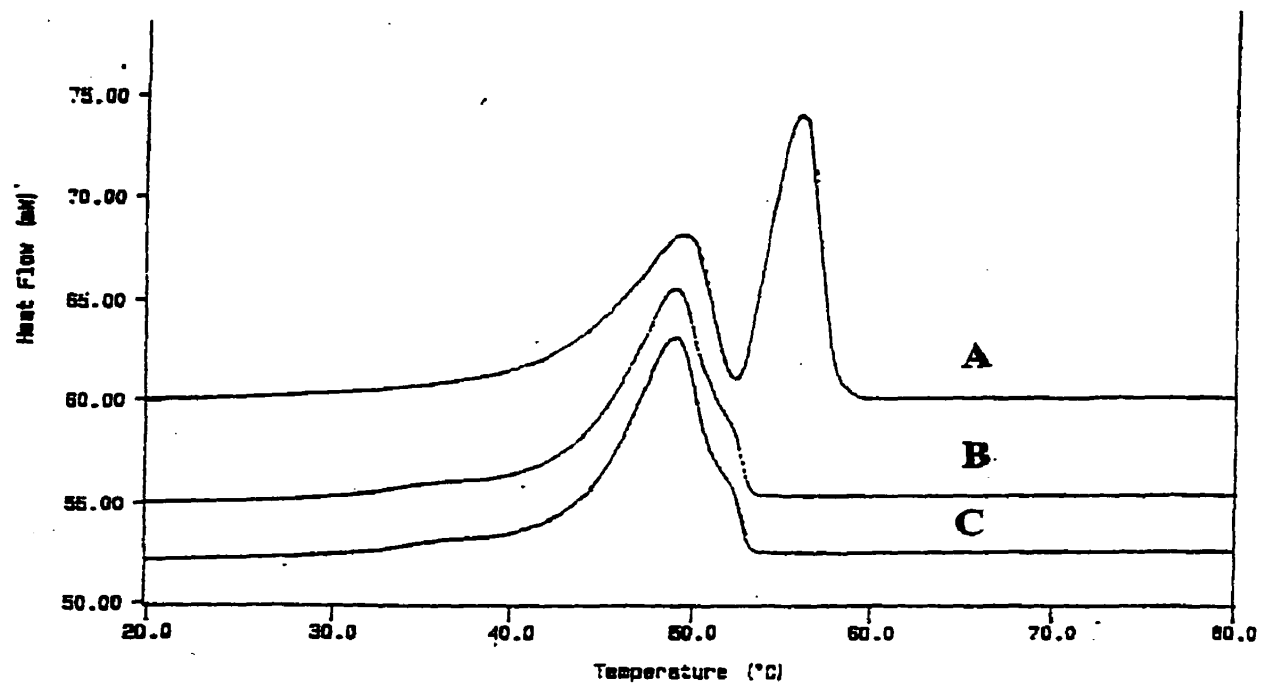


Figure 4.5. Thermographs of repeated runs of on one PCL₄₀-b-PEO₄₄ copolymer : A) first run, B) second run, C) third run.

second and third runs, display only a single endotherm which begins at 41 °C. It appears that the crystallinity of the PEO block develops much faster on cooling.

4.1.3.3. Aggregation Studies of the PCL-*b*-PEO Copolymers by Static Light Scattering Measurements

The aggregation of poly(ϵ -caprolactone)-*b*-poly(ethylene oxide) (PCL-*b*-PEO) diblock copolymers in solution was studied by static light scattering. The copolymer was dissolved in THF, a common solvent for both blocks of the copolymer. The addition of water causes the aggregation of the PCL-*b*-PEO copolymers since it is a good solvent for PEO but not for PCL. Due to the aggregation, the scattered light intensity increases suddenly and the solution appears cloudy.

Figure 4.6 shows the experimental curves of the scattered light intensity of PCL₉₆-*b*-PEO₄₄ copolymer in THF at various copolymer concentrations as a function of water content in the solvent mixture. For each solution, as long as the water content is relatively low (< 7%), the scattered light intensity changes only very little., implying that the copolymer remains unassociated. A critical water content is obtained from the intercept of the near horizontal and the sloping line segments of the scattered light intensity curves. In Figure 4.6 we see that the onset of the aggregation shifts to higher water contents as the initial copolymer concentration in THF decreases, as has been observed for other amphiphilic block copolymers [23].

Figure 4.7 shows a plot of the cwc as a function of the log of the copolymer concentration for three different copolymers which have the same PEO block length but differ in the length of their PCL block. A linear relationship is found between the cwc and the logarithm of the copolymer concentration, in agreement with previous findings on other copolymer-solvent-precipitant systems. In Figure 4.7 we also see that for any one copolymer, the cwc value decreases as the copolymer concentration is increased. Also, it is shown that for a specific copolymer concentration, the cwc decreases as the length of the hydrophobic poly(ϵ -caprolactone) increases, since the copolymers with the longer poly(ϵ -caprolactone) blocks start to aggregate at a lower water content than those with the shorter PCL blocks. This behavior is also in agreement with previous findings for other copolymer systems [23].

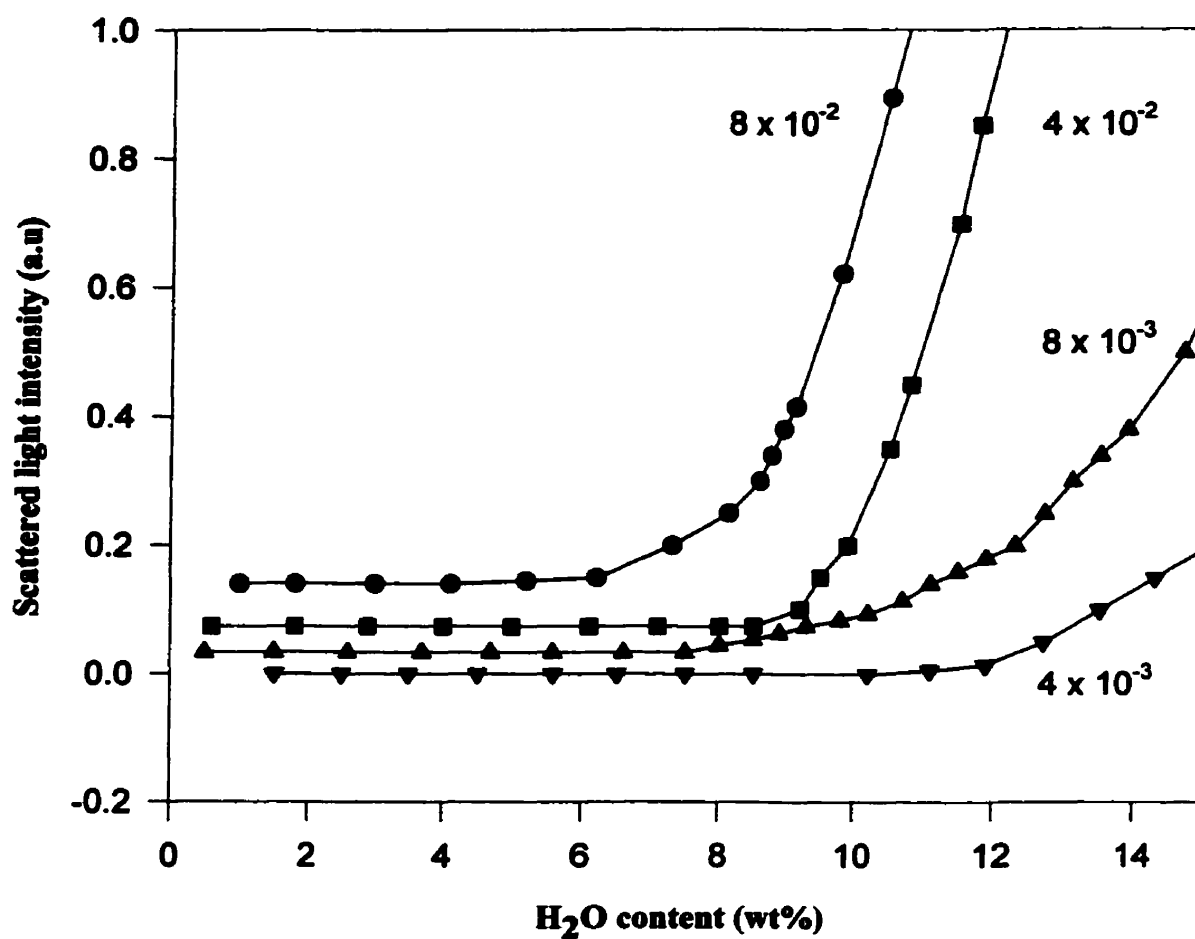


Figure 4.6. Plot of the scattered light intensity as a function of added water content for different concentrations (shown in brackets next to each curve) of PCL₉₆-b-PEO₄₄ in THF.

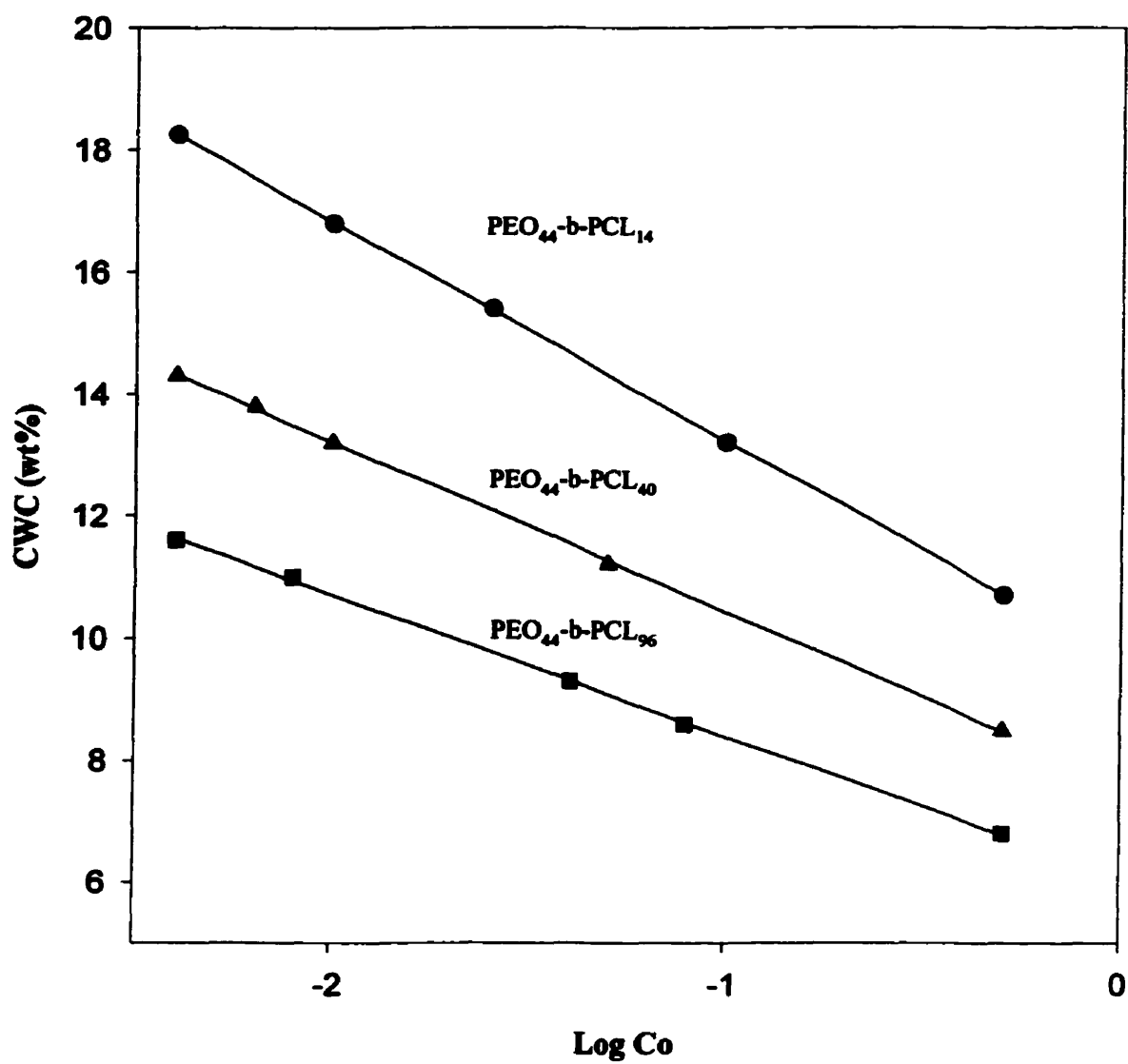


Figure 4.7. The semilogarithmic plot of the critical water content versus the copolymer concentration for various PCL-b-PEO copolymers in THF.

As expected, the relationship between the cwc and the copolymer concentration depends on the length of the PCL block; the longer the poly(ϵ -caprolactone) block, the smaller the slope $d[\text{cwc}] / d[\log C]$ of the line.

It is clear from the above that for a copolymer solution of a specific initial concentration when the water content is below a critical value the copolymer chains are unassociated. At the critical water content, the copolymers start to associate, and, as more water is added beyond the cwc, more polymer chains associate to form micelles, and the concentration of the copolymers in single-chain form decreases. Thus, it is of interest to see how the micelle fraction of the copolymers depends on the change of water content beyond the critical value. A relationship between the micelle fraction and the water content has been given in a previous paper [24]. The micelle fraction is defined as the ratio of the concentration of associated polymer to that of the total polymer, $(C_0 - C_{\text{cmc}})/C_0$ (where C_0 stands for the initial polymer concentration, and C_{cmc} for critical micellization concentration). In that solvent, the micelle fraction was found to increase rapidly within a very narrow range of water contents once microphase separation started. The micelle fraction can be calculated using the following relationship [24]:

$$(C_0 - C_{\text{cmc}})/C_0 = 1 - \exp(-2.303\Delta H_2O/A)$$

where ΔH_2O is the increment of the water content above the cwc and A is obtained from the slope $d[\text{cwc}]/d[\log C_0]$ in Figure 4.3. When the ΔH_2O value is zero or less (i.e. for water contents below the cwc), the $(C_0 - C_{\text{cmc}})/C_0$ is zero and all the copolymer chains in the solution are unassociated.

A plot of the micelle fraction against the increment of the water content is shown in Figure 4.8, with the insert showing the plot of the micelle fraction against absolute values of the water content. It is clear that the micelle fraction depends on both the length of the PCL block and the water content. Also, for copolymers with longer poly(ϵ -caprolactone) blocks, the micellization is completed within a narrower range of the increase in the water content.

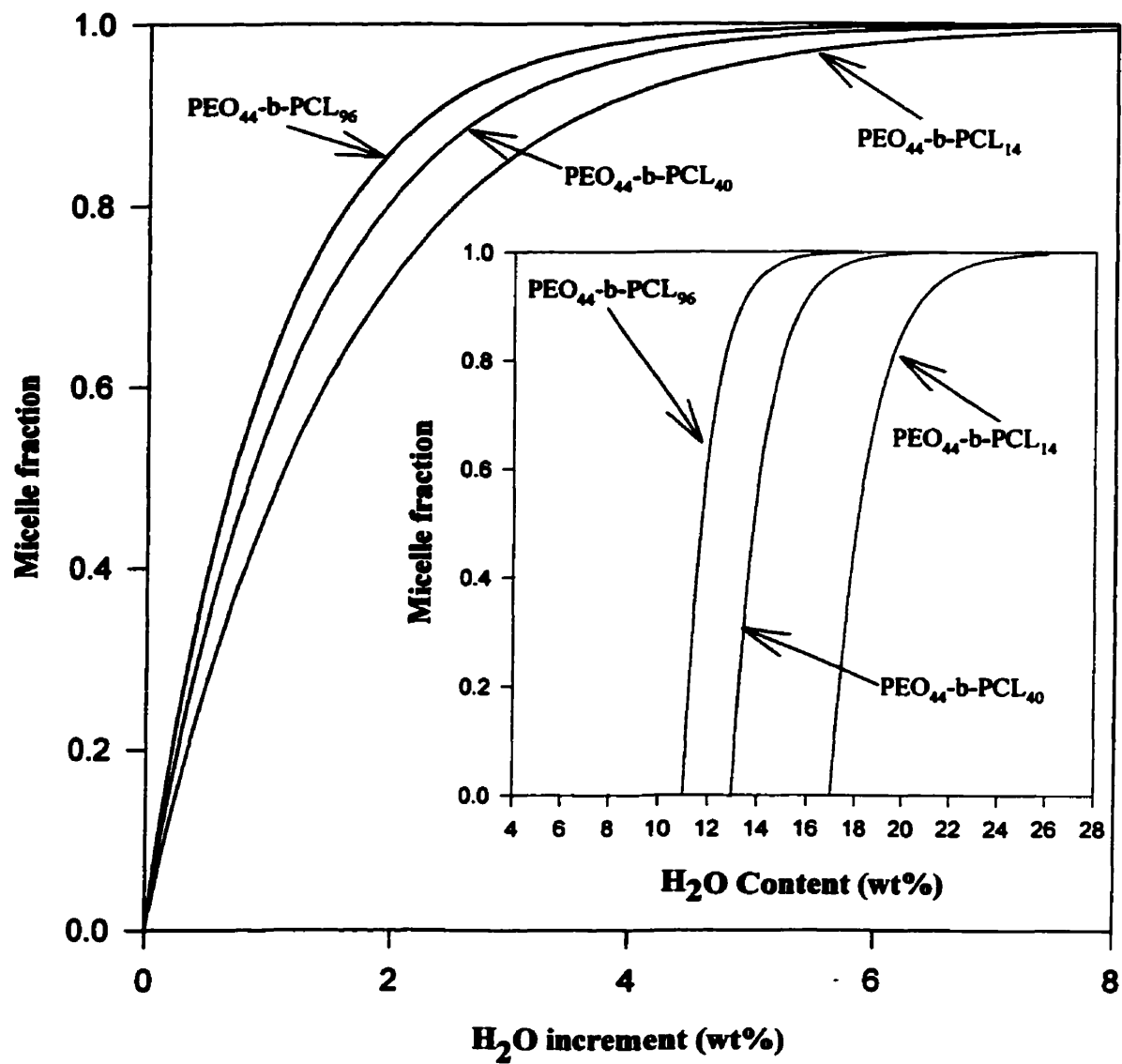


Figure 4.8. Plot of the micelle fraction as a function of the water increment beyond the critical water content for various PCL-b-PEO copolymers. The insert shows the plot against the absolute water content (1 wt%).

4.1.3.4. Crystallization of PCL block during micellization

The crystallization of the PCL block in the PCL-*b*-PEO aggregates was analyzed by DSC. The water in the PCL-*b*-PEO micelle solutions was removed and solid micelle particles were obtained by drying the samples at room temperature for two weeks. Figure 4.9 shows the thermographs of the dried micelles from three block copolymer samples; each shows an endotherm at 55° C characteristic of the melting point of PCL, indicating the PCL block crystallizes during micellization. The PEO shows a hint of a shoulder for the sample with the shortest PCL block.

4.1.3.5. CMC Determination

The determination of the critical micelle concentrations of several PCL-*b*-PEO (5-*b*-44, 12-*b*-44 and 21-*b*-44) copolymers was performed by a fluorescence method using pyrene as the probe. Pyrene is a hydrophobic compound which is sensitive to the polarity of its microenvironment. The method employed involves the measurement of the I_{338}/I_{333} ratio within the excitation spectrum of pyrene over a range of copolymer concentrations. The initial formation of micelles is marked by a large increase in the I_{338}/I_{333} ratio.

The CMC values obtained (Figure 4.10) were 1.9×10^{-5} , 8.9×10^{-7} and 2.8×10^{-7} mol/L for the PCL-*b*-PEO copolymers; 5-*b*-44, 12-*b*-44, 21-*b*-44 respectively. In units of mg/L, the CMC values are 47, 2.9 and 1.2 for the same samples. The decrease in CMC accompanying the increase in the polycaprolactone block length was anticipated.

The CMC values for PCL-*b*-PEO are in the same range as those obtained for the poly(ethylene oxide)-*b*-poly(β -benzyl L-aspartate) system (5-18 mg/L) [2a, 25] and the polylactide-*b*-poly(ethylene glycol) system (35 mg/L). The values are also in the same range as the CMC values for the polystyrene-*b*-poly(ethylene oxide) system reported by Wilhelm (1-5 mg/L) [17]. In addition, the CMC values for the PCL-*b*-PEO system are lower than the values obtained for the oligo(methyl methacrylate)-*b*-poly(acrylic acid) which has a CMC of 100 mg/L [5] and also lower than the CMC values for some of the poly(ethylene oxide)-*b*-poly(propylene oxide)-*b*-poly(ethylene oxide) systems which fall in the range of 10 - 1000 mg/L [1d]. The low CMC values obtained for the PCL-*b*-PEO system reflect the inherent stability of this system to dilution. A micellar drug delivery system is subject to sink

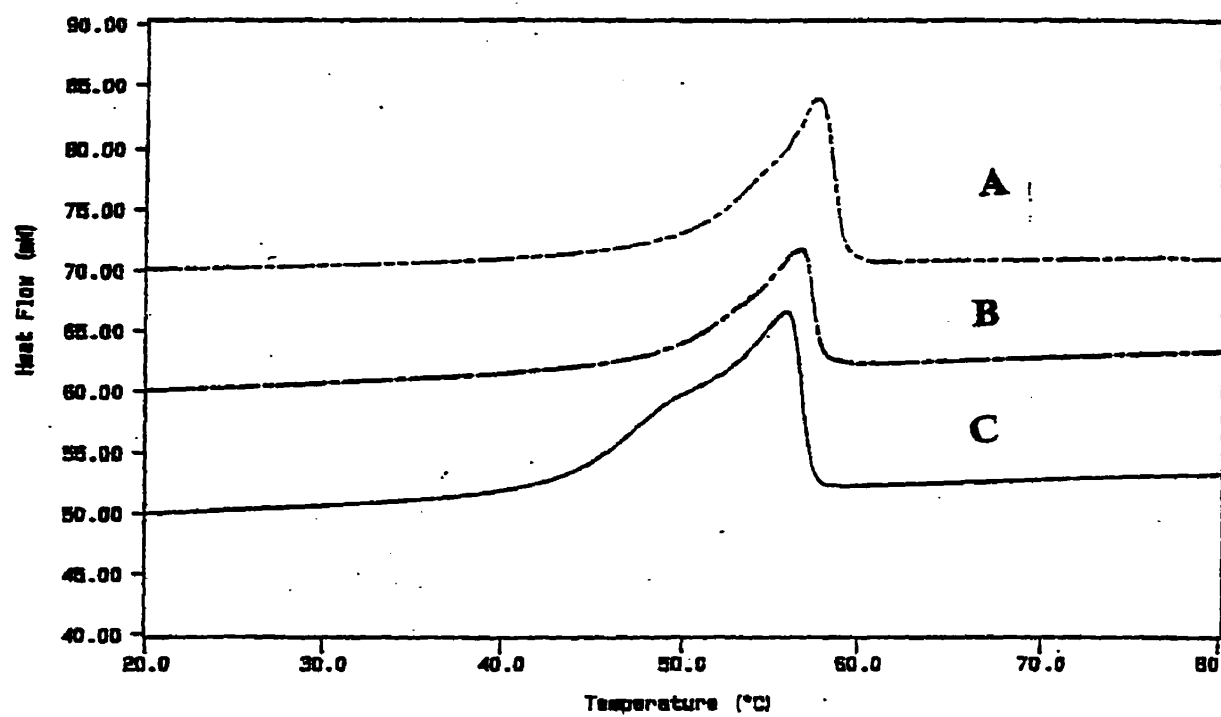


Figure 4.9. Thermographs of various PCL-b-PEO aggregates:
A. PCL₉₀-b-PEO₄₄; B. PCL₄₅-b-PEO₄₄; C. PCL₃₅-b-PEO₄₄

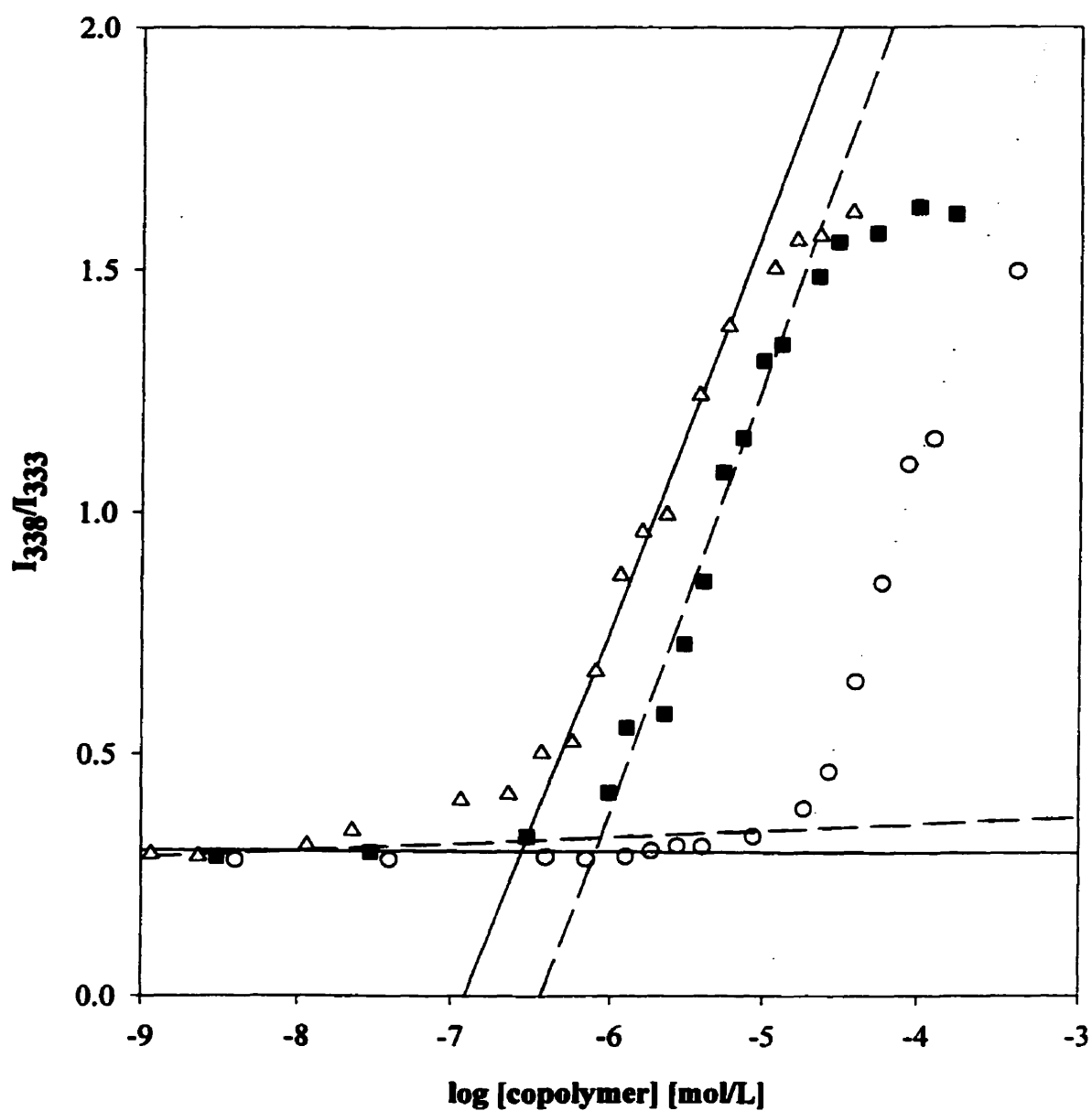


Figure 4.10. A semilogarithmic plot of the ratio of I_{338}/I_{333} of pyrene versus the copolymer concentration.

conditions upon intravenous injection into an animal or human subject. A rat, for instance, has approximately 6 % of its body weight as blood volume; thus, for a 100 g rat, the volume of blood is approximately 8 mL. Following the intravenous injection of a 100 μ L dose of a 1% (wt) solution of the PCL-*b*-PEO micelles, the concentration of copolymer in the blood will be 125 mg/L. This concentration is well above the CMC of both the PCL₁₂-*b*-PEO₄₄ and the PCL₂₁-*b*-PEO₄₄ systems and twice as high as the CMC of the PCL₅-*b*-PEO₄₄ system. Thus, given at this dose, most of the micelles will remain intact following intravenous injection. However, a 50 μ L dose of a 1% solution of the PCL-*b*-PEO micelles into a 300 g rat would result in a final concentration of 28 mg/L of copolymer in the total blood volume. This concentration is below that of the CMC of the PCL₅-*b*-PEO₄₄ system, and thus, upon injection, the micelles would convert into a population of single copolymer chains. Considerations of this type are essential in order to guarantee the most effective use of a micellar delivery vehicle [26]. Overall, a balance must be achieved between the initial stability of the micelles to sink conditions which they face upon injection, and the eventual disassembly of the micelles into single chains in order to facilitate their elimination from the body.

4.1.3.6. Determination of Micelle Morphology

Transmission electron microscopy was used as a means of studying the morphology of the PCL₂₀-*b*-PEO₄₄ micelles in water. In the first series of studies, the traditional methods of sample grid preparation were employed. In each case, the electron micrograph revealed only clusters of aggregates which did not have very clear or distinct morphologies. In addition, the aggregates were different in appearance depending on the surface (i.e mica, copper, copper coated with formvar, copper coated with carbon etc.) to which the sample had been applied. This suggested that the appearance of aggregates was surface specific and not representative of the actual morphology of aggregates in solution. For this reason freeze-fracture was adopted as a means of identifying the morphology.

The freeze-fracture technique employed revealed individual spherical aggregates of approximately 25 nm in size and larger clusters of individual aggregates strung together in a pearl necklace pattern (Figure 4.11a and 4.11b). The aggregation of the PCL-*b*-PEO

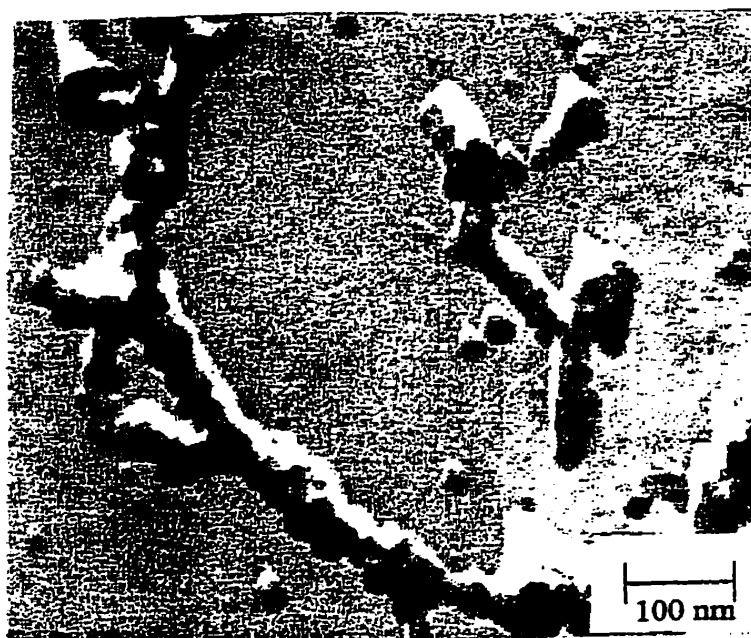
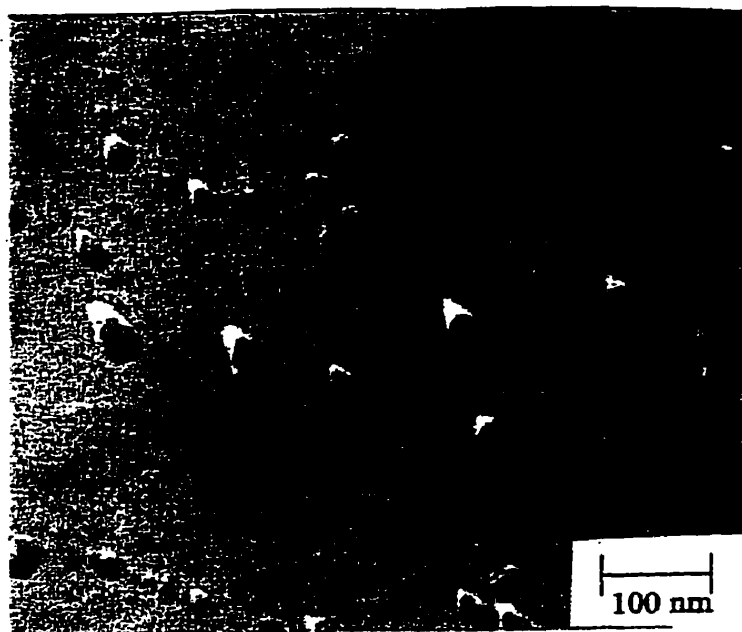


Figure 4.11a and b) The freeze-fracture/freeze etch electron micrograph of a 1% (w/w) solution of PCL₂₀-b-PEO₄₄ copolymer.

micelles into the larger clusters is in keeping with the behavior of block copolymer micelles with a poly(ethylene oxide) shell [2b, 27]. The results from the dynamic light scattering measurements of this system, which were reported elsewhere, [8] also revealed a bimodal population distribution including small aggregates of approximately 50 nm and larger aggregates of 500 nm. It was also found that the progressive dilution of a .1% (w/w) micelle solution to .02% (w/w) resulted in a shift in the bimodal population distribution from a high number of large aggregates in the more concentrated solutions to a higher number of the smaller aggregates in the solutions of lower concentration. This suggested that the larger aggregates were clusters of single micelles. The picture of the necklace-like aggregates clearly reveals that the larger aggregates are composed of individual micelles.

4.1.3.7. Incorporation of Hydrophobic Solubilizates

Determination of the Partition Coefficient for Pyrene between the PCL-*b*-PEO Micelles and Water

The values for the partition coefficient for pyrene between PCL-*b*-PEO micelles and water were found to be 240 [8], 760 and 1450 for the PCL₁₄-*b*-PEO₄₄, PCL₂₁-*b*-PEO₄₄ and PCL₄₀-*b*-PEO₄₄ systems, respectively. The increase in the partition coefficient with increasing block length reflects the increased cargo space of the PCL-*b*-PEO micelles with longer polycaprolactone blocks, assuming the aggregates are all spherical. Also, as the size of the aggregates increase the surface to volume ratio is decreased, which in turn means that in the larger aggregates a smaller fraction of the pyrene will be solubilized at the core-corona interface; this may also act to increase the I_3/I_1 ratio. The value for the partition coefficient of pyrene between the PCL₄₀-*b*-PEO₄₄ micelles and water is about three times higher than the value reported for a micelle system formed from poly(ethylene oxide)_{51/2}-*b*-poly(propylene oxide)₃₈-*b*-poly(ethylene oxide)_{51/2} micelles and water ($K_v = 460$) [19]. However, the K_v value for pyrene in PCL₄₀-*b*-PEO₄₄ micelles is an order of magnitude lower than that obtained for the poly(ethylene oxide)-*b*-poly(β -benzyl aspartate) micelles [25]. The higher value obtained for the PBLA-*b*-PEO system may be due to the presence of the benzyl group within the core-forming block, which may interact more strongly with pyrene than groups within the poly(caprolactone) block. Several studies have revealed that the compatibility between the solubilizate and the core-forming block largely influences the

extent to which solubilization occurs [28, 29]. This aspect is discussed more fully in a recent review [26].

The micropolarity of the polycaprolactone micelle core was also measured by fluorescence. The dialyzed PCL-*b*-PEO micelle solutions were found to have an I_3/I_1 ratio of 0.6. The value of 0.6 is much lower than that obtained for pyrene in the micelles formed from polystyrene-*b*-poly(ethylene oxide) copolymer, where it was reported to be 0.83 [17]. Also, for the PBLA-*b*-PEO system, the I_3/I_1 ratio was found to be 0.71 [25]. The partition coefficient for pyrene between PS-*b*-PEO micelles and water is of the order of 10^5 [17] while for the PBLA-*b*-PEO [25] system it is reported to be in the 10^4 range; furthermore for the PCL₄₀-*b*-PEO₄₄ micelles the partition coefficient is of the order of 10^3 . This demonstrates the relationship between the micropolarity of the micelle core as measured by I_3/I_1 and the extent to which the pyrene molecules are solubilized by the micelles. The greater the I_3/I_1 ratio the greater the partition coefficient of pyrene between the micelle core and water.

4.1.3.8. Loading Efficiency of the PCL-*b*-PEO Micelles for CM-DiI as a Function of Polycaprolactone Block Length.

As shown in Figure 4.12a, the loading efficiency of the PCL-*b*-PEO micelles for CM-DiI was found to increase with an increase in the length of the polycaprolactone core-forming block. The increase in the loading efficiency as a function of block length parallels the increase in the partition coefficient for pyrene as a function of polycaprolactone block length. The increase in the length of the core-forming block increases the diameter and thus the loading space within the individual micelles, assuming all aggregates are spherical. The increased hydrophobic content within the micelle core facilitates interaction between the polymer and drug molecules; this may act to enhance incorporation.

Also, as the length of the core-forming block is increased, the surface to volume ratio of the micelles decreases, assuming all micelles are spherical. During dialysis, the amount of drug lost will largely be dependent upon the amount which is located at the micelle surface.

Assuming that the conditions are such that there is little drug lost from the interior of the micelle core. Thus, as the length of the polycaprolactone block increases, less drug will be located at the micelle surface due to the decrease in the surface to volume ratio. Thus,

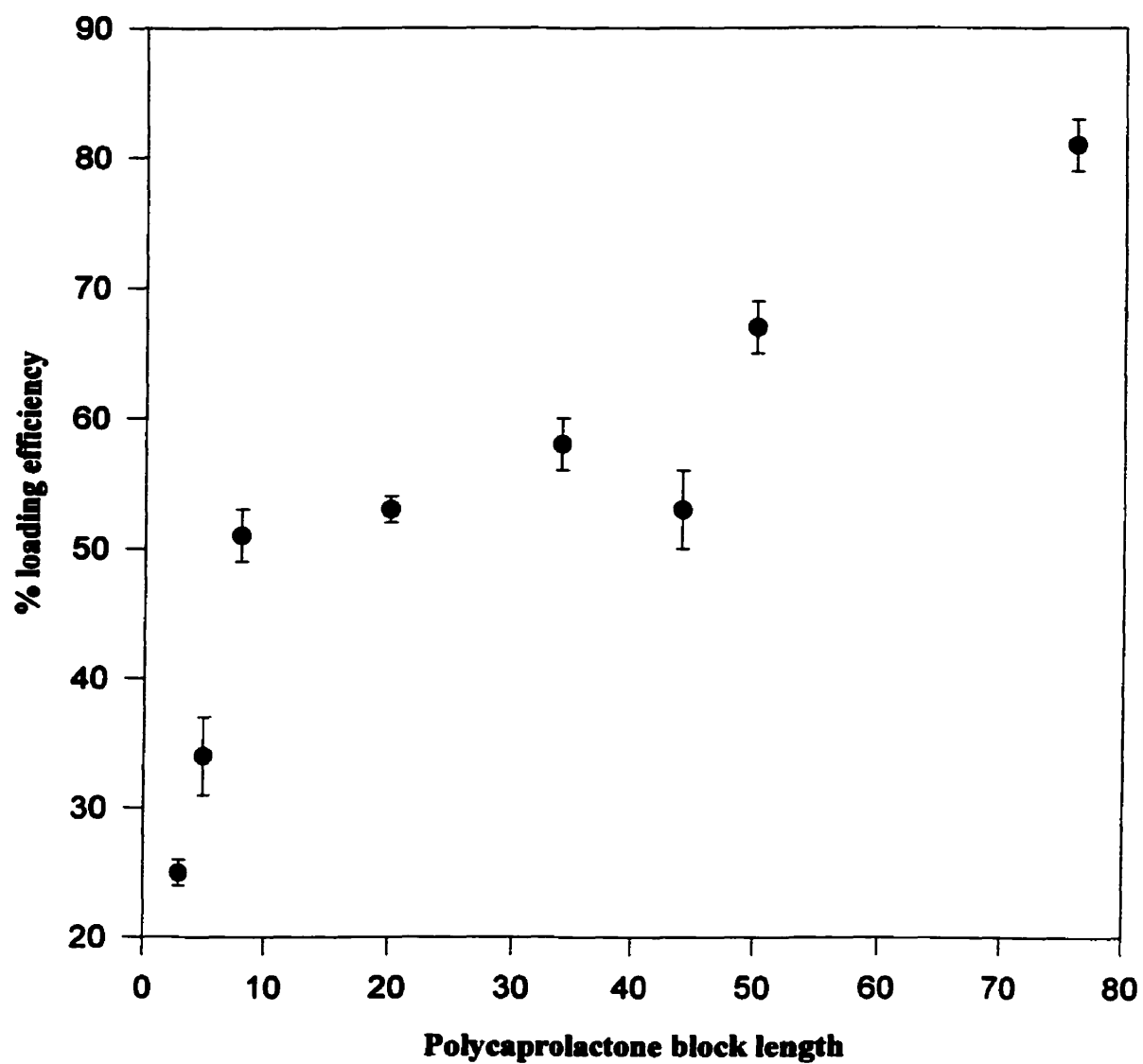


Figure 4.12 a) Plot of the % loading efficiency of CM-DiI versus the block length of polycaprolactone in the copolymer used to form the PCL-b-PEO aggregates.

during the dialysis process, more drug will be lost from the micelles with the longer polycaprolactone block lengths.

The loading efficiency of DiI into the PCL-*b*-PEO micelles was also measured as a function of the copolymer concentration (Figure 4.12b). In this case, it was found that the loading efficiency was increased as the copolymer concentration was increased from 1×10^{-6} to 1×10^{-2} g/g. However, at concentrations above 1×10^{-2} g/g the loading efficiency leveled off. Thus from 1×10^{-6} to 1×10^{-2} g/g copolymer the amount of DiI incorporated increases as the copolymer concentration is increased; however, above this concentration, the amount of DiI incorporated remains the same. This type of behavior has been previously reported in a study by Hurter and Hatton who found that there were two different patterns for the incorporation of naphthalene into PEO-*b*-PPO-*b*-PEO copolymers [30-32]. For the PEO-*b*-PPO-*b*-PEO copolymers with a higher hydrophobic content, the degree of solubilization did not increase with increasing copolymer concentration; however, for the copolymers with the higher hydrophilic content, the degree of solubilization did increase with an increase in copolymer concentration [30-32].

4.1.3.9. *In vitro* Biocompatibility of the PCL-*b*-PEO Micelles

The *in vitro* biocompatibility of the PCL-*b*-PEO micelles was assessed by incubating the different micelles with PC12 cells for a 1 – 4 day period. As previously reported [8], the *in vitro* biocompatibility of the PCL₂₁-*b*-PEO₄₄ micelles had already been confirmed for both 24 and 48 hour incubation periods. In Figure 4.13, we see the results from the incubation of several of the PCL-*b*-PEO systems (final concentration of 0.2% (w/w) in each cell well) with PC12 cells for 1-4 days. The biocompatibility of the PCL₂₁-*b*-PEO₄₄ and PCL₁₂-*b*-PEO₄₄ systems was confirmed with to be above 92 % for all incubation periods. However, in the case of micelles formed from copolymers with shorter PCL block lengths, the biocompatibility results were quite different for the 2 – 4 day incubation periods with survival falling to 66% for the PCL₅-*b*-PEO₄₄ system following the four day incubation period. At this point the reason for the lower survival rate of cells incubated with the PCL-*b*-PEO micelles with short PCL blocks for incubation periods beyond 24 hours is unknown.

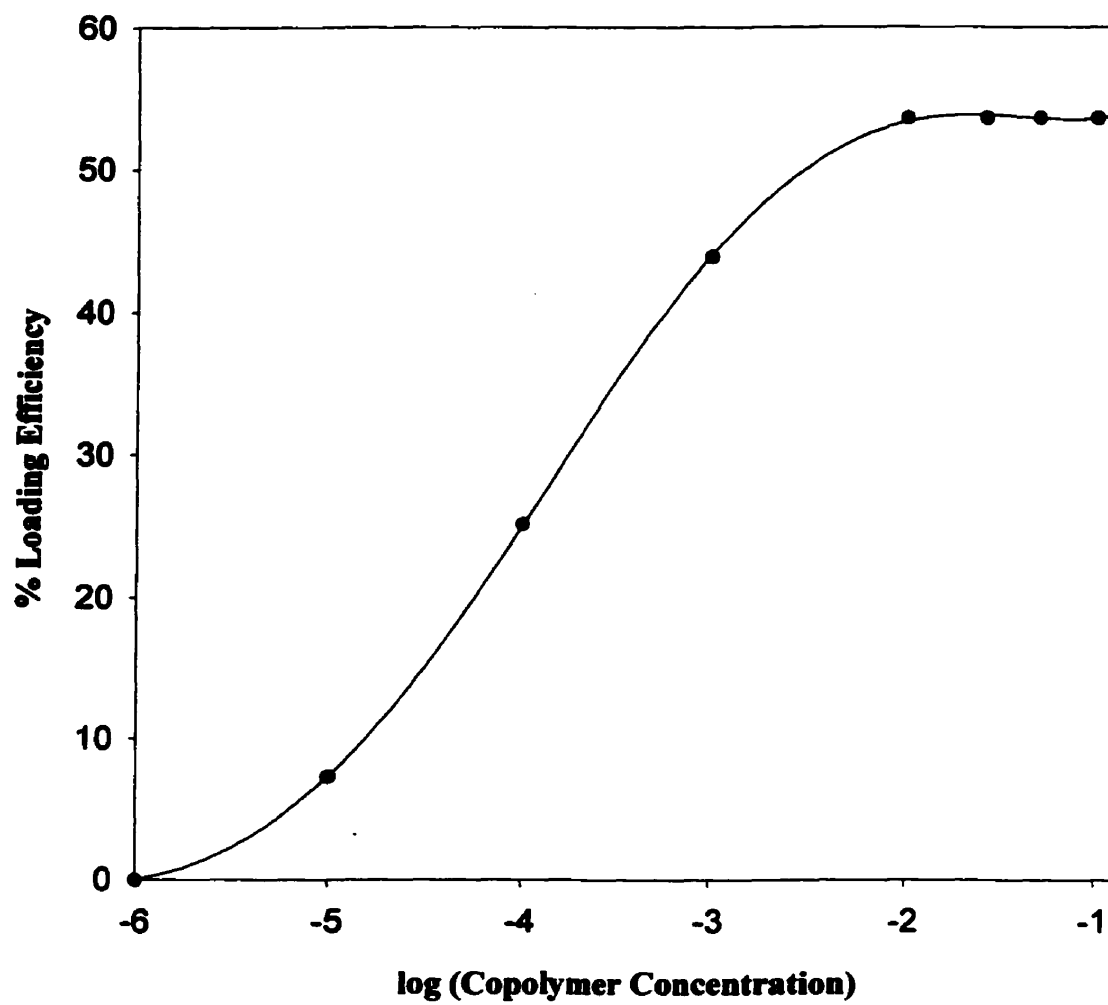


Figure 4.12b) Plot of the % loading efficiency of CM-DiI versus the PCL₂₀-b-PEO₄₄ copolymer concentration.

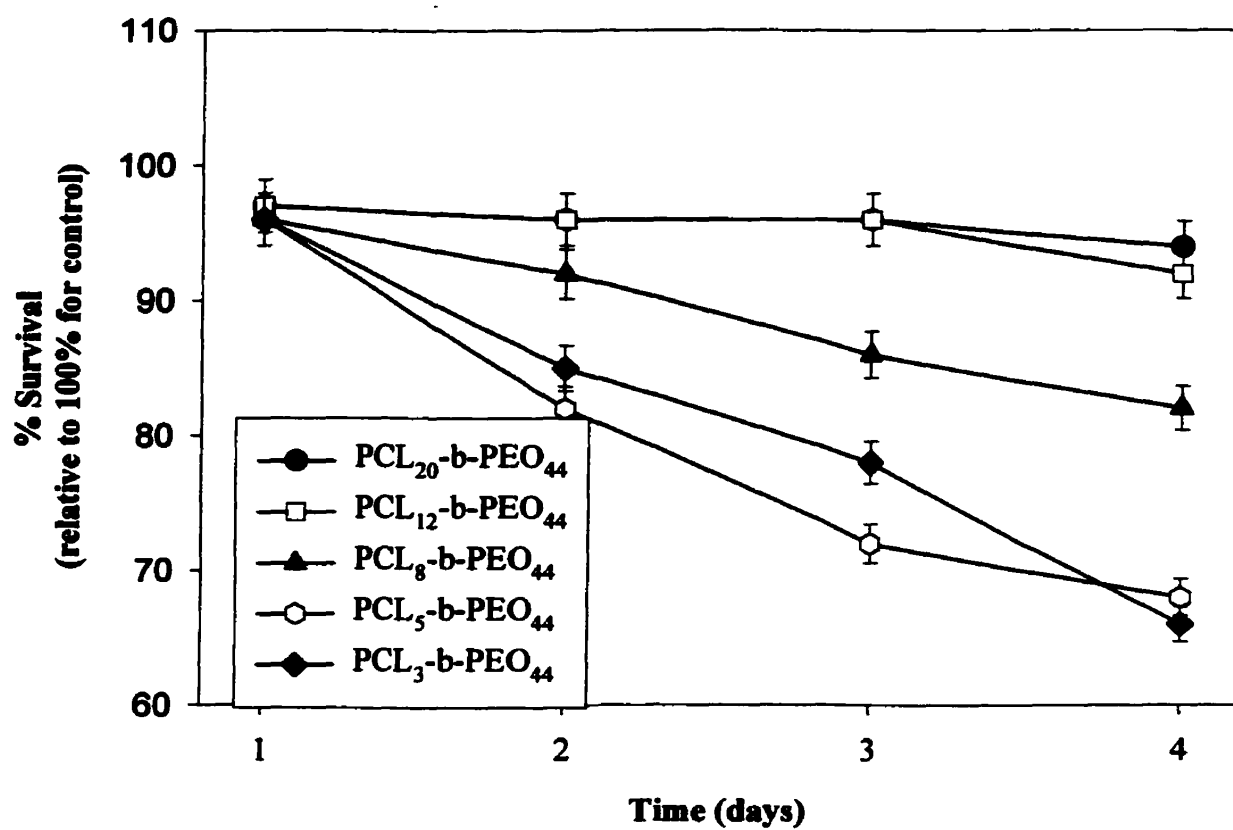


Figure 4.13. The plot of the % cell survival versus the incubation time in PC12 cell cultures.

4.1.4. Conclusion

We have reported a novel method for the synthesis of biocompatible and biodegradable copolymers of polycaprolactone-b-poly(ethylene oxide). The copolymers and the aggregates were studied with emphasis placed on characteristics of greatest interest to applications in drug delivery. Clearly, each of the properties including critical water content, critical micelle concentration, partition coefficient for pyrene, loading efficiency and in vitro biocompatibility were found to be dependent on the length of the core-forming block. This reflects the extent to which the characteristics of the micelle can be controlled by altering the properties of the copolymer used to prepare the micelle.

4.1.5. References

- 1a) Alakhov V.Y., Moskaleva E.Y., Batrakova E.V., Kabanov A.V., *Bioconjugate Chemistry* **1996**, 7, 209. 1b) Miller D.W., Batrakova E.V., Waltner T.O., Alakhov V.Y., Kabanov A.V., *J. Biocon. Chem.* **1997**, 8, 649. 1c) Batrakova E.V., Han H.Y., Alakhov V.Y., Miller D.W., Kabanov A.V., *Pharmaceutical Research* **1998**, 15, 850. 1d) V.Y. Alakhov, A.V. Kabanov, *Exp. Opin. Invest. Drugs* **1998**, 30, 49. 1e) Kabanov A. V., Kabanov V.A., *Advanced Drug Delivery Reviews* **1998**, 30, 49.
- 2a). La, S.B.; Okano, T.; Kataoka K.; *Journal of Pharmaceutical Sciences* **1996**, 85, 85.; (b) S. Cammas, K. Suzuki, C. Sone, Y. Sakurai, K. Kataoka, T. Okano, *J. Controlled Release* **1997**, 48, 157; (c). Yokoyama M., Fukushima S., Uehara R., Okamoto K., Kataoka K., Sakurai Y., Okano T., *Journal of Controlled Release* **1998**, 50, 79-92; (d).Kwon G., Naito M., Yokoyama M., Okano T., Sakurai Y., Kataoka K., *Journal of Controlled Release* **1997**, 48, 195-201; (e)Kwon G.S., Kataoka K., *Advanced Drug Delivery Reviews* **1995**, 16, 295-309.
3. Hagan S.A., Coombes A.G.A., Garnett M.C., Dunn S.E., Davies M.C., Illum L., Davis S.S. *Langmuir* **1996**, 12, 2153-2161.
4. Jeong, Y.I., Cheon J.B., Kim S.H., Nah J.W., Lee Y.M., Sung Y.K., Akaike T., Cho C.S. *J. Control. Release* **1998**, 51, 169.
5. Inoue, T., Chen G., Nakamae K., Hoffman A.S., *Journal of Controlled Release* **1998**, 51, 221.
6. Nah, J.W., Jeong Y.I., Cho C.S. *J. Polym. Sci.: Part B: Polym. Phys.*, **1998**, 36, 415.
7. Zhang X., Burt H.M., Von Hoff D., Dexter D., Mangold G., Degen D., Oktaba A.M., Hunter W.L. *Cancer Chemother. Pharmacol.*, **1997**, 40, 81.
8. Allen C., Yu Y., Maysinger D., Eisenberg A., *Bioconjugate Chemistry* **1998**, 9, 564.
9. (a) Zhang, L.; Eisenberg, A. *Science* **1995**, 268, 1728; (b) Zhang, L.; Yu, K.; Eisenberg, A. *Science* **1996**, 272, 1777. (c) Yu, Y.; Eisenberg, A. *J. Am. Chem. Soc.* **1997**, 119, 8383. (d) Cameron N., Corbiere M.K., Eisenberg A. *Canadian Journal of Chemistry* **1999** accepted. (e) Yu K., Zhang L., Eisenberg A., *Langmuir* **1996**, 5980. (f) Zhang L., Bartels C., Yu Y., Shen H., Eisenberg A., *Phys. Rev. Letters* **1997**, 79, 5034.

10. Kim S.Y., Shin I.G., Lee Y.M., Cho C.S., Sung Y.K., *Journal of Controlled Release* **1998**, 51, 13.
11. Bei, J.; Wang,Z.; and Wang, S.; Drug Release Behavior, *Chin J. Polym. Sci.*, **1995**, 2, 154.
12. Martini, L.; Collett, J.H.; and Attwood,D., *J. Pharm. Pharmacol.* **1997**, 49, 601.
13. Perret, R. and Skoulios, A. *Die Makromolekulare Chemie* **1972**, 56, 143.
- 14.Cerrai, P.; Tricoli, M.; Andruzzi, F.; Paci,M. and Paci,M. *Polymer* **1989**,30,338.
15. Bogdanov,B.; Vidts, A.; Bulcke, A Van Den; Verbeeck, R. and Schacht E., *Polymer-Letchworth* **1998**, 39, 1631.
16. Allen C., Han J., Yu Y., Maysinger D., Eisenberg A., submitted to *Journal of Controlled Release* **1999**.
17. Wilhelm, M., Zhao C., Wang Y., Xu R., Winnik M.A., Mura J., Riess G., Croucher M.D., *Macromolecules* **1991**, 24, 1033.
18. Astafieva I., Khougaz K., Eisenberg A., *Macromolecules* **1995**, 28, 7127.
19. Kabanov, A.V.; Nazarova I.R., Astafieva I.V., Batrakova E.V., Alakhov V.Y., Yaroslavov A.A., Kabanov V.A., *Macromolecules* **1995**, 28, 2303-2314.
20. Zhao J., Allen C., Eisenberg A., *Macromolecules* **1997**, 30, 7143-7150.
21. Jacobs, C.; Dubois, Ph.; Jerome, R.; and Teyssie, Ph., *Macromolecules* **1991**, 27,3027.
22. Aldrich Catalogue 1999; Polyethylene glycol homopolymer Mn = 1500, Tm = 45°C
23. Zhang L., Shen H., Eisenberg A., *Macromolecules* **1997**, 30, 1001.
24. Zhang L., Eisenberg A., *Polymers for Advanced Technologies* **1998**, 9, 677.
25. Kwon G., Naito M., Yokoyama M., Okano T., Sakurai Y., Kataoka K., *Langmuir* **1993**, 9, 945.
26. Allen C., Maysinger D., Eisenberg A., *Colloids and Surfaces B: Biointerfaces* **1999**, accepted.
27. Xu, R.; Winnik M.A.; Hallett, F.R.; Riess, G.; Croucher, M.D.; *Macromolecules* **1991**, 24, 87.
28. (a) Nagarajan, R.; Barry, M.; Ruckenstein, E. *Langmuir* **1986**, 2, 210.
29. Tian, M.; Arca, E.; Tuzar, Z.; Stephen, E.; Webber, S.E.; Munk, P. *J. Polym. Sci.: Part B: Polym. Phys.* **1995**, 33, 1713

30. Hurter P. N., Hatton T.A., *Langmuir* **1992**, 8, 1291.
31. Hurter P. N., Scheutjens J.M.H.M., Hatton T.A., *Macromolecules* **1993**, 26, 5592.
32. Hurter P. N., Scheutjens J.M.H.M., Hatton T.A., *Macromolecules* **1993**, 26, 5030.

CHAPTER 5

POLYCAPROLACTONE -*B*-POLY(ETHYLENE OXIDE) COPOLYMER MICELLES AS A NOVEL DRUG DELIVERY VEHICLE FOR NEUROTROPHIC AGENTS FK506 AND L-685,818

FK506 and its structural analogue L-685,818 were the first biologically active model compounds that we chose for our study of the PCL-*b*-PEO micelles as drug carriers. These compounds were first selected owing to their high potency and degree of lipophilicity. The polycaprolactone-*b*-poly(ethylene oxide) (PCL-*b*-PEO) micelles, like other block copolymer aggregates, have a very small cargo space; for this reason, micellar delivery vehicles are most useful for the delivery of highly potent compounds. Secondly, the availability of radiolabeled FK506 provided a method of detection of the drug necessary for studies of loading capacity, release kinetics and cell uptake. Also, *in vitro* and *in vivo* models had been established for FK506.

FK506 is a fascinating compound of great complexity and for this reason section 5.1 has been dedicated to the description of both its therapeutic effects and mechanisms of action. The model used to assess the *in vitro* delivery and biological activity of PCL-*b*-PEO micelle incorporated FK506 has been described in detail in section 5.2. Finally in section 5.3, we summarize the results obtained from the study of the *in vitro* delivery of the micelle-incorporated FK506 and L-685,818 in PC12 cell cultures.

5.1. FK506: Therapeutic Effects and Mechanisms of Action

Tacrolimus (FK506, Prograf) was discovered in 1984 by scientists from Fujisawa Pharmaceutical Company while screening for new active immunosuppressants [1].

Tacrolimus is a natural product extracted from the fermentation broth of the bacterium *Streptomyces tsukubaensis* found near Tsukuba City, Japan [2]. The compound, as shown in Figure 5.1.1, is a macrolide lactone of 822 Daltons and includes a 23 membered ring. It is a fairly lipophilic compound ($\log P = 0.386$) which is poorly soluble in water, and very soluble in organic solvents such as chloroform, acetone and ether [1].

Presently, FK506 along with cyclosporin A (CsA), are the leading immunosuppressive agents used to prevent graft rejection [3-6].

FK506 was first used in the prevention of refractory allograft rejection [7]; however it has since been proven to be effective as primary treatment following kidney, heart, lung, intestine, pancreas, and bone marrow transplantations [8]. Although FK506 and CsA are structurally distinct their mechanism of action as immunosuppressive agents are quite similar. However, FK506 has been found to be 10 fold more potent than CsA *in vitro* and 100 fold more potent *in vivo* [2,9]. The therapeutic efficacy of the two drugs has also been shown to be quite different. In 1994, the European FK506 Multicentre Liver Study Group reported on the results from a study involving 545 liver transplant patients, which compared the therapeutic efficacy of FK506 and CsA based immunosuppressive therapies [10]. The 545 patients were divided into three groups ; 16 patients received no treatment, 265 patients were treated with CsA and 264 patients were treated with FK506. In each case, the patient was examined 12 months post-transplantation. The study revealed a lower incidence of acute rejection, refractory acute rejection, and chronic rejection for

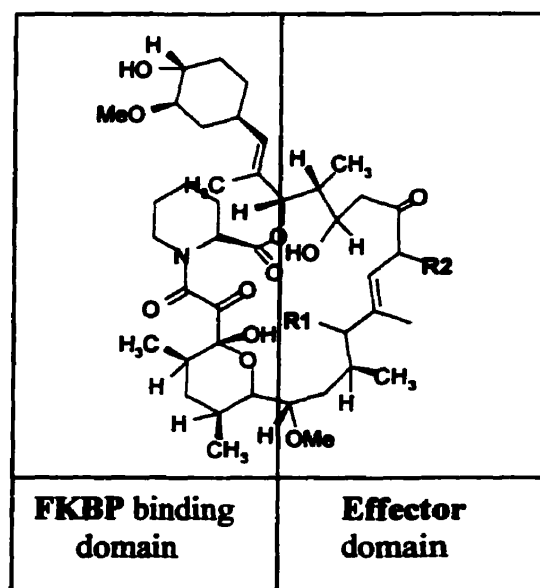


Figure 5.1.1: Structure of FK506
($R_1 = H$, $R_2 = \text{allyl}$)

patients treated with FK506 when compared to those treated with CsA. The specific results were as follows: the incidence of acute rejection was 40.5% (107 patients) and 49.8% (132 patients) for those treated with FK506 and CsA respectively; refractory acute rejection was diagnosed in 0.8% (2 patients) of those treated with FK506 and 5.3% (14 patients) of those on CsA; chronic rejection was seen in 1.5% (4 patients) of those using FK506 and 5.3% (14 patients) of patients on CsA. The survival rate for patients treated with FK506 was 77.5% (46 patients died) while that for patients treated with CsA was slightly lower at 72.6% (61 patients died). Also, the total daily dosage of corticosteroid supplement required for the treatment of rejection was less for those in the tacrolimus group than it was for those in the CsA group. These results demonstrate the slightly greater therapeutic efficacy of FK506 over CsA in the treatment of liver transplant recipients [10].

Both CsA and FK506 have been found to cause several unwanted side effects such as impaired renal function, abnormal glucose metabolism (hyperglycaemia, diabetes mellitus) and neurological effects [10]. In the study mentioned above the adverse effects induced were more severe for the group treated with FK506 in comparison to those treated with CsA. However, these results conflict with findings from another study where CsA was found to cause more severe effects on renal function than FK506 [11].

The adverse side effects that FK506 may induce often limits the allowed dosage of the drug. The incorporation of FK506 into drug delivery vehicles has been tried as a means of preventing these unwanted side effects. Several liposomal formulations have been prepared along with an oil in water emulsion formulation and a block copolymer micellar system by our group. A brief review of the delivery vehicles developed to date for FK506 will be given in section 5.1.2.

We will now discuss several aspects of FK506. The first section (Section 5.1.1) discusses the mechanism of action of several of the biological effects of FK506 including its immunosuppressant, neuroregenerative and neuroprotective activity. Finally, several of the drug delivery vehicles tried for this compound are discussed in section 5.1.2..

5.1.1. Therapeutic Effects of FK506

5.1.1.1. FK506 as an Immunosuppressive Agent

Once administered FK506 has been found to enter into both immune and non-immune responsive cells [1]. Upon entry into the cell, it binds to proteins of the immunophilin class, known as FK506-binding proteins, the predominant one being FKBP12. The FKBP immunophilins have peptidyl-prolyl cis-trans isomerase or rotamase

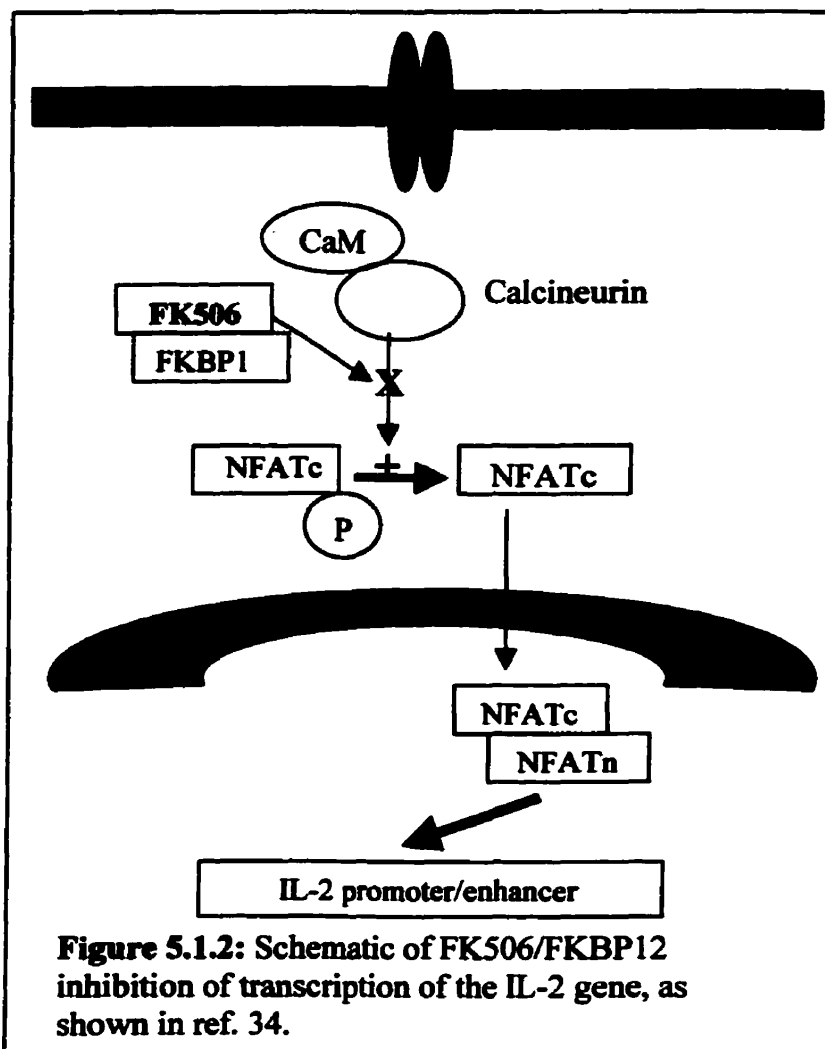


Figure 5.1.2: Schematic of FK506/FKBP12 inhibition of transcription of the IL-2 gene, as shown in ref. 34.

activity which is believed to be involved in the regulation of a range of cellular functions including protein folding [9, 12, 13]. The binding of FK506 to the FKBP's is said to inhibit their rotamase activity, however; this effect is not responsible for its immunosuppressant action [12]. This has been clearly shown by the study of analogs of FK506 (e.g. L-685,818 [14, 15]) and CsA (e.g. 6-[Me]-Ala-CsA [16]) which bind to their respective immunophilins and thus inhibit rotamase activity but have no immunosuppressive activity [13]. Instead the immunosuppressive activity of FK506 originates from its ability to inhibit the phosphatase activity of calcineurin [9].

Calcineurin also known as phosphoprotein phosphatase 2B (PP2B) is a member of the serine-threonine phosphatase family, however; it is unique in that its activity is Ca^{2+} /Calmodulin dependent. Calcineurin is a heterodimeric protein, composed of a 60kDa

catalytic subunit (A) and a 19kDa regulatory subunit (B) [9, 12]. The catalytic A-subunit includes an autoinhibitory domain and the binding site for the Ca^{2+} /CaM complex (CaM has not been found to bind in the absence of Ca^{2+}) [12]. The FK506/FKBP12 complex binds to several sites on calcineurin including the amino terminus of the B binding helix on the A subunit, the catalytic domain and the B-subunit [12]. The binding of FK506/FKBP12 to the calcineurin/CaM/ Ca^{2+} complex inhibits calcineurins phosphatase activity [9]. The inhibition of calcineurins phosphatase activity has many cellular effects; however, the immunosuppressive effect of FK506 is primarily due to the inhibition of genes encoding local mediators such as interleukin 2 (IL-2) and interferon gamma ($\text{IFN-}\gamma$) produced by CD4^{+} type 1 helper T cells (T_{H1}) [9]. For example, the transcription factor, cytoplasmic nuclear factor of activated T cells (NF-AT_{c}), is present only in activated lymphocytes where it is commonly dephosphorylated by calcineurin (Figure 5.1.2)[9]. Following, the dephosphorylation of NF-AT_{c} by active calcineurin NF-AT_{c} translocates into the nucleus where it binds with NF-At_{n} . This complex associates with the IL-2 promotor/enhancer region of the DNA to promote the transcription of the interleukin 2 (IL-2) gene [9]. The IL-2 gene is only one of the genes encoding growth-promoting cytokines whose transcription is inhibited by FK506 [9]. The inhibition of cytokine secretion from the CD4^{+} T_{H1} cells prevents the proliferation and maturation of CD8^{+} cytotoxic T lymphocytes [17].

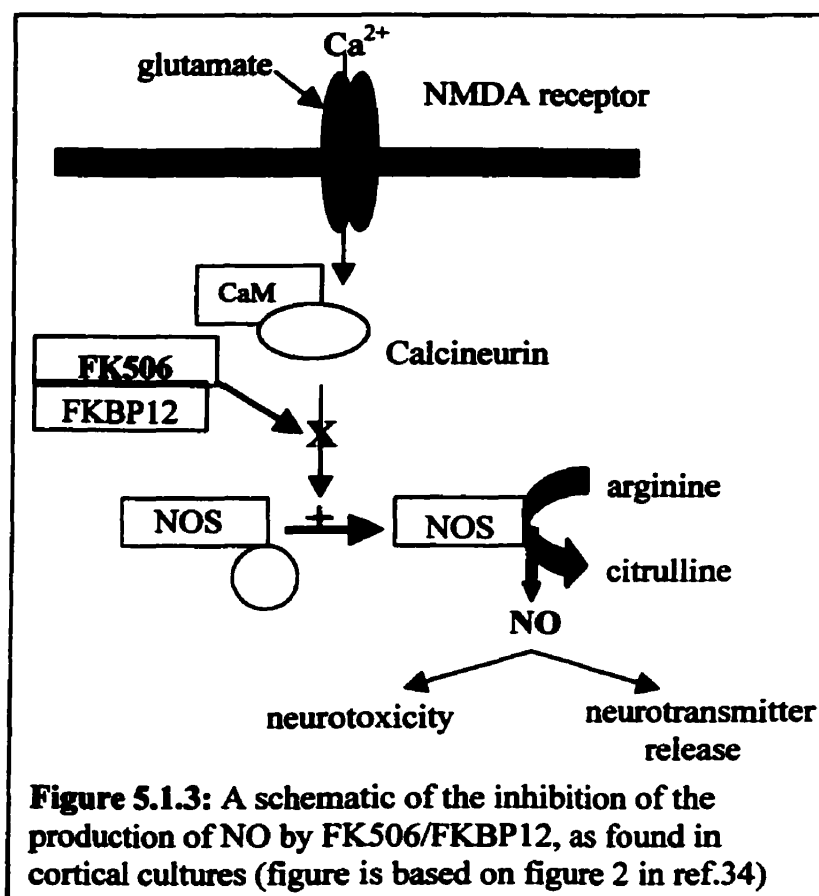
The immunosuppressive effect of FK506 is selective in that it has been found to affect mostly Type 1 helper T (T_{H1}) cells rather than Type 2 helper T (T_{H2}) cells [9]. Helper T cells aid in activating the response of other white blood cells by the secretion of lymphokines, interleukins or cytokines. Specifically, the T_{H1} cells are responsible for the activation of macrophages while the T_{H2} cells are involved in the stimulation of B cells. The selective effect of FK506 on cytokine production from the T_{H1} cells and not the T_{H2} cells may actually enhance the drugs immunosuppressive activity. Since, cytokines produced by the T_{H2} cells (e.g. IL-10) actually act to inhibit the production of IL-2 and $\text{IFN}\gamma$ by T_{H1} cells [9, 18].

Aside, from its ability to inhibit gene expression in certain cells FK506 also effects other Ca^{2+} dependent events owing to its inhibition of calcineurin. For instance,

the activation of the enzyme nitric oxide synthase is dependent on dephosphorylation by calcineurin. A few other substrates of calcineurin include phosphatase 1, CAMP-dependent protein kinase and CAMP-responsive element binding protein (CREB) [9].

In addition, it is postulated that FK506 inhibits the transcription of proinflammatory cytokines including IL-1, tumor necrosis factor α , IL-3, IL-4, IL-5, IL-6, IL-8 and granulocyte macrophage colony stimulating factor (GM-CSF) [9, 19]. The mechanism by which this occurs involves the binding of FK506 to the steroid receptor associated heat shock protein (hsp56). In binding to the glucocorticoid receptor complex FK506 stabilizes the glucocorticoid receptor preventing it from inactivation and degradation [9, 20, 21]. The stabilization of the GR complex results in an enhanced translocation of the GR to the nucleus. The binding of GR to the glucocorticoid response elements (GRE) results in the inhibition of transcription of genes encoding the aforementioned proinflammatory cytokines [19].

FK506 is also believed to prevent the degradation of the progesterone receptor and in this way enhance the transcription of genes which are promoted by the PRE. This effect of FK506 is said to be mediated by its binding to FKBP59 and their subsequent association with hsp70 and hsp90 [22, 23].



5.1.1.2. FK506 as a Neuroprotective and Neuroregenerative Agent The neuroprotective and neuroregenerative effects of FK506 are mediated by two distinct mechanisms.

Neuroprotective Activity

The neuroprotective effect of FK506 is found to be at least partially mediated *in vitro* by a calcineurin dependent mechanism which involves nitric oxide; FK506 has been shown to protect cortical cell cultures from excitotoxic death [13] (Figure 5.1.3). In this case, the calcineurin substrate of interest is nitric oxide synthase whose phosphorylated state is increased owing to the action of FK506. Nitric oxide synthase is activated by increased Ca^{2+} levels and is a calcium-calmodulin dependent enzyme [13]. This enzyme catalyzes the production of nitric oxide (NO) and citrulline from arginine. The production of nitric oxide is stimulated upon activation of a class of glutaminergic receptors termed the N-methyl-D-aspartate (NMDA) receptors [24]. The activation of these receptors causes a Ca-flux through an ion channel, leading to the activation of NOS and subsequent production of NO. The increase in the intracellular level of NO can contribute to glutamate-mediated neurotoxicity. Glutamic acid is known to be neurotoxic as it can cause overstimulation of the NMDA receptors. FK506 inhibits calcineurin and in this way inhibits the dephosphorylation and consequent activation of NOS. Snyders group demonstrated that both FK506 and CsA inhibit NMDA induced NO production in cortical cell cultures [25].

At this point, there is a discrepancy between the *in vitro* and *in vivo* data regarding the mechanism by which FK506 exerts its neuroprotective effect. The *in vivo* neuroprotective effect of FK506 is not necessarily believed to be mediated by the inhibition of the enzyme NOS. Several groups have found that NOS inhibitors do not block *in vivo* excitotoxic damage [26, 27].

Neuroregenerative Activity

The neuroregenerative effects of FK506 do not involve calcineurin, but rather originate from the inhibition of the rotamase activity of the immunophilin FKBP12. Most of the early work on immunophilins involved the study of their role in the immune system. For this reason, their name originates from the immunosuppressant drug they bind, for example the FKBP's bind FK506 and the cyclophilins bind CsA. However, the work of Snyders group later pointed to the potential

role of the immunophilins in the CNS by demonstrating that the levels of FKBP12 are 10-40 fold higher in the brain than in the immune system [28].

FKBP12 is one of approximately 50 immunophilins that have been identified to date (20 cyclophilins and 30 FKBP's) [29, 30]. The cellular location for the different immunophilins varies; FKBP12 is found in the cytosol, FKBP13 in the endoplasmic reticulum and FKBP52 is found in the nucleus and the cytosol [13]. In the cytosol, FKBP-12 is complexed to the ryanodine and inositol triphosphate receptors which both play a role in mediating intracellular Ca^{2+} levels. The ligand binding site for FKBP12 has been found to consist of a depression on the surface of the protein which is $9\text{\AA} \times 9\text{\AA}$ in area and 7\AA deep, and contains several hydrophobic residues [13]. The structure of the

human FKBP12-FK506

complex has been elucidated by means of x-ray crystallography and

NMR spectroscopy [31-33].

The FKBP binding component of FK506 is shown in Figure 5.1.1. The

specific interactions and the groups of both FK506 and

FKBP12 involved in the complex have been described in detail

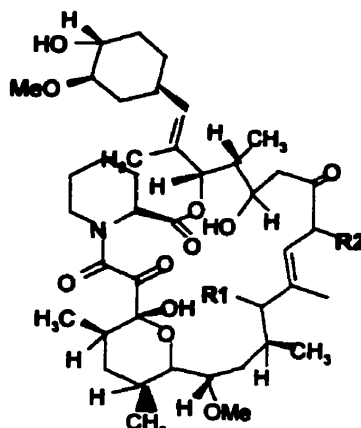
elsewhere. The binding of FKBP12 to FK506 results

in the dissociation of the immunophilin from the

ryanodine (integral membrane protein in the sarcoplasmic reticulum in muscle cells) and

inositol triphosphate receptors (integral membrane protein in the endoplasmic reticulum

[34].



FK506 ($\text{R}_1 = \text{H}$, $\text{R}_2 = \text{allyl}$)

L-685,818 ($\text{R}_1 = \text{OH}$, $\text{R}_2 = \text{ethyl}$)

FKBP12 LIGAND	Calcineurin Inhibition	Rotamase Activity IC_{50}	Neurite Outgrowth ED_{50}
FK506	YES	0.4 nM	0.5 nM
L-685,818	NO	0.7 nM	5.0 nM

Figure 5.1.4: The Structure and Activity of the FKBP12 ligands; FK506 and L-685,818, as shown in ref. 13.

The study of FK506 and its non-immunosuppressant analogue L,685-818 demonstrate that it is the inhibition of the rotamase activity of FKBP12 and not the inhibition of calcineurin that governs its neuroregenerative activity [13, 15, 35]. As summarized in Figure 5.1.4, L,685-818 does not inhibit calcineurin and so is not immunosuppressive; however, it does inhibit the rotamase activity of FKBP12 and does promote neurite outgrowth in explant cultures. In addition, both FK506 and L,685-818 were found to promote the structural and functional regeneration of lesioned sciatic nerves in rats. Also, they found that another FKBP ligand, Rapamycin, that is also not able to inhibit calcineurin is not a neuroprotectant [25]. Clearly, this shows that the neuroregenerative activity of FK506 is not mediated by a calcineurin dependent pathway. This realization prompted the design of small molecules that bind to FKBP12 and are neurotrophic but not immunosuppressant. Several small molecule FKBP12 ligands were successfully designed to contain the minimum FKBP12 binding domain [36] and have the ability to undergo the necessary hydrogen bonding interactions with FKBP12 [13]. The binding affinity of the ligands for FKBP12 was evaluated by measurement of their rotamase inhibition constant (K_i) [13, 16]. Also, experiments were performed whereby the ED_{50} of each ligand was obtained from dose response curves that were generated. In these experiments increasing concentrations of the FKBP12 ligands were incubated for 48 hours with sensory neuronal cultures [13, 37]. Following, the incubation period the extent of neurite outgrowth was assessed and a dose response curve was produced. The FKBP12 ligands studied were found to be highly potent as they were able to promote neurite extension from sensory neurons in the absence of exogenously added growth factors. It should be noted that the addition of exogenous growth factor was necessary for FK506 to induce neurite outgrowth in PC12 cells but is not required in primary neuronal cultures. The nerve growth factor is already present in primary cultures as it is produced by the Schwann cells present in culture [13].

Interestingly, there was not found to be a linear relationship between the neurotrophic potency of these ligands and their ability to inhibit the rotamase activity of FKBP12. Several of these compounds were found to have neurotrophic potencies which

were 10-100 times higher than their rotamase inhibition constants [13]. However, in all cases it was observed that binding to FKBP12 and an inhibition of its rotamase activity were required for the ligand to have neurotrophic activity. These results suggest that the inhibition of the rotamase activity of FKBP12 is necessary for the neurotrophic activity of FK506 but this inhibition is not solely responsible for the neurotrophic potency of FK506 and the other FKBP12 ligands [13].

5.1.1.3. FK506 as a Dermatological Agent

Inflammatory immunologically based skin disorders such as atopic dermatitis are found to be induced by the activation of inflammatory cells such as T cells and mast cells [38]. Since immunosuppressant agents CsA and FK506 have been found to inhibit the activation of inflammatory cells they are a likely treatment for these skin disorders. CsA was the first immunosuppressant agent to be tried in this regard [39]. Intravenous formulations of CsA have been found to be effective against psoriasis [40] and atopic dermatitis [41]; however, conflicting results have been received with topical CsA ointments. In most cases, the inefficacy of CsA topical treatments were found to be due to the insufficient penetration of CsA into the skin. Local application of FK506 has been found to be effective in the treatment of inflammatory skin disorders. The ability for FK506 to permeate human skin *in vitro* has been shown to be greater than that of CsA. This is believed to be due either to the lower molecular weight of FK506 (mol.wt = 822D, CsA mol.wt = 1202 D) or its slightly lower lipophilicity [42].

To this point it has been found that the absorption of FK506 through the skin is a passive process and that only a small amount of the topically applied dose enters the systemic circulation [43].

5.1.2. Drug Delivery Vehicles for FK506

The permissive dose of the drug is limited by its adverse effects which include primarily neurotoxicity and nephrotoxicity. For this reason, several drug delivery vehicles have been designed for FK506 with the aim of reducing the adverse effects of the drug without affecting its immunosuppressant activity [44, 45]. Several liposomal

formulations have been designed and the pharmacokinetic parameters and biodistribution of liposome incorporated FK506 have been studied. In the past, research has demonstrated that the conventional (non-sterically stabilized) liposomes are taken up by components of the RES and thus mainly accumulate in the liver and spleen. In this way, a conventional liposomal formulation of FK506 would be anticipated to reduce the neuro- and nephrotoxic effects of this drug. In a study by Ko et al. [44], the organ distribution of liposomal FK506 was compared to that of FK506 administered in an intravenous solution (Fujisawa Pharmaceutical Co. Ltd. Osaka Japan) in male Wistar rats. In this study the level of FK506 in whole blood, plasma, spleen, liver, kidney, pancreas, intestine, cerebrum and the cerebellum were measured at 10 min., 1 hour, 6hrs. and 24 hrs. post injection. It was found that the liposomal formulation of FK506 allowed for increased accumulation of FK506 in the liver and spleen when compared to the conventional i.v. solution of FK506. Also, the levels of FK506 in the kidney, cerebrum, and cerebellum were much lower when FK506 was administered in the liposomal formulation [44].

In a later study Ko et al. [45] compared the efficacy of a liposomal FK506 formulation with that of the conventional i.v. formulation of FK506 in a canine model. The model included beagle dogs which had undergone orthotopic liver transplantation. The dogs were divided into three groups: group 1, not treatment, group 2 treatment = 0.05 mg/kg/day FK506 in conventional i.v. formulation for 14 days; group 3 treatment = FK506 in a liposomal i.v. formulation 0.05 mg/kg/day for 14 days. All of the dogs in group 1 died within the two week period, those in group 2 died within 33 days; however, the dogs in group 3 survived for over 200 days. This demonstrates that the administration of FK506 in a liposomal formulation may actually enhance the therapeutic efficacy of this drug [45]. Ko et al. then compared the efficacy of the liposomal FK506 formulation with the conventional i.v. solution in the treatment of both a liver and kidney canine transplant model [46]. In this study, the beagle dogs that had undergone liver or kidney transplants were divided into the same three treatment groups described above. In the case of the liver transplant model the results were in agreement with those described above. Yet, for the kidney transplant model it was found that all animals in group 1 died within two

weeks, those in group 2 survived more than 30 days and those in group 3 only survived between 9 and 18 days. Thus, the animals treated with the i.v. liposomal formulation did not survive as long as those treated with the conventional i.v. solution [46]. These results were to be expected since the level of kidney accumulation of liposomal FK506 was previously shown to be very low; likely owing to the kidneys poor RES [45, 46].

The delivery vehicles described above for FK506 were considered for its use as an immunosuppressant agent. To our knowledge little work has been done involving the development of delivery vehicles for FK506 and other immunophilin ligands as neurotrophic agents. However, we are interested in determining if the PCL-*b*-PEO copolymer micelles are suitable as a delivery vehicle for these neurotrophic agents.

5.2. *In vitro* Model to Assess Delivery and Biological Activity of Micelle-Incorporated FK506

The *in vitro* model employed to assess the delivery and biological activity of the micelle-incorporated FK506 and L-685,818 consisted of the measurement of the extent of neurite-like outgrowth in PC12 (rat pheochromocytoma) cell cultures [37].

5.2.1. PC12 Cell Cultures

PC12 cells are often used as a model system for *in vitro* neurological studies. The PC12 cells are a clonal cell line derived from a transplantable rat adrenal pheochromocytoma [47]. They respond reversibly in a dose-dependent manner to NGF treatment and synthesize and store catecholamine neurotransmitters (dopamine and norepinephrine) [47]. PC12 cells like sympathetic neurons respond to NGF treatment by extending processes; however, unlike sympathetic neurons they do not require NGF for survival in serum containing medium. In serum-free medium the presence of NGF will promote the survival and differentiation of the PC12 cells; however, following removal of NGF the cells will die [48]. They also resemble sympathetic neurons in that they store and secrete catecholamines yet unlike sympathetic neurons the level of dopamine in PC12 cells is higher than that of noradrenaline [47].

In their optimal growth medium (85% RPMI, 10% heat inactivated horse serum, 5% calf serum, 50 units/mL penicillin and 25 µg/mL streptomycin) the PC12 cells are said to grow in clumps where the individual cells have a round polygonal shape [47]. Following one week exposure to NGF (50ng/mL) cell multiplication ceases and the cells extend neuronal-like processes [47]. These neurite-like outgrowths are said to resemble those extended by primary cultures of sympathetic neurons [47]. The response of PC12 cells to NGF is reversible in that 24 hours following replacement of the medium with NGF-depleted medium 75% of the cells lose their neurite-like outgrowths and following 72 hours cell multiplication is resumed [47].

In PC12 cells NGF mediates its effects through binding to the TrkA receptor protein tyrosine kinase [49]. The binding of the NGF ligand to its receptor initiates receptor dimerization and autophosphorylation of residues in the carboxyl terminus of the

TrkA receptor. These residues then act at “docking sites” for the Src homology 2 containing molecules which are recruited [50]. The Src homology 2 proteins are responsible for binding to activators of the Ras family of GTPases. The activation of Ras has been found to play a key role in cell signaling resulting in PC12 cell differentiation. The interaction of NGF with its receptor and the signaling pathway which leads to differentiation are described in detail elsewhere [48-50].

5.2.2. FK506 Potentiates NGF in PC12 Cell Cultures

FK506 has been shown to enhance the sensitivity of PC12 cells to NGF. Lyons et al. demonstrated that the concentration required to produce maximal outgrowth in PC12 cultures could be substantially reduced when FK506 is present [37]. For example, they found that maximal outgrowth could be achieved with either NGF alone (50ng/mL) or a combination of NGF (1ng/mL) and FK506 (1nM) [37]. FK506 has also been shown to potentiate the effects of NGF in primary cultures of dorsal root ganglia (DRG) [37]. However, for our studies we chose to use PC12 cells since the DRG cultures are primary and so would have been more difficult to work with.

In section 5.3. the study of the *in vitro* delivery and biological activity of both micelle-incorporated FK506 and L-685,818 are assessed in PC12 cell cultures.

5.3. PCL-*b*-PEO Micelles as a Delivery Vehicle for the Neurotrophic Agents FK506 and L-685,818

5.3.1. Introduction

Colloidal drug delivery vehicles such as liposomes, microspheres, nanospheres and block copolymer micelles have recently been shown to increase the therapeutic index and improve the selectivity of various potent drugs [51-58]. These vehicles have been shown to optimize the therapeutic efficacy of drugs by preventing their rapid elimination from the body [54], reducing their systemic toxicity [54], delaying their degradation and optimizing their metabolism [53, 54]. In addition, they also provide for effective delivery of drugs to specific target sites [53] and aid in overcoming both transport limitations and defense mechanisms associated with the multi-drug resistance phenotype [55].

In the recent past, there has been increasing interest in the use of micellar delivery systems formed from block copolymers [54, 56, 58]. The use of block copolymers in drug delivery was first proposed by Ringsdorf's group in the early 80's [61]. Recently the work of Kabanov's group and Kataoka's group has greatly enhanced the development of block copolymer micelles as drug delivery vehicles [54-56]. These micelles are formed from individual block copolymer molecules each of which contains a hydrophobic block and a hydrophilic block. The amphiphilic nature of the block copolymers enables them to self-assemble to form nanosized aggregates of various morphologies in aqueous solution such that the hydrophobic blocks form the core of the micelle which is surrounded by the hydrophilic blocks, which form the outer shell [62]. The inner core of the micelle creates a hydrophobic microenvironment for the nonpolar drug, while the hydrophilic shell provides a stabilizing interface between the micelle core and the aqueous medium. The properties of the hydrophilic shell, which in most cases consists of polyethylene oxide, can be adjusted to both maximize biocompatibility and avoid reticuloendothelial system uptake. The size of the micelles is usually between 10-100 nm [54]. This size is small enough to allow access to small capillaries while avoiding reticuloendothelial system uptake [54]. Micelles in this size range are also large enough to escape renal filtration, which increases their blood circulation time. Most of the existing block copolymer micelle systems are based on polyethylene oxide-*b*-polypropylene oxide-*b*-polyethylene

oxide triblock copolymer or from block copolymers which have a polypeptide or polylactic acid core forming block and a polyethylene oxide block which forms the hydrophilic corona [54-56, 58-60].

In this paper we introduce a novel block copolymer micelle system, formed from polycaprolactone-*b*-polyethylene oxide (PCL-*b*-PEO) diblocks as a potential drug delivery vehicle. The individual block components; polycaprolactone and polyethylene oxide, have been explored previously for a variety of biomedical applications [63-69].

Polycaprolactone, the hydrophobic core – forming block of the micelles is a synthetic semicrystalline biodegradable polymer. Due to the biodegradability of the polycaprolactone homopolymer, it has been tried both as a structural material in the production of medical devices such as implants, sutures, stents and prosthetics, and as a carrier for a variety of drugs [63, 64]. Polycaprolactone pastes have been developed as a drug delivery system for the anti-cancer agent taxol [65] and the antineoplastic agent bis(maltolato)oxovanadium [66]. Nanoparticle, nanocapsule and microparticle drug carriers made of polycaprolactone have been assayed for the ocular delivery of indomethacin [67]. Polyethylene oxide, the hydrophilic shell forming block of the micelles, is commonly used to impart blood compatibility to a material surface [68, 69].

Triblocks of polycaprolactone-*b*-polyethylene oxide-*b*-polycaprolactone have been used to form tablets, which were studied in terms of their biocompatibility and biodegradation [70]. In addition, recently matrices to be used as implantable drug delivery systems have been formed from the triblock copolymer polycaprolactone-*b*-polyethylene oxide-*b*-polycaprolactone (PCL₆-*b*-PEO₉₀-*b*-PCL₆) [71].

To our knowledge, there has only been one previous report on the use of diblock copolymer micelles of polycaprolactone-*b*-polyethylene oxide as a drug delivery system [72]. The novelty associated with the present application is largely due to the length of the polycaprolactone blocks. To date, diblocks with long blocks of polycaprolactone had not been synthesized; now however, owing to a new synthetic method, longer blocks are possible [73]. The longer caprolactone blocks should create a larger hydrophobic microreservoir enabling the incorporation of a greater amount of lipophilic drug. It is also

anticipated that control over the degree of incorporation and the release kinetics can be gained by varying the length of the polycaprolactone block. The degree of drug incorporated and the release kinetics of that drug are largely a function of the interaction between the drug and the core forming block. Since polycaprolactone is more hydrophobic than other polymers, commonly used as core – forming blocks (e.g. polypropylene oxide) this system may have a larger capacity for the most hydrophobic drugs.

The polycaprolactone micellar core is suitable for the incorporation of a variety of neutral, lipophilic drugs. In this paper we focus on the drugs FK506 and its analogue, L-685,818. FK506, otherwise known as tacrolimus, has been effectively used to achieve immunosuppression in organ transplant recipients [74]. FK506 binds to the immunophilin FKBP12 to form a complex which binds to and inhibits calcineurin; this, in turn, results in immunosuppression [75]. Recently, FK506 has been found to promote neuronal outgrowth which has been demonstrated in terms of the enhancement of neurite extension in PC 12 (rat pheochromocytoma) cell cultures [47] and explant cultures of rat sensory ganglia [15]. The use of FK506 for the treatment of neurodegenerative diseases is limited by its immunosuppressant activity. However, L-685,818, the structural analogue to FK506, has retained the neurotrophic action of FK506 but lost its immunosuppressant action [15]. The structural difference between FK506 and L-685,818 is only in the addition of a hydroxyl group on the analogue at C-18 and the substitution of an ethyl group for an allyl group at C-21 [15]. Recently, L-685,818 has been of interest for its potential use in the treatment of neurodegenerative diseases, as it has been shown to “enhance functional and morphologic recovery in rats with crushed sciatic nerves” [15].

At present, FK506 is administered either orally, in a capsule, or by injection as a sterile solution. In addition to this, a microemulsion formulation of FK506 has also been developed [74]. However, to our knowledge, this is the first delivery system which has been introduced for the FK 506 analogue, L-685,818.

In this communication we report on studies which explore the potential of the PCL-*b*-PEO copolymer micelles as drug delivery vehicles. In order to establish this

system as a suitable drug carrier, we studied a range of the micelle's characteristics including effective diameter, size population distributions, as well as their *in vitro* stability in various cell culture media. The micelle's affinity for lipophilic compounds was evaluated by determining the partition coefficient for the highly lipophilic compound, pyrene between the PCL-*b*-PEO micelles and water. Though each of the components, polycaprolactone and polyethylene oxide, are biocompatible, it was also necessary to assess the biocompatibility of the block copolymer as a whole. The *in vitro* biocompatibility of the copolymer was assayed by incubation of the micelles with PC 12 cells [47] and MCF-7 breast cancer cells as well as primary cultures of human microglia, astrocytes and cortical neurons. Finally, the neurotrophic drugs FK506 and L-685,818 were incorporated into the PCL-*b*-PEO micelles and the *in vitro* delivery was assayed by monitoring the degree of differentiation achieved in cultures of PC 12 rat pheochromocytoma cells.

5.3.2. Experimental Section

5.3.2.1. Materials The block copolymers were synthesized by anionic polymerization, the method has been described in detail elsewhere [73]. GPC results revealed that the polydispersity (PD) of the block copolymers was 1.16, with a symmetrical mono modal distribution. In all cases, following purification of the block copolymer there was no homopolymer present. The polycaprolactone-*b*-polyethylene oxide copolymers employed have identical polyethylene oxide block lengths (44 ethylene oxide units) but different polycaprolactone block lengths; 14 or 20 units. These polymers are designated as PCL₁₄-*b*-PEO₄₄ and PCL₂₀-*b*-PEO₄₄ respectively. All chemicals for the synthesis were purchased from Aldrich Chemical Co.

FK 506 (PrografTM) was purchased from Fujisawa Pharmaceutical, Osaka, Japan. The FK 506 analogue, L-685 818 was supplied by Merck Inc. The MCF-7 cells, and primary cultures of human microglia, astrocytes and cortical neurons were supplied by Dr. Antel at the Montreal Neurological Institute. The tissue culture reagents were all purchased from Gibco BRL. The Alamar blue was purchased from Biosource Camarillo and the Trypan blue from Gibco BRL.

5.3.2.2. Methods

Characterization of the PCL-*b*-PEO Micelles

Micelle Preparation. The PCL-*b*-PEO copolymer was dissolved in DMF and stirred overnight at room temperature. Micellization was achieved by the addition of water in a dropwise fashion to the block copolymer solution to form a micelle solution. The micelle solution was stirred overnight and then dialyzed against milli Q distilled water using dialysis tubing. The water was changed every hour for the first four hours and then every three hours for the next twelve hours.

Micelle Size Distribution. Dynamic laser light scattering (DLS) measurements on the PCL-*b*-PEO block copolymer micelles were carried out using a Brookhaven laser light scattering instrument (Brookhaven Instruments Corporation, New York, U.S.A.), with a uniphase 125 mW micro green laser at a wavelength of 532 nm at 25°C. A scattering angle of 90° was used for all measurements. The concentration of the samples ranged from 0.01 to 0.2 % w/w in filtered (.8um filter) deionized distilled Milli Q water.

***In vitro* Micelle Stability Studies.** The 1% w/w PCL-*b*-PEO block copolymer micelle solutions prepared as described above were freeze dried and dissolved in Dulbecco's Modified Eagle Medium (DMEM, Gibco), RPMI medium and water to produce both .01% and .1% w/w solutions. Dynamic laser light scattering (DLS) measurements on the solutions were carried out on a weekly basis over a 3 month period.

Determination of the Partition Coefficient for Pyrene between the PCL-*b*-PEO Block Copolymer Micelles and a DMF/H₂O Solvent Mixture. The fluorescence method used to determine the partition coefficient for pyrene between a mixed water/DMF solvent mixture (60-90 % water content) and block copolymer micelles (concentration PCL₂₀-*b*-PEO₄₄ ranges from 1×10^{-6} to 1×10^{-2} g/g), at 25° C, has been described in detail elsewhere [55b, 76, 77a]. The incorporation of pyrene into the micelle core has been described as a partition equilibrium between a micellar phase and a solvent phase [77]. Briefly, the intensity ratio of vibrational band three to vibrational band one (I_3/I_1) in the fluorescence

emission spectrum of pyrene reflects the polarity of the surrounding environment of the probe molecules. The I_3/I_1 ratio can thus be used to calculate the concentration of pyrene incorporated into the micelles and from this concentration as well as the total amount of pyrene in solution we can calculate the partition coefficient (K_v) for pyrene between the PCL-*b*-PEO micelles and the H₂O / DMF solvent mixtures. The semilogarithmic plot of the K_v versus the water content can then be extrapolated to 100 % water content.

Preparation of Solutions for the Determination of the Partition Coefficient.

Sample solutions were prepared by adding known amounts of pyrene in acetone to each of a series of empty vials, following which the acetone was evaporated. The amount of pyrene was chosen so as to give a pyrene concentration in the final solution of 1.5×10^{-9} mol/g. Different amounts of PCL₁₄-*b*-PEO₄₄ copolymer in DMF were then added. The initial volumes of the solutions were *ca.* 2mL. Micellization of the polymer was achieved by adding water at a rate of 1 drop every 10 s. The addition of water was continued until the desired water content was reached. All the sample solutions were stirred overnight before fluorescence measurements were taken.

Fluorescence Measurements. Steady-state fluorescent spectra were measured using a SPEX Fluorolog 2 spectrometer in the right-angle geometry (90° collecting optics). For the fluorescence measurements *ca.* 3 mL of solution was placed in a 1.0-cm square quartz cell. All spectra were run on air-equilibrated solutions. For fluorescence emission spectra, λ_{ex} was 339 nm. Spectra were accumulated with an integration time of 1 s/0.5 nm.

Studies involving the PCL-*b*-PEO Micelles and PC 12 Cells

Cell Cultures. PC 12 cells were maintained in DMEM supplemented with 10% horse serum, 5% fetal calf serum, 500 µg/mL penicillin, 500µg/mL streptomycin and 290 µg/mL.

***In vitro* Biocompatibility of the PCL-*b*-PEO Micelles.** PC 12 cells and the MCF-7 breast cancer cells were maintained at 37°C in 5% CO₂. The cells were plated in 96 well

plates and cultured in RPMI medium supplemented with 5 % fetal bovine serum. Aliquots of the 10% and 1% PCL-*b*-PEO micelle solutions (PCL₁₄-*b*-PEO₄₄ and PCL₂₀-*b*-PEO₄₄) were added to the wells to make the final concentration of micelles in the wells to range from 0.02% to 1% (w/v). In each case, there were controls which consisted of cells without any micelles added to the wells. The cells were incubated with the micelles for both a 24 and 48 hour period at which point the Trypan blue and Alamar blue survival assays were employed to assess cell viability in the presence of the PCL-*b*-PEO micelles.

Cell Survival Assays:(a) **Trypan blue exclusion assay.** Following the 24 or 48 hour incubation period the cells were detached with .025% Trypsin. The cell suspension was mixed with 75 μ L of PBS and 25 μ L of Trypan blue. The number of viable cells was determined by using a light microscope (Nikon, objective 20X). The percentage of viable cells was expressed as the number of viable cells divided by the total number of cells.

(b) **Alamar blue assay.** A 10 μ L aliquot of the Alamar blue was added to each cell well following a 24 hour or 48 hour incubation period. Following incubation with the dye, 50 μ L of the contents of each well was then transferred to a new 96 well plate and the absorbance at 570 nm was measured by a microplate reader (Biorad, Mode 550). Cell viability was expressed as the inverse of the absorbance. The value obtained for the controls was considered to be 100% survival.

Cell Uptake of Pyrene Incorporated Micelles. Pyrene incorporated micelles were prepared such that a total of 2×10^{-7} moles /L of pyrene had been added to the 1% (w/w) micelle (PCL₁₄-*b*-PEO₄₄) solution. An aliquot of the micelle solution was incubated with PC 12 cells cultured in DMEM at 37°C, 5% CO₂. At time 0, and 4, 8 and 24 hours, the fluorescence intensity (Perkin Elmer LS 50) of the supernatant was measured at 390 nm in order to determine the amount of pyrene remaining in the supernatant. Controls consisting of medium or medium and micelles alone were also measured. Following the removal of the aliquot of supernatant at each time point, the remaining supernatant was removed and the cells were washed three times with 100 μ L of phosphate buffer saline.

The cells were then gently scraped and fixed with aquamount on a slide and analyzed using a fluorescence microscope (Olympus BH-2).

Effect of the FK 506- and L-685,818 -incorporated PCL-*b*-PEO Micelles

Preparation of the FK506 and L-685,818 incorporated PCL-*b*-PEO micelles. Stock solutions of each drug were prepared by dissolving the drug in acetone. An aliquot of the stock solution was then added to an empty sample vial, the acetone was evaporated and preparation proceeded as described above. The FK506 drug was received as a sterile solution (PrografTM, Fujisawa Pharmaceutical, Osaka, Japan) and thus it had to be isolated prior to use. The drug was then dissolved in acetone to produce a 5.6×10^{-4} moles/L stock solution. An aliquot of the stock solution was added to an empty sample vial and the acetone was evaporated off. The PCL₂₀-*b*-PEO₄₄ block copolymer was added to the vial along with DMF, then water was added dropwise and the solution was dialysed (as described above) to produce a 1.1×10^{-5} moles/L concentration of drug in a 1% (w/w) block copolymer solution. For the L-685,818 analogue the concentration of the stock solution was 5.6×10^{-4} moles/L. The L-685,818 micelle-incorporated solution was produced in the same manner but the final concentration of the analogue was 2.3×10^{-5} moles/L in the 1% (w/w) PCL₂₀-*b*-PEO₄₄ micelle solution. It should be noted that for both the FK506 and L-685,818 micelle solutions, the concentration mentioned is the maximum quantity of drug incorporated into the micelles; some will be lost in the dialysis process.

***In vitro* Studies of free form FK506 and L-685,818 and micelle-incorporated FK506 and L-685,818.**

Cell Differentiation Assay. PC 12 cells were plated in 24 well plates at 37°C in 5% CO₂, and incubated in DMEM supplemented with 5% fetal bovine serum and the treatments described below. Neurite-like outgrowth in PC 12 cells was detected after a 48 hour period using a Nikon light microscope. For each data point 5 fields of 250-300 cells/well were analyzed. For the quantitation of neurite-like outgrowth the PC 12 cells were considered to have outgrowth if their processes were longer than the length of the diameter of the cell.

Dose-response curves for NGF, FK 506 or L-685,818 alone and the combinations of FK 506 or L-685,818 with NGF. A range of concentrations of either NGF (0.1 to 50 ng/mL), FK506 (1 to 500 nM) or L,685-818 (1 to 500 nM) alone or combinations of 0.5 or 5 ng/mL of NGF with either FK506 (5 to 500 nM) or L-685,818 (50 nM to 10 μ M), were incubated with the PC 12 cells for a 48 hour incubation period. The wells with untreated cells were used as controls.

***In vitro* effect of micelle-incorporated FK506 and L-685,818 along with NGF.** The unfiltered solution of the micelle incorporated drug was added to the cell wells at different concentrations: a 10 μ L aliquot of a FK506-micelle solution was added to each 0.5 mL cell well. The 10 μ L aliquot was produced by diluting the 1.1×10^{-5} moles/L FK506-PCL₂₀-*b*-PEO₄₄ micelle (1% w/w) stock solution. The final concentration of FK506 in the cell well was made to range from 1 to 1000 nM. In the same manner, a 10 μ L aliquot of the L-685,818 micelle solution was added to each 0.5 mL cell well, such that final concentration in the well was made to range from 10 nM to 1 μ M. In each case, 5 ng/mL NGF was also added to each cell well. Several controls were also used where the cells were treated with 5 ng/mL of NGF alone, 1% (w/w) PCL₂₀-*b*-PEO₄₄ micelles alone, 1% (w/w) PCL₂₀-*b*-PEO₄₄ micelles containing 1 nM FK 506 without NGF or 1% (w/w) PCL₂₀-*b*-PEO₄₄ micelles containing 10 nM L-685,818 .

5.3.3. Results

5.3.3.1 Micelle Size Distributions. The Dynamic Light Scattering instrument was used to measure the effective diameter of the micelles and Contin Analysis was employed to determine the population distribution of the micelles in terms of their size. The effective diameter of 0.1% (w/w) solutions of the micelles when a .45 μ m filter is used is 62 nm for the PCL₂₀-*b*-PEO₄₄ and 55 nm for the PCL₁₄-*b*-PEO₄₄. Figure 5.3.1a,b show the population distributions obtained for unfiltered solutions of the PCL₂₀-*b*-PEO₄₄ micelles (.02% and .1% w/w, Figure 5.3.1a and 5.3.1b respectively). Figure 5.3.1a shows the bimodal population distribution present in the unfiltered micelle solution; the small

aggregates were approximately 50 nm in diameter and the larger aggregates were \approx 500 nm (Figure 5.3.1a). The effect of dilution, following the preparation, on this bimodal population distribution was examined as the concentration was varied from 0.01 % to 0.2 % (w/w). In all cases, the 500 nm population was most prevalent at the higher concentration range, while dilution resulted in a gradual shift in favor of the 50 nm population.

5.3.3.2. *In vitro* Stability Studies. The micelles were monitored on a weekly basis by DLS in order to determine their relative stability in different sterile media. Over a three month period both the effective diameter of the micelles and the population size distribution remained unchanged (as per above).

5.3.3.3. *Determination of the Partition Coefficient for Pyrene.* Pyrene was used as a model hydrophobic compound. Figure 5.3.2a shows the I_3/I_1 ratio of pyrene in micelle solutions of different PCL-*b*-PEO copolymer concentrations over a range of water contents in the DMF/H₂O solvent mixtures. The I_3/I_1 ratio (Figure 5.3.2a) increases with increasing water content within the solvent mixture for a constant copolymer concentration. Likewise for a particular water content within the solvent mixture, the I_3/I_1 ratio increases as the copolymer concentration is increased. Figure 5.3.2b shows the partition coefficients calculated for pyrene between the PCL-*b*-PEO micelles and the DMF/H₂O solvent mixtures. The extrapolation of this plot to 100% water content gives a value of the order of 10^2 for the partition coefficient for pyrene between the PCL-*b*-PEO (20-*b*-44) micelles and H₂O.

5.3.3.4. *Cell Survival in the presence of the PCL-b-PEO Micelles* The incubation of the micelles with several different cell lines and primary cultures was employed as a means of testing the biocompatibility of the PCL-*b*-PEO micelles. Primary cultures of human microglia, astrocytes and cortical neurons were incubated with micelles formed from PCL₁₄-*b*-PEO₄₄ and PCL₂₀-*b*-PEO₄₄. In the cell cultures tested the PCL₁₄-*b*-PEO₄₄ induced 10-20 % cell death whereas the micelles formed from the larger polycaprolactone

block (PCL₂₀-b-PEO₄₄) did not cause any noticeable damage. For the incubation of the micelles with the PC 12 and MCF-7 cells, the results from the Trypan blue and Alamar blue survival assays found the micelles to cause little or no cell death when compared with the control wells of untreated cells. Figure 5.3.3 shows the results of the Alamar blue assay for the incubation of the PCL-*b*-PEO micelles with PC 12 cells over a 48 hour period. At almost every concentration, the micelles formed from the PCL₁₄-*b*-PEO₄₄ block copolymer appeared to have a slightly lower cell survival than the 20-*b*-44 micelles.

5.3.3.5. Cell Uptake of Pyrene Incorporated Micelles. Figure 5.3.4 shows the fluorescence intensity found for both the supernatant at 390 nm and the cells at the 0, 4, 8 and 24 hour time points. The fluorescence intensity of pyrene in the various aliquots of supernatant was found to decrease over the 24 hour incubation period indicating a decrease in the amount of pyrene remaining in the external medium. The relative fluorescence intensity at zero time was taken as 1 while after 4 hours it had decreased to 0.70 (± .05) after 8 hours 0.60 (± .05) and finally after 24 hours the intensity was 0.55 (± .05) (Figure 5.3.4). The cells were isolated at each time point and analyzed by fluorescence microscopy. The contrast relative to the intensity of fluorescence in the cells increased over the 24 hour period, from non-detectable at time zero to the maximum (arbitrarily set at 1) after 24 hours.

5.3.3.6. In vitro Studies of free form FK506 and L-685,818 and micelle-incorporated FK506 and L-685,818. In each case, the degree of neurite-like outgrowth was taken to be 100 % in the control wells of untreated PC 12 cells. The degree of differentiation in cell wells in the presence of NGF and/ or drug is expressed as a percentage relative to 100% for the control.

5.3.3.7. Dose-response curves for NGF, FK506 and L-685,818 without Micelles. Figure 5.3.5 shows the degree of neurite-like outgrowth obtained over 48 hour incubation of PC 12 cells with either NGF, FK506 or L-685,818. The degree of outgrowth in the wells where NGF had been added was found to increase from 110 to 260 % as the concentration

of NGF incubated with the cells increased. In wells incubated with FK506 or L-685,818 alone the degree of outgrowth did not vary with the concentration of drug added, rather it oscillated slightly around the 100 % value.

5.3.3.8. Dose-response curves for the Combined Effect of NGF and FK506 or L-685,818 without Micelles. The neurite-like outgrowth for cells incubated with 5 ng/mL of NGF was found to be 180 ± 6 %. As shown in Figure 5.3.6, the degree of outgrowth in cells incubated with NGF (5 ng/mL) along with FK506 (1 to 100 nM) increased from 220 to 380 % with increasing concentration of FK506. Figure 5.3.7, shows that in cells incubated with NGF (5 ng/mL) along with L-685,818 (10 to 1000 nM) the degree of outgrowth increased from 200 to 350 % as the concentration of drug was increased.

5.3.3.9. In vitro effect of micelle-incorporated FK506 and L-685,818 along with NGF. Figure 5.3.6 shows the degree of differentiation in PC 12 cells which have been incubated with PCL-*b*-PEO incorporated FK506 and 5 ng/mL NGF following a 48 hour incubation period. The degree of neurite-like outgrowth in cells incubated with 5 ng/mL of NGF was 160 ± 5 %. In cell wells incubated with micelle-incorporated FK506 (1 to 100 nM) along with 5 ng/mL of NGF the neurite-like outgrowth ranged from 170 to 300 %. In Figure 5.3.6, we see no significant difference between untreated cells and cells treated with either PCL-*b*-PEO micelles without drug or cells treated with micelle-incorporated FK506 (control vs. bar 2 and 3). There was also no significant difference between cells treated with 5 ng/mL NGF and those treated with micelle incorporated FK506 (1 nM) along with 5 ng/mL NGF (bar 1 vs. bar 7). However, there was a significant difference ($p < 0.01$) between cells treated with 5 ng/mL NGF and cells treated with 10 or 100 nM of micelle incorporated FK506 (bar 1 vs. bars 8 and 9).

Figure 5.3.7 shows the degree of differentiation in PC 12 cells which have been incubated with PCL-*b*-PEO incorporated L-685,818 and 5 ng/mL NGF following a 48 hour incubation period. The degree of differentiation seen in cells incubated with the micelle incorporated L-685,818 along with 5 ng/mL NGF increased from 163 to 290 % as the concentration of drug increased from 10 nM to 1 μ M. In Figure 5.3.7 there is no

significant difference between the untreated cells and the cells treated with micelles alone or 10 nM of micelle incorporated L-685,818 (control vs. bar 2 or bar 3). Also, no significant difference was found between cells treated with 5 ng/mL of NGF and 10 nM micelle incorporated L-685,818. There was a significant difference ($p < 0.01$) between cells treated with 5 ng/mL NGF and cells treated with 100 nM and 1 μ M of micelle incorporated L-685,818 (bar1 vs. bars 8 and 9).

5.3.4. Discussion

5.3.4.1 Characterization of the PCL-*b*-PEO Micelles

In this study we explored the potential of the novel PCL-*b*-PEO micelles as a drug delivery vehicle for lipophilic drugs. The PCL-*b*-PEO micelles cannot be prepared in water alone due to the hydrophobicity of the polycaprolactone core - forming block. For this reason, the block copolymer is first dissolved in DMF, and micellization is induced by the dropwise addition of water, followed by dialysis. The micelles formed by this method of preparation were studied by dynamic light scattering in order to measure their effective diameter and their population distribution in terms of size. Figure 5.3.1a and 5.3.1b show the population distribution of the micelles calculated by Contin analysis of the dynamic light scattering measurements. Figure 5.3.1a shows the bimodal population distribution found in a 0.02% (w/w) of PCL₂₀-*b*-PEO₄₄. The larger population, at approximately 500 nm, consists of aggregates of the small individual micelles, which we see at 50 nm. Figure 5.3.1b shows the population distribution in terms of size of a .1% (w/w) of PCL₂₀-*b*-PEO₄₄. Comparing Figures 5.3.1b and 5.3.1a we see that as the solution is diluted, decreasing the concentration from .1% to .02%, the population of the larger aggregates is decreased in favor of the smaller (50 nm) population. This suggests that the larger aggregates are composed of aggregates of small individual micelles. Micelles with a coronal shell formed from PEO are frequently seen to form larger aggregates in solution. Winnik's group suggested the large associates of PS-*b*-PEO to be either onion-like aggregates or aggregates of small individual micelles [77]. Kataoka's group agreed with the latter suggestion when explaining the large associates they observed with the PEO-*b*-

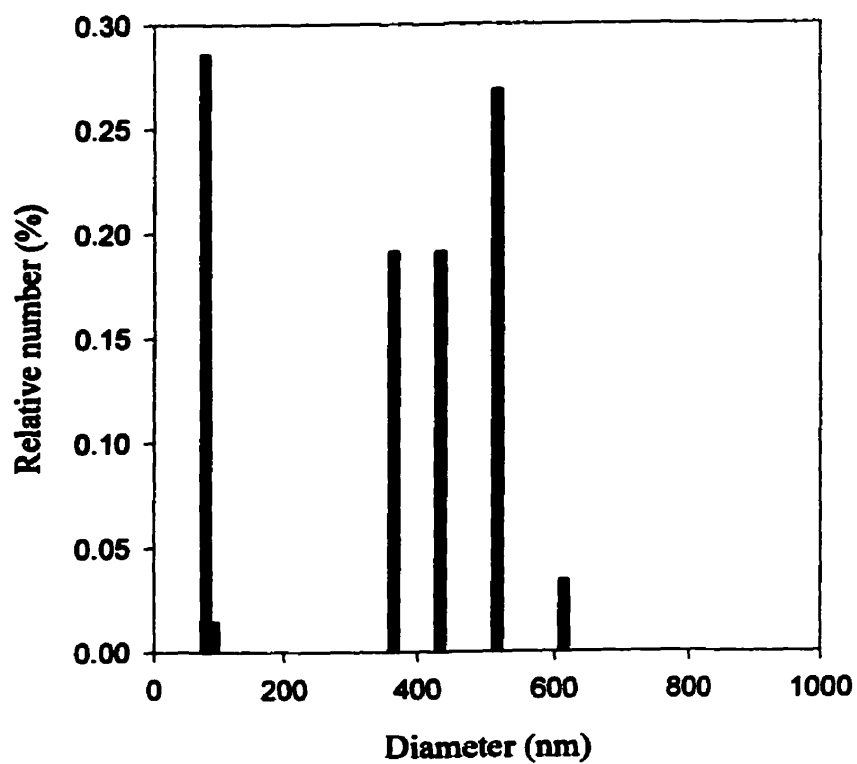


Figure 5.3.1.a) Particle size distribution of a 0.02% (w/w) solution of the PCL₂₀-*b*-PEO₄₄ copolymer micelles.

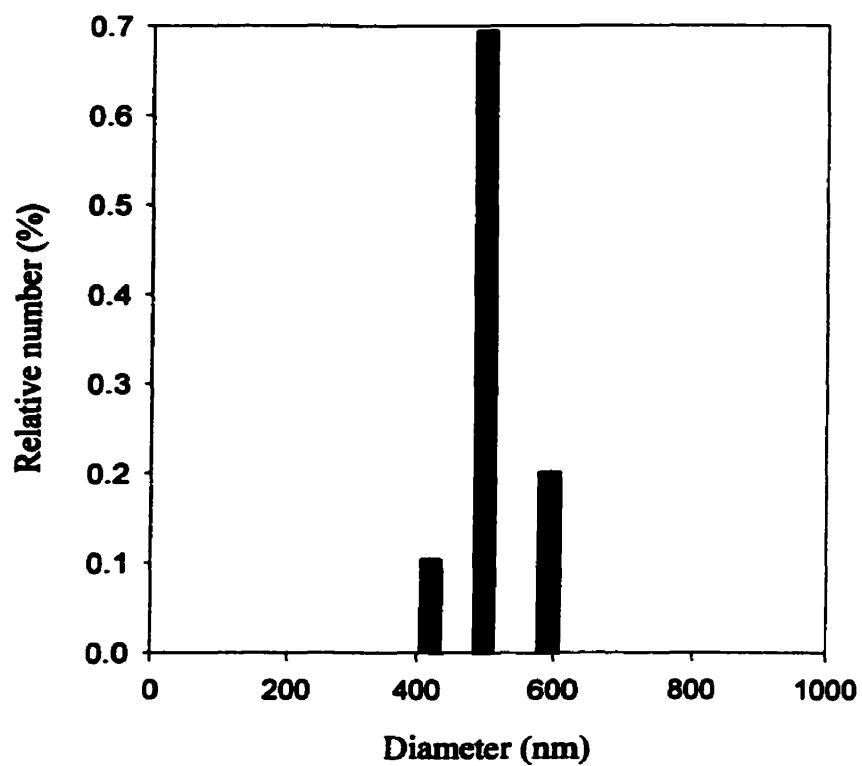


Figure 5.3.1.b) Particle size distribution of a 0.1% (w/w) solution of the PCL₂₀-*b*-PEO₄₄ copolymer micelles.

PBLA micelles [56b]. They suggest the aggregates of individual micelles may form due to either hydrophobic - hydrophobic interactions or Van der Waals interactions between the exposed cores of the individual micelles.

In our case, we had specifically chosen the PEO block to be 44 units in length, since this has most commonly been the length of the PEO stabilizing moieties employed for the steric stabilization of liposomes. However, most likely the length of the PEO blocks are too short to outweigh the hydrophobic - hydrophobic or Van der Waals interactions between the exposed polycaprolactone cores. We are now studying the relationship between the PEO chain length and the degree of aggregation achieved in the micelle solution.

Dynamic light scattering measurements were also used to monitor the *in vitro* stability of the micelles in water and the cell culture media DMEM and RPMI. Over a three month period the micelles were still intact and the population distribution of the micelles in terms of size remained relatively constant. These studies are still ongoing since the *in vitro* stability of the micelles will determine the extent to which they are suitable for various applications.

5.3.4.2 Determination of the Partition Coefficient for Pyrene between the PCL-*b*-PEO Micelles and Water.

The affinity of the PCL-*b*-PEO micelles for lipophilic compounds was assayed by the determination of the K_v for the hydrophobic model compound, pyrene, between the PCL-*b*-PEO micelles and water. This method was described in an earlier communication where it had been used to determine the K_v of pyrene between polystyrene-*b*-polyacrylic acid micelles and water. This fluorescence method is based on pyrene's sensitivity to the hydrophobicity of its microenvironment. This is reflected in changes in the ratio of the I_3/I_1 bands of its emission spectrum. The method requires the measurement of the I_3/I_1 ratio for pyrene in micelle solutions of various DMF/H₂O solvent mixtures. Figure 5.3.2a shows the increase in the I_3/I_1 ratio which accompanies an increase in the water content in the solvent mixture. The increase in the water content within the solvent mixture provides a driving force promoting the entry of pyrene into the more hydrophobic

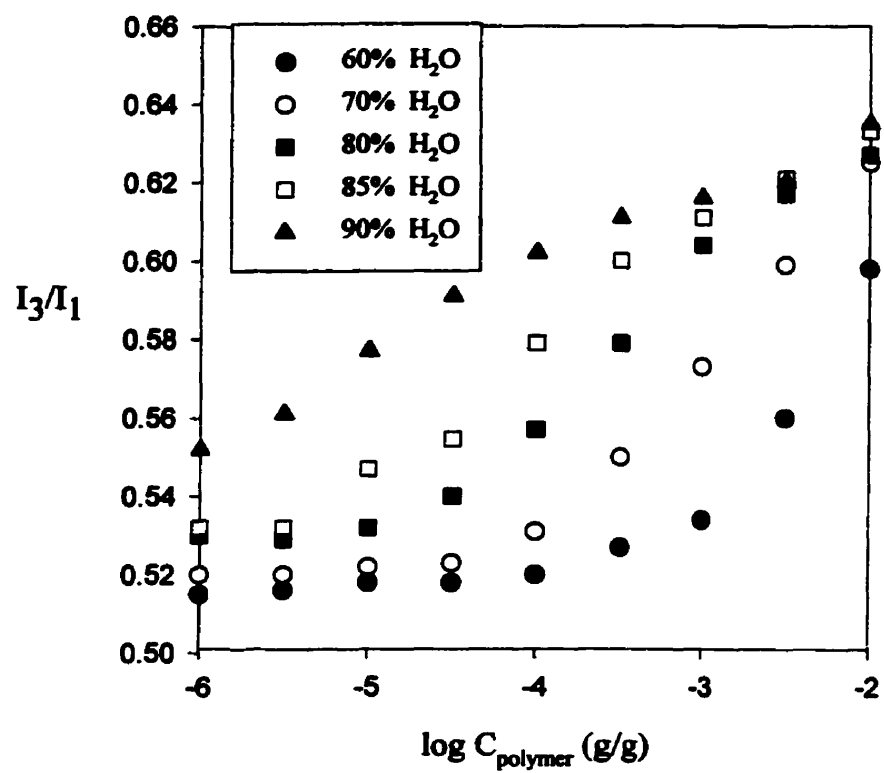


Figure 5.3.2.a) The I_3/I_1 ratio for pyrene in a solution of $\text{PCL}_{14}\text{-}b\text{-PEO}_{44}$ copolymer micelles and a DMF/ H_2O solvent mixture.

environment of the polycaprolactone micelle core. The I_3/I_1 ratio for pyrene in the many solutions was then used to calculate the partition coefficient for pyrene in each solution. Figure 5.3.2b shows the partition coefficients obtained for pyrene in the various micelle solutions, extrapolation of this plot to 100 % water content provides the value for the K_v of pyrene between the PCL-*b*-PEO micelles and water. The partition coefficient of pyrene in this micelle system was found to be of the order of 10^2 , this is low in comparison to a partition coefficient of the order of 10^5 found for pyrene between the polystyrene-*b*-polyacrylic acid (PS-*b*-PAA) micelles and water [76]. The high value for the K_v of pyrene between the PS-*b*-PAA micelles and water is thus due to the highly hydrophobic nature of both pyrene and the polystyrene core. The polycaprolactone core, though hydrophobic, is clearly less hydrophobic than polystyrene. However, this value of K_v for pyrene between the PCL-*b*-PEO micelles and water is of the same order of magnitude as that for pyrene in a solution of PEO_{m/2}-*b*-PPO_n-*b*-PEO_{m/2} ($m=51$, $n=38$) and water at the same temperature (20°C) [54b].

It should be noted, that our measurements for the determination of the partition coefficient for pyrene between the PCL-*b*-PEO micelles and water were all performed at 20°C. Previously it was found that the partition coefficient for pyrene between micelles formed from PEO-*b*-PPO-*b*-PEO and water increased by an order of magnitude when the temperature was increased from 20 to 37°C. This increase is said to be due to the decrease in the degree of hydration of the core forming block at the higher temperature. Due to the nature of the polycaprolactone core forming block, we also anticipate an increase in the partition coefficient for pyrene at higher temperatures.

Many studies, have revealed that the greatest degree of solubilization of a compound within a micelle core is achieved when there is a close match between the degree of the polarity and hydrophobicity of the compound and the micelle core [78-80].. For this reason we are now exploring the incorporation of various hydrophobic drugs into micelles with a longer polycaprolactone core forming block. Overall, the incorporation of the highly hydrophobic compound, pyrene, reveals the suitability of this micelle system as a potential carrier for even the most lipophilic compounds.

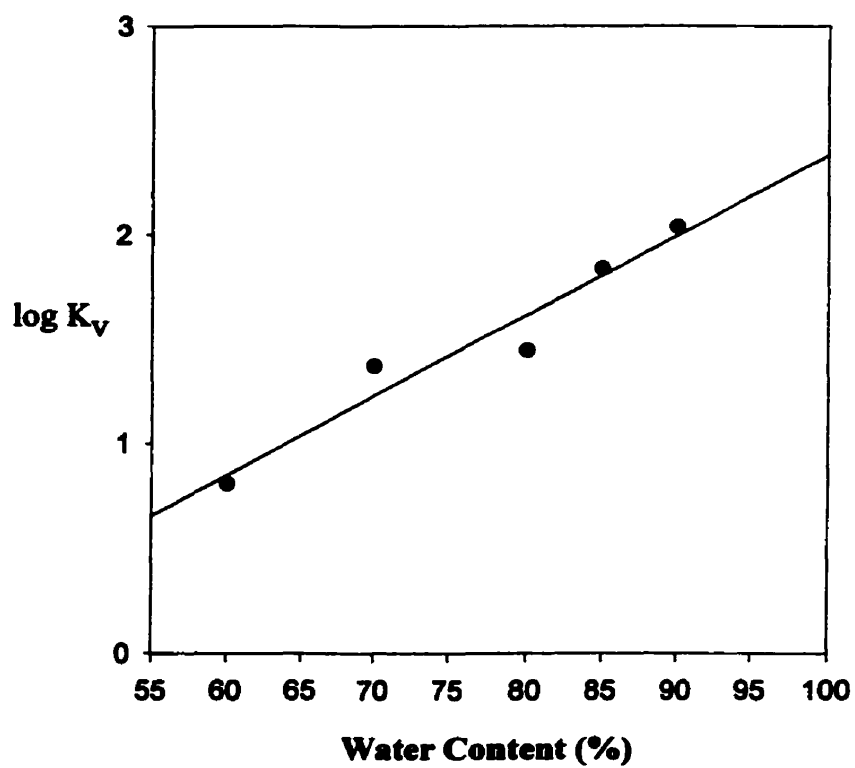


Figure 5.3.2. b) The semilogarithmic plot of the partition coefficient for pyrene in a solution of the PCL-*b*-PEO micelles and a range of H₂O/DMF solvent mixtures.

5.3.4.3. *In vitro* Biocompatibility of the PCL-*b*-PEO Micelles The *in vitro* biocompatibility of the PCL-*b*-PEO micelles (14-*b*-44, 20-*b*-44) was tested by incubating the micelles with a wide range of cell lines for both 24 hour and 48 hour periods. The Trypan blue and Alamar blue survival assays were then used to quantitate the survival rates in the presence of the PCL-*b*-PEO micelles. Figure 5.3.3 shows the percent survival obtained for the incubation of the PCL-*b*-PEO micelles (.02 to 1% (w/v)) with PC 12 cells over a 24 hour period. The survival in the presence of micelles was between 85 and 100%, except for the 70% survival obtained for the incubation of the PCL₁₄-*b*-PEO₄₄ micelles at the lowest concentration. In Figure 5.3.3 we see that at several concentrations the survival obtained with the PCL₁₄-*b*-PEO₄₄ is slightly lower than that obtained with the PCL₂₀-*b*-PEO₄₄. For this reason the 20-*b*-44 PCL-*b*-PEO system, rather than the 14-*b*-44 system, is investigated as the delivery system for FK506 and L-685,818.

The *in vitro* biocompatibility studies have shown us that addition of a PCL₂₀-*b*-PEO₄₄ micelle solution to the cell well causes little or no cell death. However, the actual destination of the micelles following their addition to the cell well is still unknown. There are several possibilities; they all remain in the supernatant, they all enter the cell, possibly only the small micelles can enter the cell while the larger aggregates remain in the supernatant, or the micelles may aggregate at the cell surface. We are currently investigating the destination of the micelles since this will largely affect the types of drugs which will most effectively be delivered by this system.

5.3.4.4. *Cell Uptake of Pyrene-Incorporated Micelles* The capability of the PCL-*b*-PEO micelle system to deliver a hydrophobic compound was first tested *in vitro* using pyrene as a model compound. The pyrene incorporated PCL-*b*-PEO micelles were incubated with PC 12 cells over a 24 hour period. At 0, 4, 8 and 24 hours, samples of the supernatant were studied by fluorescence in order to determine the quantity of pyrene remaining in the supernatant at each time point. Likewise, at each time point, cells were isolated and their fluorescence was examined under the fluorescence microscope, in order to determine if the decrease in the fluorescence within the supernatant was accompanied by an increase in fluorescence within the cells. Figure 5.3.4 shows the pronounced

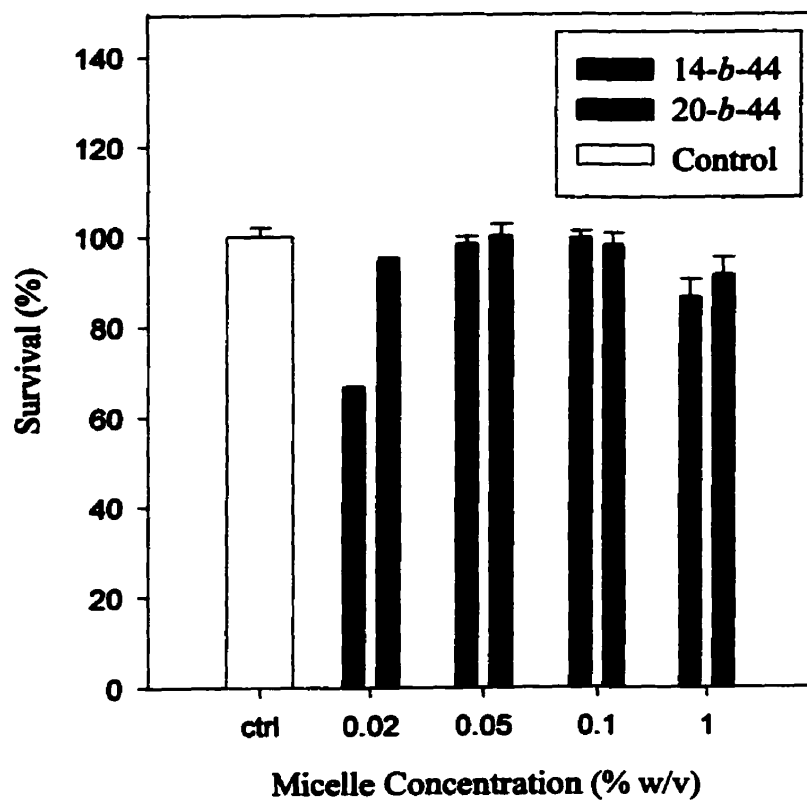


Figure 5.3.3. The *in vitro* biocompatibility of the PCL-*b*-PEO (14-*b*-44 and 20-*b*-44) micelles (0.02 to 1% w/v) as determined by the Alamar Blue survival assay. The results were confirmed by the Trypan Blue assay. Each data point represents the average of 3 independent experiments, from 6-8 wells.

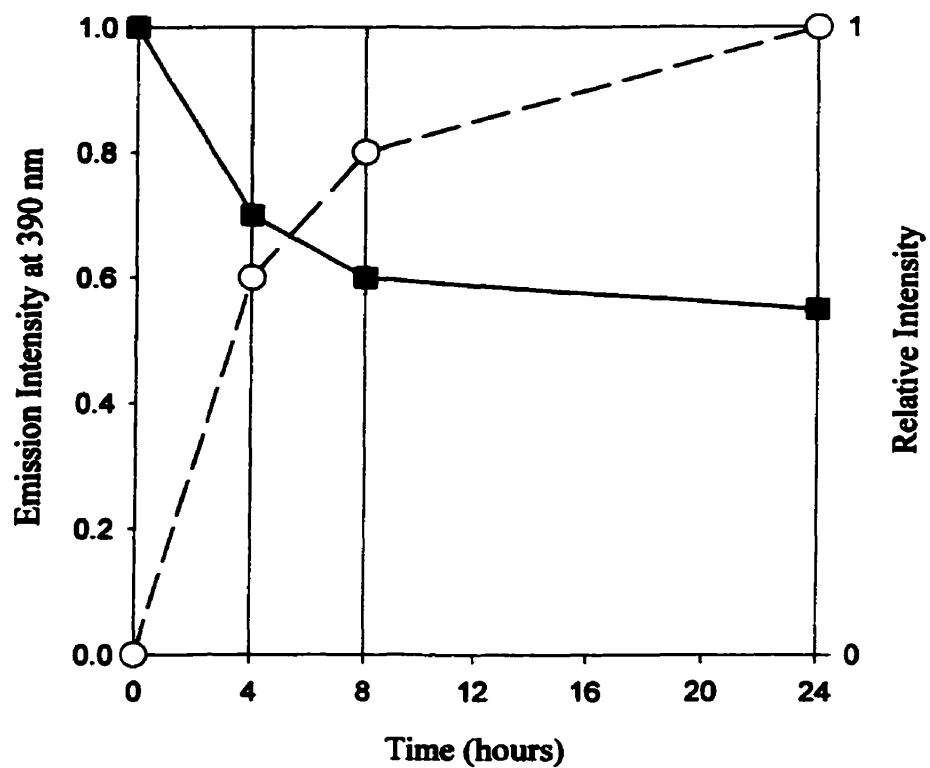


Figure 5.3.4. The change in the relative emission intensity of: pyrene in the supernatant (■), and cells (○), at 390 nm, over a 24 hour period. PC 12 cells were exposed to PCL₁₄-*b*-PEO₄₄ micelles containing pyrene and the change in the fluorescence intensity was measured at 4, 8 and 24 hour time points.

decrease in the fluorescence of the supernatant at the 4 hour time point, this decrease was found to be more gradual over the rest of the 24 hour period. A similar trend was also seen for the fluorescence of the isolated cells where the fluorescence increases gradually over the 24 hour period. At the 24 hour time point the fluorescence is quite intense and appears to be localized in small spherical aggregates.

The cell uptake studies reveal that the addition of pyrene incorporated micelles to the cells does, in fact, result in the accumulation of pyrene within the cells. However, once again, it is unknown whether or not the micelles have simply remained in the supernatant or have somehow facilitated the entry of pyrene into the cells. Since the partition coefficient for pyrene between water and the PCL-*b*-PEO micelle system is of the order of 10^2 , it seems likely that the micelles either enter the cells themselves or possibly attach themselves to the surface of the cell, enabling the drug to enter the cell without having to enter the hydrophilic cell medium.

5.3.4.5. PCL-*b*-PEO Micelles as a Delivery System for FK506 and L-685,818 The size of the PCL-*b*-PEO micelles as well as their *in vitro* stability, *in vitro* biocompatibility and their loading capacity for lipophilic compounds such as pyrene merited further study of this system as a delivery system for hydrophobic drugs. We have chosen FK506 and L-685,818 as the first hydrophobic candidate drugs to be delivered by the PCL-*b*-PEO micellar system.

As mentioned, FK506 and L-685,818 have both been shown to potentiate the effect of NGF on the outgrowth of PC 12 cells [74]. In order to compare the effect of the micelle incorporated FK506 and L-685,818 with the free drugs, it was necessary to construct dose response curves for NGF, FK506, L-685,818 alone as well as the combinations of NGF with FK506 or L-685,818. Figure 5.3.5, shows the dose response curves for each of NGF, FK506 and L-685,818 alone. Clearly, the degree of differentiation of the PC 12 cells increases with increasing concentration of NGF; however, the concentration of either FK506 or L-685,818 alone was found to have no effect on the degree of differentiation (Figure 5.3.5). These findings support previous results which have been reported in the literature [15].

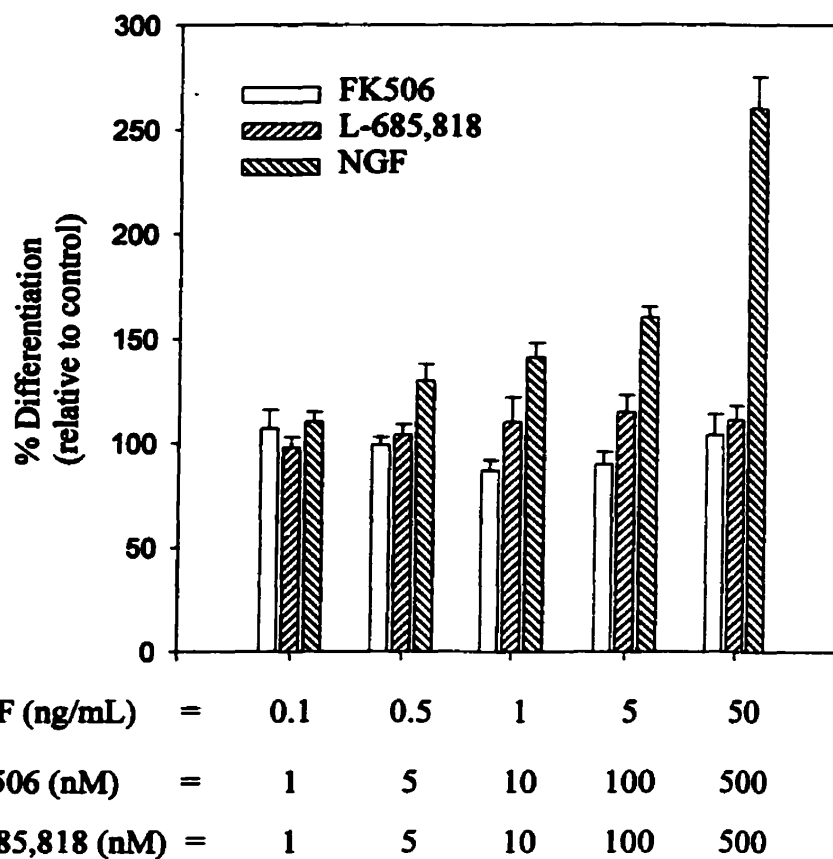
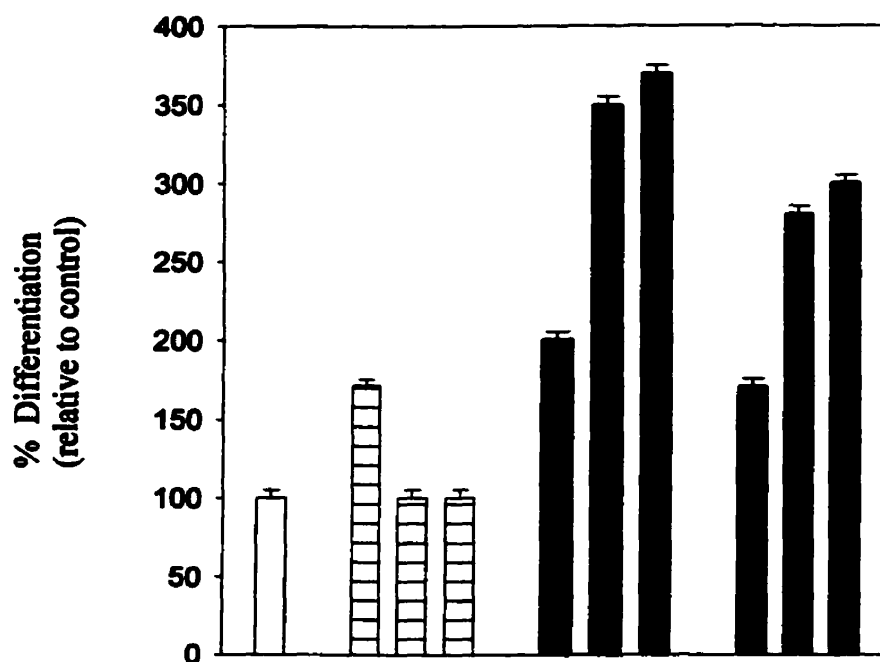


Figure 5.3.5. The degree of neurite-like outgrowth in PC 12 cells incubated with either NGF, FK506 r L-685,818, over a 48 hour period (n=3-4). The concentration of NGF incubated with the cells was C1 = 0.1, C2 = 0.5, C3 = 1, C3 = 5, C4 = 10, C5 = 50 ng/mL, the concentrations of FK506 or L-685,818 was C1 = 1, C2 = 5, C3 = 10, C4 = 100, C5 = 500 nM. The degree of differentiation in the control (absence of any treatment) is taken to be 100 % differentiation.

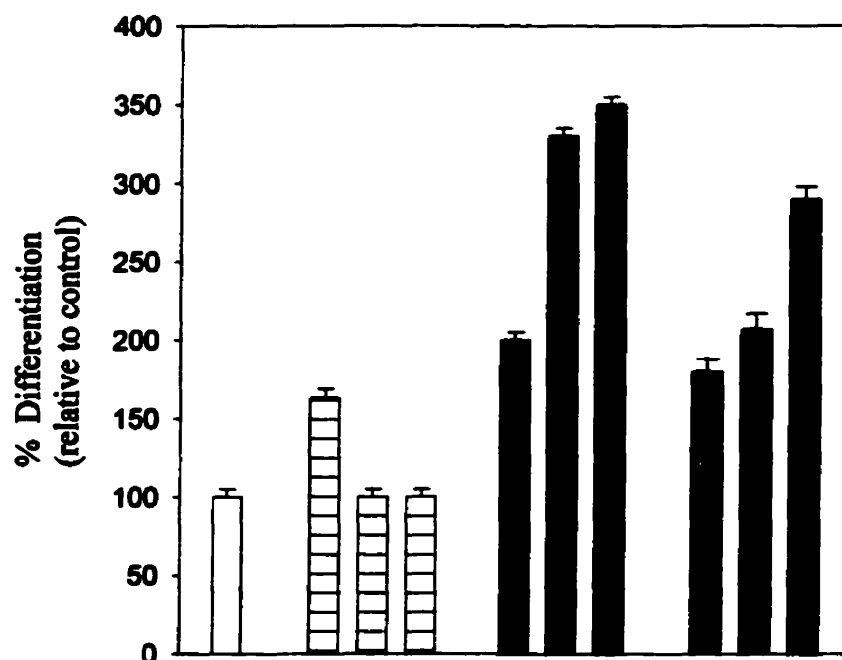
Figure 5.3.6 shows the degree of differentiation obtained in cells treated with micelle incorporated FK506 along with NGF and Figure 5.3.7 shows that for cells treated with micelle incorporated L-685,818. The PCL-*b*-PEO incorporated FK506 and L-685,818 were both found to potentiate the effect of NGF on neurite-like outgrowth in PC 12 cell cultures. Thus the ability of both FK506 and L-685,818 to potentiate the effect of NGF on neuronal outgrowth was retained despite their incorporation into the PCL-*b*-PEO copolymer micelles (Figure 5.3.6 and 5.3.7, bars 7-9). The degree of neurite-like outgrowth achieved in cell cultures treated with 5ng/mL NGF and either micelle-incorporated FK506 or L-685,818 (Fig.5.3.6 and 5.3.7, bars 7-9) was in both cases less than that obtained when the cells were treated with 5ng/mL NGF and free FK506 or L-685,818 (Fig.5.3.6 and 5.3.7, bars 4-6). This may be due to the limited 48 hour incubation period over which time only a fraction of the drug will be released from the micelles. It should be noted that, *in vitro*, a dose of FK506 as low as 1nM, is adequate to potentiate neurite-like outgrowth in PC12 cell cultures (Figure 5.3.6). Also, in several *in vivo* studies on rats it was found that 1mg/kg of FK506 was an effective dose [81]. This micellar delivery system is able to incorporate much higher concentrations of FK506 which will later be released slowly over time. In this way, it will prevent some of the damaging effects that high doses would induce.

In summary, the preliminary results obtained for the novel PCL-*b*-PEO micelle system reveal it to be a promising drug delivery vehicle for the delivery of various lipophilic drugs. The small size and indefinite *in vitro* stability of the micelles suggest that they may be useful for a wide variety of biomedical applications. Their loading capacity for the very hydrophobic compound, pyrene, encourages the incorporation of many different compounds with a high degree of hydrophobicity. Studies involving the degree of aggregation encountered in the micelle solutions are now underway with special effort placed on limiting the degree of aggregation. Also, now that the *in vitro* biocompatibility of the micelles has been established, it will be assayed *in vivo*.



NGF (ng/mL)	=	0	5	0	0	5	5	5	5	5	5
Micelles (%w/w)	=	0	0	0.1	0.1	0	0	0	0.1	0.1	0.1
FK506 (nM)	=	0	0	0	1	1	10	100	1	10	100

Figure 5.3.6. The effect of micelle-incorporated FK 506 and NGF (5 ng/mL) on the neurite-like outgrowth in PC 12 cells over a 48 hour period (n= 3-4). Control = PC 12 cells in the absence of any treatment. Bars 1-9 are PC 12 cells treated with the following: Bar 1 = 5 ng/mL NGF, Bar 2 = PCL₂₀-*b*-PEO₄₄ micelles, Bar 3= micelle-incorporated FK506 (1 nM), Bars 4-6 = FK506 (Bars 4,5,6 = 1, 10, 100 nM respectively) along with 5 ng/mL NGF; Bars 7-9 = micelle-incorporated FK506 (Bars 7,8,9 = 1, 10, 100 nM respectively) along with 5 ng/mL NGF.



NGF (ng/mL)	=	0	5	0	0	5	5	5	5	5	5
Micelles (%w/w)	=	0	0	0.1	0.1	0	0	0	0.1	0.1	0.1
L-685,818 (nM)	=	0	0	0	10	10	100	1000	10	100	1000

Figure 5.3.7. The effect of micelle-incorporated L-685,818 and NGF (5 ng/mL) on the neurite-like outgrowth in PC 12 cells over a 48 hour period (n = 3-4). Control = PC 12 cells in the absence of any treatment. Bars 1-9 are PC 12 cells treated with the following: Bar 1 = 5 ng/mL NGF, Bar 2 = PCL₂₀-b-PEO₄₄ micelles, Bar 3 = micelle-incorporated L-685,818 (10 nM), Bars 4-6= L-685,818 (Bars 4, 5, 6 = 10, 100, 1000 nM respectively)

5.3.5. References

1. Alak A.M., *Therapeutic Drug Monitoring* **1997**, 19, 338.
2. Takada K., Katayama N., Kiriya A., Usuda H., *Biopharmaceutics and Drug Disposition* **1993**, 14, 659.
3. Goto T., Kino T., Hatanaka H et al. *Transplant Proc.* **1991**, 23, 2713.
4. Jain A. B., Fung J.J., Tzakis A.G., et al. *Transplant Proc.* **1991**, 23, 2763.
5. The U.S. Multicenter FK506 Liver Study Group *New England J. Med.* **1994**, 331, 1110.
6. Venkataraman R., Jain A., Cadoff E. et al. *Transplant Proc.* **1990**, 22, 52.
7. Fung J.J., Starzl T. E., *Therapeutic Drug Monitoring* **1995**, 17, 592.
8. Mayer D.A., Dmitrewski J., Squifflet J.P., Besse T., Grabensee B. et al. *Transplantation* **1997**, 64, 436.
9. Thompson A.W., Bonham C.A., Zeevi A., *Therapeutic Drug Monitoring* **1995**, 17, 584.
10. European FK506 Multicentre Liver Study Group *The Lancet* **1994**, 344, 423.
11. Tauxe W.W., Mochizuki T., McCauley J., Starzl T.E., Jain A., Charron M., *Transplant Proc.* **1991**, 23, 3146.
12. Yakel J.:L., *TiPS* **1997**, 18, 124.
13. Hamilton G.S., Steiner J.P., *Current Pharmaceutical Design* **1997**, 176, 751.
14. Dumont F.J., Staruch M.J., Koprak S.L., *J. Exp. Med.* **1992**, 176, 751.
15. Steiner J.P., Connolly M.A., Valentine H.L., Hamilton G.S., Dawson T.M., Hester L., Snyder S.H., *Nature Medicine* **1997**, 3, 421.
16. Sigal N.H., Dumont F., Durette P., Siekierka J.J., Petersen L., Rich D., *J. Exp. Medicine* **1991**, 173, 619.
17. Thomas J., Matthews C., Carroll R., Loreth R., Thomas F., *Transplantation* **1990**, 49, 390.
18. Mosmann T.R., Coffman R.L., *Immunol. Today* **1987**, 8, 223.
19. Guyre P.N, Girard M.T., Morganelli P.M., Manganiello P.D., *J. Steroid Biochem.* **1988**, 30, 89.
20. Schmitt J., Pohl J., Stunnenberg G.H., *Gene* **1993**, 132, 267.

21. Tai P.K., Albers M.W., Chang H., Faber L.E., Schreiber S.L., *Science* **1992**, 256, 1315.
22. Tai P.K., Albers M.W., McDonnell D.P., Chang H., Schreiber S.L., Faber L.E., *Biochemistry* **1994**, 33, 1066.
23. Renoir J.M., Le Bihans S., Mercier-Bodard C., et al. *J. Steroid Biochem. Mol. Biol.* **1994**, 48, 101.
24. Choi D., *Science* **1992**, 258, 241.
25. Dawson T.M., Steiner J.P., Dawson V.L., Dinerman J.L., Uhl G.R., Snyder S.H., *Proc. Natl. Acad. Sci. U.S.A.* **1993**, 90, 9808.
26. Mackenzie G.M., Jenner P., Marsden C.D., *Neuroscience* **1995**, 67, 357.
27. Globus M.Y.T., Prado R., Sanchez-Ramos J., Zhao W., Dietrich W.D., Busto R., Ginsberg M.D., *J. Cereb. Blood Flow Metab.* **1995**, 15, 904.
28. Snyder S.H., Sabatini D.M., *Nature Medicine* **1995**, 1, 32.
29. Galat A., *Eur. J. Biochem.* **1993**, 216, 689.
30. Kay J.E., *Biochem J.* **1996**, 314, 361.
31. VanDuyne G.D., Standaert R.F., Karplus P.A., Schreiber S.L., Clardy J., *Science* **1991**, 252, 839.
32. Lepre C.A., Thomson J.A., Moore J.M., *FEBS Letters* **1992**, 302, 89.
33. VanDuyne G.D., Standaert R.F., Karplus P.A., Schreiber S.L., Clardy J. *J. Mol. Biol.* **1993**, 105.
34. Snyder S.H., Sabatini D.M., Lai M.M., Steiner J.P., Hamilton G.S., Suzdak P.D., *TiPS* **1998**, 19, 21.
35. Steiner J.P., Hamilton G.S., Ross D.T., Valentine H.L., Guo H., Connolly M.A., Liang S., Ramsey C. et al. *Proc. Natl. Acad. Sci. U.S.A.* **1997**, 94, 2019.
36. Holt D.A., Konialian-Beck A.L., Oh H.J., Yen H.K., Rozamus L.W., Krog A.J., Erhard K.F., Ortiz E. et al., *Biomed. Chem. Lett.* **1994**, 4, 315.
37. Lyons W.E., George E.B., Dawson T.M., Steiner J.P., Snyder S.H., *Proc. Natl. Acad. Sci. U.S.A.* **1994**, 91, 3191.
38. Hiroi J., Sengoku T., Morita K. et al. *Jpn. J. Pharmacol.* **1998**, 175.
39. Mueller W., Hermann B., *N.Engl. J Med.* **1979**, 301, 555.

40. Ellis C.N., Fradin M.S., Messana J.M. et al. *N. Engl.J. Med.* **1991**, 324, 277.
41. van Joost T., Stolz E., Heule F. et al., *Dermatology* **1987**, 123, 166.
42. Lauerma A.I., Surber C., Maibach H.I., *Skin Pharmacol.* **1997**, 10, 230.
43. Alaiti S., Kang S., Fiedler V.C., Ellis C.N., Spurlin D.V. et al. *J of the American Academy of Dermatology* **1998**, 16, 69.
44. Ko S., Nakajima Y., Kanehiro H. et al. *Transplantation* **1994**, 58, 1142.
45. Ko S., Nakajima Y., Kanehiro H. et al. *Transplantation* **1995**, 59, 1384.
46. Ko S., Nakajima Y., Kanehiro H. et al. *Transplantation Proc.* **1997**, 29, 529.
47. Greene L.A., Tischler A.S., *Proc. Natl Acad Sci. U.S.A.* **1976**, 73, 2424-28.
48. Mesner P.W., Epting C.L., Hegarty J.L., Green S.H., *J. of Neurosci.* **1995**, 15, 7357-7366.
49. Vambutas V., Kaplan D.R., Sells M.A., Chernoff J., *J.Bio.Chem.* **1995**, 270, 25629-25633.
50. Zhou J., Valletta J.S., Grimes M.L., Mobley W.C., *J. Neurochem.* **1995**, 65, 1146-1156.
51. Maysinger D., Morinville A. *TIBS* **1997**, 15, 410.
52. Gregoriadis G. *TIBS* **1995**, 13, 527.
53. Muller R.H., *Colloidal Carriers for Controlled Drug Delivery and Targeting: Modification, Characterization and In vivo Distribution*, CRC Press Inc., Florida **1991**.
54. Kabanov A.V., Alakhov V.Y. " Micelles of Amphiphilic Block Copolymers as Vehicles for Drug Delivery " In *Amphiphilic Block Copolymers: Self-Assembly and Applications* edited by Alexamdris P., Lindman B., Elsevier, Netherlands **1997**.
55. (a) Alakhov V.Y., Moskaleva E.Y., Batrakova E.V., Kabanov A.V. *Bioconjugate Chem.* **1996**, 7, 209. (b) Kabanov, A.V, Nazarova, I.R., Astafieva I.R., Batrakova E.V., Alakhov V.Y., Yarostavov A.A., Kabanov V.A. *Macromolecules* **1995**, 28, 2303.
56. (a) Kwon G., Naito M., Yokoyama M., Okano T., Sakurai Y., Kataoka K. *J. Controlled Release* **1997**, 48, 195. (b) La S.B., Okano T., Kataoka K. *Journal of Pharmaceutical Sciences* **1996**, 85, 85. (c) Kataoka K., Kwon G., Yokoyama M., Okano T., Sakurai Y. *J. Control. Release* **1992**, 24, 119.

57. Allen T.M. *Trends Pharmacol. Sci.*, **1994**, 15, 215.
58. Gref R., Minamitake Y., Peracchia M.T. *Science* **1994**, 263, 1600.
59. Sahli H., Tapon-Brethaudiere J., Fischer A.M., Sternberg C., Spenlehauer G., Verrecchia T., Labarre D. *Biomaterials* **1997**, 18, 281.
60. Zhang X., Burt H.M., Von Hoff D., Dexter D., Mangold G., Degen D., Oktaba A.M., Hunter W.L. *Cancer Chemother. Pharmacol.* **1997**, 40, 81-86.
61. (a) Bader H., Ringsdorf H., Schmidt B., *Angewandte Makromolekulare Chemie* **1984** 123, 457. (b) Pratten M.K., Lloyd J.B., Horpel G., Ringsdorf H. *Makromol. Chem.* **1985** 186, 725.
62. (a) Zhang L. Eisenberg A. *Science* **1995**, 268, 1728., (b) Zhang L, Yu K., Eisenberg A. *Science* **1996**, 272, 1777.
63. Woodward S.C., Brewer P.S., Moatamed F., Shindler A., Pitt C.G. *J. Biomed. Mater. Res.* **1985**, 19, 437.
64. van der Giessen W.J., Lincoff A.M., Schwartz R.S., van Beusekom H.M.M., Serruys P.W., Holmes D.R., Ellis S.G., Topol E.J. *Circulation* **1996** 94, 1690.
65. Winternitz C.I., Jackson J.K., Oktaba A.M.C., Burt H.M. *Pharm. Res.* **1996**, 13, 368.
66. Jackson J.K., Min W., Cruz T.F., Cindric S., Arsenault L., Von Hoff D.D., Hunter W.L., Burt H.M. *Br. J. Cancer* **1997**, 75, 1014.
67. Calvo P., Alfonso M.J., Vila-Jato J.L., Robinson J.R., *Journal of Pharm. Pharmacol.*, **1996**, 48, 1147.
68. Elbert D.L., Hubbell J.A., *Annu. Rev. of Mater. Sci.* **1996**, 26, 365.
69. Lee J.H., Lee H.B., Andrade J.D., Blood Compatibility of Polyethylene Oxide Surfaces *Prog. Polym. Sci.* **1995**, 20, 1043.
70. Bei J., Wang Z., Wang S., *Chinese Journal of Polymer Science* **1995**, 2, 154.
71. Martini L., Collett J.H., Attwood D. *J. Pharm. Pharmacol.* **1997**, 49, 601.
72. Kim Y.S., Shin I.L.G., Lee Y.M., Cho C. S., Sung Y.K., *J. Control. Release* **1998**, 51, 13.
73. Allen C., Yu Y., Chijiwa S., Maysinger D., Eisenberg A., to be submitted to *Macromolecules* **1999**.
74. Goral S., Helderman J.H. *Seminars in Nephrology* **1997**, 17(H), 364.

75. Marks A. R. *Physiol. Rev.* **1996**, 76, 631.
76. Zhao, J., Allen, C., Eisenberg, A. *Macromolecules* **1997**, 30, 7143.
- 77.(a) Wilhelm M, Zhao C-L., Wang Y., Xu R., Winnik M. A., Mura J.L., Riess G., *Macromolecules* **1991**, 24, 1033. (b) Xu, R.; Winnik, M.A.; Hallett, F.R., Riess, G., Croucher, M.D. *Macromolecules* **1991**, 24, 87.
78. Nagarajan, R.; Ganesh K. *J. Colloid Interface Sci.* **1996**, 184, 489.
79. Tian, M., Arca, E., Tuzar, Z., Webber S.E., Munk, P. *J. Polym. Sci., Part B: Polym. Phys.*, **1995**, 33, 1713.
80. Moroi, Y.; Mitsunobu, K.; Morisue T.; Kadobayashi, Y.; Sakai, M. *J. Phys. Chem.*, **1995**, 99, 2372.
81. Butcher S.P., Henshall D.C., Teramura Y., Iwasaki K., Sharkey J.J. *Neurosci.* **1997**, 17, 6939.

CHAPTER 6

***IN VIVO* STUDY OF POLYCAPROLACTONE-*b*-POLY(ETHYLENE OXIDE) MICELLES AS A DELIVERY VEHICLE FOR THE NEUROTROPHIC AGENT FK506**

Following our *in vitro* evaluation of the PCL₂₀-*b*-PEO₄₄ micelles as a delivery vehicle for FK506 we were interested in expanding our investigations to include *in vivo* studies. Firstly, we were interested in comparing the organ biodistribution of the micelle-incorporated drug with that known for the drug alone. Secondly, we wanted to investigate the biological activity of the micelle-incorporated drug *in vivo* using a well established model. In section 6.1. we summarize the results from our preliminary *in vivo* studies of PCL-*b*-PEO micelle-incorporated FK506. The organ biodistribution of the micelle-incorporated drug was studied both 6 and 24 hours following intravenous administration in Sprague Dawley rats. The *in vivo* biological activity of the micelle-incorporated drug was investigated using the sciatic nerve crush paradigm, an established model of peripheral nerve injury [1-5].

It is important to note that the *in vivo* biological study of a delivery vehicle requires extensive animal studies in order to properly compare the pharmacokinetic parameters and biodistribution of the delivery vehicle-incorporated drug to that of the drug alone. The *in vivo* studies that we have completed on the PCL-*b*-PEO micelles, as summarized in section 6.1., only represent the first step in a long series of studies that would be required in order to thoroughly characterize this delivery vehicle *in vivo*.

However, the results from these studies are interesting and thus suggest that further investigations of this type are worth pursuing.

6.1. *In vivo* Study of PCL-*b*-PEO Micelles as a Delivery Vehicle for the Neurotrophic Agent FK506

6.1.1. Introduction

Recently, micelles formed from amphiphilic block copolymers have been investigated as potential drug delivery vehicles for lipophilic agents. In a previous paper we described our preliminary studies of micelles formed from polycaprolactone-*b*-poly(ethylene oxide) (PCL₂₀-*b*-PEO₄₄) copolymers as a delivery vehicle for the neurotrophic agents FK506 and L-685,818 [6].

Immunosuppressant and non-immunosuppressant 12kDa-FK506 binding protein (FKBP12) ligands have been shown to have neurotrophic action [7-11]. The neurotrophic potency of the immunophilin ligands was first established with FK506 [12]. Presently, FK506 along with cyclosporin A (CsA), are the leading immunosuppressive agents used to prevent graft rejection [13-16]. As reviewed by Hamilton and Steiner [9], the neurotrophic effects of FK506 were shown by scientists at Guilford Pharmaceutical and Snyder's group to occur by a mechanism which is not mediated by calcineurin [9]. In fact they found that the structure of FK506 could be divided into an FKBP binding domain and an effector domain which interacts with calcineurin and is responsible for the immunosuppressive effect [9]. Analogues of FK506 which are unable to interact with calcineurin but retain their ability to bind to FKBP12 were found to have neurotrophic activity [9]. The neurotrophic effects of FK506 have been shown in several *in vitro* and *in vivo* models, including the potentiation of NGF in promoting neurite-like outgrowth in PC12 (rat pheochromocytoma) cells [9, 10], the production of neurite-like outgrowth in cultured chick dorsal root ganglia [9] and the enhancement of axonal regeneration in rats whose sciatic nerves had been crushed [4, 5]. The realization that the immunosuppressant and neurotrophic effects of FK506 were mediated by distinct regions of its structure prompted interest into the design of non-immunosuppressant immunophilin ligands. The design and development of delivery vehicles for this new class of drugs may enable their therapeutic potential to be fully exploited.

In the past, several carriers have been designed for the delivery of FK506 as an immunosuppressant agent, including liposomes [17-19], a water-in-oil-in-water type

emulsion [20, 21], and a dextran-conjugate [22]. To our knowledge, this is the first report of a drug carrier for the delivery of FK506 or other immunophilin ligands as neurotrophic agents.

In a previous paper we reported on our preliminary studies of micelles formed from polycaprolactone-b-poly(ethylene oxide) PCL₂₀-b-PEO₄₄ copolymers as a delivery vehicle for FK506 and L-685,818 [6]. An *in vitro* assay was used to compare the *in vitro* biological activity of drug alone and micelle-incorporated FK506 or L-685,818. The *in vitro* assay included measurement of the ability of FK506 or L-685,818 to potentiate NGF in promoting neurite-like outgrowth in PC12 (rat pheochromocytoma) cell cultures. The biological activity of the micelle-incorporated drugs were found to be retained. We now report on the *in vitro* release kinetics of FK506 from the copolymer micelles as well as their *in vivo* biodistribution 6 and 24 hours following intravenous injection into male Sprague Dawley rats. Also, the extent to which the micelle-incorporated FK506 is able to enhance functional recovery in rats whose sciatic nerves have been lesioned is assessed using a behavioral study.

The development of delivery vehicles that enhance the therapeutic potential of agents which accelerate nerve regeneration would be of great economic value to society [9]. In addition, carriers for agents which promote nerve regeneration in the peripheral and central nervous systems would be of benefit in the treatment of diseases such as Parkinson's, Alzheimer's, diabetic neuropathy and multiple sclerosis [9].

6.1.2. Materials and Methods

6.1.2.1. Materials The block copolymer PCL₂₀-b-PEO₄₄ was synthesized by anionic polymerization. All chemicals were purchased from Aldrich Chemical Company. The scintillation cocktail used in loading studies (Fisher Chemical, Fisher Scientific, ScintiSafe Econo F) and that used in the kinetic release studies (Fisher Chemical, Fisher Scientific, ScintiSafe™ Plus 50%), was purchased from V.W.R. Scientific. The radiolabelled FK506 was purchased from Nen Life Science Product-Mandel Scientific Inc. The Protosol tissue and gel solubilizer was purchased from Nen Life Science Products, Dupont. The dialysis bag used in the micelle preparation was Spectra Por®

Membrane, MWCO: 50,000 and that used for the kinetic release studies was also Spectra Por® Membrane but of MWCO: 15, 000.

6.1.2.2. Methods

Preparation of Micelle-Incorporated ^3H -FK506 A 100 μL aliquot (amount equal to 100 uCi, i.e. 1mCi = 1mL) of a ^3H -FK506 (Lot 3329491) solution in ethanol was added to an empty vial and the ethanol was allowed to evaporate. The amount of ^3H -FK506 added to the vial was 1.15 nanomoles since the specific activity of ^3H -FK506 is 87.0 Ci/mmol. 0.01g of the PCL₂₀-b-PEO₄₄ copolymer was then added to the vial along with up to 0.2g of DMF. The solution was stirred at room temperature for 4 hours, at which point 0.8g of water was added slowly to the vial to make a 1% (w/w) copolymer solution. The micelle solution was then left to stir overnight and then dialyzed against Milli Q water. The loading efficiency of the micelle solution was found to be 21% which translates to a final concentration of 240 nM FK506 in the micelle-incorporated ^3H -FK506 solution. The micelle-incorporated FK506 for the sciatic nerve crush experiments was prepared using drug extracted from 5 mg Prograf® capsules for human use (provided by Fujisawa Pharmaceutical Co.). The extracted FK506 was placed in an empty vial the solvent was evaporated and the micelles were prepared as described above. The final concentration of FK506 in the micelle solution was 6mM.

Quantitation of the Amount of ^3H -FK506 Incorporated into Micelles Aliquots (50 μL) of the micelle-incorporated ^3H -FK506 solution were placed into vials filled with 450 μL of DMF. The solution was stirred for 2 hours and then added to scintillation vials containing 4 mL of Econo-F scintillation cocktail (for organic solvents). The vials were then counted by a scintillation counter and a calibration curve was used to calculate the number of uCi of ^3H -FK506 per vial.

Measurement of the Release Profile of ^3H -FK506 from the PCL₂₀-b-PEO₄₄ Micelles

A 100 μL aliquot of the micelle-incorporated ^3H -FK506 or ^3H -FK506 alone (in a DMSO/PBS 20:80 mixture) was placed into a dialysis bag and suspended in 10 mL of warmed PBS at 37°C and pH = 7.4. At specific time intervals a 100 μL aliquot was

removed from the external medium and replaced with a fresh 100 μ L aliquot of PBS. The aliquot removed was then placed in 4 mL of Scinti-Safe-Plus 50% scintillation cocktail and counted by the scintillation counter. The counts in CPM were then converted into μ Ci and then moles of ^3H -FK506 using a calibration curve.

***In vivo* Studies**

Animal Studies All of the experiments were performed with strict adherence to the Guidelines provided by the McGill Animal Resources Center, McGill University. The animals were maintained on standard food and able to drink ad libitum.

Pharmacokinetic and Tissue Distribution Studies

Male Sprague Dawley rats weighing 75-100g were used. Rats were injected intravenously (i.v.) into the lateral tail vein with micelle-incorporated ^3H -FK506 such that each rat received 250ng/kg.

Tissue Distribution: The rats were euthanized by cervical dislocation 6 or 24 hours following i.v. injection (n = 3-4 for each time point). Organs such as the heart, spleen, liver, lungs, kidneys and brain (hypothalamus, hippocampus, cortex, cerebellum, pituitary, thalamus) were excised, rinsed with saline and weighed. A 100 mg sample of each was then placed in a scintillation vial containing 500 μ L of Protosol (tissue solubilizer) and left to stand on a shaker overnight. The following day 4 mL of scintillation cocktail was added to each vial and the were left to stand for 24 hours before being counted by a scintillation counter.

Sciatic Nerve Crush

Animals The animals used were Hanover Wistar rats weighing on average 100g. The animals were divided randomly into 3 experimental groups (each with n=6); control animals (non-lesioned, treated with 100 μ L of empty micelles), control animals (lesioned, treated with 100 μ L of empty micelles) and micelle-incorporated FK506 treated animals (lesioned, treated with 100 μ L micelle-incorporated FK506).

Drug Administration Animals received 5 mg/kg of the micelle-incorporated FK506 solution on days 0, 6 and 12 following the sciatic nerve crush. The first application was local and the others were given subcutaneously (100 μ L of micelle-incorporated FK506).

Surgical Procedure: All surgical procedures were conducted under sterile conditions. Animals were anesthetized with chloralhydrate (400 mg/kg, i.p.) and the sciatic nerves were exposed bilaterally below the sciatic notch and crushed twice with No. 7 Dumont forceps for a total of 30 seconds.

Behavioral Assessment Following, the lesion the animals were tested every 2 days for their muscle coordination on a rota-rod apparatus (Ugo Basile Treadmills for rats model 7700) for 20 days. Animals with little motor coordination dropped off the rod falling into a tray 20 cm below. Prior to the surgical procedure the animals were placed on the moving rod and those which stayed for 1 minute were chosen for this study. Also, prior to each test the rats were given a 1 minute exposure to the rotarod apparatus. Subsequently, the rats were tested over a 2 minute period whereby the endurance time was considered to be the time between the point the rat is placed on the moving rod and the point at which it falls down.

6.1.3. Results

6.1.3.1. *In vitro* Release Kinetics

Figure 6.1 shows the *in vitro* release profile of ^3H -FK506 from the PCL₂₀-b-PEO₄₄ micelle solution as measured by the dialysis method. There is a burst release of ^3H -FK506 from the micelle solution in the first 6 hours during which 40% of the drug is released. Following the 6 hour period the kinetics of the release slows down such that 100% of the drug is only released after 6 days (144 hours). Also shown is the release of ^3H -FK506 dissolved in a DMSO/ethanol solution. In this case the drug is completely released in 4 hours.

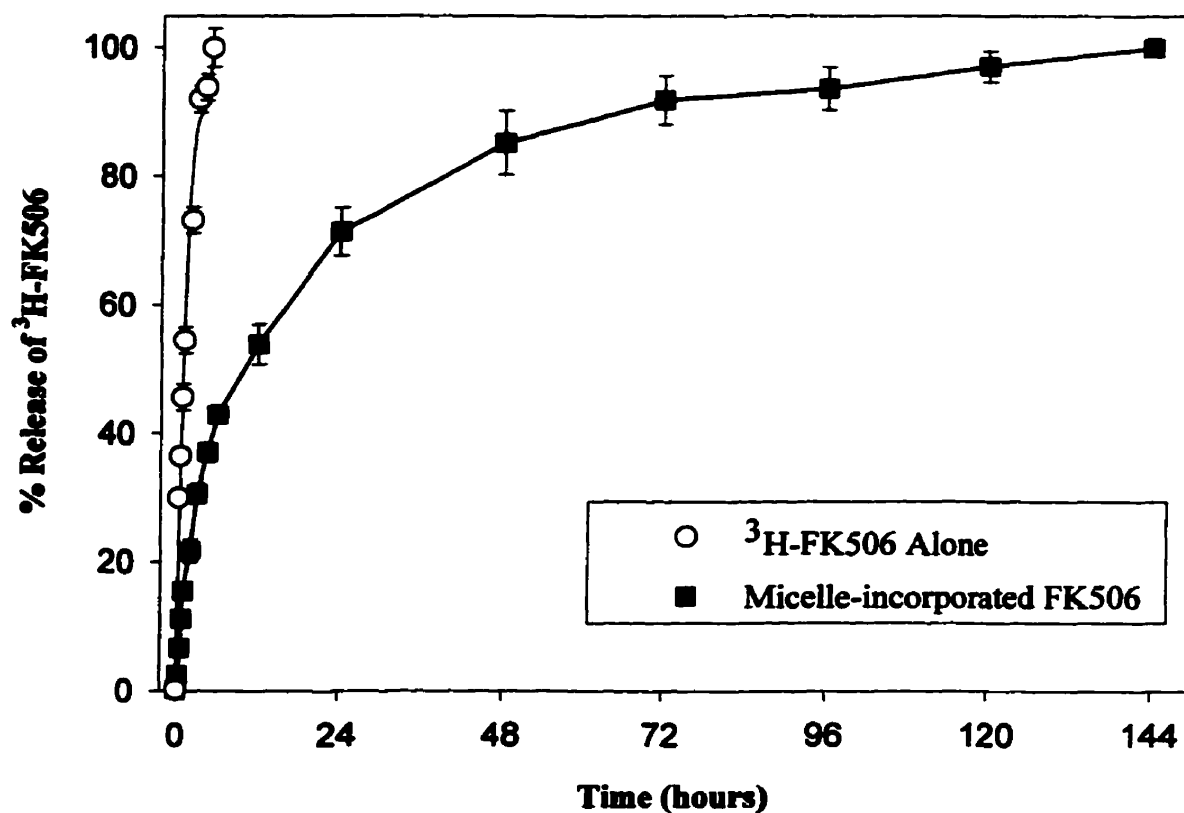


Figure 6.1. The *in vitro* release profiles of $^3\text{H-FK506}$ alone and $\text{PCL}_{20}\text{-b-PEO}_{44}$ micelle incorporated- $^3\text{H-FK506}$ as measured by the dialysis method.

6.1.3.2. Biodistribution of Micelle-Incorporated FK506 in Non-Neural Tissue

Figure 6.2a and 6.2b show the biodistribution of radiolabeled FK506, 6 and 24 hours following the intravenous injection of the PCL-*b*-PEG micelle incorporated FK506 inot male Sprague Dawley rats. In Figure 6.2a the biodistribution is expressed as the percentage of the total dose accumulated in the entire tissue. Of the tissues measured, the accumulation of the ^3H -FK506 at both 6 and 24 hours is found to be highest in the liver (13% (6hrs), 7.6% (24hrs)) and the brain (5% (6hrs), 2.1% (24hrs)). The accumulation in all other tissues at both 6 and 24 hours was far below the levels attained in the liver and the brain. Aside from the accumulation of 1.4% in the heart at 6 hours, the level of ^3H -FK506 in all other tissues was below 1% at both 6 and 24 hours.

In Figure 6.2b, the biodistribution is expressed as the % dose per gram of tissue. At 6 hours, the percent accumulation per gram of tissue for the heart, lung, liver and brain is approximately equal, ranging between 3.6% – 5%, while the levels in the spleen and kidney following 6 hours are only 1% and 1.9% respectively. Following the 24 hour period, the level of accumulation of the drug per gram of tissue is highest in the liver, brain and kidney.

6.1.3.3. Biodistribution of Micelle-Incorporated FK506 in Neural Tissue

Figure 6.3a and 6.3b show the distribution of radiolabeled FK506 in the different brain structures 6 and 24 hours following the injection of micelle-incorporated FK506. In Figure 3a, the distribution is expressed as the percentage of the total dose accumulated in the entire structure of the brain. The graph shows that the highest levels of ^3H -KF506 are attained in the rest of the brain and the cortex. When the distribution is expressed as the % dose/g of tissue the accumulation is found to be highest in the hypothalamus and the thalamus.

6.1.3.4. Behavioral Assessment of Functional Recovery

Figure 6.4 shows the endurance time attained for each of the animal groups studied on the rotarod apparatus over a 20 day period. As shown, the non-lesioned control animals almost reach the maximal endurance time (120 secs.) on day 8, and actually attain the maximal time on day 14. The lesioned animals treated with micelle-

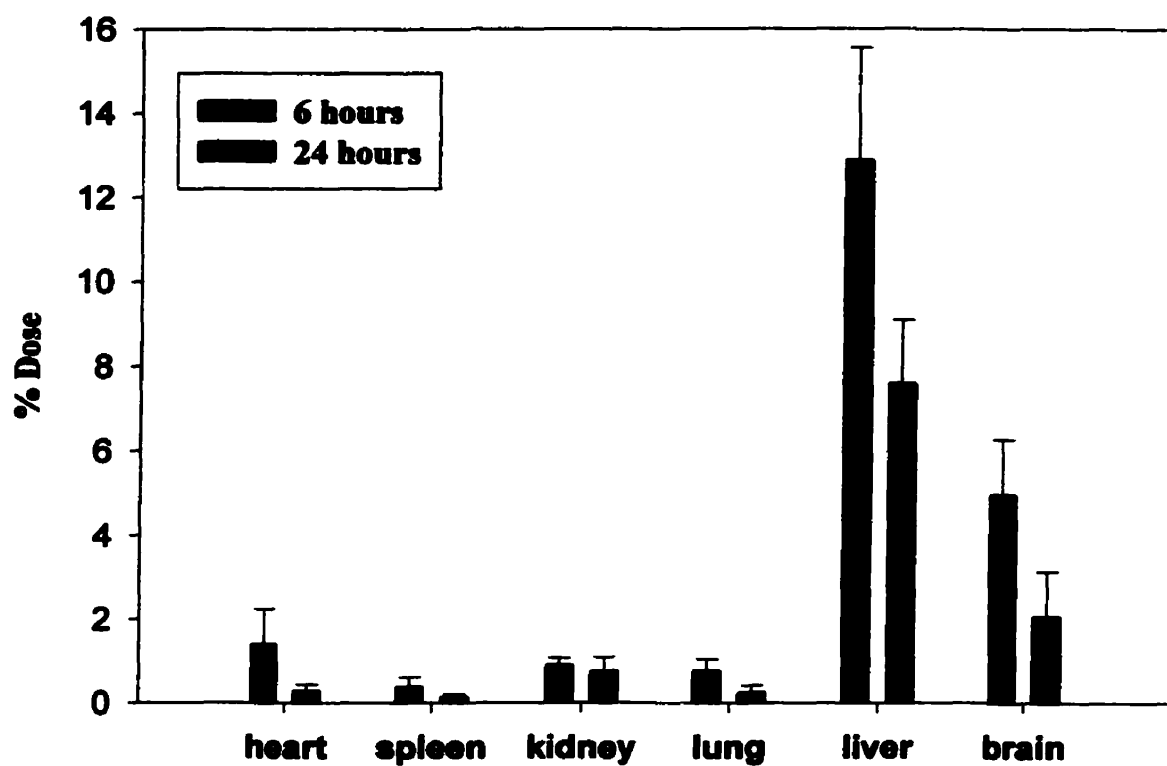


Figure 6.2.a) The biodistribution in non-neural tissue (expressed in terms of % of total dose) of radiolabeled FK506, 6 and 24 hours following intravenous injection of PCL-*b*-PEO micelle incorporated FK506 into male Sprague Dawley rats (n=3-4).

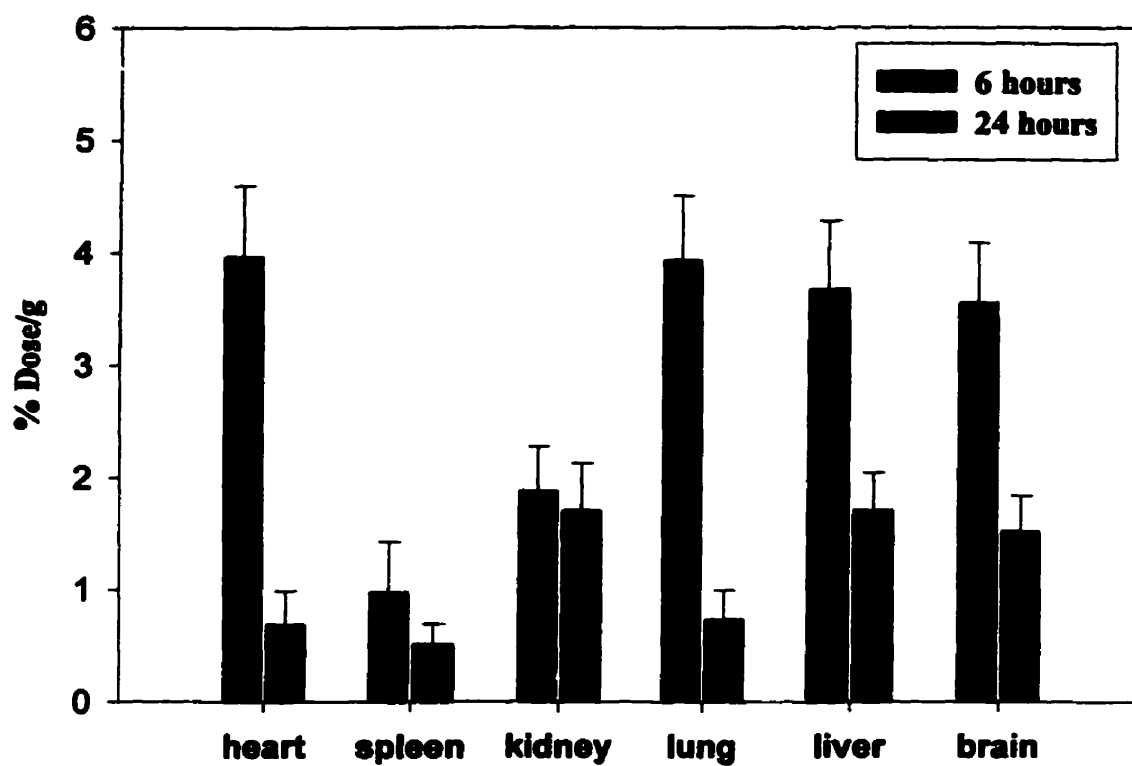


Figure 6.2.b) The biodistribution in non-neural tissue (expressed in terms of % of total dose/g tissue) of radiolabeled FK506, 6 and 24 hours following intravenous injection of PCL-*b*-PEO micelle incorporated FK506 into male Sprague Dawley rats (n=3-4).

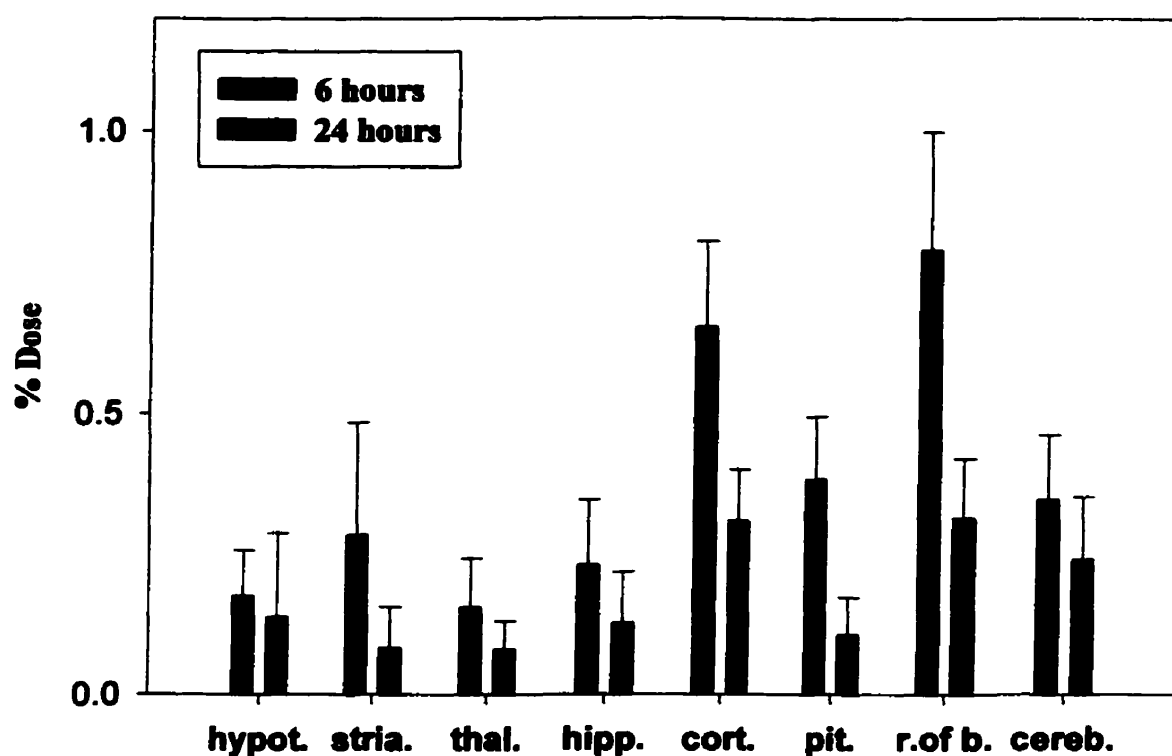


Figure 6.3.a) The distribution in neural tissue (expressed in terms of % of total dose) of radiolabeled FK506, 6 and 24 hours following intravenous injection of PCL-*b*-PEO micelle incorporated FK506 into male Sprague Dawley rats (n=3-4). (The abbreviations are as follows hypot.= hypothalamus; stria. = striatum; thal. = thalamus; hipp. = hippocampus; cort. = cortex; pit. = pituitary; r. of b. = rest of brain; cereb. =cerebellum).

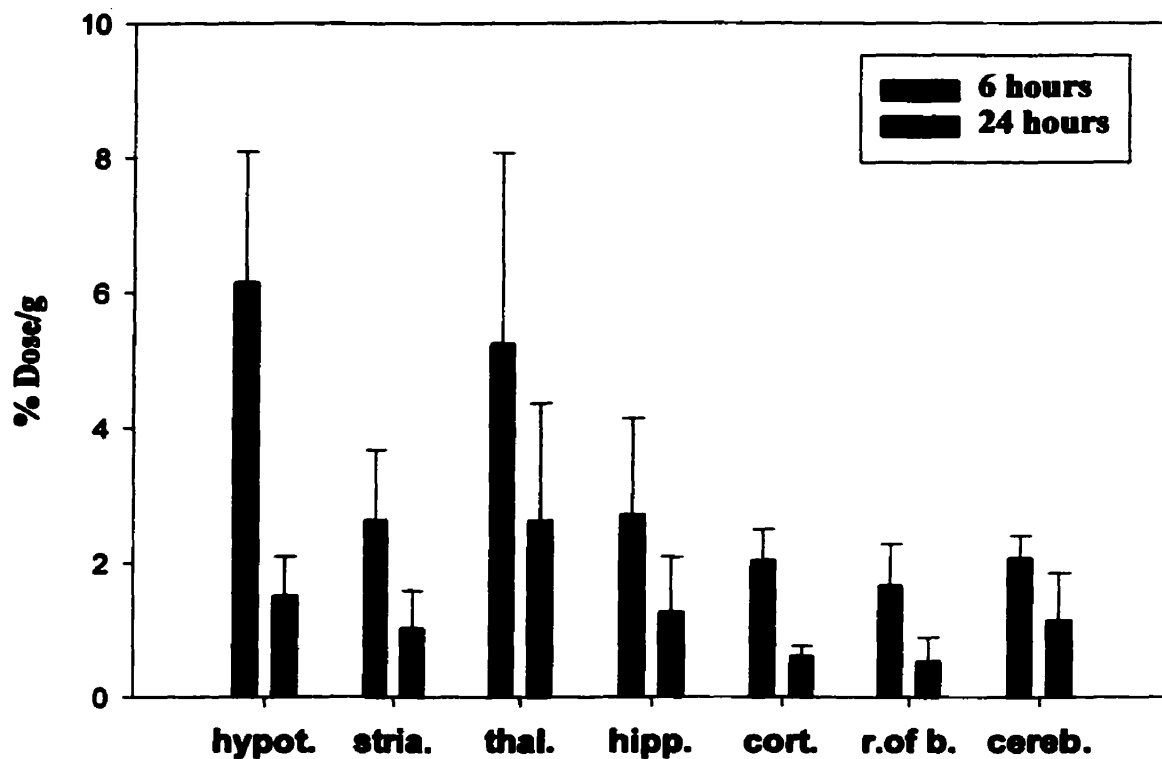


Figure 6.3.b) The biodistribution in neural tissue (expressed in terms of % of total dose/g tissue) of radiolabeled FK506, 6 and 24 hours following intravenous injection of PCL-*b*-PEO micelle incorporated FK506 into male Sprague Dawley rats (n=3-4). (The abbreviations are as follows hypot.= hypothalamus; stria. = striatum; thal. = thalamus; hipp. = hippocampus; cort. = cortex; pit. = pituitary; r. of b. = rest of brain; cereb. =cerebellum).

incorporated FK506 (5mg/kg) on days 0, 6 and 12, reach 50% of the maximal endurance time (time = 60 secs., short-dashed line) on day 6, while the lesioned animals receiving empty micelles only achieve this endurance time on day 12. The non-lesioned animals reach 75 % of the maximal endurance time (time = 90 secs., long – dashed line) by day 4, while the lesioned animals treated with the micelle-incorporated FK506 reach this point on day 10 and the lesioned animals treated with empty micelles only reach this point by day 18. The lesioned rats treated with micelle-incorporated FK506 reach the maximal endurance time achieving full functional recovery on day 16 only 2 days later than the non-lesioned animals. The lesioned control animals do not reach the maximal endurance time during the 20 day period. There is a significant difference between the endurance times of the lesioned animals treated with micelle-incorporated FK506 and those treated with empty micelles from day 8 to day 20.

6.1.4. Discussion

In this paper the PCL-*b*-PEO micelles were investigated as a delivery vehicle for the neurotrophic agent FK506. Among the various immunosuppressant and non-immunosuppressant FKBP12 ligands, FK506 was chosen as the model compound for these studies owing to its high degree of lipophilicity, the availability of both the radiolabeled and non-radiolabeled compound, the large amount of information available on the tissue distribution of FK506 administered in conventional formulations (Fujisawa Pharmaceutical Co.) or delivery vehicles, and the great extent to which the neurotrophic effects of FK506 in the sciatic nerve crush paradigm have been characterized.

The *in vitro* release kinetic profile of micelle-incorporated FK506 and FK506 alone were measured. There was a substantial difference between the release of the micelle-incorporated drug (100% released in 6 days) when compared to that of the drug alone (100% released in 4 hours). The method employed for the measurement of the release kinetics of the drug from the micelles may not be ideal. The release may be influenced by the frequency of sampling due to the fact that there is an equilibrium partitioning of the drug between the micelle and the external environment. The frequency

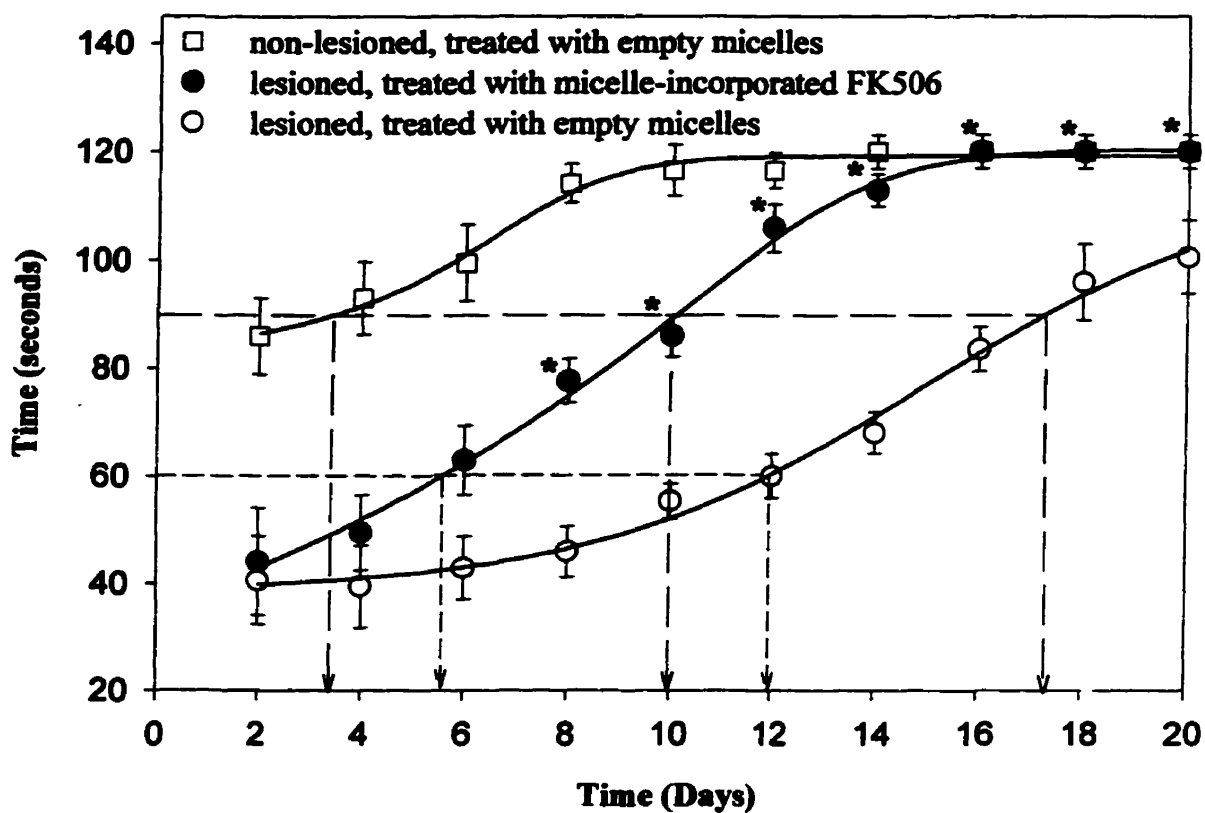


Figure 6.4. The endurance time attained for each of the animal groups (Hanover Wistar rats, $n=6$ per experimental group) studied on the rotarod apparatus over a 20 day period. Treated animals received 5 mg/kg of the micelle-incorporated FK506 solution on days 0, 6 and 12 following the sciatic nerve crush.

of sampling was much greater in the first hour than it was in the hours following, in this way, the release in the first hour may have been accelerated. A burst release is commonly seen for micelle-incorporated drugs, which is usually due to the drug which resides at the core-corona interface. However, in this case since we had dialyzed the micelles extensively following micelle preparation, the burst release would have been expected to be reduced.

The tissue distribution of the radiolabeled FK506 6 hours and 24 hours following the intravenous administration of the micelle-incorporated drug was significantly different from the biodistribution of FK506 obtained when administered in other formulations as previously reported in the literature. Yura H. et al. found that 8 hours following the intravenous administration of FK506, the biodistribution (expressed as % dose) was such that the levels of FK506 were very high in the small intestine ($\approx 60\%$ of the total dose) while the accumulation in all other tissues was quite low with approximately 5% in the liver and below 5 % in all other tissues [22]. FK506 administered in the conventional i.v. formulation (Fujisawa Pharmaceutical Co.) was reported by Kos et al. (25) to accumulate (expressed as per gram of tissue) mostly in the spleen and pancreas 6 hours following injection, and largely in the intestine, pancreas and spleen 24 hours following the intravenous injection in male Wistar rats (180-220g) [18]. The incorporation of FK506 into liposomes was found to result in an even higher accumulation in the spleen and pancreas following the 6 hour period, and the accumulation was still greatest in the spleen, pancreas and intestine following the 24 hour period [18]. Interestingly, with the PCL-*b*-PEO micelle-incorporated FK506, both 6 and 24 hours following injection the accumulation in the spleen is much less than that in the liver or brain. Since the spleen is one of the target organs for the immunosuppressive effect of FK506 for this purpose, a high accumulation in the spleen is desired. In this way, the PCL-*b*-PEO micelles may not be suitable for the delivery of FK506 as an immunosuppressant agent; however, we are interested in FK506 as a neurotrophic agent, and in this context, the block copolymer micelles may prove to be the delivery vehicle of choice.

The most striking difference between the biodistribution of the micelle-incorporated FK506 and FK506 administered in other formulations was the high degree of accumulation in the brain. FK506 is known to penetrate into the brain with ease; however, the actual levels of FK506 in the brain (% dose) are quite low when compared to the levels achieved with the micelle-incorporated FK506 [18, 22]. The administration of micelle-incorporated FK506 enables 5% of the total dose to accumulate in the brain following the 6 hour period. The high level of FK506 in the brain is not surprising when it is considered that the levels of FKBP12 are 10-40 times higher in the brain than in the immune system [9].

Due to the high accumulation in the brain we were interested in determining if, in fact, the drug was evenly distributed throughout the brain or if it was localized in specific structures. In Figure 6.3a and 6.3b we see that the drug is not evenly distributed, but rather preferentially localizes in specific brain structures. The levels of FKBP12 and calcineurin mRNA have also been reported to vary within the brain [23-25]; however, we could not clearly see a match between the preferential localization of FK506 and the regions of the brain known to contain the highest values of FKBP12 and calcineurin mRNA.

The means by which the level of radiolabeled FK506 becomes so high in the brain following the intravenous administration of the micelle-incorporated FK506 remains to be determined. It is unknown whether or not the drug penetrates into the brain as mostly free drug or while still incorporated in the micelles.

In order to determine if the biological activity of FK506 was still retained *in vivo* when administered in the PCL-*b*-PEO micelle solution, the sciatic nerve crush model of peripheral neuropathy was employed. The rats were given 5mg/kg on days 0, 6 and 12, with the first injection given locally and the other two given subcutaneously. A dose of 5mg/kg was chosen since Wang M.S. et al. found that rats with lesioned sciatic nerves receiving daily subcutaneous injections of FK506 (5mg/kg) attained full functional recovery in a shorter time period than rats receiving daily injections of 1 or 10 mg/kg [5]. Also, the group receiving 5mg/kg/day were found to have a larger number of myelinated axons and a larger mean axonal area than those receiving 1 or 10 mg/kg/day [5].

In most of the studies performed to this point on rats with lesioned sciatic nerves, the treatment involves daily subcutaneous injections of the immunophilin ligands [2-5]. However, due to the fact that the *in vitro* release kinetic measurements showed that the ³H-FK506 was only fully released from the micelles in 6 days, we chose to only inject once every 6 days.

In a previous report, rats with lesioned sciatic nerves receiving daily subcutaneous injections of 5 mg/kg FK506 were shown to attain recovery of function in 15 days [5]. In this case, we find the rats reach full functional recovery in only 16 days yet they are only administered 20 % of the drug given in the previously described experiments. Rats given 5mg/kg/day receive 90 mg/kg of drug over the 18 day period [5] in this case we only administer 15mg/kg over the 18 day period. Also, the requirement for only 3 injections of the micelle-incorporated drug increases patient compliance compared to daily s.c. injections.

6.1.5. Conclusions

The studies summarized above represent only the first step in the *in vivo* study of the PCL-*b*-PEO micelles as a delivery vehicle. The results from the organ biodistribution studies suggest that the incorporation of the drug into the micelles does in fact alter its biodistribution. However, in order to be able to best compare our results to those in the literature several additional organs should be analyzed (i.e. pancreas, intestines etc.). Also, the pharmacokinetic parameters of the micelle-incorporated drug must be determined and compared with those of the drug alone.

Finally, the results from the behavioral study suggest that the micelle-incorporated FK506 is very effective at enhancing functional recovery in rats whose sciatic nerves have been crushed. However, in order to fully substantiate these findings morphometric analysis of the nerves and measurement of the axonal regeneration rates are required.

6.1.6. References

1. Gold B.G., Storm Dickerson T., Austin D.R., *Restorative Neurology and Neuroscience* **1996**, 6, 287.
2. Gold B.G., Zeleny-Pooley M., Wang M.S., Chaturvedi P., Armistead .M., *Experimental Neurology* **1997**, 147, 269.
3. Gold B.G., Zeleny-Pooley M., Chaturvedi P., Wang M.S., *NeuroReport* **1998**, 9, 553.
4. Gold B.G., Katoh K., Storm-Dickerson T., *The Journal of Neuroscience* **1995**, 15, 7509.
5. Wang M.S., Zeleny-Pooley M., Gold B.G., *The Journal of Pharmacology and Experimental Therapeutics* **1997**, 282, 1084.
6. Allen C., Yu Y., Maysinger D., Eisenberg A. *Bioconjugate Chem.* **1998**, 9, 564.
7. Snyder S.H., Sabatinin D.M., Lai M.M., Steiner J.P., Hamilton G.S., Suzdak P.D. *TiPS* **1998**, 19, 21.
8. Snyder S.H., Sabatinin D.M *Nature Medicine* **1995**, 1, 32.
9. Hamilton G.S., Steiner J.P. *Current Pharmaceutical Design* **1997**, 3, 405.
10. Steiner J.P., Connolly M.A., Valentine H.L., Hamilton G.S., Dawson T.M., Hester S., Snyder S.H., *Nature Medicine* **1997**, 3, 421.
11. Steiner J.P., Hamilton G.S., Ross D.T., Valentine H.L., Guo H., et al. *Proc. Natl. Acad. Sci. U.S.A.* **1997**, 94, 2019.
12. Lyons W.E., George E.B., Dawson T.M., Steiner J.P., Snyder S.H., *Proc. Natl. Acad. Sci. USA* **1994**, 91, 3191.
13. Goto T., Kino T., Hatanaka H. et al., *Transplant. Proc.* **1991**, 23, 2713.
14. Jain A.B., Fung J.J., Tzakis A.G. et al. *Transplant Proc.* **1991**, 23, 2763.
15. The U.S. Multicenter FK506 Liver Study Group, *New Engl. J. Med.* **1994**, 331, 1110.
16. Venkataraman R., Jain A., Cadoff E. et al. *Transplant Proc.* **1990**, 22, 52.
17. Ko S., Nakajima Y., Kanehiro H., Horikawa M., Yoshimura A et. al., *Transplantation* **1995**, 59, 1384.
18. Ko S., Nakajima Y., Kanehiro H., Yoshimura A., Nakano H. *Transplantation* **1994**, 58, 1142.
19. Ko. S., Nakajima Y., Kanehiro H., Hisanaga M., Horikawa M., Aomatsu Y., et al., *Transplanation Proceedings* **1997**, 29, 529.

20. Uno T., Kazui T., Suzuki Y., Hashimoto H., et al. *Lipids* **1999**, 34, 249.
21. Uno T., Yamaguchi T., Li X.K., Suzuki Y., et al., *Lipids* **1997**, 32, 543.
22. Yura H., Yoshimura N., Hamashima T., Akamatsu K., et al. *Journal of Controlled Release* **1999**, 57, 87.
23. Steiner J.P., Dawson T.M., Fotuhi M., Glatt C.E., Snowman A.M., et al. *Nature* **1992**, 358, 584.
24. Dawson T.M., Steiner J.P., Lyons W.E., Fotuhi M., Blue M., Snyder S.H., *Neuroscience* **1994**, 62, 569.
25. Buttini M., Limonta S., Luyten M., Boddeke H., *Archives of Pharmacology* **1993**, 348, 679.

CHAPTER 7

CELLULAR INTERNALIZATION OF PCL₂₀-*b*-PEO₄₄ BLOCK COPOLYMER MICELLES

Following our *in vitro* study of micelle-incorporated FK506 and L-685,818 in PC12 cell cultures, we were interested in determining whether it was the drug alone or the micelle-incorporated drug that was entering the cell. This is an important issue as there is the potential to alter the intracellular trafficking pathway and fate of the drug if in fact it is the micelle-incorporated rather than the drug alone that is being internalized. If the micelles are internalized it is possible that they will facilitate accumulation of the drug in a specific subcellular organelle. This type of knowledge will allow specific drugs to be targeted to their required subcellular targets.

The ultimate goal of drug delivery is to target drugs to a specific tissue, cell-type and or subcellular organelle [1,2]. Based on the findings in the literature with "Stealth" liposomes it is unlikely that the PCL-*b*-PEO micelles will provide site-specific delivery of drugs. However, once information has been obtained on the PCL-*b*-PEO micelles alone, we can then begin surface modifications in order to optimize the distribution of the carrier.

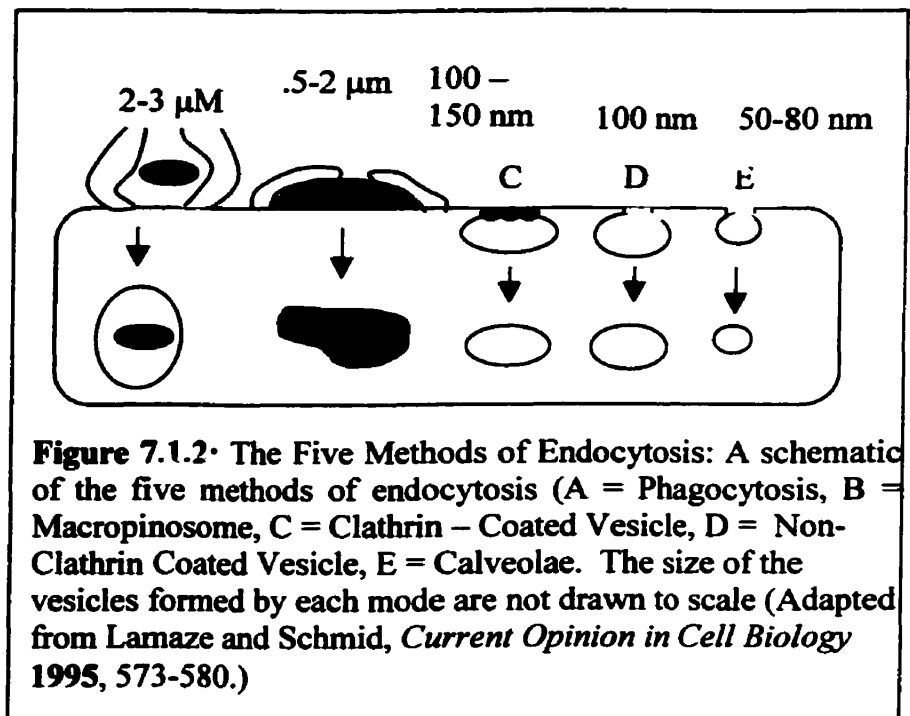
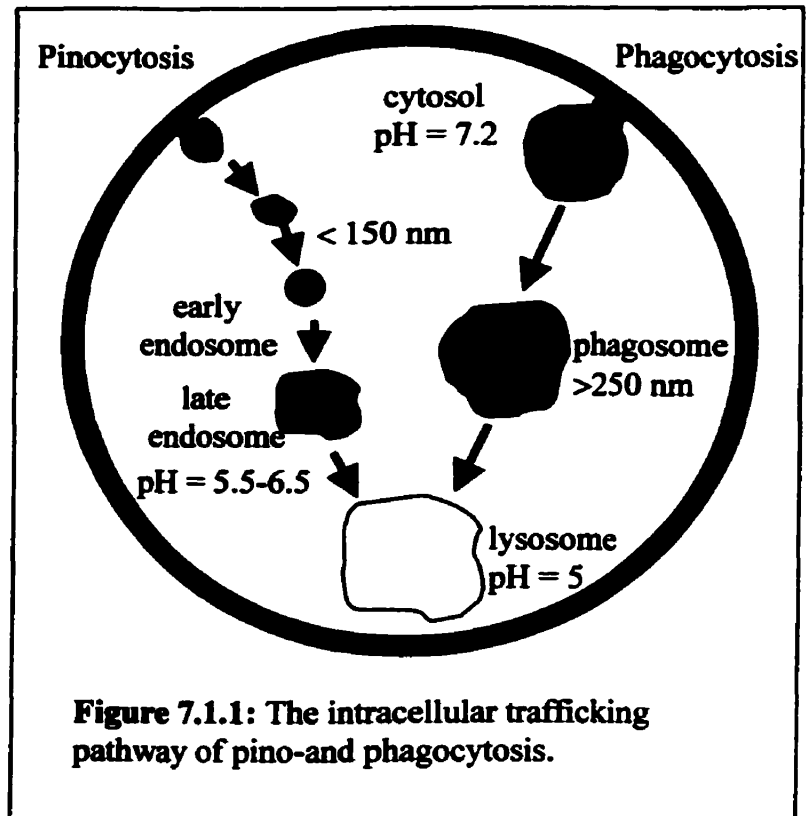
Section 7.1. includes a brief summary of the various endocytotic pathways while section 7.2. describes the initial step in the study of the cellular internalization of block copolymer micelles. In this work, we address the question of whether or not the PCL₂₀-*b*-PEO₄₄ micelles are in fact internalized into PC12 cells by an endocytotic mechanism.

7.1. Endocytosis

Endocytosis may be divided into 2 main categories, namely phagocytosis (cellular eating) and pinocytosis (cellular drinking) [3]. All eukaryotic cells are able to undergo pinocytosis while only specialized cells can undergo phagocytosis (e.g. macrophages) [3]. Whether or not the mechanism of internalization is pinocytosis or phagocytosis, most often the material internalized will be transported to the lysosomes (Figure 7.1.1). Lysosomes are

the cellular organelles (pH = 5) which contain approximately 40 types of hydrolytic enzymes responsible for the degradation of proteins, nucleic acids, oligosaccharides and phospholipids [3].

Pinocytosis can be further divided into receptor and non-receptor mediated endocytosis [4]. To this point four different



pinocytic pathways have been identified: macrophinosome, clathrin-coated vesicle, non-coated vesicle and calveolae [4]. These pathways differ in the size of vesicle that buds off from the plasma membrane and the composition of the vesicle coat (if any) (Figure 7.1.2). Also, several pharmacological manipulations have been identified which differentially block the four pinocytic pathways.

Several groups have studied the cellular internalization of different types of delivery vehicles. *In vitro* studies on the mechanism of cell uptake of conventional liposomes by phagocytic macrophages (Kupffer cells), found large amounts of liposomal material to be internalized by phagocytosis [5]. Following intravenous injection, the *in vivo* localization of conventional liposomes was mostly found to be in the fixed macrophages of the liver and spleen [6]. Specifically, studies found the internalization of liposomes into macrophage cells is an energy dependent process, and following cell entry, the liposomes are delivered to the lysosomal system resulting in their complete degradation and subsequent release of their contents [5]. By contrast, the PEO-modified sterically stabilized liposomes were found to have longer circulation times and decreased accumulation in the liver and spleen. The PEO-modified surface both enhances the surface hydrophilicity of the liposomes and provides steric stabilization which inhibits the adsorption of proteins and thus prevents non-specific recognition and consequent uptake by macrophage cells. The minimized interactions with cells of the RES allows the chance for interactions with other cell types as it has been found that it is the competition for liposome binding between different cell types that largely determines their fate *in vivo* [7]. In general, the cellular uptake of liposomes is said to be governed by the adsorption of liposomes to the surface of the cells followed by endocytic uptake. The rate and extent of cell uptake of liposomes has been found in many cases to be cell-type specific [6]. Also, the physical properties of liposomes such as size and surface charge have been found in some cases to influence the mechanism, rate and extent of cellular uptake [8-10].

7.2. The Cellular Internalization of the PCL₂₀-b-PEO₄₄ Micelles

7.2.1. Introduction

In recent years, there has been much interest in the use of block copolymer micelles as delivery vehicles for hydrophobic drugs. The micelles are formed from amphiphilic di- or triblock copolymers. In an aqueous solution, the copolymers aggregate to form micelles which contain a hydrophobic core and a hydrophilic corona. The core of the micelle serves as cargo space for hydrophobic drugs while the corona acts as an interface between the hydrophobic core and the aqueous medium. Several different hydrophobic blocks have been used to form the core of the micelles to name a few these include poly(propylene oxide) [11], poly(aspartic acid) [12-14], poly(D,L lactide) [15], poly(β -benzyl-L-aspartate) [16] and poly(caprolactone) [17,18]. By contrast, the corona forming polymer block is most often poly(ethylene oxide) though recently poly(acrylic acid) has been tried. The size of the copolymer micelles may range from 10 –100nm depending on the properties (e.g. total mol. wt., block ratio) of the individual copolymer molecules employed.

At present little is known of the mechanism or pathway of cellular internalization of block copolymer micelles or micelle-incorporated probes. Kabanov's group found that the cellular internalization (MDCK and Jurkat cells) of fluorescein containing poly(ethylene oxide)-b-polypropylene oxide-b-poly(ethylene oxide) (pluronic) micelles is inhibited at 4°C [19]. In a later study they also found that the cellular (bovine brain microvessel endothelial cells) accumulation of ³H-pluronic micelles is decreased in the presence of deoxyglucose (40mM) [20]. Together this evidence suggests that the mechanism of cellular uptake of the pluronic micelles may proceed by an endocytotic mechanism. We are now interested in determining if the cellular uptake of PCL₂₀-b-PEO₄₄ micelles proceeds by an endocytotic mechanism in PC12 [21] cell cultures.

In general, the study of the cellular internalization of drug delivery vehicles has been most extensive for liposomal carriers. To date, there are believed to be two predominant mechanisms of cell entry for liposomes, endocytosis [22-24] and fusion [25] with the plasma membrane of the cell. Recently, Bajoria et al. demonstrated that small unilamellar liposomes containing carboxyfluorescein are endocytosed by human trophoblast cells in culture [9]. They found that the rate and extent of internalization of

the liposomes was dependent on both the size and surface charge of the liposomes. Papahadjopoulos' group has shown that large (0.1 μm) negatively charged liposomes containing colloidal gold are internalized by an endocytotic mechanism in CV-1 monkey kidney cells [22]. They found the uptake pathway to progress from the localization of the liposomes in coated pits to their subsequent internalization in coated vesicles [22].

The different mechanisms of endocytosis may be divided into two broad categories, namely phagocytosis ("cellular eating") and pinocytosis ("cellular drinking") [26]. Pinocytosis includes both fluid phase pinocytosis and adsorptive or receptor-mediated pinocytosis. The many pathways of pinocytosis which have been identified include macropinosome, clathrin-coated vesicle, non-coated vesicle and caveolae. Cellular uptake by an endocytotic mechanism is known to be characterized by certain basic criteria including time, temperature, pH and energy dependence [26-28]. Many pharmacological manipulations which enable one to selectively inhibit or stimulate the individual pinocytic pathways have been identified (e.g. hypertonic treatment inhibits clathrin mediated endocytosis) [4]. It is by the exploitation of these pharmacological manipulations that the mechanism of cellular uptake of a particular macromolecule or ligand may be identified [29].

The present work describes the effect of various pharmacological manipulations on the uptake of PCL₂₀-*b*-PEO₄₄ micelles. The time, temperature, pH and energy dependence of the uptake are first investigated to determine if the basic criteria for endocytotic uptake are fulfilled. The effect of hypertonic treatment and brefeldin A on the uptake process are also studied. These studies are of importance owing to the growing interest in block copolymer micelles as drug carriers. The lack of information available on micelle-cell interactions, the cellular internalization of micelles and their intracellular fate will prevent them from being fully exploited as drug delivery vehicles.

7.2.2 Materials and Methods

7.2.2.1. Materials The PCL₂₀-*b*-PEO₄₄ (where subscripts refer to the number of monomer units in each block) block copolymer was synthesized by anionic polymerization. The description of the copolymer is provided elsewhere [18]. All chemicals for the synthesis were purchased from Aldrich Chemical Co.. The ³H-FK506

was purchased from Mandel Scientific and the fluorescent probe CM-DiI was purchased from Molecular Probes Co.. The tissue culture reagents were all purchased from Gibco BRL.

7.2.2.2. Experimental Methods

Micelle Preparation Ten milligrams of PCL-*b*-PEO block copolymer was dissolved in up to 0.2 g of dimethylformamide and stirred for four hours. Micellization was induced by dropwise addition of 0.8 g of water at a rate of approximately one drop every ten seconds. The micelles were placed in a dialysis bag and dialyzed against MilliQ distilled water. The water was changed every hour for the first four hours and then every three hours for the next twelve hours.

Preparation of Micelle-Incorporated Probes (DiI, ³H-FK506)

Micelle-Incorporated ³H-FK506 A 100uL aliquot (amount equal to 100 uCi, i.e. 1mCi = 1mL) of a ³H-FK506 solution in ethanol was added to an empty vial and the ethanol was allowed to evaporate. The amount of ³H-FK506 added to the vial was 1.19 nanomoles since the specific activity of ³H-FK506 is 84.0 Ci/mmol. 0.01g of the PCL₂₀-*b*-PEO₄₄ copolymer was then added to the vial along with up to 0.2g of DMF. The solution was stirred at room temperature for 4 hours at which point 0.8g of water was added slowly to the vial to make a 1% (w/w) copolymer solution. The micelle solution was then left to stir overnight and then dialyzed against Milli Q water. The loading efficiency of the micelle solution was found to be 28% , in this way, the final concentration of the micelle-incorporated ³H-FK506 solution was 333nM.

Micelle-Incorporated CM-DiI An aliquot of CM-DiI ($\lambda_{ex} = 553\text{nm}$) in DMF is initially added to an empty vial such that the final concentration of CM-DiI is 1×10^{-8} moles/g. Ten milligrams of PCL₂₀-*b*-PEO₄₄ copolymer is then added to the vial followed by the addition of DMF up to .2g. The solution was then allowed to stir for four hours. Micellization was achieved by the dropwise addition of water (0.8g) and then after stirring overnight the solutions were dialyzed against MilliQ water in the dark.

Electron Microscopic Analysis

Several different preparative techniques were tried in order to determine the optimal method for the electron microscopic analysis of this system. However, the freeze-fracture/freeze-etch technique was found to enable the morphology of the individual aggregates to be seen most clearly.

Freeze-Fracture/Freeze-Etch Electron Microscopy

A small drop of a 1% (wt) PCL-*b*-PEO micelle solution was placed in the center of a sample holder and dipped into liquid nitrogen-cooled liquid propane (-140°C). Following approximately 5 seconds the sample holder was removed and placed into a liquid nitrogen bath. The sample holder was then placed in the freeze-fracture apparatus (Balzers 300) wherein the temperature ranged between -100 to -120°C. Sample fracture was performed by using a liquid nitrogen cooled knife. Following freeze-fracture and freeze etch the fracture plane was shadowed with platinum/carbon (95:5) at a 30° angle and then coated with carbon at a 90° angle. The Pt/C replica was floated off the holder using distilled water and placed onto uncoated copper grids. The sample grids were analyzed by transmission electron microscopy using a JEOL microscope.

Cell Uptake Experiments

Cell Cultures PC 12 cells [21] were grown in flasks containing RPMI supplemented with 5% fetal bovine serum, 500 µg/mL penicillin and 500µg/mL streptomycin. The cells were seeded into 24 well plates containing 500 µL per well. Following a 24 hour incubation period the medium was removed and replaced by fresh medium and treatments were performed as described below.

Study of Time, Temperature and pH dependence The medium was removed and 245 µL of fresh RPMI 1640 medium was added to each well in the culture plate. A 5 µL aliquot of micelle-incorporated ³H-FK506, micelle-incorporated DiI or ³H-FK506 alone was added to each well at specific time points. The 5 µL aliquot of the micelle-incorporated ³H-FK506 or ³H-FK506 alone corresponds to 6.6 nM ³H-FK506 per well.. Following the specific incubation period the supernatant and cells were treated as described below depending on the micelle-incorporated probe used.

Temperature dependence: The cells were incubated at 4°C for 15 minutes prior to the start of the experiment. **pH dependence:** The RPMI (pH = 5) was prepared by the mixture of a specific ratio of RPMI medium and an acetic acid/Na acetate buffer solution.

Cells Treated with Micelle-Incorporated ^3H -FK506 or ^3H -FK506 Alone Following the incubation period, 200 μL of the medium was removed and placed in scintillation vials containing 4 mL of Scinti-Safe Plus 50% scintillation cocktail. The rest of the medium was removed and the cells were washed twice with 200 μL PBS. 100 μL of trypsin was then added to each well and incubated at 37°C for 15 minutes. Each well was then scraped, 100 μL of PBS was added and the contents were removed and placed in a scintillation vial containing 4 mL of Scinti-Safe scintillation cocktail. The scintillation vials were counted and the CPM value for each was recorded. A calibration curve was used to change CPM to uCi.

Cells Treated with Micelle-Incorporated DiI Following the incubation period the supernatant was removed and the cells were washed twice with 250 μL PBS. The cells were then analyzed under a fluorescence microscope (Olympus BH-2).

Study of the Effect of Hypertonic Treatment The cells were preincubated with sucrose (450 mM) containing medium for 30 mins. or 1 hour prior to the addition of 5 μL of micelle-incorporated ^3H -FK506. Following a 1 hour incubation period the cells and supernatant were treated as above.

Study of the Effect of Naz/DOG or Brefeldin A The cells were preincubated with DOG (25mM)/Naz (10mM) for 15 mins, 30 mins. or 1 hour while pretreatment with Brefeldin A was for 1 hour. The addition of 5 μL micelle-incorporated ^3H -FK506 was followed by a 1 hour incubation period after which the cells were treated as described above.

7.2.3. Results and Discussion

7.2.3.1 Characteristics of the PCL-b-PEO Micelles Employed in the Cellular Internalization Studies

The block copolymer micelles in these studies are spherical in shape and approximately 25 nm in diameter. The stability of the micelles in RPMI medium and their biocompatibility in PC12 cell cultures were previously confirmed as described elsewhere [18].

The ideal tool for these studies would be labeled block copolymer micelles; however, this was not available and for this reason we chose to use micelles containing highly lipophilic fluorescent or radioactive probes [18]. The high degree of lipophilicity of the probes ensured a high partition coefficient for the probe between the micelles and the external medium. In addition, the kinetics of the release of the selected probes from the micelles is very slow with respect to the duration of the cell uptake experiment (maximum 4 hours). In this way, the micelle-incorporated probes may be used to follow the internalization process of the micelles.

7.2.3.2. Cellular Uptake Studies:

Time, Temperature and pH dependence This study demonstrates that the micelles are internalized into PC12 cell cultures. Furthermore, these studies demonstrate that the uptake is time, temperature and pH dependent. The cellular uptake of both micelle-incorporated ^3H -FK506 and micelle-incorporated DiI were found to be time dependent as the uptake increased progressively over the 4 hour incubation period as seen in Figure 7.2.1.a and 7.2.1.b. The uptake profile of the micelles was similar to that seen for the uptake of other delivery vehicle incorporated probes, such as liposomes containing carboxyfluorescein and microparticles containing 6-coumarin [9, 30].

As seen in Figure 7.2.1.a and 7.2.1.b, a decrease in temperature from 37°C to 4°C, known to be an effective non-invasive means of inhibiting endocytosis, severely inhibits the uptake of the micelles [31]. However, there was a slight progressive increase in the uptake at 4°C over the four hour period, which is similar to the results obtained for the cellular uptake of fluorescein labeled biodegradable nanoparticles in bovine arterial smooth muscle cells over time at 4°C [32].

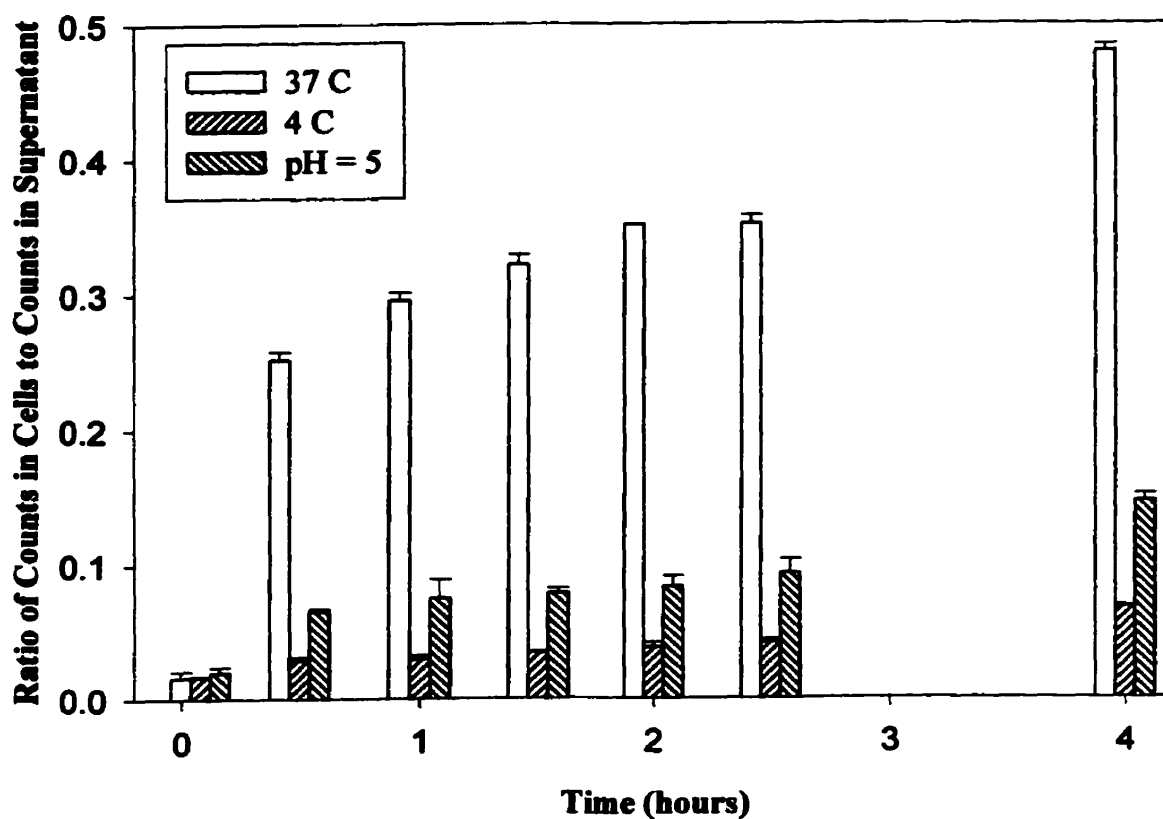


Figure 7.2.1.a) The temperature and pH dependence of the cellular internalization of PCL₂₀-b-PEO₄₄ micelle-incorporated ³H-FK506 in PC12 cell cultures. Each bar represents the mean of 4 samples \pm S.D.

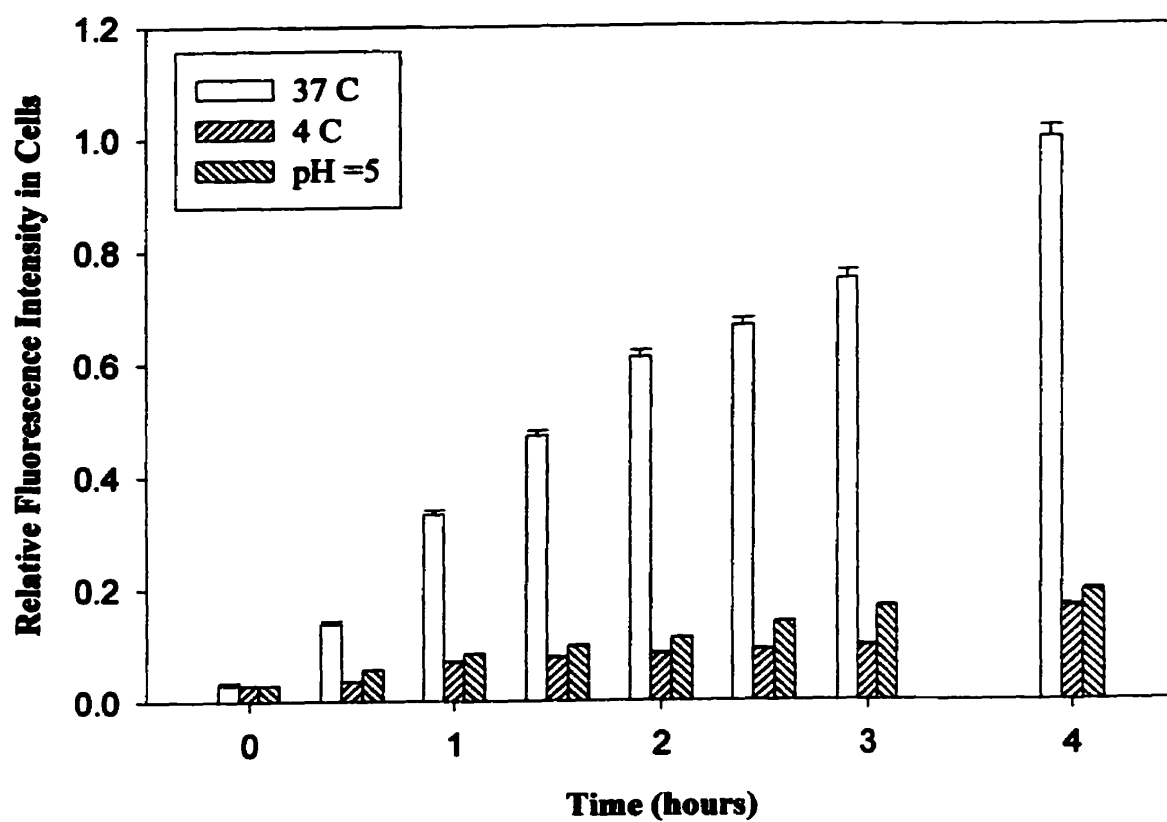


Figure 7.2.1.b) The temperature and pH dependence of the cellular internalization of PCL₂₀-b-PEO₄₄ micelle-incorporated DiI in PC12 cell cultures. Each bar represents the mean of 4 samples \pm S.D.

The pH dependence of the internalization was also confirmed (Figures 7.2.1 (a) and b). The acidification of the cytoplasm has been shown to inhibit receptor-mediated endocytosis by preventing the budding of coated pits to form coated vesicles [33-37]. Several different methods may be used to induce cytosol acidification; these include prepulsing with NH_4Cl , use of weak acids (e.g. acetic acid) which are able to penetrate the cell membrane and incubation with Nigericin in isotonic KCl [26]. In this case, we chose to induce cytosol acidification by incubating the cells with medium containing acetic acid (pH =5). The uptake of the micelles was not as great at low pH as it was at 4°C .

In addition, the time dependence of the uptake of the micelle-incorporated ^3H -FK506 was compared to the uptake of the free drug. As shown in Figure 7.2.2., the kinetics of the cellular entry of the drug alone is much faster than that of the micelle-incorporated drug. Also, it appears that much less uptake of the micelle-incorporated drug, compared to the free drug, has occurred over the four hour period.

Summary of the Effect of the Various Pharmacological Manipulations Figure 7.2.3. summarizes the effect of various pharmacological manipulations on the cellular uptake of the micelle incorporated ^3H -FK506 in PC12 cell cultures. The energy dependence of the uptake was studied by use of the metabolic poisons sodium azide (NaAz) and 2-deoxyglucose (DOG). The preincubation of the cells with Deoxyglucose (DOG) (inhibitor of glycogenolysis) and Sodium Azide (NaAz) (inhibitor of cellular respiration) for one hour decreased the uptake to 11 %. Preincubation of the cells with DOG/NaAz for 15 or 30 minutes also decreased the degree of cellular internalization of the micelle-incorporated ^3H -FK506 but not to the same extent (results not shown). The inhibition of the uptake by the metabolic inhibitors that the internalization process is energy dependent.

Hypertonic treatment by preincubation of the cells with 0.45M sucrose was also found to decrease the uptake. The inhibition of receptor-mediated endocytosis by exposure of the cells to hypertonic media was first demonstrated by Daukas and Zigmond [38]. They found that receptor-mediated endocytosis of chemotactic peptides was inhibited in polymorphonuclear leukocytes in the presence of media containing 0.43M

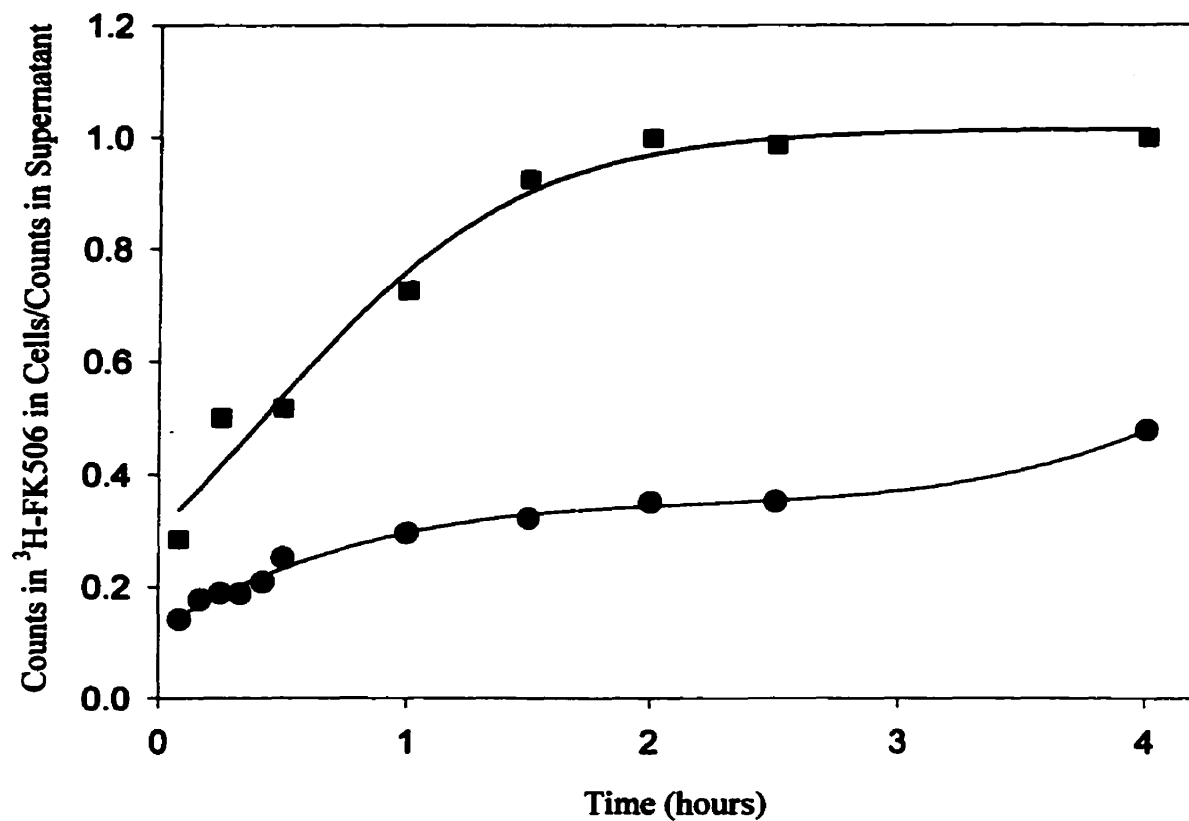


Figure 7.2.2. The time dependence of the uptake of ³H-FK506 alone (■) and PCL₂₀-b-PEO₄₄ micelle-incorporated ³H-FK506 (●) in PC12 cell cultures over a four hour period. Each point represents the mean of 4 samples ± S.D.

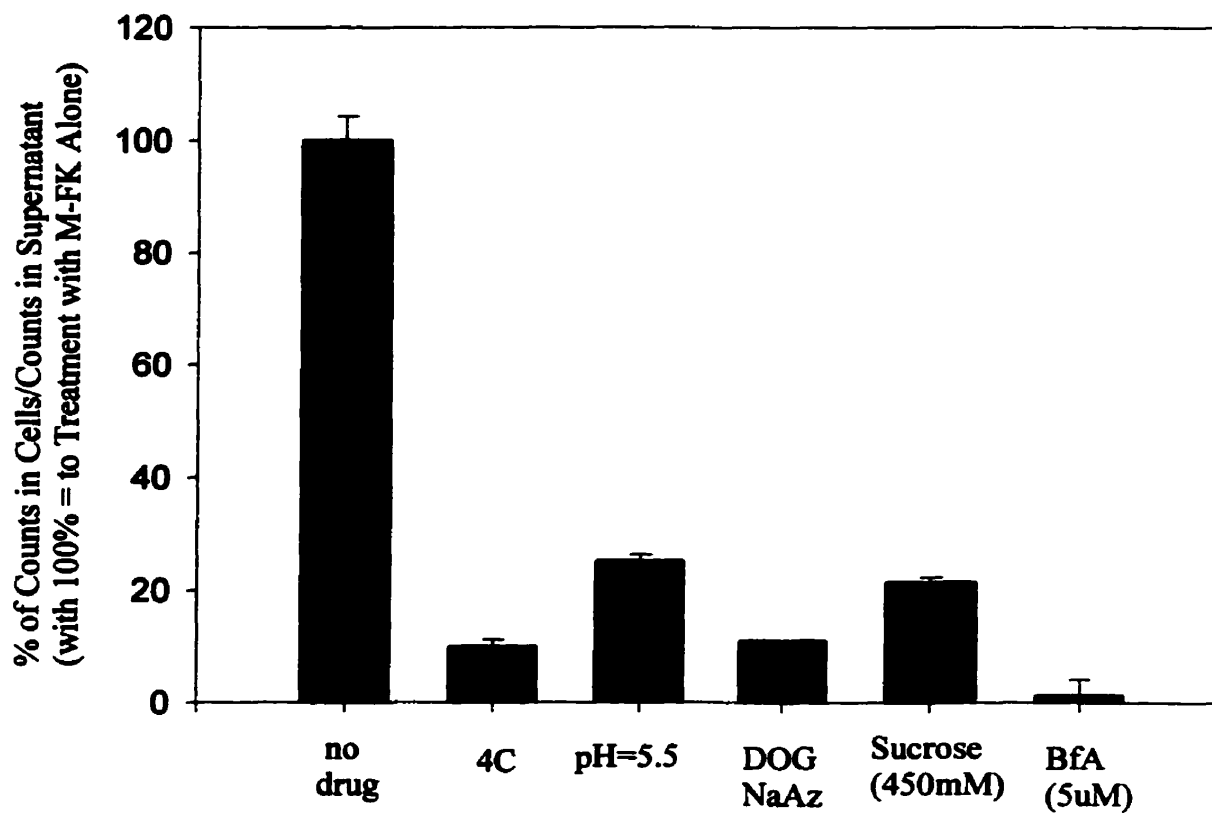


Figure 7.2.3. The effect of various pharmacological manipulations on the cellular internalization of PCL₂₀-b-PEO₄₄ micelle-incorporated ³H-FK506 in PC12 cell cultures. Each bar represents the mean of 4 samples \pm S.D.

sucrose. The specific means by which hypertonic treatment inhibits receptor-mediated endocytosis was later established by Heuser et al. [33]. They discovered that hypertonic treatment provokes inhibition in the same manner as does potassium depletion; it reduces the number of clathrin coated pits present at the cell-surface. Also, the clathrin-coated pits present were much flatter and smaller than normal and clathrin was found to be accumulated in "microcages" [34]. The fact that the hypertonic treatment did not completely abolish the uptake of the micelles may be attributed to the use of only 0.45 osmolar medium. Daukas G. et al. had found that complete inhibition of receptor-mediated endocytosis of chemotactic peptides only occurred in 0.7 osmolar medium while partial inhibition occurred in the presence of 0.45 and 0.6 osmolar medium.

In addition, the pretreatment of the cells with the macrocyclic antibiotic Brefeldin A also inhibited the internalization of the block copolymer micelles. Specifically, Brefeldin A is known to morphologically alter the endosomes by inducing the formation of tubules [28]. The inhibition of cellular uptake of the micelles in the presence of Brefeldin A is indicative that the internalization may proceed by an endocytotic mechanism.

Together, this evidence strongly suggests that the PCL₂₀-b-PEO₄₄ micelles are internalized into PC12 cells via an endocytotic mechanism. However, in order to support this finding further studies must be done using labeled micelles visible by either confocal or electron microscopy. Also, it is of interest to study the internalization of the micelles at the molecular level in order to determine which proteins are involved in the process.

The question of whether or not the block copolymer micelles are internalized into PC12 cells via an endocytotic mechanism is only the first in a series of questions that remains to be answered including: 1) what is the specific mechanism of endocytotic uptake of the micelles; (2) what intracellular trafficking pathway do they follow upon cell entry; (3) what is their final subcellular distribution or intracellular fate? and (4) are the micelles stable within the cell? The answers to these questions will be of necessity in furthering the use of block copolymer micelles in drug delivery. For instance, the knowledge of the subcellular distribution of the micelles will enable the appropriate drug

to be delivered to a particular subcellular organelle, enabling the most efficient use of the micelles as drug carriers.

7.2.4. References

1. Langer R. *Nature* **1998**, 392 Supp. 5.
2. Kato Y., Sugiyama Y. *Critical Reviews in Therapeutic Drug Carrier Systems* **1997**, 14, 287.
3. Alberts B., Bray D., Johnson A., Lewis J., Raff M., Roberts K., Walter P., Essential Cell Biology: An Introduction to the Molecular Biology of the Cell, Garland Publishing Inc. NewYork **1998** pages 472-477.
4. Lamaze C., Schmid S.L. *Current Opinion in Cell Biology* **1995**, 7, 573.
5. Scherphof G.L., Kamps J.A.A.M. *Advanced Drug Delivery Reviews* **1998**, 32, 81.
6. Miller C.R., et al. *Biochemistry* **1998**, 37, 12875.
7. Lee K.D. et al. *Biochemistry* **1993**, 32, 889.
8. Schramlova J. et al. *Folia Biologica* **1997**, 43, 161;
9. Bajoria R., Sooranna S.R. Contractor S.F. *Human Reproduction* **1997**, 12, 1343.
10. Yu H.Y., Lin C.Y. *Journal of the Formosan Medical Association* **1997**, 96, 409.
11. Alakhov V.Y., Moskaleva E.Y., Batrakova E.V., Kabanov A.V. *Bioconjugate Chem.* **1996**, 7, 209.
12. Yokoyama M., Miyauchi M., Yamada N., Okano T., Sakurai Y., Kataoka K., *Cancer Res.* **1990**, 50, 1693.
13. Yokoyama M., Okano T., Kataoka K., *J. Controlled Rel.* **1994**, 32, 269.
14. Harada A., Kataoka K. *Macromolecules* **1998**, 31, 738.
15. Hagan S.A., Coombes A.G.A., Garnett M.C., Dunn S.E., Davies M.C., Illum L, Davis S.S. *Langmuir* **1996**, 12, 2153.
16. Cammas S., Matsumoto T., Okano T., Sakurai Y., Kataoka K., *Mat. Sci. and Eng.*, **1997**, C4, 241.
17. Yeon Kim S., Gyun Shin I. L., Moo Lee Y., *J. Control. Release*, **1998**, 51, 13.
18. Allen C., Yu Y., Maysinger D., Eisenberg A., *Bioconjugate Chem.* **1998**, 9, 564.
19. Kabanov A.V., Slepnev V.I., Kuznetsova L.E., Batrakova E.V., Alakhov V.Y, Melik-Nubarov N.S., Sveshnikov P.G., Kabanov V.A., *Biochemistry International* **1992**, 26, 1035.
20. Miller D.W., Batrakova E.V., Waltner T.O., Alakhov V.Y., Kabanov A.V., *Bioconjugate Chemistry* **1997**, 8, 649.

21. Greene L.A., Tischler A.S. *Proc. Natl. Acad. Sci. U.S.A.* **1976**, 73, 2424.
22. Straubinger R.M., Hong K., Friend D.S., Papahadjopoulos D., *Cell* **1983**, 32, 1069.
23. Straubinger R.M., Papahadjopoulos D., Hong K. *Biochemistry* **1990**, 29, 4929.
24. Dijkstra J., Van Galen M., Scherphof G., *Biochim. Biophys. Acta* **1985**, 845, 34.
25. Papahadjopoulos D., Poste G., Schaeffer B., *Biochim. Biophys. Acta* **1973**, 323, 23.
26. Mukherjee S., Ghosh R. N., Maxfield F. R., *Physiological Reviews* **1997**, 77, 759.
27. Mamdough Z., Giocondi M.C., Laprade R., Le Grimmellec C., *Biochimica et Biophysica Acta* **1996**, 1282, 171.
28. Mellman I., *Annu. Rev. Cell Dev. Biol.* **1996**, 12, 575.
29. Oehlke J., Krause E., Wiesner B., Beyermann M., Bienert M., *FEBS Letters* **1997**, 415, 196.
30. Desai M.P., Labhasetwar V., Walter E., Levy R.J., Amidon G.L., *Pharmaceutical Research* **1997**, 14, 1568.
31. Steinman R. M., Mellman I.S., Muller W.A., Cohn Z.A., *The Journal of Cell Biology* **1983**, 96, 1.
32. Suh H., Jeong B., Liu F., Wan Kim S., *Pharmaceutical Research* **1998**, 15, 1495.
33. Heuser J.E., Anderson R.G.W., *The Journal of Cell Biology* **1989**, 108, 389.
34. Hansen S.H., Sandvig K., van Deurs B., *The Journal of Cell Biology* **1993**, 121, 61.
35. Heuser J.E., *Journal of Cell Biology* **1989**, 108, 401.
36. Davoust J., Gruenberg J., Howell J.E., *The EMBO Journal* **1987**, 6, 3601.
37. Sandvig K., Olsnes S., Petersen O.W., van Deurs B., *The Journal of Cell Biology* **1987**, 105, 679.
38. Daukas G., Zigmond S. H., *The Journal of Cell Biology* **1985**, 101, 1673.

CHAPTER 8

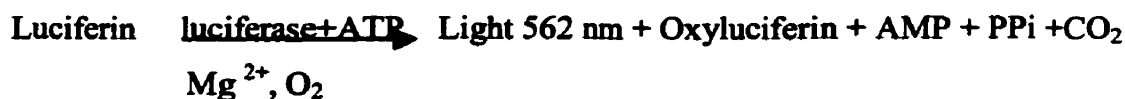
PCL-*b*-PEO MICELLES AS A DELIVERY VEHICLE FOR OTHER HYDROPHOBIC DRUGS SUCH AS DIHYDROTESTOSTERONE

Following, our evaluation of the PCL-*b*-PEO micelles as a delivery vehicle for FK506 we were interested in exploring the micelles as carriers for other drugs. Steroids such as dihydrotestosterone (DHT) are suitable candidates since they are lipophilic, relatively inexpensive and their radiolabeled analogues are readily available. Also, their properties such as polarity, hydrophobicity, solubility and molecular weight are different from those of FK506 and L,685-818. In Chapter 2, we mention that the extent of incorporation of a compound into the micelles as well as the release of the compound from the micelles is largely dependent on the compatibility between the drug and the core-forming block. For this reason, it is of interest to explore different drug - PCL-*b*-PEO micelle combinations in order to determine which drugs may be most effectively delivered by this carrier.

In section 8.2, we investigate several of the physicochemical properties of the PCL-*b*-PEO micelle incorporated DHT. Also, the in vitro delivery and biological activity of the micelle-incorporated DHT is evaluated using the model described in section 8.1.

8.1. *In vitro* Model to Assess the Delivery and Biological Activity of Micelle Incorporated Dihydrotestosterone

In the same way, that the neurite-outgrowth in NGF-treated PC12 cells was used as an *in vitro* model to assess the delivery of micelle-incorporated FK506 another model was used to evaluate the delivery of the micelle-incorporated dihydrotestosterone. The *in vitro* delivery and biological activity of the micelle-incorporated dihydrotestosterone was quantified by way of a luciferase reporter gene assay. HeLa cells were cotransfected with the MMTV luciferase reported plasmid and human androgen receptor cDNA expression plasmid. In the cotransfected HeLa cells the binding of DHT to its androgen receptor will result in the activation of transcription of the luciferase reporter gene [1]. The monomeric protein luciferase can act as a reporter enzyme directly following translation as it is said that it does not require post-translational processing to acquire enzymatic activity [2, 3]. Upon mixing the cell extract with the substrate, luciferin, the firefly enzyme will catalyze the ATP dependent oxidation of luciferin [4].



It has been found that for one molecule of luciferin oxidized there is one photon released [4]. The chemiluminescence produced can be measured using a standard scintillation counter. The luminescence decreases exponentially with time and can be divided into a fast period and a slow period.

8.2. Polycaprolactone-*b*-Poly(ethylene oxide) Copolymer Micelles as a Delivery Vehicle for Dihydrotestosterone

8.2.1. Introduction

In recent years there has been much interest in the use of androgen replacement therapy for treatment of a variety of clinical indications [5]. Currently, the most common use is for the treatment of men with hypogonadism in which case testosterone production falls below a normal range of 3-10 mg/day [6, 7]. Hypogonadism is characterized by a loss of muscle and bone mass, an increase in visceral fat, impaired immune function and altered mood. [6, 8]. Other accepted indications requiring androgen replacement therapy are microphallus in infants and delayed puberty in boys [5]. Presently, androgen therapy is under investigation for the treatment of aging men with low to normal testosterone levels [5, 9]. Serum testosterone levels have been shown to decline with aging in men; the decline is gradual in comparison to the decline in production of oestrogen in postmenopausal women and there is much inter-individual variation [5, 9]. The issue of androgen supplementation in aging men requires further investigation in order to ensure that the benefits do outweigh the risk posed to the cardiovascular system and prostate [10, 11]. However, results from studies on aging men given androgen replacement therapy have been quite promising [9, 12]. Androgen replacement therapy is also being considered for the treatment of postmenopausal women and individuals in wasting states owing to their infliction with either HIV, cancer or chronic infection [5].

The increasing interest in androgen replacement therapy has prompted the development of many androgen preparations including patches [6, 13], creams, gels [14], injectables and implants [15, 16]. Many of the oral androgen formulations have been found to have low potency and may be either rapidly cleared by the liver or potentially hepatotoxic [5]. At present the most commonly used androgen preparations worldwide are testosterone enanthate and cypionate injections [5]. However, the pharmacokinetic profile of testosterone administered in these preparations is somewhat undesirable since the serum testosterone level goes through peaks and valleys within the 14 days following injection (peak serum testosterone levels are reached following 1-3 days and then fall below physiological level between days 10-14) [5]. This type of profile does not mimic

that of the natural cycle for testosterone and gives rise to skin problems (e.g. acne, oiliness) during the peak periods and mood changes and loss of libido when testosterone levels fall below physiological levels.

To date, one of the most promising preparations for androgen replacement therapy has been biodegradable microspheres containing testosterone [17]. The administration of the microsphere preparation to hypogonadal men gave rise to physiological serum testosterone levels for 10-11 weeks following a single injection [17]. Several other colloidal carriers have been tried as drug delivery vehicles for steroids [18-21]. These have mostly included microspheres composed of homopolymer (e.g. poly (d,l-lactic acid) [18]) and copolymer (e.g. poly(lactide)-co-poly(ϵ -caprolactone) [19]) materials. Also, micelles formed from copolymers of poly(lactide)-*b*-poly(ethylene glycol) were studied as a carrier for testosterone [21]. Currently, there is a need for new delivery vehicles for androgens such as these which provide pharmacokinetic profiles which mimic the normal circadian pattern of these hormones.

In this paper we propose polycaprolactone-*b*-poly(ethylene oxide) (PCL₂₀-*b*-PEO₄₄ where subscripts refer to block lengths) copolymer micelles as potential carriers for androgens. The characterization of the PCL₂₀-*b*-PEO₄₄ micelles has been described in detail elsewhere [22]. Block copolymer micelles have been investigated extensively as delivery vehicles for lipophilic compounds [21-29]. The amphiphilic nature of the copolymer molecules enables them to self-assemble to form micelles in an aqueous medium. In this way, the micelle is composed of a hydrophobic core which serves as cargo space for the lipophilic drugs and a hydrophilic corona which acts as an interface between the core and the external medium.

In this paper we report on the physico-chemical characterization and *in vitro* study of PCL₂₀-*b*-PEO₄₄ micelles as a delivery vehicle for dihydrotestosterone. The loading capacity of the micelles are determined and several parameters are evaluated including the number of DHT molecules per micelle, the apparent partition coefficient of DHT which partitions between the micelle and the external medium and the release profile of the micelle-incorporated DHT. In addition, the *in vitro* cytotoxicity of a range of concentrations of the PCL₂₀-*b*-PEO₄₄ copolymer micelles are studied in HeLa cells and evaluated using the MTT survival assay. The biological activity of the micelle-

incorporated DHT is then evaluated in HeLa cells which have been cotransfected the MMTV-LUC reporter gene and the androgen receptor.

8.2.2. Materials and Methods

8.2.2.1. Materials The block copolymer PCL₂₀-b-PEO₄₄ was synthesized by anionic polymerization as described elsewhere [30]. All chemicals were purchased from Aldrich Chemical Company. The scintillation cocktail used in loading studies (Fisher Chemical, Fisher Scientific, ScintiSafe Econo F) and that used in the kinetic release studies (Fisher Chemical, Fisher Scientific, ScintiSafe™ Plus 50%), was purchased from V.W.R. Scientific. The radiolabelled DHT was purchased from Mandel Scientific while the cold 5 α -dihydrotestosterone (DHT) was purchased from Sigma. The dialysis bag used in the micelle preparation was Spectral Por® Membrane, MWCO: 50,000 and that used for the kinetic release studies was also Spectral Por® Membrane but of MWCO: 15, 000.

8.2.2.2. Methods

Preparation of Dihydrotestosterone Incorporated PCL₂₀-b-PEO₄₄ Micelles. To a small glass vial, 0.005g of the PCL₂₀-b-PEO₄₄ copolymer and an aliquot of a DHT stock solution containing a known ratio of hot to cold drug were dissolved in 0.15g of dimethylformamide (DMF). This solution was stirred using a magnetic stir bar for 4 hours. To induce micelle formation, a 0.35g of double distilled water was added slowly with stirring (one drop every ten seconds) to the copolymer-drug solution. The total mass of this mixture was 0.5g, which yielded a 1% polymer solution by weight. This solution was stirred for 12 hours. To remove the DMF and the excess DHT, the solution was dialyzed in double distilled water for 12 hours. (The water was changed twice every four hours then once every hour for four hours.) After dialysis, the micelle solution was available for use. We did not use any specific analytical method to detect the amount of DMF remaining in the micelle preparation following dialysis. However, the total core volume in our experiments is typically less than 0.5% (w/w) and even if 1% of that were DMF (highly unlikely in view of the dialysis procedure) the toxic effects on the cells would be far below detectable levels.

Measurement of the Amount of DHT Loaded in PCL₂₀-b-PEO₄₄ Micelles. An aliquot of the micelle solution was dried in a vacuum dessicator in a small glass vial. The micelles were then dissolved in 450μL of DMF, stirred by vortex and then counted using 4mL of scintillation cocktail (Wallac Liquid Scintillation Counter). The number of counts per minute for 100μL of micelle solution was used to extrapolate the number of counts for a 500μL sample. The counts per minute for each solution were then converted to moles using a calibration curve.

Kinetic Release of DHT from PCL₂₀-b-PEO₄₄ Micelles. The release kinetics of DHT from PCL₂₀-b-PEO₄₄ micelles was performed using previously dried 100μL aliquots of micelle solution. To the dried micelles, 100μL of phosphate buffer solution, PBS (pH 7.4) was added. The size and size population distribution of the micelles was shown previously to be unaffected by the re-dispersion process in PBS [22]. To ensure that the micelles were well dispersed in PBS, the solutions were vortexed. The dispersed micelles were left to stand at 37°C until the solution had reached that temperature. The micelle solution (8mM or 40mM micelle-incorporated DHT) was then placed in a dialysis bag which was immersed in a large vial containing warmed PBS (10mL PBS, pH=7.4, 37°C). At the appropriate time intervals, a 100μL aliquot of PBS was removed from outside the dialysis bag in the large vial to count the amount of DHT released from the micelles. (The aliquot was dispersed in 4mL of scintillation cocktail, then counted.) Following the removal of each 100uL aliquot a 100uL aliquot of fresh PBS was added.

Apparent partition coefficient for DHT between the PCL₂₀-b-PEO₄₄ Micelles and the External Medium. Immediately after the dialysis of micelles, 100μL aliquots of solution were placed into eppendorf vials. The solutions were then centrifuged at 14,000 rpm for 10 minutes (Eppendorf Centrifuge 5402). A speed of this order of magnitude had been previously established to precipitate micelles of this size [31]. This speed is sufficient for precipitation since a 1% (w/w) solution of PCL₂₀-b-PEO₄₄ has been shown to consist mostly of aggregates of 500-600 nm in size [22, 30]. The supernatant was removed carefully by pipette and placed into a glass vial containing 450μL of DMF . The precipitate (micelles) was left in the eppendorf and to it 450μL of DMF was added.

These solutions were stirred using the vortex for several minutes. Each of the solutions were then added to vials containing 4mL of scintillation cocktail and counted by the scintillation counter.

***In vitro* Experiments**

Cell Culture HeLa cells (ATCC) were grown in 6 well plates (Falcon) in DMEM medium supplemented with penicillin (1%) and streptomycin (1%) and 10% fetal bovine serum to reach 60% confluency. HeLa cells were chosen since they are often the cell line used for transfections and they do not secrete dihydrotestosterone or testosterone.

***In vitro* Cytotoxicity of PCL₂₀-b-PEO₄₄ Micelles** The cells were split into 24 well plates (500 μ L medium per well) for the cytotoxicity studies. An aliquot of a stock solution of PCL₂₀-b-PEO₄₄ micelles was added to each well such that the concentration of empty micelles ranged from 1×10^{-6} to 1×10^{-3} (g/g) per well. Following 24, 48 or 72 hours the cell survival was measured using the MTT assay. The MTT dye was added to each well following the specific time period and incubated for 4 hours at 37°C. The cells were then placed on ice and the supernatant was removed by aspiration. An aliquot of trypsin was then added to each well and the cells were left on ice for 20 minutes. DMSO was then added to each well and the cells were collected and centrifuged at 14 000 rpm for 20 minutes at 4°C. The supernatants were then collected and the absorbance of each was measured at $\lambda = 595$ nm.

Cell Transfection The medium was changed 4 hours prior to the transfection procedure. HeLa cells were transfected by applying the calcium phosphate transfection protocol [32]. The cells were transfected with expression vectors encoding the androgen receptor and the reporter plasmid MMTV-LUC (kindly provided by Dr. Albert O. Brinkmann, Erasmus University Rotterdam). The full description of the AR construct is described elsewhere [33]. Following a 48 hour period the medium was removed and replaced by androgen free medium (serum treated with charcoal to eliminate steroids) and the cells were treated as described below.

Cell Treatment To assess the effects of dihydrotestosterone and micelle-incorporated dihydrotestosterone on the induction of the integrated MMTV-LUC gene the

cells were treated as follows: no treatment (negative control), empty micelles (200 μ L of a 1%(w/w) solution, negative control), DHT alone (positive control) or micelle-incorporated DHT (200 μ L of a 1mM micelle-incorporated DHT solution in a total volume of 2 mL) such that the final concentration of DHT in each well was 100 nM. Each condition was assessed in triplicate per experiment and three separate experiments were carried out (n=9). The cells were allowed to incubate with treatment for 24 hours prior to performing the luciferase assay.

Assay for Luciferase Activity in Transfected HeLa Cells The treated or non-treated transfected HeLa cells were lysed in a standard lysis buffer: 25mM triphosphate, pH 7.8; 8mM magnesium chloride; 1mM DTT; 1mM EDTA; 1% Triton X-100; 1% BSA and 15% glycerol. Upon cell lysis the cells were scraped with a rubber policeman and the lysates were collected in eppendorf tubes and stored at -80°C . The lysates were then thawed and centrifuged for 15 minutes at 13 000rpm and 4°C . The luciferase assay was performed using the Promega luciferase assay system and all steps were performed on ice [4]. A 100 μ L aliquot of the luciferase assay reagent was then added to 100 μ L of the extract in an eppendorf tube. An aliquot of the luciferase assay substrate was added to the sample, mixed and the sample was introduced into the counting chamber. A constant time interval was maintained between substrate addition and data acquisition (10-15 secs). The data acquisition was carried out over 2 minutes.

Light Intensity Measurements The light intensity was measured using a LKB model 1211 Rackbeta liquid scintillation counter [4].

8.2.3. Results

8.2.3.1. Loading Capacity of $\text{PCL}_{20}\text{-}b\text{-PEO}_{44}$ Micelles for Dihydrotestosterone In the final stage of micelle preparation the micelles are dialyzed against double distilled water in order to remove the organic solvent (DMF). During this stage both drug that was not incorporated into the micelles and some of the drug that was incorporated is lost and goes to waste. Figure 8.1, shows the plot of the amount of DHT loaded in the micelle solution versus the total amount of DHT added (0.3 – 17.4 μ moles) during the preparation of 0.1 mL of a 1% (w/w) solution of $\text{PCL}_{20}\text{-}b\text{-PEO}_{44}$ micelles. The amount of DHT incorporated into the 0.1 mL volume of the micelle solution increases as the amount of

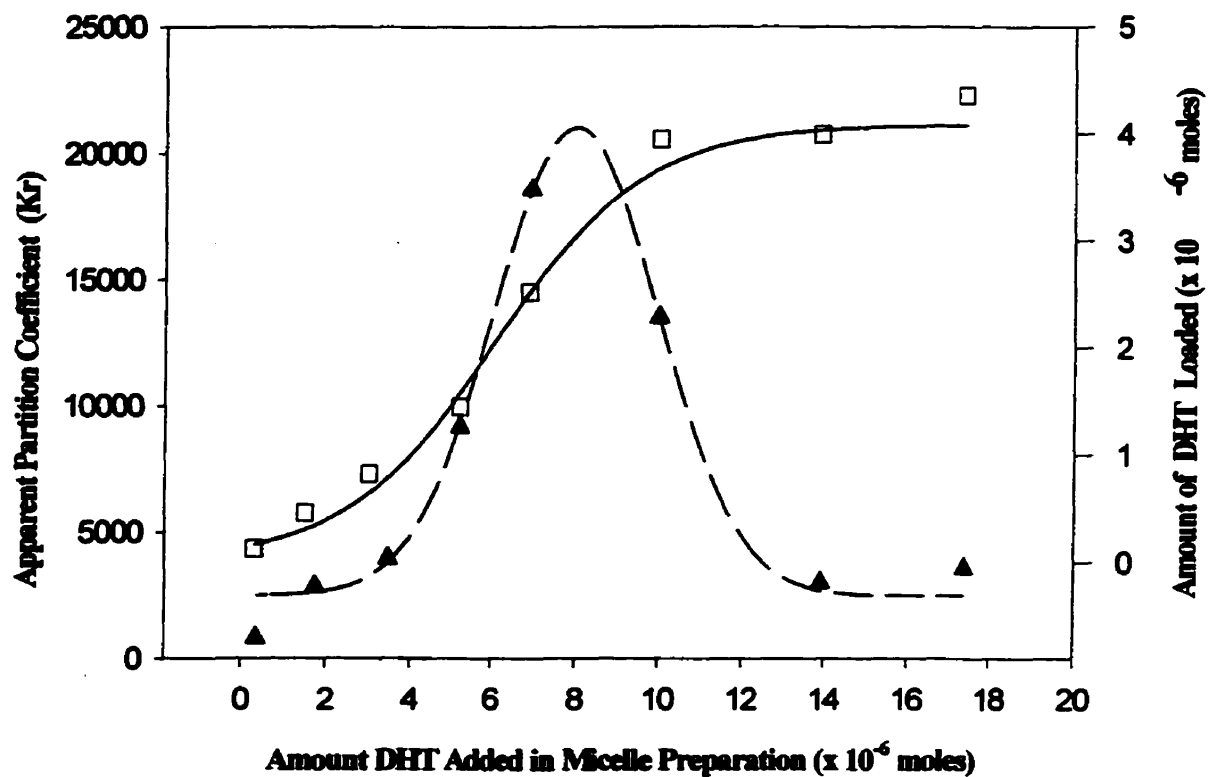


Figure 8.1: The plot of the apparent partition coefficient for DHT (left axis) between the PCL₂₀-b-PEO₄₄ micelles and the external medium versus the amount of DHT added during micelle preparation. The amount of DHT loaded into the PCL₂₀-b-PEO₄₄ micelles (right axis) versus the amount of DHT added during micelle preparation.

DHT added during micelle preparation is increased until a maximum loading capacity is reached. The maximum amount of DHT that may be loaded into the 0.1 mL volume was found to be 4.4 μ moles which corresponds to 1.3 mg of DHT. This maximum loading capacity is reached when 10 μ moles or more of DHT is added during micelle preparation. In this way, the loading efficiency meaning the percentage of the total drug added during micelle preparation that is loaded into the micelle solution decreases from 39% when 10 μ moles DHT is added during preparation to 23% when 17 μ moles is added.

8.2.3.2. Apparent Partition Coefficient for DHT between the Micelles and the External Medium

For the drug that has been incorporated into the micelle solution an equilibrium exists whereby the drug partitions between the micelle cores and the external medium. The partition coefficient (K_v) for drugs or model hydrophobic compounds (pyrene) between the micelles and the external medium has been described in detail elsewhere [34-36]. In this case, since the measurements of the amount of drug in the micelles and the external medium are carried out following dialysis we term this the apparent partition coefficient (K_r) rather than the partition coefficient (K_v) since the process has been influenced by the dialysis process. It should be recalled that the partitioning of the drug between micelles and the external medium is a process that involves not only the incorporation of the drug into the micelle core but also the core-corona interface and the corona region. The localization of the drug will determine to some extent the amount lost during the dialysis process by burst release; in this way, the apparent partition coefficient is not constant. The apparent partition coefficient (K_r) may be described by the following equation:

$$\frac{[\text{DHT}]_{\text{micelles}}}{[\text{DHT}]_{\text{water}}} = \frac{K_r \chi_{\text{PCL}} C}{\rho_{\text{PCL}}}$$

where $[\text{DHT}]_{\text{micelles}}$ is the concentration of DHT in the micelles (precipitate following centrifugation), $[\text{DHT}]_{\text{water}}$ is the concentration of DHT in the external medium (supernatant following centrifugation), χ_{PCL} is the weight fraction of PCL in the

PCL₂₀-*b*-PEO₄₄ copolymer ($\chi_{\text{PCL}} = 0.55$), C is the concentration of copolymer in g/mL and ρ_{PCL} is the density of PCL in g/mL ($\rho_{\text{PCL}} \cong 1$).

Figure 8.1 also shows the plot of the apparent partition coefficient (K_r) versus the amount of DHT added during micelle preparation. The value of K_r is found to range from a minimum of 850 to a maximum of 18500. As shown in Figure 8.1, fitting of the curve suggests that the maximum value may even be higher than 18500. The value of the K_r increases as the amount of DHT during micelle preparation increases from 0.35 to 6.94×10^{-6} moles at which point it reaches a maximum value of 19000. Beyond this point the apparent partition coefficient decreases as more of the DHT is found in the external medium.

8.2.3.3. Number of Molecules Loaded per Micelle From the known amount of DHT incorporated into the micelles it is possible to calculate the number of molecules incorporated per micelle [34]. The number of micelles present in solution may be calculated if the aggregation number (N_A) for the copolymer is known. The aggregation number is the number of copolymer molecules which aggregate to form a micelle. The aggregation number for PCL₂₀-*b*-PEO₄₄ is $N_A = 125$. Figure 8.2 includes the plot of the number of DHT molecules incorporated per micelle versus the amount of DHT added during micelle preparation. The number of molecules per micelle was found to range from a minimum of 55 to a maximum of 2200. The plot of the maximum number of molecules per micelle if all the DHT had been incorporated is also shown (dashed line). Clearly, that is much higher than the actual values attained. This large difference is due mostly to the drug lost during the dialysis process and also to the drug which is present in the micelle solution but in the external medium. It should be noted that for the calculation of the number of micelles in solution the aggregation number was assumed to be 125 for all drug loading levels. It is possible that as the amount of drug loaded increases the aggregation number may change; however, since during the assembly process the micelle core is highly swollen with solvent the presence of other solvent-like molecules (e.g. drug) in the core would not be expected to change the aggregation number dramatically.

The percentage of the weight of drug loaded to the weight of the core copolymer may also be calculated since the amount of drug loaded into the micelles is known. The

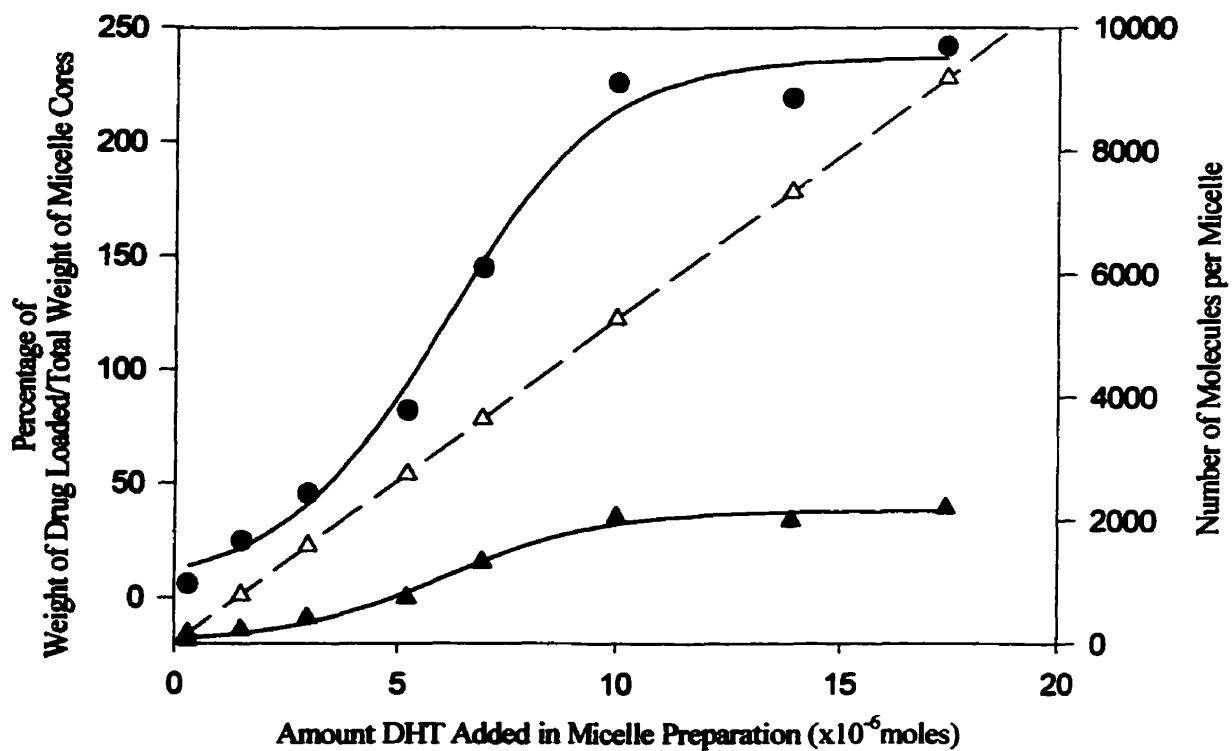


Figure 8.2: The percentage of the weight of drug loaded to the total weight of micelle cores (left axis) versus the amount of drug added during micelle preparation. The plot of the number of molecules of DHT loaded per micelle (right axis) versus the amount of DHT added during micelle preparation.

percentage is found to increase from a minimum value of 10 to a maximum value of 240 where it plateaus. The maximum value is reached when 10 μ moles or more of DHT are added during micelle preparation.

8.2.3.4. *In vitro* Release Kinetic Profile of Micelle-Incorporated DHT The dialysis method was used to study the release of DHT from two micelle solutions which differed in the amount of DHT that they contained. The concentration of the solutions studied were 8 mM and 40 mM. The release kinetic profiles of the two micelle-incorporated DHT solutions and the control (drug alone) over a 10 day period are plotted in Figure 8.3. As shown the release of DHT from the 8 mM micelle-incorporated solution is much faster than that from the 40 mM solution. The release of the control solution is complete in 3 hours by contrast 90 % of the DHT from the 8 mM micelle solution is released in 8 days (192 hours) and 100% of the DHT from the 0.04M solution is only released after 30 days (720 hours, point not shown).

8.2.3.5. *In vitro* Studies

Cytotoxicity of PCL₂₀-b-PEO₄₄ copolymer micelles in HeLa cell cultures The cytotoxicity of the empty micelles was studied in HeLa cell cultures for 24, 48 and 72 hour periods. The concentration of PCL₂₀-b-PEO₄₄ copolymer was varied from 1×10^{-6} to 1×10^{-3} g/g. A concentration of 1×10^{-3} g/g and the 24 hour period correspond to the conditions used in the transfection assays. Figure 8.4, shows the % survival of cells exposed to different copolymer concentrations (1×10^{-6} to 1×10^{-3} g/g) for the specified time periods. The % survival was expressed relative to the control (no copolymer added) which was taken to be 100% survival for all incubation periods (0 - 72hours). The copolymer concentration of 1×10^{-3} g/g caused an insignificant degree of cell death as the percent of cell survival fell to a low of 82% for the 72 hour incubation period.

***In vitro* Biological Assay** Figure 8.5 shows the luciferase activity in HeLa cells cotransfected with expression vectors for MMTV-LUC and androgen receptor. The activity was determined using a highly sensitive luciferase assay system whereby light intensity is proportional to luciferase concentration within a range of 10^{-16} – 10^{-8} M. Bar 1

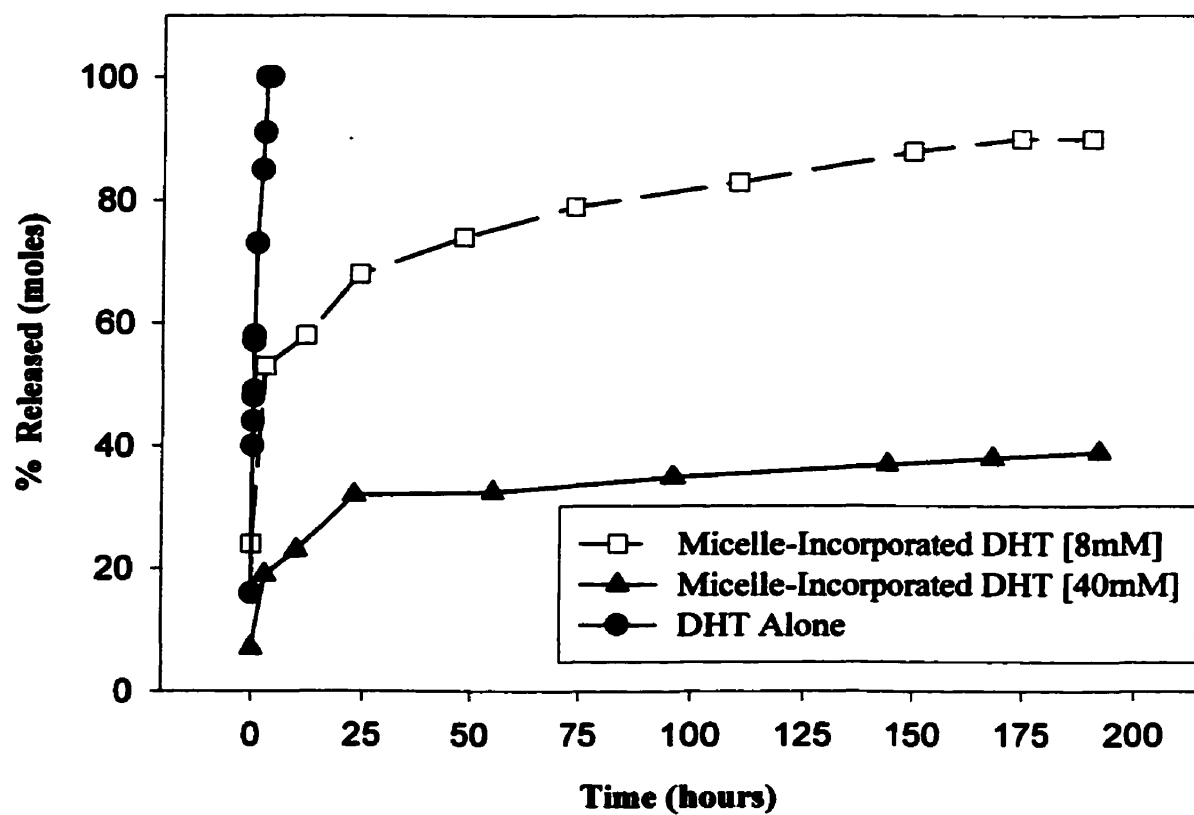


Figure 8.3: The release of DHT alone, 8mM micelle-incorporated DHT, 40mM micelle-incorporated DHT over time.

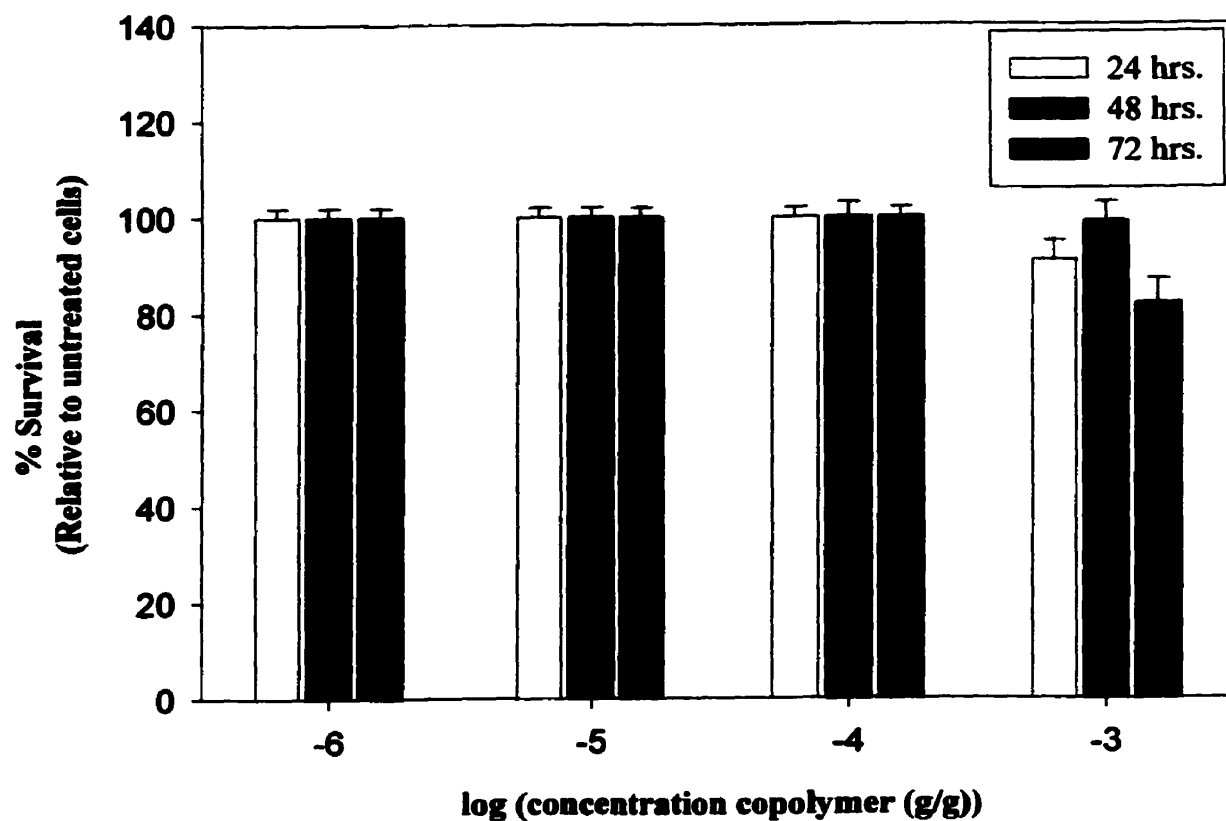


Figure 8.4: The *in vitro* biocompatibility of PCL₂₀-b-PEO₄₄ micelles in HeLa cells for 24-72 hours as measured relative to the untreated control which is taken to be 100% survival.

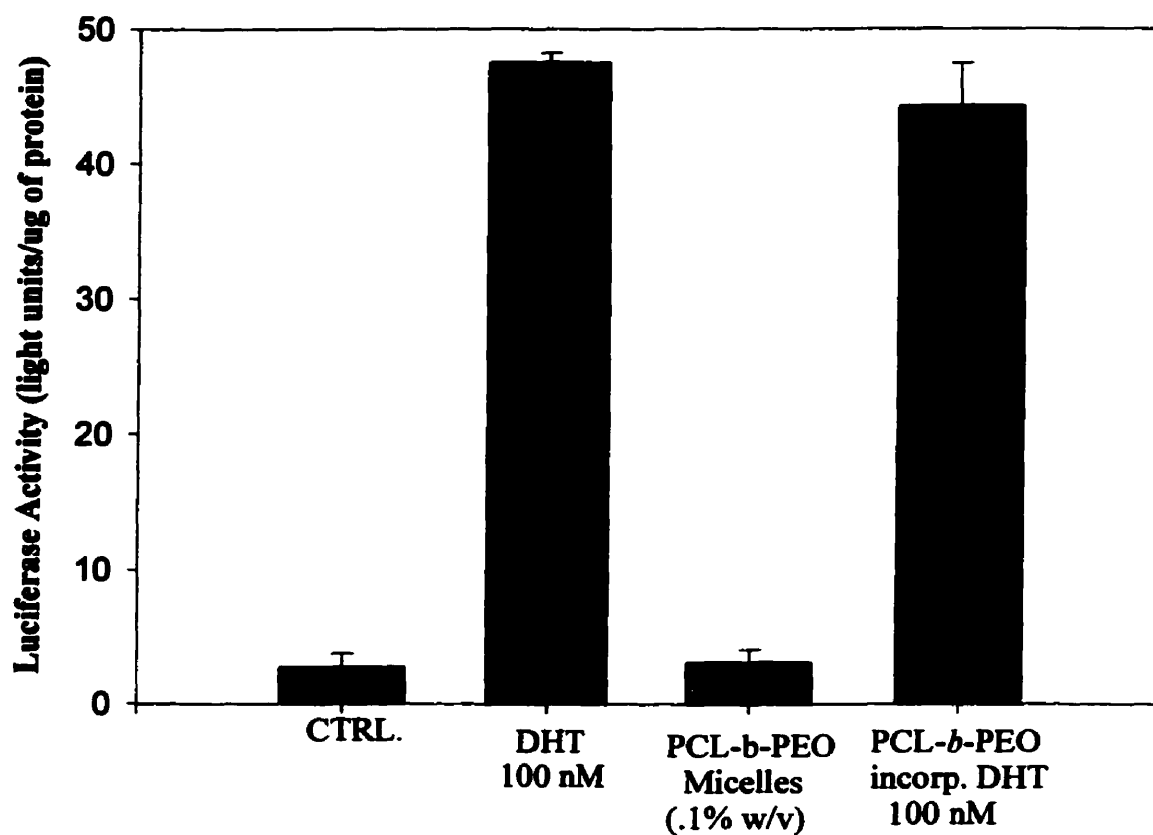


Figure 8.5: The luciferase activity in HeLa cells cotransfected with MMTV-LUC and the androgen receptor and treated with either nothing (control), 100nM DHT alone, empty PCL₂₀-b-PEO₄₄ micelles or PCL₂₀-b-PEO₄₄ micelle-incorporated DHT 100nM.

in Figure 8.5 demonstrates the basal level of luciferase activity in cells which are untreated (negative control). As a positive control the transfected cells were treated with 100 nM DHT (bar 2), in this case the luciferase activity was 47 light units per μg of protein. As a second negative control the cells were treated with empty PCL₂₀-*b*-PEO₄₄ micelles, with this treatment the luciferase activity was indistinguishable from the level of activity in untreated cells. The transfected cells were also treated under identical conditions with the PCL₂₀-*b*-PEO₄₄ micelle-incorporated DHT such that the final concentration per well was 100nM. There was a highly significant increase in the luciferase activity induced by both treatment with free DHT (bar 2) and micelle-incorporated DHT (bar 4). There was no significant difference between the luciferase activity induced with free drug or micelle-incorporated drug.

8.2.4. Discussion

Results from these studies show that the highly lipophilic model molecule DHT can be effectively incorporated into the PCL₂₀-*b*-PEO₄₄ copolymer micelles providing a novel delivery system for DHT with a prolonged and steady release. This delivery system may be used for other compounds which are highly lipophilic or toxic. The advantage of block copolymer micelles as delivery vehicles is that they may be tailor – made (e.g. size, morphology, hydrophobicity and polarity of core) to suit a particular application by changing the properties of the copolymer (e.g. block composition, block length, block ratio) and the conditions used in micelle preparation. The copolymer micelles can also be made to be small in size (10-100nm) and have a high degree of stability.

One of the major roles of a delivery vehicle is to enhance the solubility of highly lipophilic drugs in an aqueous medium. The maximum amount of DHT that could be loaded into 0.1mL of a 1% (w/w) PCL₂₀-*b*-PEO₄₄ micelle solution was found to be 1.3mg (Figure 8.1). This amount is equivalent to 12.8g in one liter of a 1% (w/w) PCL₂₀-*b*-PEO₄₄ micelle solution while the solubility for DHT in water is only 42 mg/L at 25°C [37]. The PCL₂₀-*b*-PEO₄₄ micelles have enhanced the solubility of DHT in water by a factor of 300.

However, the ideal micelle-incorporated DHT solution will not only correspond to that which contains the maximum amount of DHT. The ideal solution of micelle-

incorporated DHT would also have a high apparent partition coefficient (K_r) and a slow release profile. As mentioned previously, in a micelle solution the drug partitions between the micelles and the external medium. The ratio of the drug in the micelles to that in the external medium may be termed the apparent partition coefficient. In Figure 8.1, we see that as an increasing amount of drug is added during micelle preparation more drug is incorporated and the apparent partition coefficient increases. Yet, as the maximum loading capacity of the micelles is neared more of the drug is present in the external medium of the micelle solution so the K_r decreases. The maximum value of K_r is reached just prior to the point at which the loading capacity is attained (see Figure 8.1). In this way it may be best to use the solution that has the highest value of K_r but slightly less DHT loaded into the micelle solution.

Another factor to consider is the amount of copolymer required to deliver a specific quantity of drug. It is of course important that the delivery vehicle carries a sufficient quantity of drug to justify its use. The calculation of the number of drug molecules per micelle enables one to realize the extent to which the micellar delivery vehicle provides a loading space for the drug. A maximum of 2000 molecules were found to be loaded per micelle (Figure 8.2). Also, a maximum value of 240 was obtained for percentage of the weight of drug loaded to the weight of the micelle cores this demonstrates that the micelles are very efficient carriers of DHT.

The study of the kinetic release profiles of two of the micelle-incorporated DHT solutions, which differed in the amount of DHT incorporated, revealed that the more concentrated solution has the optimal release profile (Figure 8.3). The release profile of the 40 mM micelle-incorporated DHT solution did not have the same initial burst release which the 8 mM solution was found to have. Also, the slow steady release from the 40 mM DHT-micelle solution was found to continue for one month. The decrease in the release rate which was found to accompany an increase in the amount of drug loaded parallels behavior previously described in the literature [38]. Kim et al. recently reported that the release rate of indomethacin from PCL-*b*-PEO micelles decreased as the loading level of the drug was increased [38]. This may be due to the increase in the compatibility between the core and the drug which may accompany an increased loading level. As we described in a recent review [39], both the degree of incorporation of a drug into micelles

and the release of the drug from the micelles are greatly influenced by the compatibility between the core of the micelle and the drug to be incorporated.

The 40 mM micelle-incorporated DHT solution appears to be a promising preparation to be considered for androgen replacement therapy. However, the release kinetic profile *in vitro* may not be indicative of the pharmacokinetic profile *in vivo*. To this point, the mode of administration that has been most investigated for block copolymer micelle preparations has been by intravenous injection; however, in this instance administration by intramuscular injection may be more convenient. *In vivo* studies are presently underway in order to provide data on the pharmacokinetic parameters and organ biodistribution of micelle-incorporated DHT.

The study of the *in vitro* biocompatibility of the PCL₂₀-*b*-PEO₄₄ micelles in HeLa cells was required in order to ensure that this cell line could be used for the *in vitro* biological assay. The incubation of the PCL-*b*-PEO micelles for 24-72 hours in the concentration used in the transfection assay caused no noticeable cell death in comparison to the untreated control (Figure 8.4). The *in vitro* biocompatibility of the micelles had been previously confirmed in PC12 cells, MCF-7 cells and primary cultures of human microglia, astrocytes and cortical neurons [22].

The *in vitro* assay used to examine the biological activity of micelle-incorporated DHT included HeLa cells which had been cotransfected with expression vectors for MMTV-LUC and the androgen receptor. The results (Figure 8.5) demonstrate that the preparation of micelle-incorporated DHT does not diminish the biological activity of the drug. It was expected that the biological activity of the micelle-incorporated DHT would be equivalent to that of the drug alone since the DHT would likely be completely released from the micelles over the 24 hour period. As mentioned previously, 200 μ L of a 1 mM micelle-incorporated DHT stock solution were incubated with the HeLa cells. From the release kinetic experiments we see that as the amount of drug loaded is decreased the release rate is increased and since for the 8 mM micelle-incorporated DHT solution the release was over in 8 days it follows that the release of the 1mM solution would likely be over in approximately one day. These results also show that the drug is released from the micelle and able to bind to the androgen receptor. The ongoing experiments in the laboratory are designed to test several possibilities involving the release of micelle-

incorporated DHT and subsequent binding to the androgen receptor. The three possibilities which exist are the following: 1- the micelles remain outside the cell and the drug is released into the external medium following which it enters the cell; 2- the micelles enter the cell and release the drug into the cytoplasm after which it is transported into the nucleus; 3- the micelles enter the nucleus where the drug is then released. Studies which employ fluorescent or radiolabeled copolymer are currently ongoing in order to determine the localization of the micelles when incubated with HeLa cells. We have recently, confirmed that the PCL₂₀-*b*-PEO₄₄ micelles are internalized into PC12 (rat pheochromocytoma) cells [40] by an endocytotic mechanism [41]. Similar studies must be done with HeLa cells and other cell lines since it is known that the rate and extent of cellular internalization of small particles is cell type specific [42]. In this way, the internalization results obtained from studies on one specific cell type cannot be assumed for the internalization into another cell type. To this point, it appears that the cellular internalization of the PCL₂₀-*b*-PEO₄₄ micelles into HeLa cells proceeds at a much slower rate when compared to the rate in PC12 cell cultures.

8.2.5. Conclusion

The PCL₂₀-*b*-PEO₄₄ copolymer micelles were shown to be efficient carriers of dihydrotestosterone as they enhanced the solubility of DHT in water by 300 fold. Also, the micelle-incorporated DHT was shown to have a slow steady release profile in PBS at 37°C. The biocompatibility of the delivery vehicle in HeLa cells was confirmed over 24-72 hour periods. Finally, the biological activity of the micelle-incorporated DHT was found to be retained as measured in HeLa cells. The results clearly demonstrate that the micelle-incorporated drug is able to reach its nuclear target.

8.2.6. References

1. Wang L.G., Liu X.M., Kreis W., Budman D.R., *Biochemical Pharmacology* **1998**, 55, 1427-1433.
2. Wood K.V., et al. *Biochem. Biophys Res. Comm.* **1984**, 124, 592.
3. DeWet J.R. et al., *Proc. Natl. Acad. Sci. U.S.A.* **1985**, 82, 7870.
4. Nguyen V.T., Morange M., Bensaude O. *Analytical Biochemistry* **1988**, 171, 404-408.
5. Wang C., Swerdloff R. S. *Ann Med.* **1997**, 29 365.
6. McClellan K.J., Goa K. L. *Drugs* **1998**, 55, 253.
7. Mazer N.A., Heiber W.E. Moellmer J.F. et al. *J. Controlled Release* **1992**, 19, 347.
8. Gooren L.J.G. *Molecular and Cellular Endocrinology* **1998**, 145 153.
9. Tenover J.S. *J. Clinical Endocrinol. Metab.* **1992**, 75, 1092.
10. Carter H.B., Pearson J.D., Metter E.J., Chan D.W. Andres R., Fozard J.L., Rosner W., Walsh P.C. *Prostate* **1995**, 2725.
11. Snyder P.J., Development of criteria to monitor the occurrence of prostate cancer in testosterone clinical trials. In: Bhasin S., Gabelnick H.L., Swerdloff R.S., Wang C., (Eds), *Pharmacology, Biology and Clinical Applications of Androgens*. Wiley-Liss, New York pp. 143-150.
12. Morley J.E. Perry H.M., Kaiser F.E., Kraenzle D., Jensen J., Houston K., Mattammal M., Perry H.M. *J. Am. Geriatr. Soc.* **1993**, 41 149.
13. Arver S., Dobs A.S., Meikle A.W., Caramelli K.E., Rajaram L., Sanders S.W., Mazer N.A., *Clinical Endocrinology* **1997**, 47, 727.
14. Schaison G., Nahoul G., Couzinet B. Percutaneous dihydrotestosterone system. In: Nieschlag E., Behre H.M., (Eds.) *Testosterone: Action, Deficiency and Substitution*. Berlin: Springer Verlag, 1990: 155-164.
15. Handelsman D.J., Mackey M.A., Howe C., Turner L., Conway A.J. *Clinical Endocrinology* **1997**, 47, 311.
16. Jockenhovel F., Vogel E., Kreutzer M., Reinhardt W., Lederbogen S., Reinwein D. *Clinical Endocrinology* **1996**, 45, 61.
17. Bhasin S., Swerdloff R.S., Steiner B., et al. *J. Clin. Endocrin. Metab.* **1992**, 74, 75.

18. Kobayashi D., Tsubuku S., Yamanaka H., Asano M., Miyajima M., Yoshida M. *Drug Development and Industrial Pharmacy* **1998**, 24, 819.
19. Buntner B., Nowak M., Kasperczyk J., Ryba M., Grieb P., Walski M., Dobrzynski P., Bero M. *Journal of Controlled Release* **1998**, 56, 159.
20. Tsukubu S., Sugarawa S., Miyajima M., Yoshida M., Asano M., Okabe K., Kobayashi D., Yamanaka H., *Drug Development and Industrial Pharmacy* **1998**, 24, 927.
21. Hagan S.A., Coombes A.G.A., Garnett M.C., Dunn S.E., Davies M.C., Illum L., Davis S.S. *Langmuir* **1996**, 12, 2153.
22. Allen C., Yu Y., Maysinger D., Eisenberg A., Polycaprolactone-b-poly(ethylene oxide) *Bioconjugate Chem.* **1998**, 9, 564.
23. Yokoyama M., Fukushima S., Uehara R., Okamoto K., Kataoka K., Sakurai Y., Okano T. *J.Control. Release* **1998**, 50, 79.
24. Yokoyama M., Okano T., Kataoka K. *J. Controlled Rel.* **1994**, 32, 269.
25. Kwon G., Naito M., Yokoyama M., Okano T., Sakurai Y., Kataoka K. *J. Control. Release* **1997**, 48, 195.
26. Alakhov V.Y., Moskaleva E.Y., Batrakova E.V., Kabanov A.V. *Bioconjugate Chem.* **1996**, 7, 209.
27. Miller D.W., Batrakova E.V., Waltner T.O., Alkhov V.Y., Kabanov A.V., *Bioconjugate Chemistry* **1997**, 8, 649.
28. Inoue T., Chen G.H., Nakamae K., Hoffman A.S. *J. Control. Release* **1998**, 51, 221.
29. Zhang X., Burt H.M., Von Hoff D., Dexter D., Mangold G., Degen D., Oktaba A.M., Hunter W.L. *Cancer Chemother. Pharmacol.*, **1997**, 40, 81.
30. Yu Y., Allen C., Chijiwa S., Maysinger D., Eisenberg A. submitted to *Macromolecules* **1999**.
31. Ding J., Liu G. *J. Phys. Chem. B.* **1998**, 102, 6107.
32. Current Protocols in Molecular Biology supplement 36, p 9.1.4-9.1.6
33. Cor. W. Kuil, Eppo Mulder *Endocrinology* **1996**, 37, 1870.
34. Zhao J., Allen C., Eisenberg A. *Macromolecules* **1997**, 30, 7143.
35. Wilhelm M., Zhao C.L., Wang Y., Xu R., Winnik M.A., Mura J.L., Riess G., Croucher M.D. *Macromolecules* **1991**, 24, 1033.

36. Kabanov A.V., Nazarova I.R., Astafieva I.R., Batrakova E.V., Alakhov V.Y., Yarostavov A.A., Kabanov V.A. *Macromolecules* **1995**, 28, 2303.
37. Handbook of Physical Properties of Organic Chemicals. Lewis Publishers. CRC Press Inc. 1997 p.363.
38. Kim S.Y., Shin I.G., Lee Y.M., Cho C.S., Sung Y.K.. *Journal of Controlled Release* **1998**, 51, 13.
39. Allen C., Maysinger D, Eisenberg A. *Colloids and Surfaces B: Biointerfaces*, accepted **1999**.
40. Greene L.A., Tischler A.S. *Proc. Natl. Acad. Sci. U.S.A.* 1976, 73, 2424.
41. Allen C., Yu Y., Eisenberg A, Maysinger D. *Biochimica Biophysica Acta* accepted **1999**.
42. Straubinger R.M., Papahadjopoulos D, Hong K. *Biochemistry* **1990**, 29, 4929.

CHAPTER 9

CONCLUSIONS, CONTRIBUTIONS TO ORIGINAL KNOWLEDGE AND SUGGESTIONS FOR FUTURE WORK

9.1. Conclusions and Contributions to Original Knowledge

The aim of the work summarized in this thesis has been the preparation, characterization and application of block copolymer micelles as drug delivery vehicles. In Chapter 2, we outlined the physico-chemical properties of the micelle which influence their potential as drug delivery vehicles. It was hoped that this discussion would demonstrate the extent to which the block copolymer micelles can be tailor-made to suit a particular application. Studies of the physico-chemical characterization of micelles as drug carriers were mostly described in Chapters 3, 4, 5, and 8. While the biological studies of the micelles as drug carriers were described in Chapters 5, 6, 7, and 8.

In Chapter 3, we described our results from studies of the partitioning of the model compound, pyrene, between PS-*b*-PAA copolymer micelles and a H₂O/DMF solvent mixture as a function of both the copolymer concentration and the water content in the solvent mixture. The partition coefficient for pyrene between the micelles and the external medium was found to increase linearly with an increase in the water content in the solvent mixture. The number of molecules of pyrene per micelle was found to vary with both the copolymer concentration and the solvent composition. The partition coefficient was used to calculate the equilibrium constant which was, in turn, used to calculate the free energy of transfer of pyrene from the solvent phase to the micelle phase. The free energy of transfer was found to decrease as the water content in the solvent mixture was increased. These studies demonstrate that the incorporation of a

hydrophobic solubilize may be enhanced by changing the composition of the external medium such that it becomes increasingly uncomfortable for the solubilize.

As mentioned previously, the fluorescence method employed for measurement of the partition coefficient of pyrene between the PS-*b*-PAA micelles and a H₂O/DMF solvent mixture was based on previously developed methods. However, in the second part of these studies we took the partition coefficients obtained by the fluorescence method and used them to calculate values of the I_3/I_1 ratios, the amount of pyrene absorbed and the number of pyrene molecules per micelle. The calculated values were then compared with the experimental values in order to check the self-consistency of the approach. This also enabled us to identify any shortcomings which may arise through the use of this fluorescence method. Deviations were found at the highest copolymer concentrations between the two sets of I_3^U values, and at the lowest copolymer concentrations between the values of the number of pyrene molecules per micelle.

The value of the partition coefficient for pyrene between a micelle system and water serves to some extent as a measure of the affinity of the micelles for hydrophobic solubilizes. This is clearly shown when we compare the values obtained for the partition coefficient for pyrene between the PS-*b*-PAA micelles and water, found to be of the order of 10^5 (Chapter 3), with that for pyrene between the PCL-*b*-PEO micelles and water, found to be of the order of 10^2 (Chapter 4). Since the partition coefficient for pyrene between a micelle system and water is a standard parameter used to evaluate the degree of hydrophobicity of the core-forming block, it was important to establish a fluorescence method, in which we were aware of its shortcomings and breakdowns in order to be able to calculate this value reliably.

In Chapter 4, we reported on a novel method for the synthesis of the biocompatible and biodegradable copolymers of poly(caprolactone)-*b*-poly(ethylene oxide). We described the characterization of a series of PCL-*b*-PEO copolymers which have a constant PEO block length and different PCL block lengths. We also reported on the physico-chemical characteristics of the PCL-*b*-PEO aggregates, focusing mostly on

properties which are of interest to applications in drug delivery. As anticipated, both the characteristics of the copolymer and the physico-chemical properties of the aggregates were found to vary depending on the block length. This finding highlights the extent to which the parameters of the micelles can be tailored by altering the properties of the copolymer materials employed in micelle preparation.

The determination of the physico-chemical characteristics of the PCL-*b*-PEO copolymers and aggregates is essential to maximally exploiting these micelles as drug delivery vehicles. For example, knowledge of the critical micelle concentration of the copolymer will enable one to know which dilutions can be used in particular biological experiments. In this way, the properties of the PCL₂₀-*b*-PEO₄₄ system described in Chapter 4 served as important pieces of information in the biological studies described in Chapters 5-8.

In addition, as mentioned in Chapter 2, it is unlikely that there will be one universal micellar drug delivery vehicle which would serve as the best carrier for all hydrophobic solubilizates. For this reason, if we fully characterize each of the individual micelle systems, based on copolymers with different hydrophobic blocks, we would be able to create a database of micelles from which one could choose the best system to delivery a specific drug.

In Chapters 5 and 6, we summarized the *in vitro* and *in vivo* studies of the PCL₂₀-*b*-PEO₄₄ micelle system as a drug carrier for the neurotrophic agent FK506. To our knowledge, this was the first report on a colloidal drug delivery vehicle for FK506 as a neurotrophic agent. In Chapter 5, we confirmed the *in vitro* biocompatibility of the PCL₂₀-*b*-PEO₄₄ aggregates in MCF-7 and PC12 cell cultures as well as primary cultures of human microglia, astrocytes and cortical neurons. Also, the *in vitro* delivery and biological activity of the micelle-incorporated FK506 was proven in PC12 cell cultures. In Chapter 6, we reported on the *in vivo* biological distribution of the micelle-incorporated drug in Sprague Dawley rats 6 and 24 hours following intravenous administration. The most striking difference between the biodistribution of the micelle-

incorporated FK506 and FK506 administered in other formulations was the high degree of accumulation in the brain which accompanied the administration of the drug in micelle form.

In order to determine if the biological activity of FK506 was still retained *in vivo* when administered in the PCL-*b*-PEO micelle solution, the sciatic nerve crush model of peripheral neuropathy was employed. The rats were given 5mg/kg on days 0, 6 and 12, with the first injection given locally and the other two given subcutaneously. Rats with lesioned sciatic nerves and receiving daily subcutaneous injections of 5 mg/kg of FK506 were shown to attain recovery of function in 15 days. In this case, we find that the rats reach full functional recovery in 16 days, yet they are only administered 20 % of the drug given in the experiments previously reported in the literature. Rats given 5mg/kg/day receive 90 mg/kg of drug over the 18 day period; in this case we only administer 15mg/kg over the 18 day period. The requirement for only 3 injections of the micelle-incorporated drug also increases patient compliance compared to the requirement for daily s.c. injections.

In Chapter 7, we report on a study of the cellular internalization of the PCL₂₀-*b*-PEO₄₄ micelles in PC12 cell cultures. Specifically, we employed various pharmacological manipulations to determine whether or not the uptake proceeded by an endocytotic mechanism. The evidence accumulated throughout these studies strongly suggests that the micelles are, in fact, internalized by endocytosis. However, as mentioned previously, this is the first step in a series of studies which must be performed in order to gain more information on the cellular internalization of block copolymer micelles.

Finally, in Chapter 8 we report on the investigation of the PCL₂₀-*b*-PEO₄₄ micelles as a delivery vehicle for dihydrotestosterone. These studies were initiated in order to explore the PCL-*b*-PEO micelles as carriers for drugs other than FK506. The PCL₂₀-*b*-PEO₄₄ copolymer micelles were shown to be efficient carriers of dihydrotestosterone as they enhanced the solubility of DHT in water by 300 fold. Also, the micelle-incorporated

DHT was shown to have a slow steady release profile in PBS at 37°C. In addition, the biological activity of the micelle-incorporated DHT was found to be retained as measured in HeLa cells. The results clearly demonstrate that the micelle-incorporated drug is able to reach its nuclear target.

9.2. Suggestions for Future Work

The overall aim of this thesis was the development of a delivery vehicle based on block copolymer micelles. This aim was divided into several goals including the preparation, characterization and *in vitro/in vivo* biological study of the delivery vehicle. Since there were multiple goals it was not possible to fully expand the studies in any one area. Therefore this thesis only serves as a foundation from which the research can be easily expanded into many directions.

In terms of the physico-chemical characterization of the PCL-*b*-PEO micelles as drug carriers there are several studies which may be of interest for the future. For instance, it may be useful to study the extent of solubilization of compounds with different physical properties (i.e. degree of hydrophobicity, polarity, charge, molecular weight etc.) into the PCL-*b*-PEO micelles. In this way, we may be able to deduce which drugs could be most efficiently delivered by this specific micelle system.

An extensive study of the stability of the PCL-*b*-PEO micelles in biologically relevant media has yet to be conducted. In order for the delivery vehicle to be fully implemented, its stability must be further explored. In these studies the length of the corona forming block as well as other micelle properties should be varied in order to determine their effect on stability. Also, studies of the interactions of various proteins with the micelles could be included in this area.

The morphologies of the PCL-*b*-PEO aggregates formed under the different conditions remain to be determined. As mentioned in Chapter 2, aggregates of different morphologies may have interesting applications in drug delivery. Also, to date, block copolymer aggregates of different morphologies have not been formed from biocompatible and biodegradable copolymers.

In terms of the biological study of the micelles as drug carriers, this thesis has only explored micelle-incorporated drugs rather than studies of the micelles alone. For example, in Chapter 7, we investigate the cellular internalization of micelles by following

micelles containing radio- or fluorescent-labeled probes. Labeled micelles would be the ideal tool to truly determine both the extent and mechanism of uptake of micelles in different cell lines. Also, the *in vivo* biodistribution of the micelles alone could be determined through the use of labeled micelles. Finally, in order to achieve site-specific delivery, the surface of the PCL-*b*-PEO micelles could be modified by attachment of targeting moieties.